THERMOCHEMICAL VALORISATION OF RESIDUAL BIOMASS TO HIGH VALUE MOLECULES AND ENERGY

Jacky Cheikh wafa

THERMOCHEMICAL VALORISATION OF RESIDUAL BIOMASS TO HIGH VALUE MOLECULES AND ENERGY

Jacky Cheikh Wafa

Doctoral Thesis

Tarragona

2023

Jacky Cheikh Wafa

THERMOCHEMICAL VALORISATION OF RESIDUAL BIOMASS TO HIGH VALUE MOLECULES AND ENERGY

DOCTORAL THESIS

Supervised by Dr. Christophe Bengoa

Chemical Engineering Department

UNIVERSITAT
ROVIRA i VIRGILI

Tarragona
2023

UNIVERSITAT
ROVIRA i VIRGILI

Departament d'Enginyeria Química

Avinguda Països Catalans, 26

43007 Tarragona (Spain)

Tel. 977559619

Fax. 977559621

E-mail: christophe.bengoa@urv.cat

I STATE that the present study, entitled "Thermochemical Valorisation of residual biomass to High Value Molecules and Energy", presented by Jacky Cheikh Wafa for the award of the degree of Doctor, has been carried out under my supervision at the Department of Chemical Engineering of this university.

Tarragona, 3rd of November 2023

Dr. Christophe Bengoa
Doctoral Thesis Supervisor

58

59 **To the sustainable future**

60 **To the upcoming generation**

Acknowledgments

Words cannot express my gratitude to my supervisor Dr. Christophe Bengoa not only for giving me the opportunity to achieve another degree, but also for providing me with his invaluable and continuous support, patience, advices, motivation and help. I also would like to express my deepest appreciation to Dr. Esther Torrens, who without her, none of the problems could have been solved. Without both of you, this journey would not have been possible!

I would like to acknowledge Dr. Ursel Hornung and KIT, Karlsruhe Institute of Technology, for your kind welcome. I had the privilege to work with you.

PISET members, I'm glad that I got to work with you. Chicas (Vidingas), thank you for the best memories and for being amazing friends.

Kasia, I´m so lucky to call you not only a co-worker, but also a true friend. Thank you so much for everything! Jessica, Mary and Christine, thank you for making me feel HOME away from HOME, LEBANON.

Sisters and brother, nephews and nieces, thank you for providing me with the daily dose of energy.

أمي و أبي، بشكركم من كل قلبي على كل الدعم .أنا كتير فخورة لأنو أنا بنتكم.من وراكم أنا عم حقق أحلامي و طموحاتي .بحبكن كتير.

My Ragazzo, thank you for always motivating me to be my best. I really appreciate your ¨can-do¨ attitude every day. Thank you for never losing patience with me, even when I was acting crazy. I love you!

Table of contents

Summary

Fossil fuels have been the primary sources of energy for several centuries. However, they come with several significant disadvantages like the environmental impact including the releases of greenhouse gases such as carbon dioxide (CO_2), which contribute to global warming and climate change. In addition, Fossil fuels are finite resources, and their extraction can lead to resource depletion.

In response to these challenges, biofuels, derived from renewable organic materials, offer a more sustainable and environmentally friendly alternative. Biomass represents a versatile and valuable resource for energy production. It is derived from forestry residues and agricultural crops to municipal and industrial organic wastes. Among all, primary sludge is rich in lipids, proteins and carbohydrates and contains a high content of water.

Hydrothermal liquefaction is an innovative thermochemical process that play a significant role in the waste management as it deals with high moisturized materials. It operates at high conditions and converts the biomass into biocrude, biochar, aqueous phase and biogas. It's feasible to primary sludge as it contains around 4% of total solids.

Several parameters including temperature, reaction time and water:total solid ratio affect the yield and quality of biocrude and other products. In this study, according to the results obtained, the highest yield of biocrude was reached at 270°C of temperature and 30 min of reaction time. However, the best quality of biocrude was reached at higher temperature, 300°C. Definitely, longer reaction time gives better results. Here, all the results of biocrude obtained at 30 min were better than that obtained at 0 min. 2% load of PS gave higher yield of biocrude than 8% load of PS. By increasing the water content, the hydrolysis is easier and faster, resulting in higher amounts of organics in the biocrude phase.

As for the optimization of the HTL process, two scenarios were completed: The implementation of catalysts, either in homogeneous or heterogeneous form, and the change of solvent, either by using a pure organic solvent or by mixing an organic solvent with water.

According to the results obtained, the best improvement in biocrude yield was shown when 10% of $CuSO_4$ was added. Also, an important increase was noticed when pure methanol was used as a solvent.

HTL of other biomasses (buffalo, swine manure, rice straw and spirulina platensis) was accomplished. When comparing the results with the one of primary sludge, it offers the best conversion efficiency. Co-HTL of primary sludge with other biomasses was done as well. Apparently, the presence of primary sludge did improve the yield of biocrude, when comparing to the results obtained from HTL of biomass alone.

For all these runs, the complete separation of the four products was completed. Also, the yield for each phase was calculated. The characterization using different analytical method was done as well.

Despite all the manipulations done (change in temperature, change in reaction time, addition of catalyst, change of solvent and the change of solid load), biocrude didn’t attain standards needed to be used as an alternative for fossil fuels.

Regarding the high content of heavy compounds, biocrude should be subjected to hydrotreating and hydrocracking in order to minimize the oxygen content and to obtain more hydrocarbon chains.

1

Introduction

380

381

1. Fossil fuels and CO_2 emissions

Nobody is doubting the fact that energy is the most significant parameter to maintain the prosperity of the global. Currently, 80.3 % of the world´s primary energy is originated from fossil fuels (Renewables 2021 global status report, 2022). Interconnection of advancement in the economy and industrialization and rapid population growth has given rise in the energy consumption in the past years (Paramati et al., 2022). It was observed by many worldwide societies that counting only on fossil fuels does not offer important energy efficiency or vigorous advantages for nature. Carbon dioxide (CO_2), eluted from the huge combustion of oil and coal, is the principal promoter for global warning (Xu et al., 2023; Al Naimat et al., 2023). In addition, fossil fuels are damaging the environment and causing several dangerous effects on the planet, reflected by the increase of the global temperature and ozone layer weakening (Al Naimat et al., 2023; Xu et al., 2022). Some researchers noted atmospheric problem uncertainties including risky weather actions, very cold winters, very hot summers, a rise of sea levels, leading to an increase in the overall earth temperature (Yaduvanshi., 2021). The changes in the earth temperatures according to NASA are presented in Figure 1. It´s clear that, all over the years, the temperature is in increment direction.

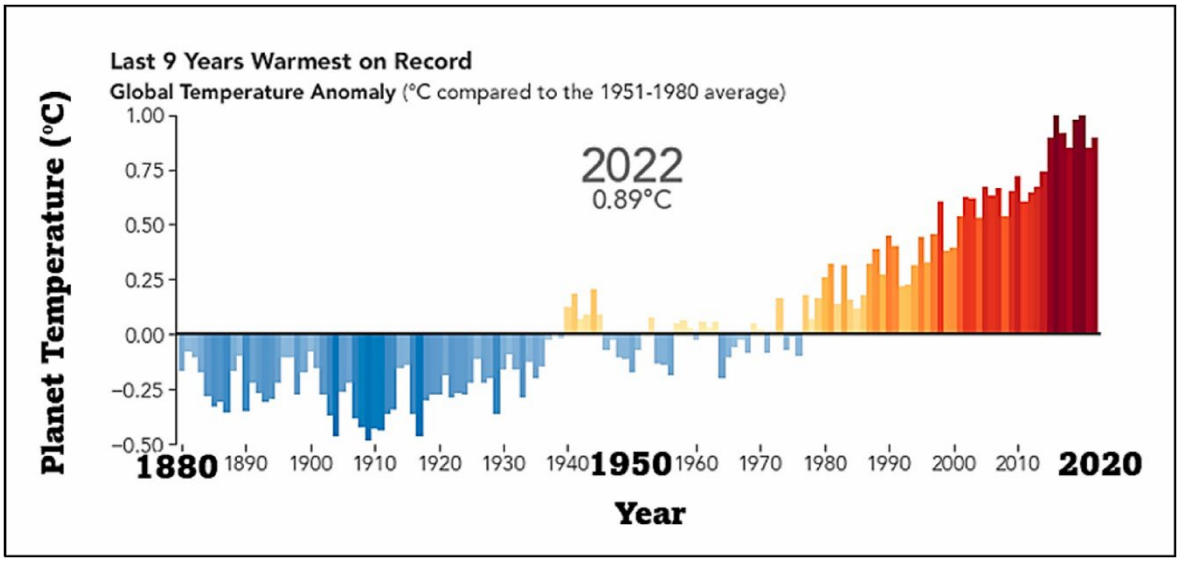

Figure 1. The increase rates of the earth´s temperature annually (NASA, 2023).

On the other hand, fuel resources are not distributed equally, resulting in a situation where some countries rely on others for energy, and their usage is affected by the political instability of the country reserve holders. Also, the accessibility of these reserves is getting more difficult, which is anticipated to result in high prices (Yesilyurt., 2023). All this initiated diverse research on renewable energy development to replace fossil fuels by using available sources. To minimize carbon emissions and fight the climate change and other problems, many countries focused on reducing energy consumption and offering low-carbon power systems (Zang et al., 2023).

2. Renewable energy resources

New generations will have the chance to enjoy green environment and safe living. Renewable Energy, Photovoltaic panels, wind farms, bioenergy, biogas, hydroelectric power, tide and ocean energies, and other types of sustainable resources have demonstrated their important values and extensive contributions to supply green job opportunities, notable cost-effectiveness of electrical power, and lower GHG emissions, specifically CO_2 (Al Naimat et al., 2023; Bui et al., 2023). The behaviour of the electricity generation from different sources in the OECD countries from 2000 to 2020 is shown in Figure 2. The rely on the renewable energy as an electricity source has become a major concern.

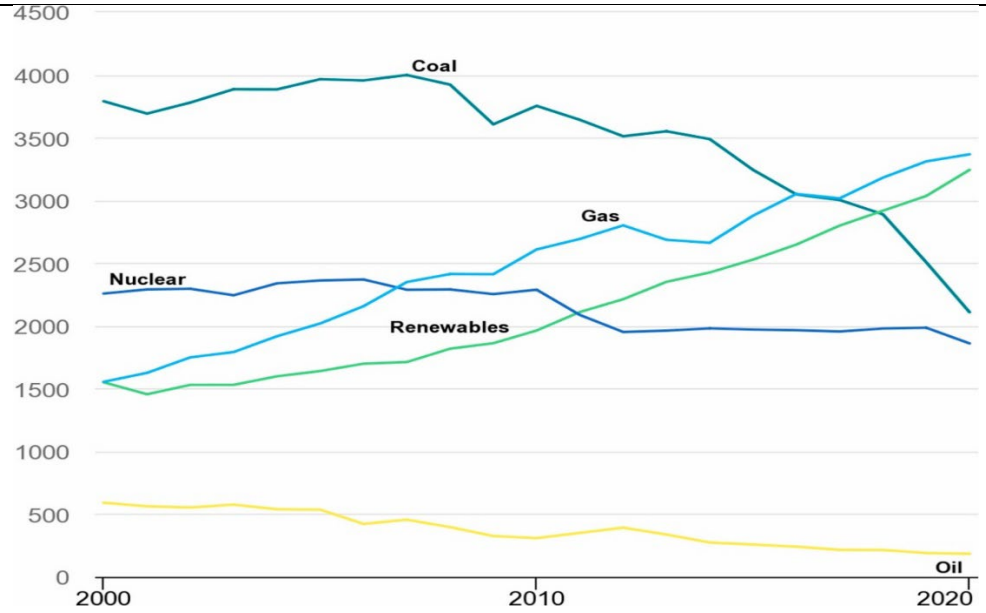

Figure 2. Electricity generation from different sources in OECD countries (Köse et al., 2020).

Renewable power capacity is predicted to rise by 2400 gigatons from 2022 to 2027, decreasing global warming to 1.5 °C globally (Khan et al., 2023). Certainly, biofuels/bioenergy were seen to be an eco-friendly substitute to conventional fuel. In fact, the acceptance of biomass for processing biofuels for electricity and transportation production resulted in increasing the demand for renewable energy (Van Ga et al., 2022). As indicated by reports, a considerable

part of the net energy demand of most of the developed countries is projected to be fulfilled by biomass-derived energy by 2050 (Kumar et al., 2015).

3. Biomass

¨Biomass¨ is any living or recently dead matter, generated from direct or indirect photosynthesis of animals or plants (Pocha et al., 2023). It contains 550–560 billion tons of carbon (Bar-On et al., 2018). Also, the production of biomass per year reached 100 billion tons (Wang et al., 2017). Biomass is considered to be an organic-rich feedstock used for synthesis of transportation fuels heat energy and electricity, and carbon-rich materials such as biochar, activated carbon, and carbon nanotubes (Bui et al., 2023). It´s one of the most significant resources for future sustainable energy as it can be converted to various liquid and gaseous biofuels including biogas/syngas, biodiesel, alcohol and bio-oil (Chew et al., 2017; Kasinath et al., 2021). Among the commonly explored biomass for energy utilization include agricultural and forestry wastes including saw dust and rice husk, municipal and food wastes, energy crops including switchgrass and algae and animal by-products including animal manure are all considered common biomasses for energy production, presented in Figure 3 (Saravanan et al., 2022; Tripathi et al., 2016).

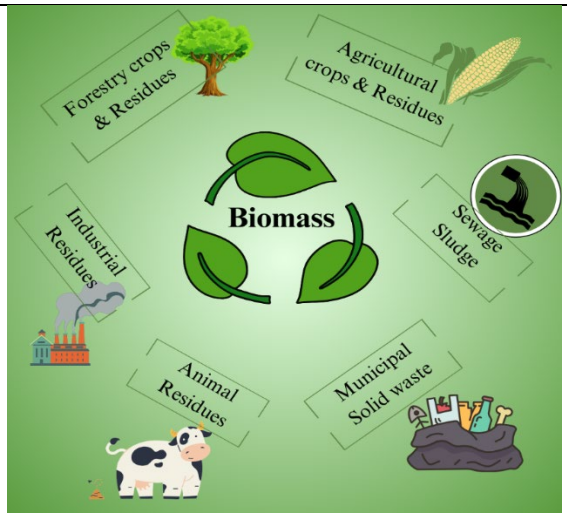

Figure 3. Different types of biomasses.

First generation biomass (crop plants) has been avoided because of interference with food chain and food supply (Kumar et al., 2023). Second generation biomass (non-edible lignocellulosic materials) may disturb food production, resulting in an increase in the food prices which prompts difficulties in accessing foodstuff (Akgül et al., 2019). Subsequently, the disadvantages of first and second generations resulted in exploitation of third and fourth generation biomass. Sewage sludge has many benefits over other biomass types including microalgae and biomass. First of all, sewage sludge is produced in huge amounts in all commercial and residential areas while others need proper land, weather condition and more time to grow (Jahromi et al., 2022). Consequently, sewage sludge is an efficient feedstock for bioenergy production.

4. Conversion techniques to bioenergy

Many communities disagreed the use of municipal sludge as a fertilizer (land application) due to environmental problems including its contamination with pathogens, heavy metals and micropollutants. Other conventional sludge treatments like incineration and co-compositing

458 emit toxic substances into the atmosphere (Jahromi et al., 2022). Through biochemical and
459 thermochemical conversion processes, sewage sludge can be converted to bioenergy (Cai et
460 al., 2017). However, the biochemical conversion techniques, like anaerobic digestion, utilize
461 microorganisms or enzymes to degrade biomass into smaller compounds including methane-
462 rick gases, are time consuming. The thermochemical conversion techniques, including
463 liquefaction, combustion, pyrolysis and gasification generate energy products through heat
464 (Shahbeig et al., 2020). Among all, hydrothermal liquefaction is considered a convenient
465 process for converting wet organic biomass, like sewage sludge, into biocrude that can be
466 additionally upgraded into feasible biofuels and valuable products (Thomsen et al., 2024).
467

468 **5. Hydrothermal liquefaction**

469 The development of the hydrothermal liquefaction technique through time from 2008 to
470 2022 is shown in Figure 4. The selection of biomass was initially studied. Then, the interest
471 in optimizing the process and improving biocrude yield through understanding the effect of
472 many parameters and the introduction of catalysts and co-solvents brought the HTL process
473 into a higher stage. Continuous HTL process has been also established, and the economic
474 feasibility of biocrude production from HTL was conducted by a techno-economic analysis.
475 Recently, a research group developed kinetic modelling of HTL of biomass, providing not
476 only the prediction of yields of HTL products under different conditions, but also the
477 provision of perceptions into potential reaction pathways (Yu et al., 2023).

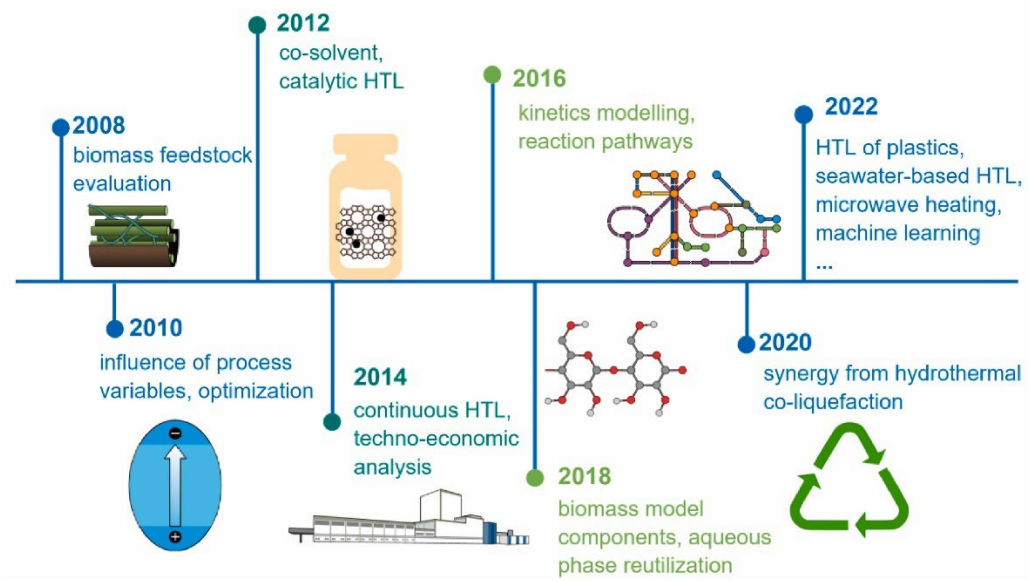

Figure 4. Hydrothermal liquefaction technique development timeline (Yu et al., 2023).

5.1.Process

HTL is a thermochemical conversion pathway with high energy efficiency rate and high conversion that operates at high temperatures (250–375 C), high pressures during a short reaction time (Thomsen et al., 2024). Under these conditions, the rigid structure of polymer of the biomass decomposes into a liquid biocrude as a main product (Sanchez et al., 2021). This technique is favourable for sludge as it deals with biomasses that contain high moisture content, resulting in higher conversion efficiency as pre-heat-drying of feedstock is not necessary (Jahromi et al., 2022). Figure 4 presents an overview of HTL process. The conversion of biomass through HTL process results in four products: biocrude, biochar, biogas and aqueous phase. HTL is performed either in a batch or in a continuous reactor (Thomsen et al., 2024). An extraction solvent like dichloromethane, methanol, toluene or acetone is usually used in batch systems to extract oil phase (Jahromi et al., 2022). In addition, the different variables,

492 temperature, time, feedstock concentration and stirring rate, beside the presence or the absence
493 of catalysts and solvents (other than water) affect greatly the distribution of products.

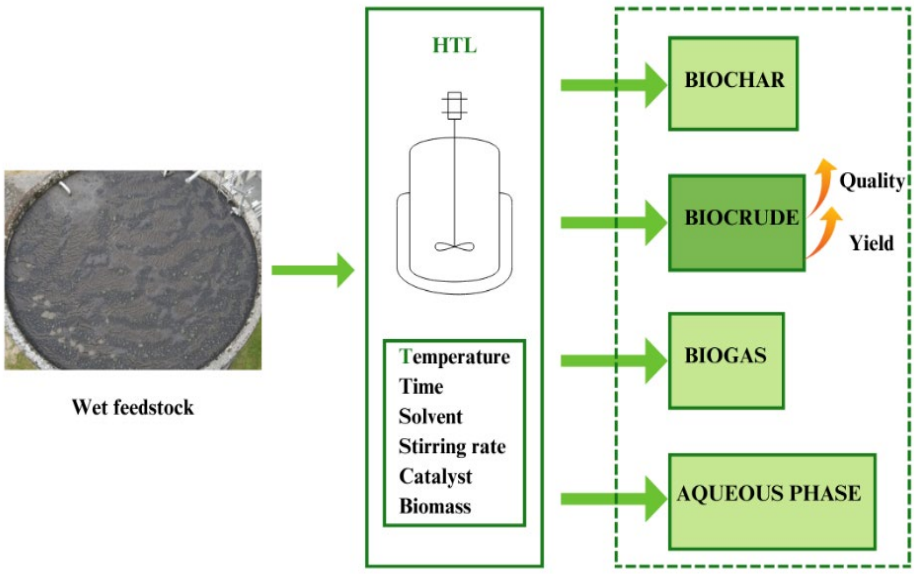

Figure 5. The basic concept of HTL process.

494

495 Several studies investigated the HTL conversion of sewage sludge into biocrude using
496 different conditions, shown in Table 1.

Table 1. HTL results of sludge from different sources at different conditions.

Feedstock	Parameters	Biocrude yield %	Reference
Secondary sludge	350 ºC, 15 min, K_2CO_3	45.22	Shah et al., 2020
Primary sludge	300 ºC, 20 min	46.80	Thomsen et al., 2024
Secondary sludge	360 ºC, 0 min, $CuSO_4$	47.45	Wang et al., 2018
Sewage sludge	220 ºC, 30 min	34.90	Lai et al., 2018
Sewage sludge	399.85 ºC, 60 min	26.80	Qian et al., 2017

Primary sludge	300 ºC, 30 min	37.66	Experimental work

497

498

499 **5.2.Parameters**

500 Researchers have adopted different strategies, including the change in the parameters, to
501 improve the biocrude yield and quality. Temperature, reaction time, catalyst and solvent used
502 could affect not only the conversion efficiency of biocrude, but also the properties of the by-
503 products.

504 **5.2.1. Temperature**

505 Temperature is the most important parameter in the HTL process, which greatly
506 affects product yield. It was demonstrated that high temperature can improve the
507 quality of biocrude, the yield of gas with lower water-soluble substance yield, total
508 organic carbon content in the aqueous phase and solid yield (Xu et al., 2018). This
509 scenario is attributed to the boost of the hydrolysis process of biomass at higher
510 temperature and the endothermic properties of HTL process (Mastalinezhad et al.,
511 2023). In other words, high temperature favours the hydrolysis of organic
512 compounds and the production of monomers and oligomers by mean of dehydration,
513 condensation and decarboxylation reactions. However, when the temperature passes
514 the threshold value, a depolymerization occur and the yield of biocrude decreases
515 (Fan et al., 2022). For example, biocrude yield from HTL of primary sludge has
516 increased from 28 % to 42 % when the temperature has increased from 300 ºC to
517 325 ºC. However, when the temperature became 350 ºC, the yield has decreased
518 again to 32 % (Thomsen et al., 2024). In addition, a low yield of biocrude was
519 produced from HTL ranging between 180 ºC and 330 ºC, due to the compounds

formed from the decomposition of lipids. While at higher conditions, cellulose and proteins were decomposed as well, resulting in higher biocrude yield (Reddy et al., 2016).

5.2.2. Reaction time

Reaction time is another important factor in the production of biocrude. The selection of the reaction time in the middle of the chosen time interval should be enough to attain the maximum yield of biocrude, preventing additional decomposition of organic compounds in the aqueous phase and decreasing the cost of the product (Mastalinezhad et al., 2023). At long reaction time, some biocrude compounds could be transferred to gas and solid phase due to re-polymerization and decomposition of lighter compounds (Fan et al., 2022). The rate of hydrolysis is usually fast, so short time is enough to decompose organic compounds effectively. In one study, the overall conversion biomass reached its optimal value along with the increase of reaction time from 0 to 60 min. However, above that time, no changes were noticed (Remón et al., 2019). In another study, the optimal time condition of HTL of domestic sewage sludge was 45 min with a 13.81 % increase in the yield of biocrude when compared to 30 min reaction time. However, a longer time to 60 min was followed by an increase in the solid and aqueous phase yields resulting in lower biocrude production (Mishra et al., 2020). Elsewhere, by increasing the reaction time from 15 min to 45 min, no significant changes were noticed in the biocrude yield at 320 ºC and 350 ºC. Only at lower temperature, 280 ºC, the yield of biocrude was altered by the reaction time. Probably, at higher temperature, biocrude could be thermally converted to gaseous molecules. Polymerisation may not be the main

reaction at high conditions, resulting in more compounds in gaseous and aqueous phases (Villaver et al., 2018).

5.2.3. Catalyst

Homogeneous and heterogeneous catalysts are both concerned in the improvement of biocrude yield. The addition of catalyst may decrease the activation energy and respectively increases the yield of biocrude. In addition, they are able to minimize the repolymerization and condensation reactions of the intermediate products, resulting in high biocrude yield and lower biochar yield (Fan et al., 2022). Alkali acids and metal salts are usually utilized as homogeneous catalysts, and transition metal oxides, rare metals are commonly used as heterogeneous catalysts in HTL process (Chen et al., 2017). Several advantages associated with heterogeneous catalysts favour their use over homogeneous catalysts. In fact, heterogeneous catalysts could be recuperated easily and reduces reactor corrosion. Also, their use doesn´t only increase the yield of biocrude but also improves the quality of biocrude by minimizing the heteroatoms (Wang et al., 2018). Consequently, biocrude becomes much more appropriate for combustion Sharma et al., 2021). In a study, HTL biocrude yield was optimized to 47.45 % in the presence of $CuSO_4$ (Wang et al., 2018). In another one, the HTL of wood at 280 ºC for 15 min with K_2CO_3 has produced the highest yield of biocrude, 34 % (Jindal et al., 2015). The HTL of microalgae using red mud as catalyst improved the biocrude yield by 30 % (Saral et al., 2021).

5.2.4. Solvent

The selection of the solvent is significant for the optimisation of the HTL conversion. Water is the common solvent medium used. However, its critical conditions require additional energy input. Therefore, the replacement of water by another organic solvent having lower dielectric constant could improve the production of biocrude with better quality (Fan et al., 2022). Methanol, ethanol, propanol and acetone are examples of organic solvents that can replace water in HTL process. They are characterized by their high dissolution, moderate operating conditions, reaction intermediate stabilization that edges char formation and their incorporation in the deoxygenation reactions, resulting in biocrude containing low acidity and higher energy content (Madikizela et al., 2022). Also, aliphatic compounds were successfully extracted by n-hexane in wet biomass (Olkiewicz et al., 2014). The extraction of crude sludge oil (CSO) from wet sewage sludge (WSS) was efficient at a temperature above 260 ºC with a production yield of 22.8-24.2 % (Wu et al., 2017). The highest yield of biocrude from HTL of municipal sludge without any additional was 9.34 %. While in the presence of Ni-Co/AC as catalyst and ethanol as solvent, the yield has increased to 61.51 % (Hao et al., 2023). By comparing the behaviour of HTL sludge in n-hexane-water medium and methanol-water medium, the maximum biocrude yield was reached in methanol-water medium with 46.5 wt% (Li et al., 2018).

5.3. Products

Biomass is depolymerized through HTL process into four different products: biocrude, biochar, aqueous phase and biogas.

5.3.1. Biocrude

Biocrude is a dark and viscous oil, considered as a major energy product from HTL. However, it cannot be utilized directly as a biofuel because it has low heating value and high heteroatom content (Leng et al., 2020). Also, the high viscosity prevents its direct usage in vehicles, especially because of the incomplete combustion resulted from the pool pumping capacity (Summers et al., 2022). Consequently, it should be upgraded to improve its properties. One solution is to apply the catalytic hydrodeoxygenation where biocrude can be converted to biofuel in the presence of catalyst and hydrogen with oxygen removal (Xia et al., 2016). On the other hand, the co-processing of biocrude and its distillate fractions with petroleum could minimize capital costs, and adjust to present refining downstream facilities (Lavanya et al., 2016).

5.3.2. Biochar

Biochar is the solid phase residue from HTL, rich in carbon. It´s cheap, extremely porous, rich in carbon and characterized by its renewable content (Qiu et al., 2018). Biochar can be utilized in various applications like a solid fuel, a catalyst and an adsorbent. In addition, biochar can be used to remove heavy metals and dyes from aqueous medium. Also, biochar can be utilized to remove organic pollutants (nitrate, ammonia, phosphorus) from municipal wastewater (Mahima et al., 2021). Also, it´s likely to generate new biochar composites by modifying and adding nanoparticles onto biochar (Qiu et al., 2018).

5.3.3. Aqueous phase

Aqueous phase is the product generated from the conversion of the moisture content of the initial feedstock. Due to its high chemical oxygen demand (COD) concentration and high carbon-hydrogen content (20-40 % of initial biomass), it was difficult to deal with it. Recently, the valorisation of HTL aqueous phase though different techniques like anaerobic digestion, bioconversion, aqueous phase reforming and gasification won a great attention (Li et al., 2021). Also, the reuse of nutrients of HTL-AP through recycling was applied in order to reach an overall economic sustainability of the process (Mahima et al., 2021).

5.3.4. Biogas

Biogas is the gas phase released from the HTL process. Non-condensable gases were found including CO, CO_2, CH_4 and H_2 beside the flammable gases like C_2H_6 and C_2H_4 (Lu et al., 2022). Among all these gases, only H_2 can be utilized in the hydrotreatment of biocrude while the rest are considered as greenhouse gases that cause to global warming (Fan et al., 2022).

6. Objective

The overall objective of the experimental research work (Figure 6) is the thermochemical valorisation of residual biomass to high value molecules and energy. In order to attain the goal, the process has passed through many steps:

- Study the influence of temperature on the hydrothermal liquefaction of the municipal primary sludge at 30 min of reaction time (Chapter 2).
- Study the influence of temperature on the hydrothermal liquefaction of the municipal primary sludge at 0 min of reaction time (Chapter 3)

- Study the effect of homogeneous and heterogeneous catalysts on the products distribution from HTL conversion (Chapter 4)
- Study the effect of organic solvents and co-solvents on the quality and yield of biocrude and other products obtained from HTL (Chapter 5)
- Perform HTL of other biomasses and co-HTL of primary sludge with other biomasses for the purpose of HTL optimization (Chapter 6).

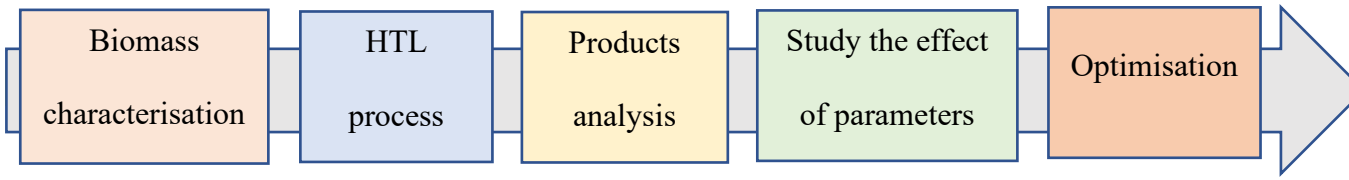

Figure 6. Main objectives of the thesis.

7. Thesis outline

The research work is divided into seven chapters outlined below:

- Chapter 1 presents the reason behind this research work and its objectives
- Chapter 2 includes the whole HTL process of primary sludge with the separation and the characterization of all the products at different temperatures for a reaction time of 30 min.
- Chapter 3 studies the quality and yield of products obtained from HTL of primary sludge at different temperature for a reaction time of 0 min.
- Chapter 4 investigates the HTL of primary sludge with the presence of catalysts (homogeneous and heterogeneous). Also, all the characterization products obtained is achieved for optimization purpose.

- Chapter 5 presents the HTL of primary sludge with the presence of solvents other than water and co-solvents with water. In addition, all the characterization products obtained is achieved for optimization purpose.
- Chapter 6 presents the behaviour of HTL with other types of biomasses. Also, co-HTL of primary sludge with other biomasses is performed for process conversion optimization.
- Chapter 7 includes the main conclusions of the research work and the future plan in that field.

References

"Global Temperatures,"The National Aeronautics and Space Administration (2023). NASA.

Akgül, A., & Seçkiner, S. U. (2019). Optimization of biomass to bioenergy supply chain with tri-generation and district heating and cooling network systems. *Computers & Industrial Engineering*, *137*, 106017. *https://doi.org/10.1016/j.cie.2019.106017*

Al Naimat, A., Liang, D. (2023). Substantial gains of renewable energy adoption and implementation in Maan, Jordan: A critical review. *Results in Engineering*, 19, 101367. https://doi.org/10.1016/j.rineng.2023.101367

Bar-On, YM., Phillips, R., Milo R. (2018). The biomass distribution on Earth. *Proceedings of the National Academy of Sciences*, 115 (25). *https://doi.org/10.1073/pnas.1711842115*

Bui, V. D., Hoang, V., Nguyen, H. P., Duong, X. Q., Nguyen, D. T., Pham, M. T., & Nguyen, P. Q. P. (2023). Techno-economic assessment and logistics management of biomass in the conversion progress to bioenergy. *Sustainable Energy Technologies and Assessments*, *55*, 102991. *https://doi.org/10.1016/j.seta.2022.102991*

679 Cai, J., He, Y., Yu, X., Banks, S. W., Yang, Y., Zhang, X., Yu, Y., Liu, R., & Bridgwater, A.
680 V. (2017). Review of physicochemical properties and analytical characterization of
681 lignocellulosic biomass. *Renewable & Sustainable Energy Reviews*, *76*, 309–322.
682 *https://doi.org/10.1016/j.rser.2017.03.072*
683 Chen, W., Yang, H., Chen, Y., Xia, M., Chen, X., & Chen, H. (2017). Transformation of
684 Nitrogen and Evolution of N-Containing Species during Algae Pyrolysis.
685 *Environmental Science & Technology*, *51*(11), 6570–6579.
686 *https://doi.org/10.1021/acs.est.7b00434*
687 Chew, K. W., Yap, J. Y., Show, P. L., Suan, N. H., Juan, J. C., Ling, T. C., Lee, D. H., &
688 Chang, J. S. (2017). Microalgae biorefinery: High value products perspectives.
689 *Bioresource Technology*, *229*, 53–62. *https://doi.org/10.1016/j.biortech.2017.01.006*
690 Fan, Y., Hornung, U., & Dahmen, N. (2022). Hydrothermal liquefaction of sewage sludge for
691 biofuel application: A review on fundamentals, current challenges and strategies.
692 *Biomass & Bioenergy*, *165*, 106570. *https://doi.org/10.1016/j.biombioe.2022.106570*
693 Hao, B., Xu, D., Wang, Y., Wang, Y., Kapusta, K., & Guo, Y. (2023). Catalytic hydrothermal
694 liquefaction of municipal sludge for biocrude production over non-noble bimetallic
695 catalyst in ethanol solvent. *Fuel*, *331*, 125812.
696 *https://doi.org/10.1016/j.fuel.2022.125812*
697 Jahromi, H., Rahman, T., Roy, P., & Adhikari, S. (2022). Hydrotreatment of solvent-extracted
698 biocrude from hydrothermal liquefaction of municipal sewage sludge. *Energy*
699 *Conversion and Management*, *263*, 115719.
700 *https://doi.org/10.1016/j.enconman.2022.115719*

Jindal, M. K., & Jha, M. K. (2015). Catalytic hydrothermal liquefaction of waste furniture sawdust to bio-oil. *Indian Chemical Engineer*, *58*(2), 157–171. https://doi.org/10.1080/00194506.2015.1006145

Kasinath, A., Fudala-Książek, S., Szopińska, M., Byliński, H., Artichowicz, W., Remiszewska-Skwarek, A., & Łuczkiewicz, A. (2021). Biomass in biogas production: Pretreatment and codigestion. *Renewable & Sustainable Energy Reviews*, *150*, 111509. https://doi.org/10.1016/j.rser.2021.111509

Khan, Kh., Su, Ch., Khurshid, A., Qin, M. (2023). Does energy security improve renewable energy? A geopolitical perspective. *Energy*, 128824. https://doi.org/10.1016/j.energy.2023.128824

Köse, N., Bekun, F. V., & Alola, A. A. (2020). Criticality of sustainable research and development-led growth in EU: the role of renewable and non-renewable energy. *Environmental Science and Pollution Research*, *27*(11), 12683–12691. https://doi.org/10.1007/s11356-020-07860-y

Kumar, A., Kumar, N., Baredar, P., & Shukla, A. (2015). A review on biomass energy resources, potential, conversion and policy in India. *Renewable & Sustainable Energy Reviews*, *45*, 530–539. https://doi.org/10.1016/j.rser.2015.02.007

Kumar, J., Sathish, S., Prabu, D., Renita, A. A., Saravanan, A., Deivayanai, V., Anish, M., Jayaprabakar, J., Baigenzhenov, O., & Hosseini-Bandegharaei, A. (2023). Agricultural waste biomass for sustainable bioenergy production: Feedstock, characterization and pre-treatment methodologies. *Chemosphere*, *331*, 138680. https://doi.org/10.1016/j.chemosphere.2023.138680

Lai, F., Chang, Y., Huang, H., Wu, G., Xiong, J., Pan, Z., & Zhou, C. (2018b). Liquefaction of sewage sludge in ethanol-water mixed solvents for bio-oil and biochar products. *Energy*, *148*, 629–641. https://doi.org/10.1016/j.energy.2018.01.186

Lavanya, M., Meenakshisundaram, A., Renganathan, S., Chinnasamy, S., Lewis, D. M., Nallasivam, J., & Bhaskar, S. (2016). Hydrothermal liquefaction of freshwater and marine algal biomass: A novel approach to produce distillate fuel fractions through blending and co-processing of biocrude with petrocrude. *Bioresource Technology*, *203*, 228–235. https://doi.org/10.1016/j.biortech.2015.12.013

Leng, L., Zhang, W., Peng, H., Li, H., Jiang, S., & Huang, H. (2020). Nitrogen in bio-oil produced from hydrothermal liquefaction of biomass: A review. *Chemical Engineering Journal*, *401*, 126030. https://doi.org/10.1016/j.cej.2020.126030

Li, B., Liu, Y., Yang, T., Feng, B., Xing, K., Wang, S., & Li, R. (2021). Aqueous phase reforming of biocrude derived from lignocellulose hydrothermal liquefaction: Conditions optimization and mechanism study. *Renewable Energy*, *175*, 98–107. https://doi.org/10.1016/j.renene.2021.04.127

Li, R., Ma, Z., Yang, T., Li, B., Wei, L., & Sun, Y. (2018). Sub–supercritical liquefaction of municipal wet sewage sludge to produce bio-oil: Effect of different organic–water mixed solvents. *Journal of Supercritical Fluids*, *138*, 115–123. https://doi.org/10.1016/j.supflu.2018.04.011

Lu, J., Watson, J., Liu, Z., & Wu, Y. (2022). Elemental migration and transformation during hydrothermal liquefaction of biomass. *Journal of Hazardous Materials*, *423*, 126961. https://doi.org/10.1016/j.jhazmat.2021.126961

745 Madikizela, M., & Isa, Y. M. (2022). Effect of operating conditions on the hydrothermal
746 valorization of sewage sludge. *Biofuels, Bioproducts and Biorefining*, *17*(2), 403–414.
747 *https://doi.org/10.1002/bbb.2429*
748 Mahima, J., Sundaresh, R. K., Gopinath, K. P., Rajan, P. S. S., Arun, J., Kim, J. S., &
749 Pugazhendhi, A. (2021). Effect of algae (Scenedesmus obliquus) biomass pre-treatment
750 on bio-oil production in hydrothermal liquefaction (HTL): Biochar and aqueous phase
751 utilization studies. *Science of the Total Environment*, *778*, 146262.
752 *https://doi.org/10.1016/j.scitotenv.2021.146262*
753 Mastalinezhad, F., Osfouri, S., Azin, R. (2023). Production and characterization of biocrude
754 from Persian Gulf Sargassum angustifolium using hydrothermal liquefaction: Process
755 optimization by response surface methodology. Biomass and Bioenergy, 178, 106963,
756 *https://doi.org/10.1016/j.biombioe.2023.106963*
757 Olkiewicz, M., Caporgno, M. P., Fortuny, A., Stüber, F., Fabregat, A., Font, J., & Bengoa, C.
758 (2014). Direct liquid–liquid extraction of lipid from municipal sewage sludge for
759 biodiesel production. *Fuel Processing Technology*, *128*, 331–338.
760 *https://doi.org/10.1016/j.fuproc.2014.07.041*
761 Paramati, S. R., Shahzad, U., & Doğan, B. (2022). The role of environmental technology for
762 energy demand and energy efficiency: Evidence from OECD countries. *Renewable &*
763 *Sustainable Energy Reviews*, *153*, 111735. https://doi.org/10.1016/j.rser.2021.111735
764 Pocha, C. K. R., Chia, W. Y., Silvanir, Kurniawan, T. A., Khoo, K. S., & Chew, K. W. (2023).
765 Thermochemical conversion of different biomass feedstocks into hydrogen for power
766 plant electricity generation. *Fuel*, *340*, 127472.
767 *https://doi.org/10.1016/j.fuel.2023.127472*

768 Qian, L., Wang, S., & Savage, P. E. (2017). Hydrothermal liquefaction of sewage sludge under
769 isothermal and fast conditions. *Bioresource Technology*, *232*, 27–34.
770 *https://doi.org/10.1016/j.biortech.2017.02.017*
771 Qiu, Z., Wang, Y., Bi, X., Zhou, T., Zhou, J., Zhao, J., Miao, Z., Yi, W., Fu, P., & Zhuo, S.
772 (2018). Biochar-based carbons with hierarchical micro-meso-macro porosity for high
773 rate and long cycle life supercapacitors. *Journal of Power Sources*, *376*, 82–90.
774 *https://doi.org/10.1016/j.jpowsour.2017.11.077*
775 Reddy, H. K., Muppaneni, T., Ponnusamy, S., Sudasinghe, N., Pegallapati, A., Selvaratnam,
776 T., Seger, M., Dungan, B., Nirmalakhandan, N., Schaub, T., Holguín, F. O., Lammers,
777 P. J., Van Voorhies, W., & Deng, S. (2016). Temperature effect on hydrothermal
778 liquefaction of Nannochloropsis gaditana and Chlorella sp. *Applied Energy*, *165*, 943–
779 951. *https://doi.org/10.1016/j.apenergy.2015.11.067*
780 Remón, J., Randall, J. D., Budarin, V. L., & Clark, J. H. (2019). Production of bio-fuels and
781 chemicals by microwave-assisted, catalytic, hydrothermal liquefaction (MAC-HTL) of
782 a mixture of pine and spruce biomass. *Green Chemistry*, *21*(2), 284–299.
783 *https://doi.org/10.1039/c8gc03244k*
784 Renewables 2021 global status report (2022). REN21. https://www.ren21.net/wp-
785 content/uploads/2019/05/GSR2021_Full_Report.pdf
786 Sanchez, E. L., Pedersen, S. B., Paulsen, M. M., Rosendahl, L., & Pedersen, T. H. (2021).
787 Techno-economic evaluation of carbon capture via physical absorption from HTL gas
788 phase derived from woody biomass and sewage sludge. *Energy Conversion and*
789 *Management: X*, *11*, 100089. *https://doi.org/10.1016/j.ecmx.2021.100089* ç

Saral, J. S., & Ranganathan, P. (2021). Catalytic hydrothermal liquefaction of Spirulina platensis for biocrude production using Red mud. *Biomass Conversion and Biorefinery*, *12*(1), 195–208. https://doi.org/10.1007/s13399-021-01447-4

Saravanan, A., Kumar, P. S., Aron, N. S. M., Jeevanantham, S., Karishma, S., Yaashikaa, P., Chew, K. W., & Show, P. L. (2022). A review on bioconversion processes for hydrogen production from agro-industrial residues. *International Journal of Hydrogen Energy*, *47*(88), 37302–37320. https://doi.org/10.1016/j.ijhydene.2021.08.055

Shah, A. A., Toor, S., Conti, F., Nielsen, A. H., & Rosendahl, L. (2020). Hydrothermal liquefaction of high ash containing sewage sludge at sub and supercritical conditions. *Biomass & Bioenergy*, *135*, 105504. https://doi.org/10.1016/j.biombioe.2020.105504

Shahbeig, H., & Nosrati, M. (2020). Pyrolysis of municipal sewage sludge for bioenergy production: Thermo-kinetic studies, evolved gas analysis, and techno-socio-economic assessment. *Renewable & Sustainable Energy Reviews*, *119*, 109567. https://doi.org/10.1016/j.rser.2019.109567

Sharma, N., Jaiswal, K. K., Kumar, V., Vlaskin, M. S., Nanda, M., Rautela, I., Tomar, M. S., & Ahmad, W. (2021). Effect of catalyst and temperature on the quality and productivity of HTL bio-oil from microalgae: A review. *Renewable Energy*, *174*, 810–822. https://doi.org/10.1016/j.renene.2021.04.147

Summers, S., Yang, S., Watson, J., & Zhang, Y. (2022). Diesel blends produced via emulsification of hydrothermal liquefaction biocrude from food waste. *Fuel*, *324*, 124817. https://doi.org/10.1016/j.fuel.2022.124817

Thomsen, L., Anastasakis, K., Biller, P. (2024). Hydrothermal liquefaction potential of wastewater treatment sludges: Effect of wastewater treatment plant and sludge nature

on products Distribution. *Fuel*, 355, 129525. *https://doi.org/10.1016/j.fuel.2023.129525*

Tripathi, M. P., Sahu, J., & Ganesan, P. (2016). Effect of process parameters on production of biochar from biomass waste through pyrolysis: A review. *Renewable & Sustainable Energy Reviews*, *55*, 467–481. *https://doi.org/10.1016/j.rser.2015.10.122*

Van Ga, B., Bui, T. M. T., Ong, H. C., Nižetić, S., Bui, V. H., Nguyen, T. T. X., Atabani, A., Štěpanec, L., Pham, L. H. P., & Hoang, A. T. (2022). Optimizing operation parameters of a spark-ignition engine fueled with biogas-hydrogen blend integrated into biomass-solar hybrid renewable energy system. *Energy*, *252*, 124052. *https://doi.org/10.1016/j.energy.2022.124052*

Villaver, W. S., Carpio, R. B., Yap, K. J. R., & De Leon, R. L. (2018). Effects of temperature and reaction time on yield and properties of biocrude oil produced by hydrothermal liquefaction of Spirulina platensis. *International Journal of Smart Grid and Clean Energy*, *7*(1), 32–41. *https://doi.org/10.12720/sgce.7.1.32-41*

Wang, S., Griffiths, D. L., Yang, H., & Luo, Z. (2017). Lignocellulosic biomass pyrolysis mechanism: A state-of-the-art review. *Progress in Energy and Combustion Science*, *62*, 33–86. *https://doi.org/10.1016/j.pecs.2017.05.004*

Wang, W., Qi, Y., Meng, H., Han, W., Li, J., & Zhang, J. (2018). Catalytic liquefaction of municipal sewage sludge over transition metal catalysts in ethanol-water co-solvent. *Bioresource Technology*, *249*, 361–367. *https://doi.org/10.1016/j.biortech.2017.09.205*

Wang, W., Xu, Y., Wang, X., Zhang, B., Tian, W., & Zhang, J. (2018). Hydrothermal liquefaction of microalgae over transition metal supported TiO2 catalyst. *Bioresource Technology*, *250*, 474–480. *https://doi.org/10.1016/j.biortech.2017.11.051*

Wu, S., Liu, F., Huang, S., Wu, Y., & Gao, J. (2017). Direct n -hexane extraction of wet sewage sludge at thermal and pressurized conditions: A preliminary investigation on its process and product characteristics. *Fuel Processing Technology*, *156*, 90–97. *https://doi.org/10.1016/j.fuproc.2016.07.020*

Xia, Q., Chen, Z., Shao, Y., Gong, X., Wang, H., Liu, X., Parker, S. F., Han, X., Yang, S., & Wang, Y. (2016). Direct hydrodeoxygenation of raw woody biomass into liquid alkanes. *Nature Communications*, *7*(1). *https://doi.org/10.1038/ncomms11162*

Xu, B., & Lin, B. (2023). Assessing the green energy development in China and its carbon reduction effect: Using a quantile approach. *Energy Economics*, 106967. https://doi.org/10.1016/j.eneco.2023.106967

Xu, D., Lin, G., Liu, L., Wang, Y., Jing, Z., & Wang, S. (2018). Comprehensive evaluation on product characteristics of fast hydrothermal liquefaction of sewage sludge at different temperatures. *Energy*, *159*, 686–695. *https://doi.org/10.1016/j.energy.2018.06.191*

Xu, F., Xie, Y., Zhou, D. (2022). Air pollution's impact on the settlement intention of domestic migrants: evidence from China. *Environ. Impact Assess. Rev.,* 95,106761. https://doi.org/10.1016/j.eiar.2022.106761

Yaduvanshi, A., Nkemelang, T., Bendapudi, R., & New, M. (2021). Temperature and rainfall extremes change under current and future global warming levels across Indian climate zones. *Weather and Climate Extremes*, *31*, 100291. *https://doi.org/10.1016/j.wace.2020.100291*

Yesilyurt, M., Ozcan, H., Yavasoglu, H. (2023). Co-simulation-based conventional exergy evaluation of a hybrid energy generation-vanadium redox flow battery-air source heat pump System. *Energy*, 281, 128301. *https://doi.org/10.1016/j.energy.2023.128301*

Yu, J., Lin, X., Huang, J., Ye, W., Lan, Q., Du, Sh., Liu, Z., Wu, Y., Zhao, Z., Xu, X., Yang, G., Changotra, R., Hu, Y., Wu, Y., Yan, Ch., Yang, J., He, Q. (2023). Recent advances in the production processes of hydrothermal liquefaction biocrude and aid-in investigation techniques. Renewable Energy, 218, 119348, *https://doi.org/10.1016/j.renene.2023.119348*

Zang, X., Li, H., Wang, Sh. (2023). Optimal design of energy-flexible distributed energy systems and the impacts of energy storage specifications under evolving time-of-use tariff in cooling-dominated regions. Journal of Energy Storage, 72, 108462. *https://doi.org/10.1016/j.est.2023.108462*

2

Conversion of high lípids and carbohydrates content municipal primary sludge by hydrothermal liquefaction

ABSTRACT

WWTPs problem is the continuous production of huge amount of sludge contributing to human, health and environmental concerns. Hydrothermal liquefaction is a process that converts wet biomass into biocrude, biochar, aqueous phase and vented gas at high conditions. This study assessed the valorisation of primary sludge through HTL and the influence of temperature on the product distribution. The experiments were conducted at different temperatures, 30 minreaction time, and 100 rpm stirring rate. The maximum yield of biocrude produced was 39.47% at 270°C. In all cases, the quality of products obtained were better than that of the original feedstock.

873

874

875 **1. Introduction**

876 Population growth, consumption of groundwater reserves, agricultural and industrial activities,
877 climate change, all together promotes the increase of water usage. This high consumption
878 implies alarming levels of gap between the demand and the supply, causing a risk to human
879 existence in some parts of the world (Shannag et al., 2021). For the moment, one-third of the
880 EU countries undergo a water stress all over the year because of climate change (Truchado et
881 al., 2021). Therefore, an extensive water plan and wastewater management layouts are
882 absolutely needed to decrease that gap in a simple and efficient way. Municipal wastewater
883 treatment plants have the power to treat the wastewater and bring it to a standard, then, treated
884 water can be securely discharged into receivers, land or managed for reuse (Marcal et al., 2021).
885 However, the obstacle that is continuously faced by the wastewater treatment plants is the
886 production of a by-product, called sewage sludge. It is a biomass composed of microorganisms,
887 lipids, carbohydrates, proteins, toxic compounds, heavy metals, and organic contaminants (Gao
888 et al., 2021). Following mechanical treatment (grit and screen removal), the wastewater is
889 treated by primary clarification, aeration, and secondary clarification. The sludge produced
890 from primary and secondary treatments is usually passed through the anaerobic digester where
891 organic materials are stabilized (Senfter et al., 2021). The production of sludge has reached
892 11.5 million tons (dry matter basis) in the countries of the European community and, it is
893 expected to increase to 13.0 million tons in 2020 (Thomsen et al., 2020). The common ways
894 for sludge disposal are the followings: landfilling, land disposal, land application and
895 incineration. 4.75 million dry metric tons of municipal sewage sludge were produced in the
896 U.S.A. in 2019. Among this huge amount produced, only 52 % was employed in land
897 applications, whereas the rest was disposed of through landfilling (22%), incineration (16%)
898 and other management applications (10%) (US EPA, 2021). Nevertheless, the environmental

problems resulted from these routes, promoted the management of sludge, and made its reuse an important interest (Thomsen et al., 2020; ~~Hodaei et al., 2021~~). The use of wastewater sludge has become a domain of advancing research and investment around the world (Biller et al., 2018). The management of sludge resulting from water treatment is both a challenge and an opportunity for the economic sustainability of wastewater treatment plants. Anaerobic digestion is capable of stabilizing biodegradable organic substances contained in sludge, but cannot recover much of the chemical energy present in sludge. Then, other processes are needed to solve this environmental problem (Cabrera et al., 2023).

The continuous availability, the presence of organic matter (lipids, proteins, carbohydrates and lignin), its high calorific value, make the municipal sludge to be seen as a sustainable feedstock for any thermochemical conversion process (Rahman et al., 2021; Hao et al., 2023). Among the sustainable thermochemical technologies, hydrothermal liquefaction has been considered as a transpiring technique to convert biomass into bioenergy (Liu et al. 2022).

Hydrothermal liquefaction (HTL) is a thermochemical depolymerization approach that converts organics contained in wet biomass, into high-valuable products (~~Edifor et al., 2021~~) (De Aguiar Do Couto et al. 2018). In the hydrothermal liquefaction, the high amount of water plays one of the principal roles, because the water contained in the sludge is the reaction medium and catalyses the process. HTL process is a suitable option for handling high moisture content solids where water is used as the medium for breaking down the organic matter into nearly simpler chemicals at high temperatures and pressures (Wu et al. 2022). Usually, hydrothermal liquefaction operates at a temperature ranging from 280 to 400°C and under pressure from 10 to 25 MPa (Rahman et al., 2021). These operating conditions are the cause of the role of water. In the region near the critical point, water acts as a non-polar solvent, being an extremely effective reaction medium for organics. The other benefits of the hydrothermal

liquefaction are high conversion, high separation, and energy efficiency. The sludge is principally converted into biocrude (main product) and three by-products, namely, biochar, aqueous phase, and biogas. HTL has proven that it is a valorising process able to produce energetically dense biocrude oils from wet feedstocks without any previous removal of water (Haider et al., 2023). As the drying step of the sludge can be skipped during HTL process, this contributes to important cost savings, considering the high moisture content of sludge, between 95 and 98% (Guo et al., 2022). The biocrude is deep dark brown, close to black, and has a high viscosity like bitumen or distillation vacuum residue. On the other hand, biocrude has in its composition a high content of heteroatoms, like oxygen or nitrogen. This fact is common in biocrudes from almost all types of feedstocks treated by hydrothermal liquefaction (Castello et al. 2019). Recent studies have been focused on the hydrothermal liquefaction of mainly digested sludge and activated sludge. For example, the highest conversion to biocrude reached from municipal secondary sludge was 18.25% (dry basis), and 26.75% (dry basis) after HCl pre-treatment, at a temperature of 300ºC and a time of reaction of 30 min (Liu et al., 2018). In the case of municipal digested sludge, the highest conversion to biocrude was 41.6% (volatile solids basis) working with ethylene environment and without any catalyst, while in an inert environment (nitrogen), the conversion was 37.1% (volatile solids basis) also without catalyst, both at a temperature of 350ºC and a time of reaction of 60 min (Rahman et al., 2021). All these results are obtained at optimum operating conditions, specifically, temperature and of reaction time. These parameters are responsible of the quality and quantity of the products. Some studies concluded that low temperature and short time promotes the formation of heavy biocrude (Liu et al., 2018). Biocrude and by-products yields are distributed differently depending on the temperature. The reaction temperature is one of the parameters that have a significant influence on HTL products distribution (Rahman et al., 2021). The yield of biocrude

947 increases progressively with the increase of temperature until reaching a maximum value.
948 When this value is exceeded, the excessive temperature provokes the cracking of the biocrude
949 phase into gaseous products and the formation of high molecules by additional re-
950 polymerisation (Li et al., 2018). The quality of biocrude and the gas yield are improved with
951 the increase of temperature, whereas the yields of solid and water-soluble substance and the
952 total organic carbon content in the aqueous phase have been decreased. The maximum biocrude
953 yield was obtained at 340°C with a value of 22.9 wt. % (TS basis) (Xu et al., 2018). Primary
954 sludge is obtained using the mechanical wastewater treatment process. It is a thick fluid, grey
955 in colour, slimy and with highly ghastly odours. Primary sludge is drawn at solids
956 concentrations of 2-6 % out of which 55 to 70 % are organic (Biller et al., 2018). It has more
957 than 40% of proteins and carbohydrates (Wang et al., 2021). HTL doesn't only convert lipid,
958 but also proteins and carbohydrates, contributing to high biocrude yield (De Aguiar Do Couto
959 et al. 2018). In one study, primary sludge containing 11.9% of TS was converted to 39.8 %
960 (VS basis) at 339 °C (Snowden-Swan et al., 2016). In another one, 37.3% (VS basis) was
961 obtained from primary sludge comprising 11.9% of TS at 347°C (Marrone et al., 2018).
962 The aim of this work is to produce biocrude from municipal primary sludge through HTL. The
963 utilization of primary sludge in this process has a great interest in waste management
964 approaches. The work will focus on the influence of the temperature on the product
965 distribution. Beside this, the objective of the work is to attain a complete mass balance. Finally,
966 biocrude is upgraded by separation into two phases: light and heavy oil. This full
967 characterization will allow to define several routes to valorise the products, as a perfect
968 example of circular economy.
969

970 ## 2. Materials and methods

971 ### 2.1. Reagents

972 Dichloromethane 99.9 % (ref.: 32222), Toluene 99.7 % (ref.: 32249) and 2-Propanol 99.9 %
973 (ref.: 59300) were purchased from Honeywell. Methanol (ref.: 412722), HPLC-GOLD-
974 Ultragradient grade, was brought from Carlo Erba reagents. n-Hexane 95 % (ref.: 363242),
975 high performance chromatography grade, and phenol crystalline (ref: 144852.1211) and n-
976 heptane (ref.: 162062.1611) were provided by PanReacAppliChem. Sulfuric acid reagent (ref:
977 34632), orange reagent (ref: 131130.1612), sulfuric acid 95.0–97.0 % (ref: 30743), bovine
978 serum albumin (BSA) (ref: A9647), sodium hydroxide 98 % (ref: 30620), sodium carbonate
979 (ref: 222321), potassium sodium tartrate tetrahydrate (ref: 217255), copper (II) sulphate
980 pentahydrate (ref: 209198), Folin&Ciocalteu's phenol reagent (ref: F9252), magnesium
981 sulphate monohydrate (ref: 434183), anhydrous sodium sulphate (ref: 239313) and fuming
982 hydrochloric acid (ref: 84418), high analytical reagent grade, were supplied by Sigma -
983 Aldrich.
984

985 ### 2.2. Primary sludge collection and managing

986 Samples of primary sludge were provided by the municipal wastewater treatment plant of Reus
987 in Tarragona, Spain. 500 mL bottles of primary sludge were sampled after partial gravity
988 thickening of the primary treatment. They were stored in a freezer at -15°C and defrosted in an
989 oven at 60°C for 5 hours. The bottles of primary sludge were used directly as received.
990

991 ### 2.3. Characterization of primary sludge

992 Figure 1 shows the analytical techniques performed to fully characterise the primary sludge.
993 The characterisation of primary sludge was carried out in triplicate. Total solids (TS), volatile

994 solids (VS) and ash content were measured according to standard methods 2540B and 2540E
995 respectively (Rice et al., 2012). The extraction of lipids was achieved in a Soxhlet apparatus
996 using hexane as a solvent, according to standard method 5520E (Rice et al., 2012). Total
997 carbohydrates percentage was determined by phenol-sulfuric acid Dubois method (Dubois et
998 al., 1956). Shortly, 0.05 mL of 80% phenol solution was added to 2 mL of diluted sludge sample
999 in a glass tube. Then, 5 mL concentrated sulfuric acid was quickly added. The tubes were kept
1000 under room temperature for 10 min and then placed into a thermostatic bath at 30°C another
1001 15 min. The absorbance was measured at 480 nm. Proteins content was determined with Lowry
1002 method (Lowry et al., 1951). The proteins solubilization in the sludge samples was carried out
1003 by heating the samples with 2 M sodium hydroxide at 100°C for 10 min. The absorbance was
1004 measured at 750 nm. Finally, ultimate analysis was realized by Serveis Técnics de Recerca at
1005 Universitat de Girona. Analysis was performed using an ultimate analyser (Perkin Elmer model
1006 EA2400). C, H and N were determined, and O was calculated by difference. A field emission
1007 of variable pressure environmental scanning electron microscopy (ESEM) with X-ray
1008 microanalysis (Quanta 600, FEI Company), characterised by a high resolution (3 nm) was
1009 utilized to detect heavy metals of primary sludge.
1010

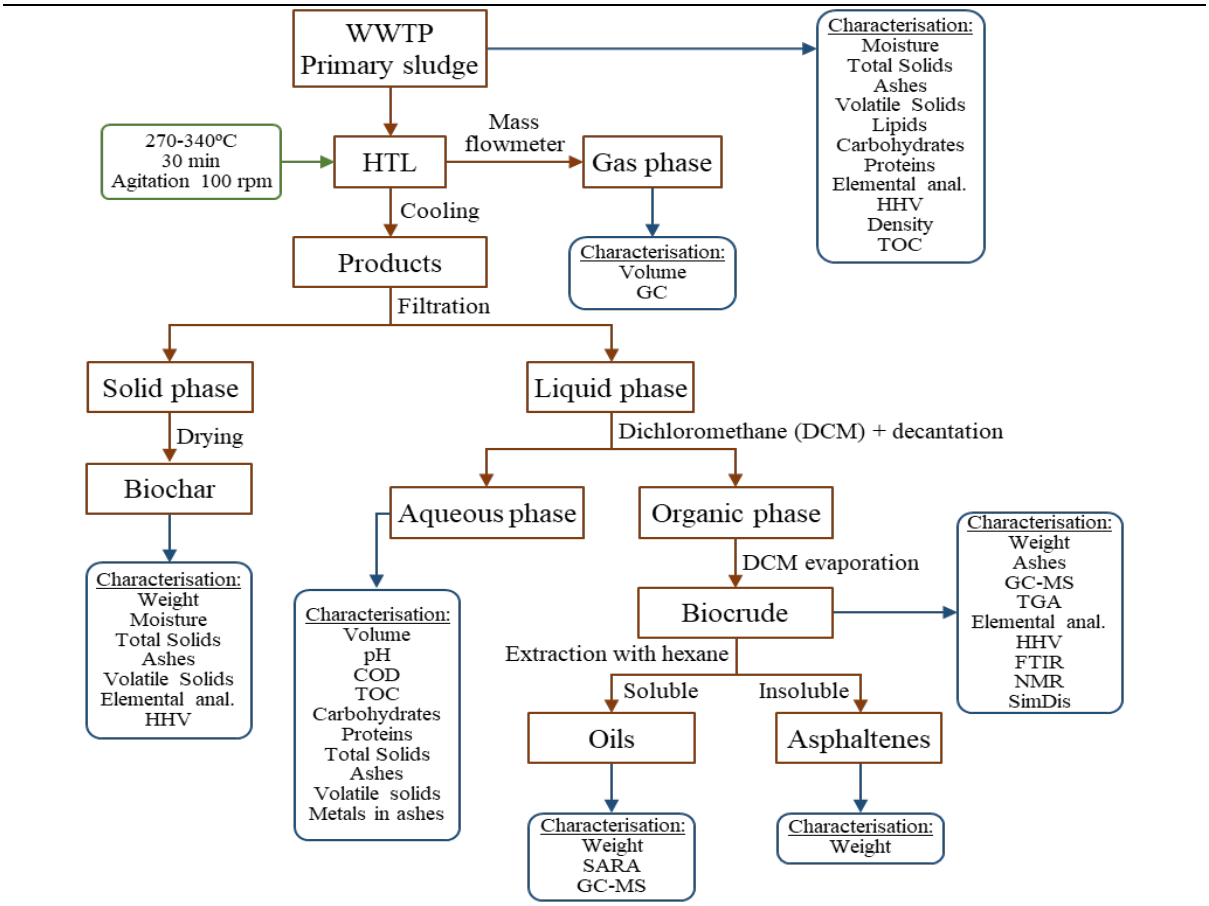

Figure 1. Separation methodology of products of HTL of primary sludge.

2.4. Hydrothermal liquefaction of primary sludge

The experiments were performed in a 1 L Stainless Steel Autoclave (Autoclave Engineers model EZE Seal) encountered by a movable heating shell, a fixed MagneDrive® stirrer (magnetically coupled, packless rotary impeller system) and an operating condition controller. The reactor is connected to a gas line through an inlet valve allowing the introduction of nitrogen. The outlet valve is linked to a gas flow meter and a Tedlar bag push lock valve 0.6 L (Superlco 30289-U) for gas collection. A bottle containing exactly approximately 500 g of primary sludge was emptied in the reactor. Pure nitrogen gas was purged three times to create

an oxygen-free atmosphere and then pressurized up to 1 bar as an initial pressure. HTL experiments were achieved at five different temperatures and their corresponding pressures: 240°C (~33.7 bar), 270°C (~55.6 bar), 300°C (~86.9 bar), 320°C (~114.0 bar) and 340°C (~146.8 bar). Reaction time after attaining desired temperature was always 30 min and continuous agitation of 100 rpm. The pressure of the reaction was not controlled and maintained as auto generated with respect to its reaction temperature. The heating up time was recorded based on the selected temperature, ranging between 1 hour and 3 hours. After achievement of each batch experiment, the reactor was cooled down in a room temperature water bath (~25°C) until going back to its initial condition.

2.5. Cleaning of the reactor and separation of products

Figure 1, also presents the schematic diagram of the experimental separation procedures after hydrothermal liquefaction of primary sludge. The products obtained are distributed into 4 different phases: gas, organic, aqueous, and solid. When the reactor was back to atmospheric pressure and laboratory ambient temperature, the gas phase was released. The output gas was passed through a flow meter, indicating the volume of the gas mixture, and collected in a gas bag. After that, the reactor was opened, and the mixture was poured into a large beaker. The solid part was separated from the liquid part via vacuum filtration. The liquid part, mainly containing the aqueous phase and a small part of the organic phase, was transferred into a bottle. Meanwhile, the reactor was washed repeatedly with dichloromethane until being totally clean to recover the organic remaining part, deposited on the walls, on the cover of the reactor and, in the agitation module. Then the mixture, where a part of solids was entrapped into the organics, was separated by vacuum filtration. The liquid part containing the organic phase and the dichloromethane was transferred into another bottle. The solid retained on the filter paper,

biochar, and ashes, was washed with dichloromethane several times. The biochar was dried in the oven for 24 hours at 105ºC and quantified by weighting. A small volume of dichloromethane was added to the aqueous phase. Then, the mixture was centrifuged at 8000 rpm for 5 minutes. The upper phase is the dichloromethane containing the small part of organic phase. This was added to the organic phase previously separated. The lower phase is the aqueous phase containing soluble organic molecules. Dichloromethane was evaporated from the organic phase by the rotary evaporation, at 65ºC and atmospheric pressure. The viscous organic liquid obtained is the biocrude, that it was further weighted for quantification. Finally, biocrude was separated into oils and asphaltenes by Soxhlet extraction using 200 mL of hexane. Oils were separated from hexane by rotary evaporation at 65ºC and atmospheric pressure. Asphaltenes were quantified by the difference between biocrude and oils. The biocrude yield was calculated from equation (1):

$$\text{Biocrude yield (\%)} = \frac{\text{Mass of biocrude}}{\text{Mass of volatile solids}} \times 100 \quad (1)$$

The aqueous phase yield was calculated from equation (2):

$$\text{Aqueous phase yield (\%)} = \frac{\text{Mass of solids dissolved in aqueous phase}}{\text{Mass of volatile solids}} \times 100 \quad (2)$$

The solid yield was calculated from equation (3):

$$\text{Solid yield (\%)} = \frac{\text{Mass of solid residue}}{\text{Mass of volatile solids}} \times 100 \quad (3)$$

The gas yield was calculated from equation (4):

$$\text{Gas yield (\%)} = \frac{\text{Mass of gas}}{\text{Mass of volatile solids}} \times 100 \quad (4)$$

In all the equations, mass of volatile solids is referred to that of primary sludge.

2.6. Biocrude characterization and quantification

Figure 1 again, shows the characterisation performed with the biocrude, which was very extensive: weight, ashes, gas chromatography/mass spectrometry (GC/MS), thermogravimetric analysis (TGA), elemental (ultimate) analysis, determination of higher heating value (HHV), Fourier transform infrared spectroscopy (FTIR), nuclear magnetic resonance (NMR) and simulated distillation (SimDis). Finally, saturated, aromatics, resins and asphaltenes (SARA) fractions of biocrude were characterised.

2.6.1. Gas chromatography/mass spectrometry spectroscopy of biocrude

The samples of biocrude at all temperatures were characterized by gas chromatography-mass spectroscopy (GC/MS) using a Perkin Elmer Turbo Mass Gold GC/MS, equipped with a Supelco SLB®-5ms capillary GC column (L × I.D. 30 m × 0.25 mm, d_f 0.25 μm). Dichloromethane was used as solvent. The GC oven was maintained at 70ºC for 1 min, heated to 180ºC at a rate of 7ºC/min, then heated to 240ºC at a rate of 12ºC/min and finally 7 min hold at 330ºC.

2.6.2. Thermogravimetric analysis of biocrude

The weight loss properties of biocrudes were studied by thermogravimetric analysis (TGA). In each test, about 3 to 4 mg of sample was heated from 30°C to 800°C at a nitrogen flow of 60 mL/min and a 10 K/min heating rate ~~(Zhu et al., 2022).~~

2.6.3. Elemental analysis and HHV of biocrude

Ultimate analysis of biocrude samples was also realized by Serveis Técnics de Recerca at Universitat de Girona as commented in section 2.2. C, H and N were quantified, and O calculated by difference. Then, the higher heating values of (HHVs) of biocrude were

calculated using Dulong formula (5), taken from Hong's study, where HHV is expressed in MJ/kg (Hong et al., 2021):

$$\mathrm{HHV}\ (\%) = 0.3383 \cdot \mathrm{C} + 1.443 \cdot \left(\mathrm{H} - \frac{\mathrm{O}}{8}\right) \quad (5)$$

C, H and O are the mass percentages of carbon, hydrogen, and oxygen from the ultimate analysis of the samples, respectively.

2.6.4. FTIR of biocrude

FTIR spectra were collected using a Thermo Nicolet Nexus 670 Fourier Transform Infrared Spectrophotometer equipped with a single-bounce diamond attenuated total reflectance (ATR) accessory (Specac Golden Gate) and KBr beam splitter. Spectra were collected from 4000 to 500 cm^{-1} with 0.98-cm^{-1} resolution and averaged over 50 replicate scans using Omnic software. Background scans were conducted of the dry accessory at ambient temperature. The spectra were then collected after smearing about 30 mg of sample directly on the ATR crystal surface.

2.6.5. ^{1}H NMR of biocrude

^{1}H NMR spectra were collected using a Varian Unity 400-MHz spectrometer outfitted with a 5-mm broadband probe. 50–75 mg of biocrude were dissolved in deuterated chloroform containing 0.03% tetramethylsilane (TMS) as an internal reference. Samples were then filtered (0.22-lm PTFE) to remove any suspended particulates before loading into 5 mm diameter NMR tubes. ^{1}H spectra were acquired with a 90^{o} pulse angle, spinner frequency of 20 Hz, sweep width of 8000 Hz across 32 transients.

2.6.6. Simulated distillation of biocrude

Simulated distillations were modeled after ASTM-D2887 method and performed using a HP 5890 Series II FID gas chromato-graph and a Durabond DB-HT-SimDis GC column by Agilent-J&WScientific (5 m0.53 mm id, 0.15µm film). Helium (56.4 mL/min) was used as the carrier gas. The oven temperature was initially set to 36°C, and raised to 400°C at 10°C/min and then held constant for 10 min. The injector volume was set to 0.5 µL and the injector temperature was set to 350ºC. Detector temperature was set to 375°C, hydrogen gas set to 40 ml/min, airflow set to 400 ml/min, and helium makeup set to 24 ml/min. Samples (1% w/w) and reference standards (0.5% w/w) were dissolved in DCM. Samples were filtered (0.22 µm PTFE) to remove any suspended particulates. Boiling points were determined in accordance to a D2887 calibration mix and a D2887 Reference Gas Oil standard, both purchased from sigma Aldrich. Data (retention time and areas) were collected. Each sample was distributed between fractions (%wt) and boiling points were calculated accordingly.

2.6.7. Gas chromatography/mass spectroscopy of oils separated from biocrude

Oils were also characterized by gas chromatography-mass spectroscopy (GC/MS). The same procedure than for biocrude was used (see section 2.6.1.), but hexane was utilized as solvent.

2.6.8. Quantification of SARA fractions of biocrude

SARA fractions of biocrude were analysed. The separation of light phase and heavy phase was repeated as mentioned above, but with n-heptane. The separated maltenes were fractionated into saturated hydrocarbons with 20 mL of n-heptane using activated alumina in a glass chromatographic column. Then, aromatic compounds were extracted through 20 mL of toluene. Finally, resins were removed from the adsorbent using 20 mL of a mixture of toluene

and 2-propanol (1:1). More polars were also removed using 20 ml of methanol. Each eluted fraction was recovered by solvent removal using a Rotary evaporator.

2.7. Biochar characterization and quantification

Figure 1 too, presents the characterisation performed with the biochar. Total solids, moisture content, volatile solids and ash content were determined in biochar according to standard methods 2540B and 2540E respectively (Rice et al., 2012). Also, ultimate analysis and heavy metals detection were done by following the same procedures described above.

2.8. Aqueous phase characterization

Figure 1 as well, shows the characterisation performed with the aqueous phase. COD, TOC, TN, proteins, and carbohydrates were measured or analysed for the aqueous phase. COD analysis was performed according to standard method 5220D (Rice et al., 2012). TOC was analysed by using a TOC analyser TOC-L Series based on a specific standard calibration curve. Total organic carbon (TOC) was measured by ASI-L auto sampler Shimadzu into a Shimazdu TOC-L CSN TOC analyser provided with a NDIR detector and calibrated with standard solutions of hydrogen potassium phthalate. Total dissolved nitrogen was measured in the same TOC analyser coupled with TNM-L ROHS unit (Ponces-Robles et al., 2018). Protein amount was measured according to Lowry method (Lowry et al., 1951) and carbohydrates were quantified following Dubois method (Dubois et al., 1956) as described in the previous section (2.3). Total solid (TS), volatile solid (VS) and ash content were measured in the aqueous phase as well. A specific volume of aqueous phase was dried in a weighted crucible for 24 hours in the oven at 100ºC then burned in the furnace at 550ºC for 1 hour, as detailed by the standard methods 2540B and 2540E respectively (Rice et al., 2012). Measurement of pH value in the

HTL aqueous phase was performed by pH meter. Heavy metals were analysed in the ash of the solid dissolved in the aqueous phase by following the same procedure mentioned before.

2.9. Gas phase characterization

Figure 1 likewise, shows the characterisation performed with the gas phase. Identification and quantification of biogas were finalized by a gas chromatograph (micro-GC, Agilent, 990) equipped with a thermal conductivity detector (TCD). A MS5A SS 10MX0.25MMX30UM BF RTS, CP-PORABOND Q 5MX0.25MMX3UM column (column 1) was used to separate the light gases using Argon as a carrier gas and a PORAPLOT Q UM 10MX0.25MMX8UM BF, CP-PORABOND Q 1MX0.25MMX3UM column (column 2) was used to separate heavy gases using helium as a carrier gas. Column 1 was maintained at injector temperature 100ºC, injection time 40 ms, column temperature 100ºC and initial pressure 200 kPa. Column 2 was maintained at injector temperature 100ºC, injection time 40 ms, column temperature 60ºC and initial pressure 150 kPa. The run time was 120 s. The mole percentage of each gas was determined with respect to gas standards prepared by Carburos Metálicos, S.A.

3. Results and discussion

3.1. Characterization of primary sludge and suitability of its use in HTL

The characterisation of primary sludge is outlined in Table 1. As it can be seen in the table, the primary sludge, as received, contained 4.3 ± 0.1% of total solids (w/w wet sludge basis). The moisture, calculated by difference, accounted to 95.7 ± 0.1% (w/w wet sludge basis). These values are close to the obtained in other studies of the research group with primary sludge from the WWTP of Reus (Tarragona, Spain): 4.2 ± 1.2% (Olkiewicz et al., 2015) or 3.9 ± 0.1% (Glinska et al., 2020). Ashes were 22.9 ± 0.3% (w/w total solids basis) of the total solids. Then,

volatile solids were calculated by difference from ashes, 77.1 ± 0.3% (w/w total solids basis). On the other hand, the density of primary sludge was 1.012 g/mL, comparable to that of water. The volatile solids were analysed for carbohydrates, proteins, and lipids contents. Carbohydrates was found to be the predominant fraction (29.84%). Indeed, the values of lipids (oil, greases, fats, and long fatty acids) (23.41%) and proteins (21.15%) were considered significant. These results are comparable with those obtained in previous studies with the primary sludge of the same origin: lipids (19.6 ± 0.6%), carbohydrates (31.3 ± 0.1%), proteins (27.7 ± 0.1%) and ashes (16.0 ± 0.1%), values obtained in a study of recovery of cellulose from primary sludge (Glinska et al., 2020) or, lipids (27.2 ± 0.4%), carbohydrates (26.2 ± 2.6%), proteins (24.2 ± 1.4%) and ashes (20.1 ± 0.4%), results from a primary sludge used to produce biodiesel. One of the characteristics in the total solids of the primary sludge of the Reus WWTP is the similar composition of the ingredients, all always between 20 and 30% in w/w total solids basis.

The ultimate analysis gave the following results: primary sludge had low nitrogen content (3.71%), low hydrogen content (5.34%), high carbon content (36.86%) and finally, a very high oxygen content (31.19%), this last one, obtained by difference. These values allowed to calculate the higher heating value (HHV) of dried primary sludge. In the calculation, the mass of the ashes has been discounted to obtain a more realistic value. In these conditions the HHV was 14.55 MJ/kg. This value is comparable with that obtained in other works: 10.55 MJ/kg (Kulikova et al., 2022) or 17.31 MJ/kg (Adedeji et al., 2022).

Table 1. Characterization of primary sludge from WWTP of Reus.

Feedstock characterization	**Percentage %**
Moisture content (w/w wet sludge basis) *	95.7 ± 0.1

Total solids (w/w wet sludge basis) *	4.3 ± 0.1
Volatile solids (w/w total solids basis) *	77.1 ± 0.3
Ashes in total solids (w/w total solids basis) *	22.9 ± 0.3
Proteins in volatile solids (w/w total solids basis) *	21.2 ± 1.7
Carbohydrates in volatile solids (w/w total solids basis) *	29.8 ± 1.2
Lipids in volatile solids (w/w total solids basis) *	23.4 ± 0.8
C	36.86
H	5.34
N	3.71
O [#]	31.19
Density of wet sludge (g/mL)	1.01
TOC in wet sludge (mg/L)	6290
HHV of wet sludge (MJ/kg)	14.55
Mass balance (Ashes + Proteins + Carbohydrates + Lipids) *	97.3 ± 4.0

* Average of at least three assays

[#] By difference

1207

1208

1209 SEM images and EDX spectra of ash in primary sludge are presented in Figure SM1
1210 (supplementary material). SEM images show that the ashes have an irregular structure. The
1211 particles have different size and are irregular. It seems that the bigger particles are formed by
1212 aggregation of smaller ones. The image magnified 6000 times (location (c)) shows asymmetric
1213 cavities and a surface full of granules. In the case of metals contained in the ashes, EDX spectra

identified in average: O (41.2%), Ca (17.1%), Fe (13.4%), Si (7.0%), P (5.3%), Al (4.3%), S (2.9%), Cl (1.7%), Na (1.6%), K (1.3%), Mg (1.2%) and Ti (0.7%). The origin of these oxides should be the drinking water that has high calcium content, the dust dragged by rainwater and the erosion caused in the sewage system.

Concerning the suitability to use primary sludge in HTL process, the value of total solids in the primary sludge is low, 4.3% (w/w wet sludge basis). This value is consistent with the values obtained in other works, which usually vary between 1 and 5%, such as 5.0% (Biller at al., 2018) or 4.5% (Marrone et al., 2018). This means that the water content present in the sludge is very high. As it was commented in introduction, HTL process is a very good option to treat wet biomass, where water is used as the medium for breaking down the organic matter.

Lipids in primary sludge are formed from free fatty acids in the range of C10 to C18 which are precursors for esters production. Also, proteins are approved to be promoters for biocrude production through HTL. Maillard reactions represent an important part in the distribution of biocrude and composition, originated from the reaction of amine groups present in proteins with carbonyl groups present in reducing carbohydrates (Fan et al., 2021). WWTP primary sludge is rich in lipids, proteins and carbohydrates. Therefore, HTL is assumed to be a suitable option for thermally hydrolysing the macromolecules into valuable chemicals. Then, primary sludge assists in demonstrating an economically viable and energy-efficient sludge biorefinery approach.

3.2. Hydrothermal liquefaction of primary sludge

HTL experiments of primary sludge, sample around 500 g, were always performed at a reaction time of 30 minutes and a stirring rate of 100 rpm. Five different operating temperatures were utilised: 240, 270, 300, 320 and 340ºC. After the completion of the reaction time, the reactor

was cooled down to ambient conditions and the four products (gaseous phase, biocrude, containing organics aqueous phase and biochar) were separated following experimental procedure depicted in Figure 1. The quantification and characterization of the products obtained during the HTL of the sludge will be presented in the different sections presented below.

3.3. Conversion of primary sludge to biocrude

3.3.1. Results

The biocrude yields from primary sludge HTL at different temperatures are illustrated in Table 2. Obviously, the most interesting phase produced during HTL is the biocrude. Overall, the biocrude yield initially increased and then decreased with temperature increasing from 270 to 340ºC. The maximum value was obtained at 270ºC, 39.47% (w/w_{VS}). This value is consistent with other works, where a close value of 42.20% (w/w_{VS}) was obtained in the HTL of primary sludge at 330ºC for 10 min (Madsen et al., 2019), and comparable to that obtained with HTL of municipal sludge, 34.00% (w/w_{VS}), at 325ºC for 30 min (Prestigiacomo et al., 2020).

A slight drop, ~2.0% (w/w_{VS}), from 300ºC to 340ºC should be caused by gas formation through biocrude conversion. Similarly, temperature also has a critical effect on the distribution of biocrude between oils and asphaltenes. Herein, the maximum value of oils, 23.96% (w/w_{VS}), was reached at 300ºC. At 320ºC, oils yield has faced a sharp decrease to 21.24% (w/w_{VS}). The results obtained confirm the significant effect of temperature on the biocrude yield. In other words, an important biocrude yield is supported by a high reaction temperature (Mishra et al. 2020, Thomsen et al. 2020, Zhang et al. 2021). As mentioned elsewhere, higher temperature could boost the energy needed to break the bonds that strengthen hydrolysis and depolymerization of high-volatile biomass (carbohydrates, proteins, and lipids) (Liu et al.

2022). Nevertheless, an increase in temperature over the optimal limit develops a thermal cracking of biocrude that reduce the biocrude yield and promotes the formation of coke and water-soluble gas products (Li et al., 2018). This was validated by the decrease of biocrude yield when the temperature became higher than 270ºC.

Table 2. Biocrude, oils and asphaltenes yields after HTL experiment, 30 min of reaction time and 100 rpm stirring rate.

	Biocrude		Oils *		Asphaltenes *	
T (ºC)	Weight (g)	(%)	Weight (g)	(%)	Weight (g)	(%)
240	5.86 ± 0.35	35.17 ± 2.03	3.47 ± 0.68	22.67 ± 0.80	2.10 ± 0.52	12.50 ± 0.47
270	6.66 ± 0.12	39.47 ± 0.74	4.02 ± 0.06	23.87 ± 0.40	2.64 ± 0.18	15.60 ± 0.34
300	6.29 ± 0.13	37.66 ± 0.66	4.08 ± 0.16	23.96 ± 0.71	2.21 ± 0.26	13.70 ± 1.63
320	6.11 ± 0.20	37.42 ± 0.33	3.69 ± 0.32	21.24 ± 0.89	2.42 ± 0.51	16.18 ± 1.34
340	5.82 ± 0.15	34.97 ± 0.28	2.92 ± 0.22	17.47 ± 0.92	2.89 ± 0.22	17.50 ± 0.60

* Oils and asphaltenes were obtained from biocrude by separation with hexane

3.3.2. Ultimate analysis and HHV of biocrude

The ultimate composition C, H, N and O, atomic ratios, higher heating values HHV and the energy recovery ER of biocrude are presented in Table 3. Also, the properties of petroleum are listed as well to perceive the quality of biocrude (Shah et al. 2020). The ultimate composition of biocrude was not really affected by the effect of temperature, because results are close. The percentages of C and O reacted with temperature in an opposite way. We can notice that the carbon content in biocrude kept increasing with temperature until reaching an optimum value of 76.94 % at 340 ºC. Whereas, the oxygen content was generally in decline, from 9.87% to 7.85% at 340ºC. The nitrogen content values have been quite constant and have remained within the interval 3.65-4.38%. In the same way, the hydrogen content was rather constant for the five temperatures. Values are contained in the interval 10.81-11.59%. This last value was reached at 240ºC (11.59%). With these values, HHV was always high, around 40 MJ/kg. Comparing the results obtained to the one of petroleum biocrude, the value attained at 340ºC, 40.50 MJ/kg, was very close to the value of petroleum, 42.75 MJ/kg. On the other hand, the increase of HHV with respect to the original sludge (10.40 MJ/kg) is very important, close to 300% in all cases. On the other hand, the atomic ratios H/C and O/C have been calculated. The result of these calculations allows to represent the Van Krevelen diagram (Shah et al., 2020). The diagram allows to evaluate the origin and the degree of maturity of the oil. It also allows visualizing the differences between this and other synthetic or biomass-derived fuels. Figure 2 presents the Van Krevelen diagram for primary sludge and biocrude. As can be seen in the figure, the O/C atomic ratio of biocrudes is much lower than that of primary sludge, there is a factor of one order of magnitude. This fact indicates that the transformation of primary sludge to biocrude has been carried out through dehydration and decarboxylation reactions, which allows the reduction of the O/C atomic ratio and therefore improves the stability and viscosity

of the biocrude. Also, biocrude upgrading would require less hydrogen. On the contrary, the H/C atomic ratio of the primary sludge is very similar to that of the biocrudes. But on the other hand, this ratio is still a bit low compared to that of oil. This indicates that the H/C atomic ratio has to be improved by eliminating heteroatoms, as the only way for biocrude to be used as a substitute for petroleum-derived fuels. Even these results are encouraging, there is still a huge difference between the oxygen percentages in biocrude and fossil petroleum. The high content of O makes biocrude soluble in polar solvents including methanol and acetone, but badly mergeable with fossil fuels (Zhang et al. 2021). The target of the study is to obtain an intensification of energy density in biocrude to be qualified to be used in further applications, including biofuel. Therefore, upgrading biocrude is necessary to fit with the petroleum conditions. This can be done by either the introduction of catalysts, working under hydrogen environment, by the utilisation of an organic solvent or, a combination of all.

Table 3. Ultimate analysis and HHV of biocrude, 30 min of reaction time and 100 rpm stirring rate.

Samples		% C	% H	% N	% O	H/C	O/C	HHV (MJ/kg) *	ER (%)
Primary sludge		36.72	5.38	3.58	54.31	1.76	1.11	10.40 #	---
Biocrude	240ºC	74.89	11.59	3.65	9.87	1.86	0.10	40.28	287
	270ºC	75.11	10.81	4.38	9.69	1.73	0.10	39.26	278
	300ºC	75.06	11.31	4.07	9.56	1.81	0.10	39.99	285
	320ºC	75.82	10.95	4.17	9.06	1.73	0.09	39.81	283
	340ºC	76.94	11.01	4.20	7.85	1.72	0.08	40.50	289
Petroleum @		83.0-87.0	10.0-14.0	0.1-1.0	0.1-3.0	---	---	~ 42.75	---

* Calculated with Dulong equation: $\text{HHV}\ (\%) = 0.3383 \cdot \text{C} + 1.443 \cdot \left(\text{H} - \frac{\text{O}}{8}\right)$ (Hong et al., 2021)

Dried in the oven during 24 h at 105ºC

@ Shah et al., 2020

1306

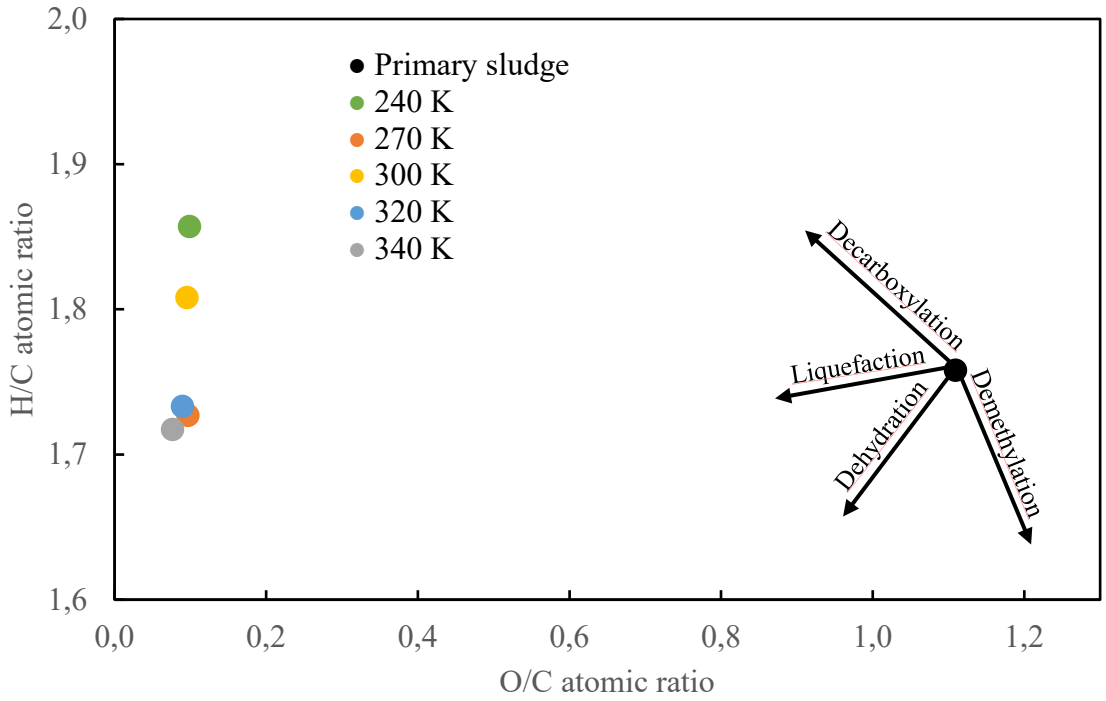

Figure 2. Van Krevelen diagram for primary sludge and biocrudes. 30 min of reaction time and 100 rpm stirring rate.

1307

1308

1309 **3.3.3. GC/MS analysis of biocrude**

1310 Usually, there are more of 300 substances identified by GC/MS in the biocrude. The main
1311 substances identified from the ingredients of sludge as lipids, protein, carbohydrate and lignin,
1312 were cyclic terpanes and terpenes, along with nitrogenous, oxygenated, and phenolic

components (Al-juboori et al., 2023). Chemical compounds of the biocrude obtained at different temperatures were identified by GC–MS analysis. The detailed compounds information of the biocrude from HTL at 300ºC are presented in Table SM1 (supplementary material). As it can be seen in the table, biocrude displayed various chemical groups. Oil compounds were mostly with chain structures and contained different number of nitrogen elements. Moreover, GC/MS results showed sufficient molecules in a cyclic form, suggesting the transform of hydrophilic molecule from sludge to the oil phase through recombination reactions (Xiao et al., 2019). On the other hand, more types of N-containing long-chain structure molecules were found in biocrude, implying the improved combination of alkane with amine generated from the deamination of the organics in the feedstock (Leng et al., 2020). Phenols were conceivably produced from the cyclization/condensation of carbohydrates resulting from cellulose and hemicellulose component (Zhao et al. 2021). The chromatogram of biocrude at 300ºC is depicted in Figure SM2 (supplementary material).

3.3.4. TGA analysis of biocrude

TGA analysis was applied to study the three stages of weight loss of the biocrude. The TGA curves of the 5 samples of biocrude from HTL of primary sludge are shown in Figure 3. All HTL biocrudes show the same TGA curve progression, with a similar *decomposition process*. A relatively significant weight loss takes place at 215.04°C in HTL-240°C with 70.52% of weight loss, 220.66 °C in HTL-270°C with 75.25 % of weight loss, 186.90°C in HTL-300°C with 74.69 % of weight loss, 237.56 °C in HTL-320°C with 81.26 % of weight loss, 232.12 °C in HTL-340°C with 76.15 % of weight loss.

(a)

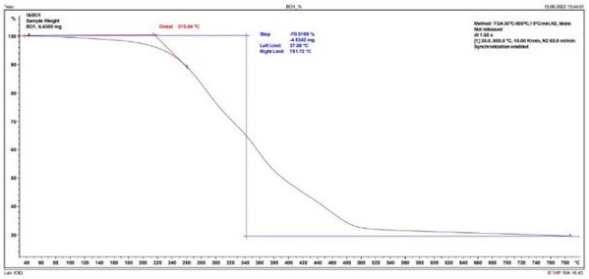

(b)

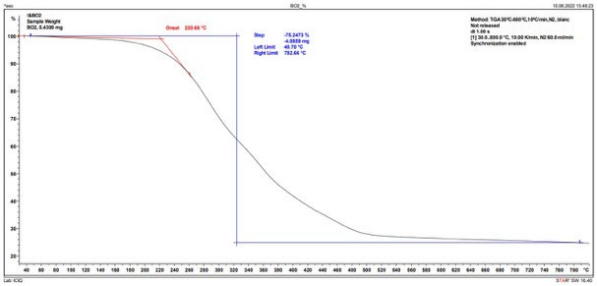

(c)

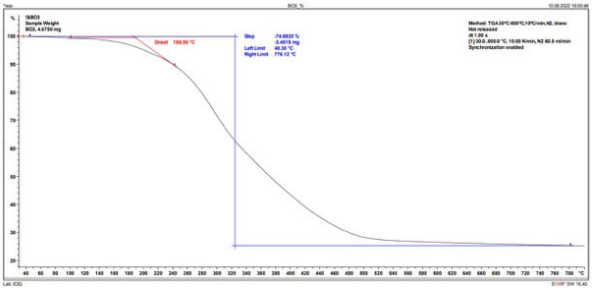

(d)

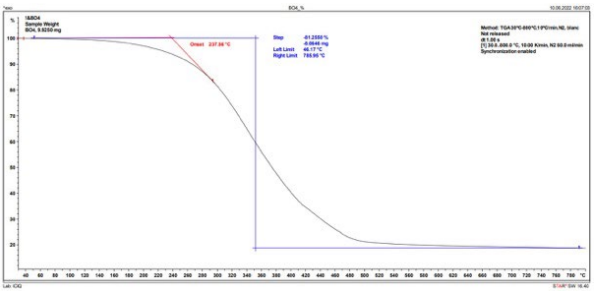

(e)

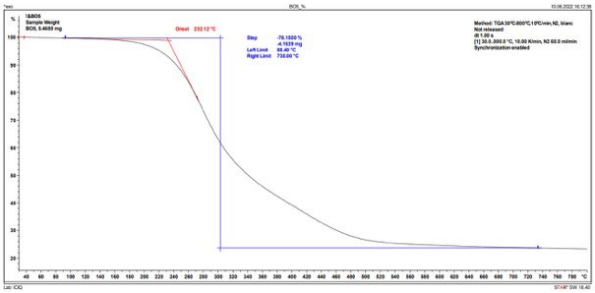

Figure 3. Thermal gravimetric analysis of samples of biocrude: (a) 240ºC; (b) 270ºC; (c) 300ºC; (d) 320ºC; (e) 340ºC. 30 min of reaction time and 100 rpm stirring rate.

3.3.5. FTIR of biocrude

FTIR spectroscopy identifies functional groups present in biocrude and allows for a more comprehensive comparison of these groups when compared to GC/MS analysis. Figure 4 shows FTIR spectra for biocrudes via hydrothermal liquefaction at 240ºC and 340ºC for the same reaction time (30 min). Confirming ultimate analysis, the high hydrogen and carbon content of HTL biocrude at both conditions produced important saturated C-H stretching with CH_2 and CH_3 bending around 2919 cm^{-1} and 2850 cm^{-1}, unsaturated stretching around 1657 cm^{-1} and aromatics around 720 cm^{-1}. Biocrude was observed with C-O stretching peaks (1035–1456 cm^{-1}) that belong to esters and phenols. C=O stretching peaks around 1707 cm^{-1} and 1780 cm^{-1} correspond to the functional groups of carboxylic acids, ketones, quinones and esters as expected from GC/MS chromatogram. The moderate proteins content was reflected in the biocrude with N-H bending peaks at 3195 cm^{-1} and 3215 cm^{-1}. The peaks around 457 cm^{-1} and 403.3 cm^{-1} indicated the presence of C-Br or C-Cl bonds. Both spectra were very similar. They contained the same functional groups. However, the spectra of the HTL of biocrude at 340 ºC detected more peaks that correspond to C=O functional groups, indicating the presence of wider variety of acids, ketones and esters.

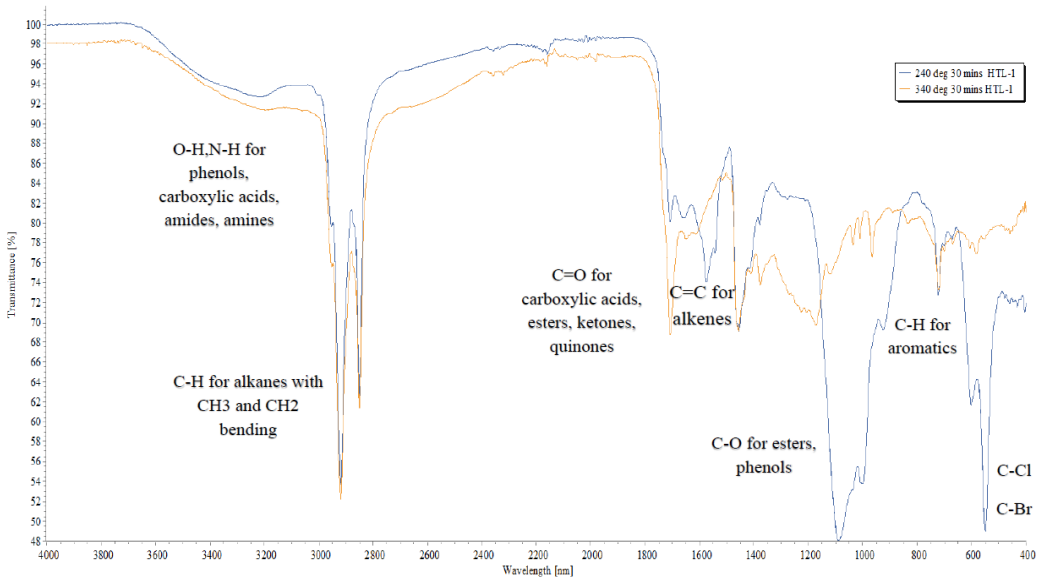

Figure 4. FT-IR plot of samples of biocrude: 340ºC (orange) and 240 ºC (blue). 30 min of reaction time and 100 rpm stirring rate.

3.3.6. ^{1}H NMR of biocrude

NMR spectra provided complementary functional group information to FTIR spectra. Figure 5 presents the ^{1}H NMR spectra of samples of biocrude at 240ºC and 340ºC for the same reaction time (30 min). Similar to FTIR, ^{1}H NMR spectra showed a percentage of aliphatic functional groups of alkane functional groups (0.8–1.2 ppm). HTL biocrude exhibited unsaturated functionality (alkenes) (1.8–2.4 ppm). However, the same section can be assigned to carboxylic acids, ketones and esters. The high peak intensity here confirmed that most of the biocrude from HTL of sludge was contributed by the decomposition of lipids-derived compounds (Massoumi et al., 2021). Aromatics were also observed (2.2–2.4 ppm) in agreement with findings from FTIR. The chemical shifts, located between 5.2 to 5.5 ppm, represented amide protons, that can be associated to the large number of nitrogen compounds. The big peak around

7.2 ppm corresponded to the solvent used. Even though both conditions contributed to the same functional groups, but their peak intensities were very distinct. It can be noted clearly that the peaks of the biocrude at HTL 340 ºC were way higher than that of HTL 240ºC. It can be concluded that more compounds were produced when the temperature has increased. This was also confirmed by GC/MS and FTIR.

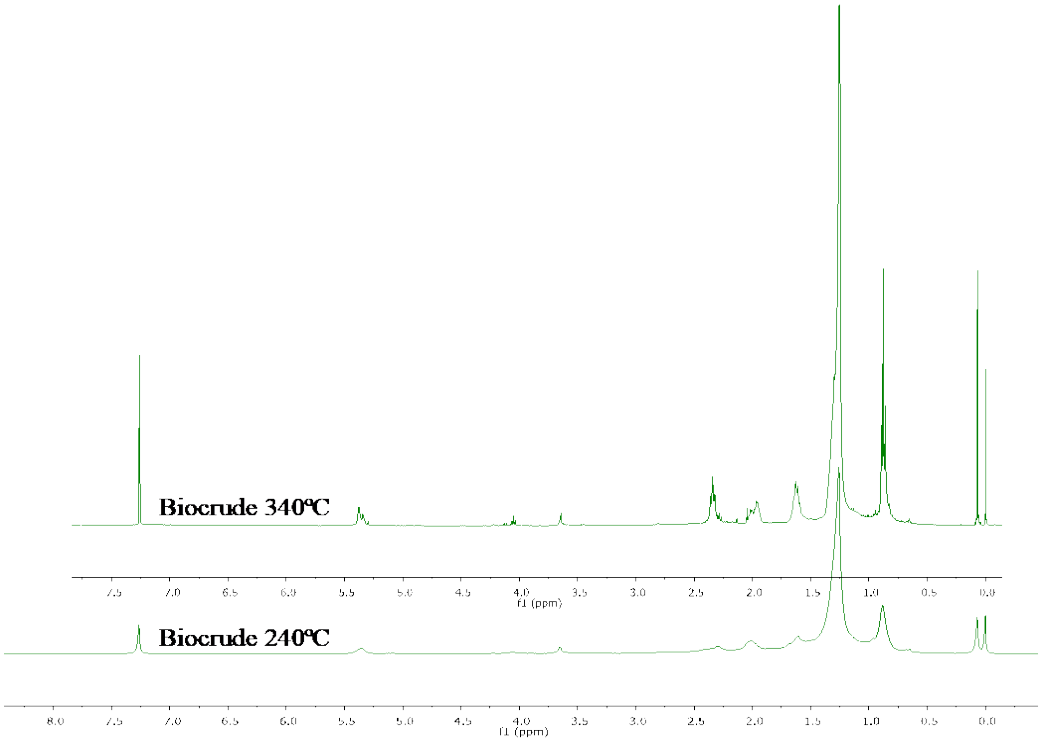

Figure 5. 1H NMR plots of samples of biocrude at 240 and 340ºC. 30 min of reaction time and 100 rpm stirring rate.

3.3.7. Quantification of SARA fractions of biocrude

SARA fractions quantification was performed to all conditions and the results are presented in Table 4. The composition of biocrude produced was distributed between maltenes including saturates, aromatics and resins, and asphaltenes. The amount of asphaltenes occupied almost

50 % of the total amount of biocrude obtained. At 320ºC, the percentage was the highest (62.80 %). The amount of saturates was predominant. Although it didn't change at low and mild conditions (≈ 30 %), a slight decrease was noted at high temperatures (25 %). Aromatics were just few. Their maximum attaint was even lower than 8 %. Polar compounds were observed in all biocrudes. They decreased with the increase of the temperature until reaching a minimum value of 6.70 % at 320 ºC then increased again to 9.92 % at 340 ºC. The results obtained from SARA analysis complied with the peaks detected by GC/MS. These results are presented in Table SM2 (supplementary material).

Table 4. SARA fractions characterization of biocrude, 30 min of reaction time and 100 rpm stirring rate.

Temperature	Oils				% Asphaltenes
	% Oils	% Saturates	% Aromatics	% Resins	
240 ºC	50.40	30.80	6.22	13.38	49.60
270ºC	45.25	30.14	4.50	10.61	54.75
300ºC	42.43	29.00	4.74	8.69	57.57
320ºC	37.23	25.59	4.94	6.70	62.77
340ºC	41.98	24.20	7.86	9.92	58.02

3.3.8. Simulated distillation of biocrude

Figure 6 shows the conversion of chromatograms from simulated distillation of biocrudes to their respective mass fractions depending on their boiling point. As it can be seen in the figure, the biocrudes produced at all temperatures offer very similar behaviours. The differences

between the studied temperatures are not significant, being always below 10%. None of the five biocrudes have a fraction in the range of gasoline. Only less than 10% of the biocrude fraction is in the Jet Fuel range. The substances included in this fraction are usually produced from protein and lignin (Al-juboori et al., 2023). Similarly, less than 30% of the biocrude fraction is in the Diesel range. The elements involved in this fraction are essentially formed from protein, and in minor quantity from lipids, carbohydrates and lignin (Al-juboori et al., 2023). In fact, 70% of the biocrude fractions are in the vacuum gasoil range. The substances involved in this fraction are essentially formed from lipids (Al-juboori et al., 2023). This fact demonstrates that biocrude requires further treatment in order to be considered as an alternative viable fuel for locomotion vehicles. As can be seen in other works (Haider et al., 2018), the use of biocrude to produce fuels requires refining after liquefaction. This post-refining must use commercial hydrotreating catalysts and hydrogen, both to improve the quality of the hydrocarbons and to eliminate the heteroatoms present in the biocrude mixtures. Table SM3 (supplementary material) displays the values of composition of biocrudes by fractional cuts. The table was made using the boiling cuts presented by Haider (Haider et al., 2018).

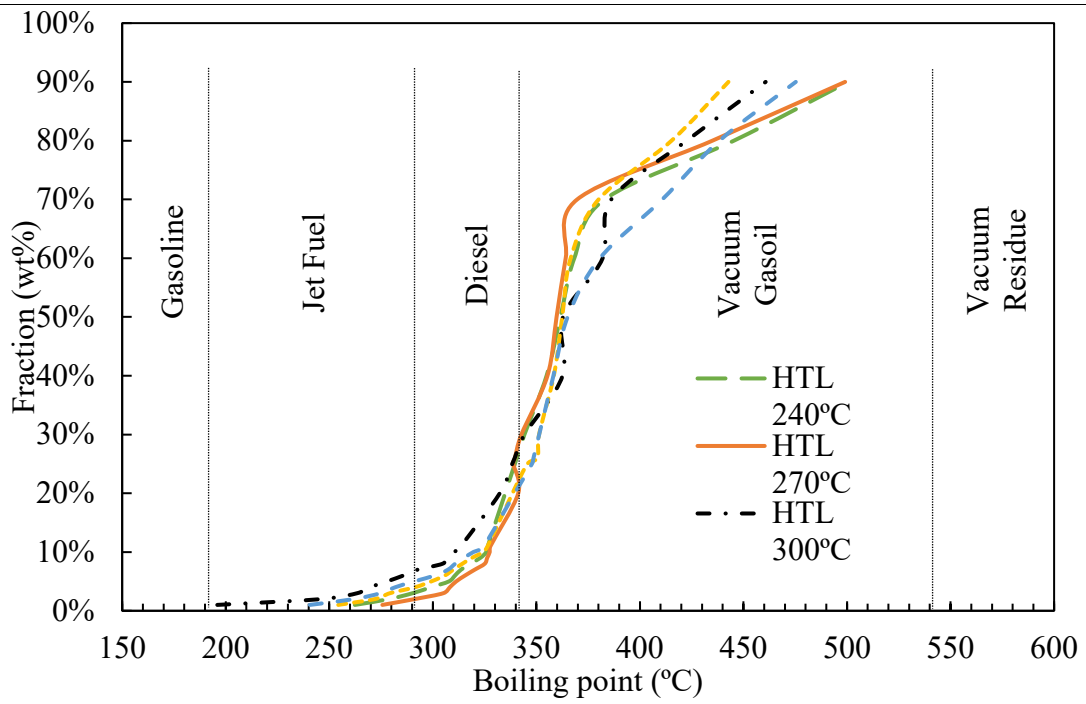

Figure 6. Simulated distillation of biocrude. 30 min of reaction time and 100 rpm stirring rate (Haider et al., 2018).

3.4. Aqueous liquid phase and its characterization

After the separation of organic phase from the liquid phase, aqueous phase was fully characterized. The liquid phase is essentially the moisture of primary sludge with water soluble organic species. The effects of temperature on the composition of aqueous phase are elucidated in Table 5. Apparently, with temperature rising from 240 to 300ºC, the TOC and COD concentrations have increased from 5130 to 5700 mg/L and from 10130 to 15700 mg/L. At 320ºC, the values of TOC and COD have decreased again to 5685 mg/L and 13500 mg/L. The much higher TOC and COD concentrations here suggests that large amounts of organic species

in primary sludge are transferred into the aqueous phase during primary sludge HTL as dissolved organics. In all the scenarios, the value of COD is higher than 10000 mg/L and the value of TOC is higher than 5000 mg/L. The amounts of proteins and carbohydrates in the aqueous phase are very low, compared to the ones of primary sludge. HTL is carried out by hydrolytic breakage of bio-constituents of the wet biomass and by the improvement of the depolymerisation products to simpler organic molecules (Zhu et al., 2022). Here, by increasing the temperature, the fractions of proteins and carbohydrates in primary sludge were hydrolysed and transformed to organic products with simple chains. The density of aqueous phase is the same at all conditions and is comparable to the one of water. pH values were slightly increasing with temperature, indicating the existence of N-rich compounds. The percentage of dissolved solids in the aqueous phase was respectively low. Ash content and VS were changing oppositely with temperature. With the increase of temperature, the VS content in the aqueous phase was always dropping. Consequently, the ash percentage was increasing. SEM images and EDX spectra of ash in aqueous phase are presented in Figure SM3 (supplementary material). Very little heavy metals remained in the ash of the dissolved solid in the aqueous phase.

Table 5. Aqueous phase characterization after HTL

	Temperature				
	240ºC	270ºC	300ºC	320ºC	340ºC
Weight (g)	427.98	447.00	451.14	398.01	438.09
Proteins (%, TS basis)	1.6	1.3	1.4	1.3	1.4
Carbohydrates (%, TS basis)	0.1	0.1	0.1	0.0	0.0
TOC (mg/L)	5130	5560	5700	5685	5440
COD (mg/L)	10130	10230	15700	13500	12500
Density (mg/L)	1.00	1.00	1.00	1.00	1.00
pH	6.34	6.56	6.81	6.91	7.71
TS (%, dry basis)	0.86	0.66	0.42	0.45	0.32
Ash (%, TS basis)	13.7	17.2	22.5	24.0	29.6
VS (%, TS basis)	86.3	82.8	77.5	76.0	70.4

3.5. Biochar and its characterization

3.5.1. Experimental results

Biochar is the solid phase recovered after process. It's a black solid that contains carbonized organics and ashes. The results obtained from its analysis are presented in Table 6. The effect of temperature on the bio-char yield was always negative. When the temperature increased from 240ºC until 300ºC, the percentage of biochar decreased from 26.2 until 19.9% (w/w). However, when passing the threshold condition, the percentage of biochar was raised again. The calculated yields were 30.81% at 320ºC and 26.9% at 340ºC. At high temperatures, the biocrude was broken, favouring the production of higher amount of solid phase and gaseous

products. Ash and VS contents were dependent on the operating temperature. High temperature was promoting the amount of ash in biochar, resulting in lower VS. While the organic part in biochar was transferred to biocrude, the probability for its usage in further applications was decreasing.

Table 6. Biochar characterization, 30 min of reaction time and 100 rpm stirring rate.

	Temperature (ºC)				
	240	270	300	320	340
Biochar weight (g)	6.24	3.32	4.22	6.52	5.53
Biochar yield % (dry basis)	34.01	29.24	28.10	39.85	34.10
Ash % (dry basis)	33.2	58.4	60.6	62.93	76.8
VS % (dry basis)	66.8	41.6	39.4	37.07	23.2
C %	53.17	68.08	71.47	82.33	76.55
H %	7.22	8.13	9.75	11.84	10.13
N %	2.69	4.40	2.97	2.56	3.06
O % *	36.92	19.40	15.81	3.26	10.26
HHV (MJ/Kg)	22.51	30.04	33.48	41.00	37.56

* By difference

3.5.2. Ultimate analysis

The ultimate analysis of the solid phase, biochar, is also presented in Table 6. Solid phase from HTL of primary sludge could be implemented in different applications in various sectors due to its high energy density and high carbon percentage, especially at high conditions (320 and 340ºC). For example, solid phase reached a HHV of 41 MJ/kg with a carbon content of 82.33 %. Therefore, biochar can be considered a potential bioenergy feedstock. In addition, it can be used in different applications in soil amendment, storage material for hydrogen, catalysts for bioenergy conversion processes and construction materials (Sharifyadeh et al. 2019). Moreover, biochar can be utilized as well as biosorbent and carbon supplement in anaerobic digestion (Mishra et al. 2019). SEM images of biochar and ash in biochar are presented in Figure SM4 (supplementary material).

3.5.3. Heavy metals

EDX spectra of biochar and ash in biochar are also presented in Figure SM4 (supplementary material). As carbon was the most abundant element in biochar, heavy metals were shown in small quantities. On the other hand, ash was rich in salts or oxides containing K, Ca, Mg, Fe, Na, S, Cl and Si. It was reported in some studies that heavy metals are accumulated in the solid residue from HTL using sewage sludge as feedstock (Li et al., 2018).

3.6. Biogas

The composition of biogas produced from HTL of primary sludge at 270, 300 and 320 ºC is presented in Table 7. In general, the fraction of biogas produced at all conditions were very small. At 270ºC, only 0.0465 mol % C_2H_4 and 0.004 mol % CO_2 were produced. At 300 ºC and 320ºC, the percentages of CO_2 and C_2H_4 didn't change significantly, but more biogases

were noted. CH_4 was observed with 0.038 mol % and 0.035 mol %. CO was detected with 0.115 mol % and 0.052 mol %. At 320 ºC alone, some C_3H_6 was found with 0.002 mol %. The increase of temperature induced the production of more gases. Figure SM5 (supplementary material) shows an example of the chromatograms obtained with the two columns.

Table 7. Biogas composition, 30 min of reaction time and 100 rpm stirring rate.

Temperature (ºC)	Biogas Volume	Biogas Composition (mol fraction) *				
		CH_4	CO	CO_2	C_2H_4	C_3H_6
270	471.20	N.D.	N.D.	0.0465	0.0040	N.D.
300	857.67	0.0380	0.1150	0.0520	0.0040	N.D.
320	917.60	0.0350	0.0520	0.0480	0.0030	0.0020

* Values of H_2O, N_2, O_2 are not shown

4. Conclusions

39.47% (w/w_{VS}) of biocrude was achieved at 270°C and 23.96% (w/w_{VS}) of oils was attained at 300°C. These maximum values are important because only temperature was optimised. Biocrude contains heavy hydrocarbons and N-compounds. HHV attained a value of 40.50 MJ/kg. Aqueous phase still contains organics which makes it an interesting source to recover chemical energy. Biochar conversion is always higher than 20% with a HHV of 41 MJ/kg % at 320ºC, an interesting bioenergy feedstock. In definitive, HTL of primary sludge is a very attractive process where a residual biomass is converted in four products, all with industrial interest.

Acknowledgements

Authors thank the collaboration of the public company Gestió Ambiental i Abstament S.A. (WWTP in Reus, Spain). Jacky Cheikhwafa thanks the Agència de Gestió d'Ajuts Universitaris i de Recerca (AGAUR) of Catalan Government for the pre-doctoral contract (Ajuts per a la contractació de personal investigador predoctoral en formació, 2019 FI-B 00743). This work is part of the PECT "Cuidem el que ens uneix/Pobles Vius i Actius/Ebrebioterritori" project, within the frame of the RIS3CAT and ERDF Catalonia Operational Programme 2014-2020. It is co-financed by the Catalan Government and the Provincial Council of Tarragona. The authors from Universitat Rovira i Virgili are recognised by the Comissionat per a Universitats i Recerca del DIUE de la Generalitat de Catalunya (2017-SGR-396) and supported by the Universitat Rovira i Virgili (2017PFR-URV-B2-33).

References

Al-juboori, J.M., Lewis, D.M., Hall, T., van Eyk, P.J. 2023. Characterisation of chemical properties of the produced organic fractions via hydrothermal liquefaction of biosolids from a wastewater treatment plant. Biomass and Bioenerg, 170, 106703. https://doi.org/10.1016/j.biombioe.2023.106703.

Biller, P., Johannsen, I., dos Passos, J.S., Ottosen, L.D.M. 2018. Primary sewage sludge filtration using biomass filter aids and subsequent hydrothermal co-liquefaction. Water Res, 130, 58–68. https://doi.org/10.1016/j.watres.2017.11.048.

Cabrera, D.V., Barria, D.A., Camu, E., Celis, C., Tester, J.W. Labatut, R.A. 2023. Enhancing energy recovery of wastewater treatment plants through hydrothermal liquefaction. Environ Sci-Wat Res, 9, 474-488. *https://doi.org/10.1039/d2ew00752e*.

Castello, D., Haider, M. S., & Rosendahl, L. (2019). Catalytic upgrading of hydrothermal liquefaction biocrudes: Different challenges for different feedstocks. Renewable Energy, 141, 420–430. https://doi.org/10.1016/j.renene.2019.04.003

De Aguiar Do Couto, E., Pinto, F., Varela, F. J., Reis, A. O. A., Costa, P. P. C., & Calijuri, M. L. (2018). Hydrothermal liquefaction of biomass produced from domestic sewage treatment in high-rate ponds. Renew Energy, 118, 644–653. https://doi.org/10.1016/j.renene.2017.11.041

DuBois, M., Gilles, K.A., Hamilton, J.K., Rebers, P.A., Smith, F. 1956. Total sugar determination by phenol sulphuric method. Anal Chem, 28, 350-356.

Gao, F., Zhou, Ch., Du, J., Zhang, Y., Wu, W., Liu, G., Li, D. 2021. Effect of gaseous agents on co-combustion characteristics of sewage sludge and coal. J Environ Chem Eng, 9, 106227. https://doi.org/10.1016/j.jece.2021.106227.

Glińska, K., Stüber, F., Fabregat, A., Giralt, J., Font, J., Mateo-Sanz, J.M., Torrens, E., Bengoa, C. 2020. Moving municipal WWTP towards circular economy: Cellulose recovery from primary sludge with ionic liquid. Resour Conserv Recycl Adv, 154, 104626. https://doi.org/10.1016/j.resconrec.2019.104626.

Guo, Y., Guo, L., Jin, C., Zhao, Y., Gao, M., Ji, J., She, Z., Giesy, J. P. 2022. Comparison of primary and secondary sludge carbon sources derived from hydrolysis or acidogenesis for nitrate reduction and denitrification kinetics: Organics utilization and microbial community shift. Environ Res, 212, 113403. https://doi.org/10.1016/j.envres.2022.113403.

Haider, M.S., Castello, A., Michalski, K.M., Pedersen, T.H., Rosendahl, L.A. 2018. Catalytic hydrotreatment of microalgae biocrude from continuous hydrothermal liquefaction:

heteroatom removal and their distribution in distillation cuts. Energies, 11, 3360. https://doi.org/10.3390/en11123360.

Haider, M.S., Chiaberge, S., Siviero, A., Isik, M.A., Castello, A., Pedersen, T.H., Rosendahl, L.A. 2023. Understanding the demetallization of nitrogen-rich hydrothermal liquefaction biocrudes by FTICR mass spectrometry: Recalcitrant effect of metalloporphyrins and basic nitrogenates. Fuel, 334, 126755. https://doi.org/10.1016/j.fuel.2022.126755.

Hao, B., Xu, D., Wang, Y., Wang, Y., Kapusta, K., Guo, Y. 2023. Catalytic hydrothermal liquefaction of municipal sludge for biocrude production over non-noble bimetallic catalyst in ethanol solvent. Fuel, 331, 125812. https://doi.org/10.1016/j.fuel.2022.125812.

Hong, C., Wang, Z., Si, Y., Li, Z., Xing, Y., Hu, J., Li, Y. 2021. Effects of aqueous phase circulation and catalysts on hydrothermal liquefaction (HTL) of penicillin residue (PR): Characteristics of the aqueous phase, solid residue and bio oil. Sci Total Environ, 776, 145596. https://doi.org/10.1016/j.scitotenv.2021.145596.

Kulikova, Y., Babich, O., Tsybina, A., Sukhikh, S., Mokrushin, I., Noskova, S., Orlov, N. 2022. Feasibility of Thermal Utilization of Primary and Secondary Sludge from a Biological Wastewater Treatment Plant in Kaliningrad City, Energies, 15, 5639. https://doi.org/10.3390/en15155639.

Leng, S., Leng, L., Chen, L., Chen, J., Chen, J., Zhou, W. 2020. The effect of aqueous phase recirculation on hydrothermal liquefaction/carbonization of biomass: A review. Bioresource Technol, 318, 124081. https://doi.org/10.1016/j.biortech.2020.124081.

Li, H., Lu, J., Zhang, Y., Liu, Z. 2018. Hydrothermal liquefaction of typical livestock manures in China: Biocrude oil production and migration of heavy metals. J Anal Appl Pyrol, 135, 133-140. https://doi.org/10.1016/j.jaap.2018.09.010.

Li, R., Ma, Z., Yang, T., Li, B., Wei, L., Sun, Y. 2018. Sub–supercritical liquefaction of municipal wet sewage sludge to produce biocrude: Effect of different organic–water mixed solvents. J Supercrit Fluid, 138, 115–123. https://doi.org/10.1016/j.supflu.2018.04.011.

Liu, R., Tian, W., Kong, S., Meng, Y., Wang, H., Zhang, J. 2018. Effects of inorganic and organic acid pretreatments on the hydrothermal liquefaction of municipal secondary sludge. Energ Convers Manage, 174, 661–667. *https://doi.org/10.1016/j.enconman.2018.08.058*.

Liu, Q., Zhang, G., Liu, M., Kong, G., Xu, R., Han, L., & Zhang, X. (2022). Fast hydrothermal liquefaction coupled with homogeneous catalysts to valorize livestock manure for enhanced biocrude oil and hydrochar production. Renew Energy, 198, 521–533. https://doi.org/10.1016/j.renene.2022.08.090

Lowry, O.H., Rosebrough, N.J., Farr, A.L., Randall, R.J. 1951. Proteins measurement with the folin phenol reagent. Biol Chem, 193, 265-275.

Marcal, J., Bishop, T., Hofman, J., Shen, J. 2021. From pollutant removal to resource recovery: A bibliometric analysis of municipal wastewater research in Europe. Chemosphere, 284, 131267. https://doi.org/10.1016/j.chemosphere.2021.131267.

Mishra, S., Mohanty, K. 2020. Co-HTL of domestic sewage sludge and wastewater treatment derived microalgal biomass – An integrated biorefinery approach for sustainable biocrude production. Energ Convers Manage, 204, 112312. https://doi.org/10.1016/j.enconman.2019.112312.

Mishra, S., Roy, M., Mohanty, K. 2019. Microalgal bioenergy production under zero-waste biorefinery approach: Recent advances and future perspectives. Bioresource Technol, 292, 122008. https://doi.org/10.1016/j.biortech.2019.122008.

Olkiewicz, M., Fortuny, A., Stüber, F., Fabregat, A., Font, J., Bengoa, C. 2015. Effects of pre-treatments on the lipid extraction and biodiesel production from municipal WWTP sludge. Fuel, 141, 250-257. https://doi.org/10.1016/j.fuel.2014.10.066.

Ponce-Robles, L., Polo-López, M.I., Oller, I., Garrido-Cardenas, J.A., Malato, S. 2018. Practical approach to the evaluation of industrial wastewater treatment by the application of advanced microbiological techniques. Ecotox Environ Safe, 166, 123-131. https://doi.org/10.1016/j.ecoenv.2018.09.044.

Rice, E.W., Baird, R.B., Eaton, A.D., Clesceri, L.S. 2012. Standard Methods for the Examination of Water and Wastewater, 22nd edn. APHA AWWA WEF, Washington.

US EPA O. Basic Information about Biosolids. US EPA 2021. https://www.epa.gov/biosolids/basic-information-about-biosolids (accessed May 18, 2021).

Rahman, T., Jahromi, H., Roy, P., Adhikari, S., Hassani, E., Oh, T.-S. 2021. Hydrothermal liquefaction of municipal sewage sludge: Effect of red mud catalyst in ethylene and inert ambiences. Energ Convers Manage, 245, 114615. https://doi.org/10.1016/j.enconman.2021.114615.

Senfter, T., Fritsch, L., Berger, M., Kofler, T., Mayerl, C., Pillei, M., Kraxner, M. 2021. Sludge thickening in a wastewater treatment plant using a modified hydrocyclone. Carbon Resour. Convers, 4, 132–141. https://doi.org/10.1016/j.crcon.2021.03.001.

Shah, A.A., Toor, S.S., Conti, F., Nielsen, A.H., Rosendahl, L.A. 2020. Hydrothermal liquefaction of high ash containing sewage sludge at sub and supercritical conditions. Biomass and Bioenerg, 135, 105504. https://doi.org/10.1016/j.biombioe.2020.105504.

Shannag, H.K., Al-Mefleh, N.K., Freihat, N.M. 2021. Reuse of wastewaters in irrigation of broad bean and their effect on plant-aphid interaction. Agr Water Manage, 257, 107156. https://doi.org/10.1016/j.agwat.2021.107156.

Sharifzadeh, M., Sadeqzadeh, M., Guo, M., Borhani, T.N., Murthy Konda, N.V.S.N., Garcia, M.C., Wang, L., Hallett, J., Shah, N. 2019. The multi-scale challenges of biomass fast pyrolysis and biocrude upgrading: Review of the state of art and future research directions. Prog Energ Combust, 71, 1-80. https://doi.org/10.1016/j.pecs.2018.10.006.

Stratiev, D., Shishkova, I., Dinkov, R., Nenov, S., Sotirov, S., Sotirova, E., Kolev, I., Ivanov, V.S., Ribagin, S., Atanassov, K.T., Stratiev, D.D., Yordanov, D., Nedanovski, D. 2023. Prediction of petroleum viscosity from molecular weight and density. Fuel, 331, 125679. https://doi.org/10.1016/j.fuel.2022.125679.

Thomsen, L.B.S., Anastasakis, K., Biller, P. 2021. Wet oxidation of aqueous phase from hydrothermal liquefaction of sewage sludge. Water Res, 117863. https://doi.org/10.1016/j.watres.2021.117863.

Thomsen, L., Carvalho, P., Dos Passos, J., Anastasakis, K., Bester, K., Biller, P. 2020. Hydrothermal liquefaction of sewage sludge; energy considerations and fate of micropollutants during pilot scale processing, Water Res, 183, 116101, https://doi.org/10.1016/j.watres.2020.116101.

Tong, Y., Yang, T., Li, B., Kai, X., Li, R. 2021. Two-stage liquefaction of sewage sludge in methanol-water mixed solvents with low-medium temperature. J Supercrit Fluid, 168, 105094. https://doi.org/10.1016/j.supflu.2020.105094.

Truchado, P., Gil, M.I., López, C., Garre, A., López-Aragón, R.F., Böhme, K., Allende, A. 2021. New standards at European Union level on water reuse for agricultural irrigation:

Are the Spanish wastewater treatment plants ready to produce and distribute reclaimed water within the minimum quality requirements? Int J Food Microbiol, 356, 109352. https://doi.org/10.1016/j.ijfoodmicro.2021.109352.

Vardon, D.R., Sharma, B.K., Scott, J., Yu, G., Wang, Z., Schideman, L., Zhang, Y., Strathmann, T.J. 2011. Chemical properties of biocrude oil from the hydrothermal liquefaction of Spirulina algae, swine manure, and digested anaerobic sludge. Bioresource Technol, 102, 8295–8303. https://doi.org/10.1016/j.biortech.2011.06.041.

Wang, J., Liu, G., Shao, Y., Zhang, Q., Wei, Q., Luo, F., Sun, W., Liu, S., Liu, Y., Zhang, J., Qi, L., Wang, H. 2021. Regulation of anaerobic fermentation for producing short-chain fatty acids from primary sludge in WWTPs by different alkalis. J Environ Manage, 299, 113623. *https://doi.org/10.1016/j.jenvman.2021.113623*.

Wu, H., Li, X., Zhang, Q., Zhang, K., Xu, X., & Xu, J. (2022). Promoting the conversion of poplar to bio-oil based on the synergistic effect of alkaline hydrogen peroxide. Renew Energy, 192, 107–117. https://doi.org/10.1016/j.renene.2022.04.101

Xiao, H., Zhai, Y., Xie, J., Wang, T., Wang, B., Li, S., Li, C. 2019. Speciation and transformation of nitrogen for spirulina hydrothermal carbonization. Bioresource Technol, 286, 121385. https://doi.org/10.1016/j.biortech.2019.121385.

Xu, D., Lin, G., Liu, L., Wang, Y., Jing, Z., Wang, S. 2018. Comprehensive evaluation on product characteristics of fast hydrothermal liquefaction of sewage sludge at different temperatures. Energy, 159, 686–695. *https://doi.org/10.1016/j.energy.2018.06.191*.

Zhang, L., Li, W., Lu, J., Li, R., Wu, Y. 2021. Production of platform chemical and bio-fuel from paper mill sludge via hydrothermal liquefaction. J Anal Appl Pyrol, 155, 105032. https://doi.org/10.1016/j.jaap.2021.105032.

Zhao, B., Li, H., Wang, H., Hu, Y., Gao, J., Zhao, G., Ray, M. B., & Xu, C. (2021). Synergistic effects of metallic Fe and other homogeneous/heterogeneous catalysts in hydrothermal liquefaction of woody biomass. Renew Energy, 176, 543–554. *https://doi.org/10.1016/j.renene.2021.05.115*

1667

1668

3

Use of chemical energy from municipal WWTP primary sludge through hydrothermal liquefaction

ABSTRACT

Hydrothermal liquefaction allows the valorisation of municipal WWTP primary sludge into products with higher added value. The process permits the recovery of the chemical energy contained in the sludge to generate more useful substances. The effect of temperature on the quality of the products has been evaluated. Best biocrude yield, 39.4% (w/w_{VS}), best maltene yield, 22.8% (w/w_{VS}), best HHV, 42.2 MJ/kg and, best energy recovery, 88%, have been obtained at 300ºC. In the range of studied temperatures (240-340ºC), all biocrude yields were greater than 34.8% (w/w_{VS}), all maltene yields were superior than 19.4% (w/w_{VS}), all HHV values were larger than 34 MJ/kg and, all energy recovery were bigger than 60%. Simulated distillation of all biocrude samples associated them with high vacuum gasoil cut. Gases, biocrude, aqueous fraction and biochar were extensively characterised.

1670

1. Introduction

The current picture of wastewater sludge is more perceived as an energy and nutrients resource, rather than just a waste, with the potentiality of net energy removal and nutrient conservation (Biller et al. 2017). Municipal waste sludge can be noted in urban areas as a waste stream from wastewater of the wastewater treatment plants (WWTPs), containing chemical energy potential represented as chemical oxygen demand (COD). It is considered a very likely waste feedstock, because it's cheap, sustainable and easily accessible, and it contains a wide range of organic matters and nutrients (Fan et al. 2020). Different types of sludge are generated from the disposal process of wastewater: primary sludge, secondary sludge, and digested sludge. Each one is discharged in a different way, depending on the treatment type and stage (Shah et al. 2020). Among all, primary sludge is normally discharged after the primary treatment and presents settled organic matter coming from raw wastewater. It's black in color and has a total solid of 4%. It contains 55-70% of highly degradable organics including lipids, proteins, and carbohydrates (Wang et al. 2021). Primary and other types of sludge are subjected to different traditional disposal techniques including landfill and incineration as well as land application for agriculture. Nevertheless, economic and environmental problems have limited these applications (Thomsen et al. 2020). Therefore, new strategies and approaches are needed to convert these wastes into environmentally and physically sustainable resources. In fact, the waste valorization policy, including sewage sludge processing, is one of the main goals on the agenda of the European Union EU regulations (Budych-Gorzna et al. 2021). Several methodologies are implemented for the conversion of waste sludge. In research and development R & D; hydrothermal liquefaction HTL undergoes great attention as a highly adaptable process that is capable to convert a wide range of organic feedstock. Because it guarantees an economic and ecological performance, HTL process might be a competitive

substitute to other biomass production processes. HTL offers important potential advantages for wastewater treatment. It is transforming wet sludge into low-odor solids, sterilized, a particle and toxic-free waste, and profitable biocrude (Marrone 2016); also, it's converting 72% of carbon and decreasing dry solid mass by 76% (Snowden-Swan et al. 2017). Lipids in PS are composed of free fatty acids in the range of C10 to C18 which are precursors for esters production. In addition, proteins are confirmed to be promoters for biocrude production through HTL. Maillard reactions represent a significant part in the distribution of biocrude and composition, originated from the reaction of amine groups present in proteins with carbonyl groups present in reducing carbohydrates (Fan et al., 2021). In HTL, the conversion of biomass into a highly viscous bio-oil, referred to as biocrude, is usually performed at temperatures of 300-420°C and pressures of 15-35 MPa (Penke et al. 2021). Co-products including solid, gas and aqueous phases are obtained as well. In addition, it employs water at sub-critical conditions in the conversion process, thus HTL process is convenient for biomass with high water content. Also, water acts as catalyst that changes the activation energy for some reactions and promotes new reaction pathways to the biomass-water ratio at ambient conditions (Obeid et al. 2022). However, one main withdraws of using this technique is the production of high concentrated wastewater, called aqueous phase. Sludge contains a high moisture content, which is converted through the process into an aqueous phase that forms a predominant part of the products (Song et al. 2022). Many researchers have focused on the biocrude as the main product. Hydrothermal liquefaction HTL of digested sewage sludge with 21.25 % of TS has produced. 21.26 % of biocrude. However, between 36.6 and 50.6 % wt/wt of aqueous phase was generated as well (Fan et al. 2020). In the study of Liu and his colleagues, HTL of mixed sludge (primary and secondary) with TS of 20% was derived to 40.7-48.3% of biocrude and 35.6-42.1% of aqueous phase depending on the operating conditions (Liu et al., 2022).

The purpose of this study is to evaluate the effect of temperature in HTL not only on the biocrude phase, but also on the aqueous phase. In addition, a complete characterization and mass balance are other duties to be attained including the biogas produced.

2. Materials and methods

2.1. Reagents

Dichloromethane 99,9 % (ref.: 32222) was purchased from Honeywell. n-Hexane 95 % (ref.: 363242), high performance chromatography grade and phenol crystalline (ref: 144852.1211) were provided by PanReacAppliChem. Reagents, sulfuric acid reagent (ref: 34632), orange reagent (ref: 131130.1612), sulphuric acid 95.0–97.0 % (ref: 30743), bovine serum albumin (BSA) (ref: A9647), sodium hydroxide 98 % (ref: 30620), sodium carbonate (ref: 222321), potassium sodium tartrate tetrahydrate (ref: 217255), copper (II) sulphate pentahydrate (ref: 209198), Folin&Ciocalteu's phenol reagent (ref: F9252), magnesium sulphate monohydrate (ref: 434183), anhydrous sodium sulphate (ref: 239313), and fuming hydrochloric acid, high analytical reagent grade, (ref: 84418) were supplied by Sigma - Aldrich.

2.2. Sludge collection and managing

Samples of primary sludge were supplied by the municipal wastewater treatment plant of Reus in Tarragona, Spain. Bottle, filled with 500 ml of sludge, were collected after partial gravity thickening of the primary treatment. They were stored in a freezer at -15 °C and defrosted before use in an oven at 60 °C for 5 hours. The bottles of sludge were used directly as received.

2.3. Characterization of sludge by conventional methods

A full characterization of primary sludge was carried out in triplicate. Total solids (TS), volatile solids (VS) and ash content were measured according to standard methods 2540B and 2540E respectively (Rice et al., 2012). Extraction of lipids was achieved in a Soxhlet apparatus using hexane as a solvent, according to standard method 5520E (Rice et al., 2012). Total carbohydrate percentage was detected by phenol-sulfuric acid Dubois method (Dubois et al., 1956). Shortly, 0.05 mL of 80 % phenol solution was added to 2 mL of diluted sludge sample in a glass tube. Then, 5 mL concentrated sulfuric acid was quickly added. The tubes were kept under room temperature for 10 min and then placed into a thermostatic bath at 30 ℃ another 15 min. The absorbance was measured at 480 nm. Protein content was determined with Lowry method (Lowry et al., 1951). The protein solubilization in the sludge samples was carried out by heating the samples with 2 M sodium hydroxide at 100°C for 10 min. The absorbance was measured at 750 nm. Finally, elemental analysis was realized by Serveis Técnics de Recerca at Universitat de Girona. Analysis was performed using an elemental analyzer (Perkin Elmer model EA2400). C, H and N were determined, and O was calculated by difference.

2.4. Hydrothermal liquefaction of primary sludge

The experiments were conducted using a 1 L Stainless Steel Autoclave (Autoclave Engineers model EZE Seal) equipped with a movable heating shell, a fixed MagneDrive® stirrer (a packless rotary impeller system that operates magnetically), and a control system for maintaining operating conditions. The reactor was connected to a gas line, allowing the introduction of nitrogen, and had an inlet valve for gas input. The outlet valve was connected to a gas flow meter and a Tedlar bag push lock valve 0.6 L (Superlco 30289-U) for gas collection.

The experimental setup involved placing approximately 500 g of primary sludge into the reactor. To create an oxygen-free environment, pure nitrogen gas was purged three times. Subsequently, the system was pressurized to 1 bar as the initial pressure. The HTL experiments were conducted at five different temperatures and their corresponding pressures: 240°C (~33.7 bar), 270°C (~55.6 bar), 300°C (~86.9 bar), 320°C (~114.0 bar), and 340°C (~146.8 bar). The reaction time after reaching the desired temperature was always 0 minute, with continuous agitation at 100 rpm. The reaction pressure was not actively controlled but was automatically generated based on the reaction temperature. The heating time varied between 1 hour and 3 hours, depending on the selected temperature. After each batch experiment, the reactor was cooled down using a room temperature water bath (~25°C) until it returned to its initial condition.

2.5. Cleaning of the reactor and separation of products

Figure 1, also presents the schematic diagram of the experimental separation procedures after hydrothermal liquefaction of primary sludge. The products obtained are distributed into 4 different phases: gas, organic, aqueous, and solid. When the reactor was back to atmospheric pressure and laboratory ambient temperature, the gas phase was released. The output gas was passed through a flow meter, indicating the volume of the gas mixture, and collected in a gas bag. After that, the reactor was opened, and the mixture was poured into a large beaker. The solid part was separated from the liquid part via vacuum filtration. The liquid part, mainly containing the aqueous phase and a small part of the organic phase, was transferred into a bottle. Meanwhile, the reactor was washed repeatedly with dichloromethane until being totally clean to recover the organic remaining part, deposited on the walls, on the cover of the reactor and, in the agitation module. Then the mixture, where a part of solids was entrapped into the

organics, was separated by vacuum filtration. The liquid part containing the organic phase and the dichloromethane was transferred into another bottle. The solid retained on the filter paper, biochar, and ashes, was washed with dichloromethane several times. The biochar was dried in the oven for 24 hours at 105ºC and quantified by weighting. A small volume of dichloromethane was added to the aqueous phase. Then, the mixture was centrifuged at 8000 rpm for 5 minutes. The upper phase is the dichloromethane containing the small part of organic phase. This was added to the organic phase previously separated. The lower phase is the aqueous phase containing soluble organic molecules. Dichloromethane was evaporated from the organic phase by the rotary evaporation, at 65ºC and atmospheric pressure. The viscous organic liquid obtained is the biocrude, that it was further weighted for quantification. Finally, biocrude was separated into oils and asphaltenes by Soxhlet extraction using 200 mL of hexane. Oils were separated from hexane by rotary evaporation at 65ºC and atmospheric pressure. Asphaltenes were quantified by the difference between biocrude and oils.

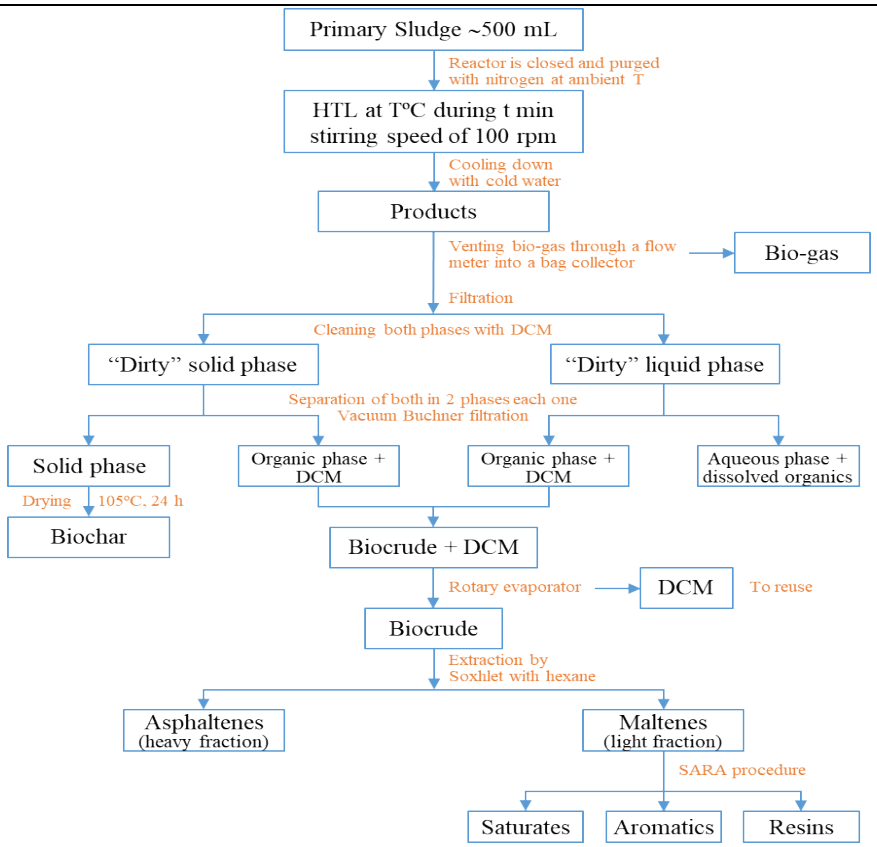

Figure 1. Process overview of primary sludge HTL.

2.6. Biocrude quantification and characterization

A comprehensive characterization was conducted on the biocrude, encompassing various analytical techniques and parameters. The analysis included weight determination, assessment of ashes content, gas chromatography/mass spectrometry (GC/MS), thermogravimetric analysis (TGA), elemental (ultimate) analysis, determination of higher heating value (HHV), Fourier transform infrared spectroscopy (FTIR), nuclear magnetic resonance (NMR), and simulated distillation (SimDis). Furthermore, the saturated, aromatics, resins, and asphaltenes (SARA) fractions of the biocrude were characterized.

2.6.1. Gas chromatography/mass spectrometry spectroscopy

Biocrude samples were characterized by gas chromatography-mass spectroscopy (GC-MS) using a Perkin Elmer Turbo Mass Gold GC-MS, equipped with a Supelco SLB®-5ms capillary GC column (L × I.D. 30 m × 0.25 mm, d_f 0.25 μm). The solvent used was dichloromethane. The GC oven was maintained at 70ºC for 1 min, heated to 180ºC at a rate of 7ºC/min, then heated to 240ºC at a rate of 12ºC/min and finally 7 min hold at 330ºC. Oils were also characterized by gas chromatography-mass spectroscopy (GC-MS) using the same procedure but using hexane as solvent.

2.6.2. FTIR and ^{1}H NMR

Further functional group data was interpreted from FTIR and ^{1}H NMR spectroscopic analysis. FTIR spectra were obtained from a Thermo Nicolet Nexus 670 Fourier Transform Infrared Spectrophotometer equipped with a single-bounce diamond attenuated total reflectance (ATR) accessory (Specac Golden Gate) and KBr beam splitter. Spectra ranging from 4000 to 500 cm^{-1} with 0.98-cm^{-1} resolution and averaged over 50 replicate scans were collected using Omnic software. Background scans were conducted of the dry accessory at ambient temperature. The spectra were then collected after smearing about 30 mg of sample directly on the ATR crystal surface.

^{1}H NMR spectra were assembled using a Varian Unity 400-MHz spectrometer outfitted with a 5-mm broadband probe. 50–75 mg of biocrude were dissolved in deuterated chloroform containing 0.03% tetramethylsilane (TMS) as an internal reference. Samples were then filtered (0.22- μm PTFE) to remove any suspended particulates before loading into 5 mm diameter NMR tubes. ^{1}H spectra were obtained with a 90 pulse angle, spinner frequency of 20 Hz, sweep width of 8000 Hz across 32 transients.

2.6.3. Elemental analysis and HHV

Elemental analysis of biocrude samples was also realized by Serveis Técnics de Recerca at Universitat de Girona as commented in section 2.2. C, H and N were quantified, and O calculated by difference. Then, the higher heating values of (HHVs) of biocrude were calculated, using Dulong formula taken from Hong's study where HHV is expressed in MJ/kg (Hong et al., 2021).

2.6.4. Thermogravimetric TGA analysis of biocrude

The weight loss properties were studied by *thermogravimetric analysis* (TGA). In each test, about 3 to 4 mg of sample was heated from 30 to 800 C at a nitrogen flow of 60 mL/min and a 10 K/min heating (Zhu et al., 2022).

2.6.5. Quantification and identification of SARA fractions of biocrude

SARA of biocrude was performed as well. The separation of light phase and heavy phase was repeated as mentioned above. The separated maltenes were fractionated into saturates hydrocarbons with 20 mL of n-hexane using activated alumina in a glass chromatographic column. Then, aromatic compounds were extracted by 20 mL of toluene. Finally, resins were removed from the adsorbent using 20 mL of a mixture of toluene and 2-propanol (1:1). More polars were also removed using 20 ml of methanol. Each eluted fraction was recovered by solvent removal using a Rotary evaporator. All the fractions obtained were filtered and injected on GC-MS for identification following the procedure mentioned in 2.6.1.

2.6.6. Simulated distillation (Sim-Dis) of biocrude

Sim-Dis was displayed after ASTM-D2887 method and performed using a HP 5890 Series II FID gas chromato-graph and a Durabond DB-HT-SimDis GC column by Agilent-J&WScientific (5 m0.53 mm id, 0.15µm film). Helium (56.4 mL/min) was the carrier gas. The oven temperature was initially set to 36°C, and increased to 400°C at 10°C/min and then held constant for 10 min. The injector volume was set to 0.5 µL and the injector temperature was set to 350ºC. Detector temperature was set to 375°C, hydrogen gas set to 40 ml/min, airflow set to 400 ml/min, and helium makeup set to 24 ml/min. Samples (1% w/w) and reference standards (0.5% w/w) were dissolved in DCM. Samples were filtered (0.22-µm PTFE) to remove any suspended particulates. Boiling points were determined in accordance to a D2887 calibration mix and a D2887 Reference Gas Oil standard, both purchased from sigma Aldrich. Data (retention time and areas) were collected. Each sample was divided into fractions (%wt) and boiling points were calculated accordingly.

2.7. Quantification and characterization of biochar

Total solids, moisture content, volatile solids and ash content were determined in biochar according to standard methods 2540B and 2540E respectively (Rice et al., 2012). Also, elemental analysis was done by following the same procedure described above.

2.8. Quantification and characterization of aqueous phase

COD, TOC, TN, protein, and carbohydrates were measured or analyzed for the aqueous phase. COD analysis was performed according to standard method 5220D (Rice et al., 2012). TOC was analyzed by using a TOC analyzer TOC-L Series based on a specific standard calibration curve. Total organic carbon (TOC) was measured by ASI-L auto sampler Shimadzu into a Shimazdu TOC-L CSN TOC analyzer provided with a NDIR detector and calibrated with

standard solutions of hydrogen potassium phthalate. Total dissolved nitrogen was measured in the same TOC analyzer coupled with TNM-L ROHS unit (Ponce-Robles et al., 2018). COD removal and TOC removal percentages were calculated using the equations retrieved from another study (Thomsen et al. 2022). Protein amount was measured according to Lowry method (Lowry et al., 1951) and carbohydrate were quantified following Dubois method (Dubois et al., 1956) as described in the previous section (2.3). Total solid (TS), volatile solid (VS) and ash content were measured in the aqueous phase as well. A specific volume of aqueous phase was dried in a weighted crucible for 24 hours in the oven at 100 ºC then burned in the furnace at 550 ºC for 1 hour, as detailed by the standard methods 2540B and 2540E respectively (Rice et al., 2012).

2.9. Characterization of Biogas

Identification and quantification of biogas were finalized by a gas chromatograph analyser (micro-GC, Agilent, 990) equipped with a thermal conductivity detector (TCD). A MS5A SS 10MX0.25MMX30UM BF RTS, CP-PORABOND Q 5MX0.25MMX3UM column (column 1) was used to separate the light gases using Argon as a carrier gas and a PORAPLOT Q UM 10MX0.25MMX8UM BF, CP-PORABOND Q 1MX0.25MMX3UM column (column 2) was used to separate heavy gases using helium as a carrier gas. Column 1 was maintained at injector temperature 100ºC, injection time 40 ms, initial pressure 200 kPa and column temperature 100ºC. Column 2 was maintained at injector temperature 100ºC, injection time 40 ms, initial pressure 150 kPa and column temperature 60ºC. The run time was 120 s. The mole percentage of each gas was determined with respect to gas standards prepared by E. DE CARBUROS METÁLICOS S.A.

2.10. Calculation methods

All experiments were accomplished in triplicates and products were calculated with the following equations. Equations (1) - (4) estimated the yield of biocrude, aqueous phase, aqueous phase, gaseous phase, higher heating value, and energy recovery, respectively. The mass of volatile solids in the equations is referred to the one of primary sludge (ash-free feedstock).

$$\text{Biocrude yield (\%)} = \frac{\text{Mass of bio-oil}}{\text{Mass of volatile solids}} \times 100 \quad (1)$$

$$\text{Aqueous phase yield (\%)} = \frac{\text{Mass of solids dissolved in aqueous phase}}{\text{Mass of volatile solids}} \times 100 \quad (2)$$

$$\text{Biochar yield (\%)} = \frac{\text{Mass of solid residue}}{\text{Mass of volatile solids}} \times 100 \quad (3)$$

$$\text{Gas yield (\%)} = 100 - (1) - (2) - (3) \quad (4)$$

$$\text{HHV (MJ/kg)} = 0.3383\ \text{C} + 1.443\ \left(\text{H} - \frac{\text{O}}{8}\right) \quad (5)$$

C, H and O are the mass percentages of carbon, hydrogen, and oxygen from the elemental analysis of the samples, respectively.

$$\text{ER (\%)} = \text{Biocrude yield (\%)} \frac{\text{HHV}\left(\frac{\text{MJ}}{\text{kg}}\right) \text{of biocrude}}{\text{HHV}\left(\frac{\text{MJ}}{\text{kg}}\right) \text{of primary sludge}} \quad (6)$$

$$\text{COD removal (\%)} = \frac{\text{COD (Aqeous phase)} - \text{COD (primary sludge)}}{\text{COD (primary sludge)}} \times 100 \quad (7)$$

$$\text{TOC removal (\%)} = \frac{\text{TOC (Aqeous phase)} - \text{TOC (primary sludge)}}{\text{TOC (primary sludge)}} \times 100 \quad (8)$$

3. Results and discussion

3.1. Characterization of primary sludge

Table 1 provides an overview of the characterization conducted on the primary sludge. The initial composition of the sludge revealed a total solids content of 4.3 ± 0.1% (w/w wet sludge basis), with the remaining percentage being moisture (95.7 ± 0.1%). These values align closely

with previous studies conducted by the research group on primary sludge from the Reus WWTP, which reported total solids contents of 4.2 ± 1.2% (Olkiewicz et al., 2015) and 3.9 ± 0.1% (Glinska et al., 2020). The ash content, expressed as a percentage of the total solids, was determined to be 22.9 ± 0.3%, while the volatile solids were calculated as the difference from the ash content and accounted for 77.1 ± 0.3% (w/w total solids basis). The density of the primary sludge was found to be 1.012 g/mL, similar to that of water.

Table 1. Characterization of primary sludge from Reus municipal WWTP.

Feedstock characterization	**Percentage % (dry basis) ***
Moisture content	95.70 ± 0.1
Dry matter	4.30 ± 0.1
Volatile matter	77.12 ± 0.3
Ash content	22.88 ± 0.3
Protein	21.15 ± 1.7
Carbohydrate	29.84 ± 1.2
Lipid	23.41 ± 0.8
C	36.86
H	5.34
N	3.71
O	54.12
Density(g/mL)	1.01
TOC (mg/L)	6290
TN (mg/L)	1544.60
COD (mg/L)	35180
HHV (MJ/kg)	18.37

*Average of at least three assays

The volatile solids were further analyzed to determine the proportions of carbohydrates, proteins, and lipids. Carbohydrates were identified as the predominant fraction, representing 29.84% of the volatile solids. Lipids (23.41%) and proteins (21.15%) were also found in significant amounts. These findings are consistent with previous studies on primary sludge

from the same source, which reported lipid contents of 19.6 ± 0.6%, carbohydrate contents of 31.3 ± 0.1%, protein contents of 27.7 ± 0.1%, and ash contents of 16.0 ± 0.1% in a study on cellulose recovery from primary sludge (Glinska et al., 2020). Another study on primary sludge used for biodiesel production reported lipid contents of 27.2 ± 0.4%, carbohydrate contents of 26.2 ± 2.6%, protein contents of 24.2 ± 1.4%, and ash contents of 20.1 ± 0.4% [22] (Glinska et al., 2020).

The ultimate analysis of the primary sludge revealed low nitrogen (3.71%) and hydrogen (5.34%) contents, high carbon content (36.86%), and a substantial oxygen content (31.19%), calculated by difference. These values were used to determine the higher heating value (HHV) of the dried primary sludge, taking into account the mass of the ashes. The calculated HHV under these conditions was 14.55 MJ/kg, comparable to values obtained in other studies, such as 10.55 MJ/kg (Kulikova et al., 2022) and 17.31 MJ/kg (Adedeji et al., 2022).

Figure 2 showcases scanning electron microscopy (SEM) images and energy-dispersive X-ray spectroscopy (EDX) spectra of the ash in the primary sludge.

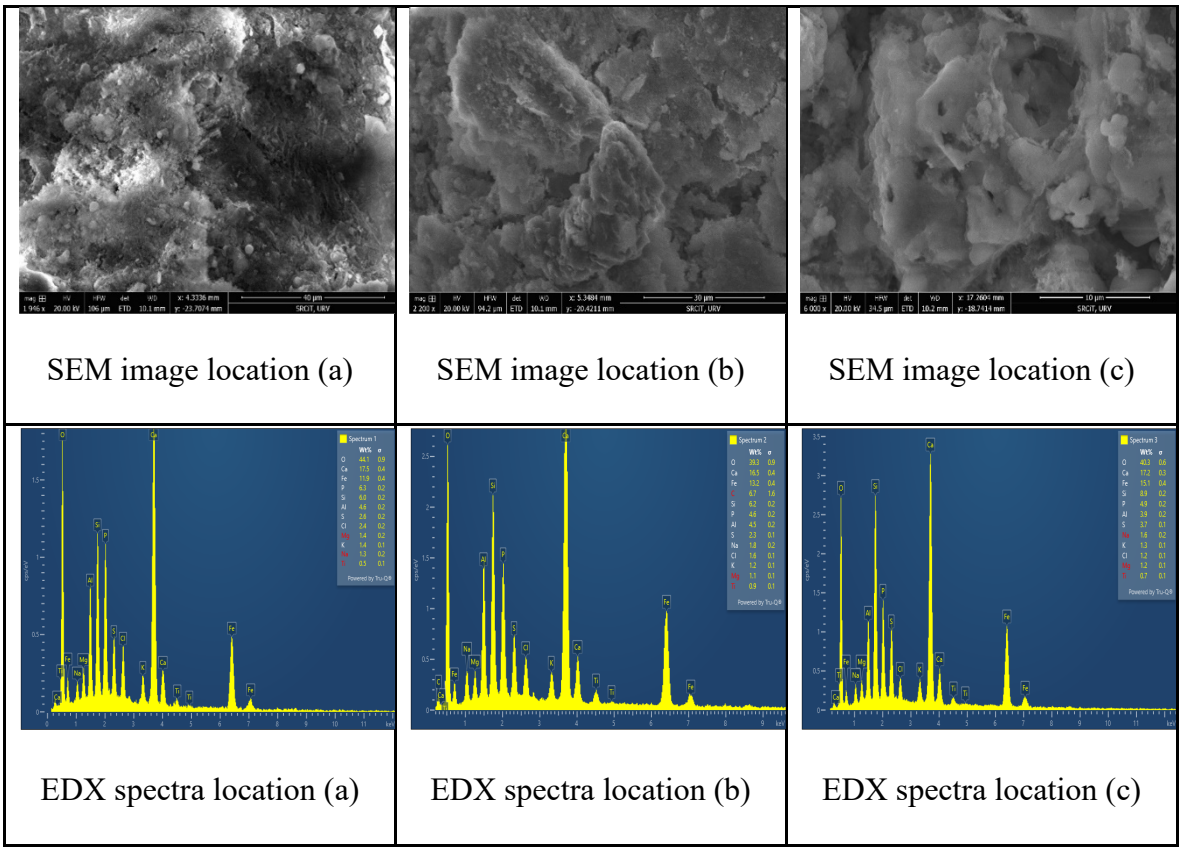

Figure 2. SEM images and EDX spectra of ash in primary sludge. (a), (b), and (c) denote distinct observation sites of the sample.

3.2. HTL of primary sludge

The HTL experiments conducted on the primary sludge involved a sample size of approximately 500 g. These experiments were consistently performed with a reaction time of 0 minute and a stirring rate of 100 rpm. The operating temperatures varied across five different levels: 240°C, 270°C, 300°C, 320°C, and 340°C. Upon completion of the designated reaction time, the reactor was gradually cooled to ambient conditions. The resulting products, namely the gaseous phase, biocrude, aqueous phase containing organics, and biochar, were separated

using the experimental procedure illustrated in Figure 1. The subsequent sections will present the quantification and characterization of the products obtained throughout the HTL process for the sludge.

Table 1. Biocrude yields at different temperatures. Time of reaction: 0 min. Stirring: 100 rpm.

T (ºC)	Biocrude (% w/w_{vs})	Maltenes [a] (% w/w_{vs})	Asphaltenes [b] (% w/w_{vs})
240	32.5 ± 5.9	19.4 ± 1.4	13.1 ± 4.5
270	35.4 ± 1.0	22.6 ± 0.2	12.8 ± 0.8
300	39.4 ± 2.0	22.8 ± 1.7	16.6 ± 0.3
320	36.2 ± 1.4	21.5 ± 0.3	14.7 ± 1.2
340	35.8 ± 0.5	19.6 ± 0.0	16.2 ± 0.5

[a] Maltenes are the light phase of biocrude, obtained after Soxhlet extraction with hexane

[b] Asphaltenes are the heavy phase of biocrude, calculated by difference

The yields and distributions of biocrude obtained from primary sludge HTL at different temperatures are listed in Table 2. Generally, the biocrude yield at the beginning increased to a maximum value and then decreased with temperature increasing from 240 to 340ºC.

The optimum value was obtained at 300ºC, 38.30% (w/wVS). This result is comparable to that obtained with HTL of mixed sludge (primary and secondary), 42.6% (w/wVS) at 350ºC for 15 min (Liu et al. 2023) and with HTL of WSS, 37.1 (w/wVS) at 340ºC for 20 min (Li et al. 2018). A slight drop, ~3.0% (w/wVS), from 300ºC to 340ºC is derived from the biogas formation

through the conversion process. In addition, temperature has a significant effect on the distribution of biocrude between oils and asphaltenes. In this study, the optimum value of oils, 23.18% (w/wVS), was reached at 320ºC. The results obtained validate the important effect of temperature on the biocrude yield. High reaction temperature implies significant biocrude yield. According to other studies, high temperature provides a medium with low density of polarity of water, which accelerates the hydrolysis, depolymerization, decomposition and reformation reactions (Shah et al. 2020; Xu et al. 2018). However, it looks that after the initial hydrolysis, primary products obtained underwent additional reactions (e.g., gasification) and high molecular weight solids were formed by additional repolymerization at very high temperature (Qian et al. 2020; Li et al. 2018). This was approved by the decrease of biocrude yield when the temperature has exceeded the threshold limit, higher than 300 ºC.

3.3. Characterization of biocrude

3.3.1. Ultimate analysis and HHV

The corresponding results of the elemental analysis C, H, N and O with HHV and ER of biocrude obtained at different operating conditions are represented in table 3. The HTL process of primary sludge formed a product with high energy source then initially. Temperature had an obvious effect on the distribution of elements in biocrude. The percentages of C and O reacted in an opposite way with the increase of temperature. From 240ºC until 300ºC, C % was improved significantly until reaching a maximum value of 78.3% then decreased slightly at higher temperatures to 76.71%. Whereas O % decreased sharply from 20.3% to 5.9% then increased again to near 9.2%.

Table 3. Elemental analysis of biocrude at different temperatures. Time of reaction: 0 min. Stirring: 100 rpm.

T (ºC)	Elemental analysis (%)				HHV [b] (MJ/kg)	ER (%)
	C	H	N	O [a]		
240	66.3	11.1	2.3	20.3	34.8	0.60
270	75.3	11.2	3.8	9.7	39.9	0.75
300	78.3	11.6	4.2	5.9	42.2	0.88
320	76.7	11.4	3.8	8.1	40.9	0.79
340	76.7	9.8	4.3	9.2	38.4	0.73

[a] Calculated by difference (O = 100 - N - H - C)

[b] Calculated with Dulong equation

Hydrogen content was not really affected by the temperature. Values were very close at all temperatures. A small change was noticed at 340 ºC. the percentage of nitrogen was increasing with the rise of temperature, but slowly. Finally, using the equation of Dulong, it can be said that HHV was improved along with temperature. The quality of biocrude as an energy source was the best at 300 ºC with a HHV value of 41.99 MJ/kg, very close to the one of petroleum crude oil, between 42 and 47 MJ/k (31). In this case, the energy recovery is close to 0.9 showing the benefits of the process.

3.3.2. Gas chromatography- Mass spectroscopy GCMS

Figure 3 illustrates a chromatogram of GC/MS analysis of a sample of biocrude obtained at

300ºC, with a reaction time of 0 min. On the other hand, Table 4 lists the identification of peaks of all biocrudes produced at different temperatures, showing the existence of many different organic compounds. Only compounds with compatibility higher than 70% were considered. Based on GCMS results, clearly, the biocrude was classified into N-containing compounds (N and O heterocyclic compounds and amides), Oxygenated compounds (aldehyde, acids, esters and ketones), and hydrocarbons. Considering the complex nature of primary sludge, it's difficult to explain the right pathways of the retrieved compounds. The presence of fatty acids can be explained by the hydrolysis of lipids. Nitrogen – and – Oxygen - containing heterocycle compounds can be synthesized from the dimerization of amino acids or Maillard reactions between amino acids and reducing sugars, products of the hydrolysis of proteins and sugars (Zhu et al., 2022; Xu et al. 2018).

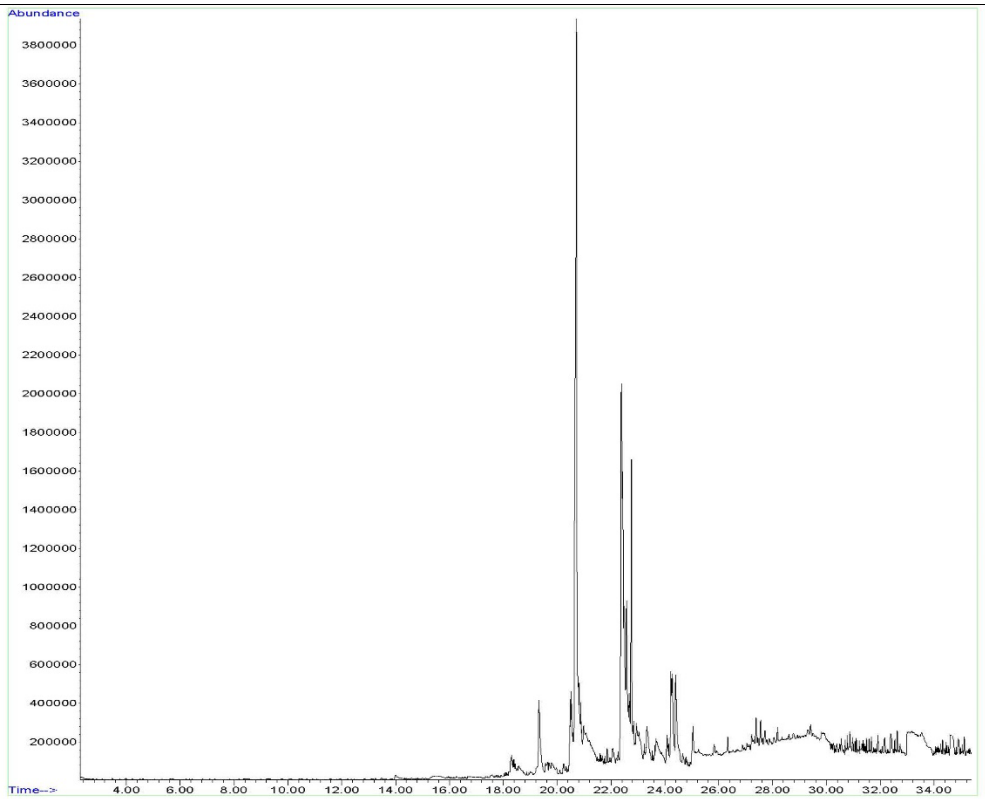

Figure 3. Chromatogram of GC/MS of biocrude produced at 300ºC. Time of reaction: 0

min. Stirring: 100 rpm.

2018

2019 Amides appeared from partly hydrolysing reactions in such a short residence time (0 min) (Zhu
2020 et al. 2018). Ketones were generated from cellulose by cyclization, dehydration, and hydrolysis.
2021 Long chain hydrocarbons were derived from decarboxylation of fatty acids (Shah et al. 2020).
2022 Note that some compounds could not be detected on GC-MS because of their extra high boiling
2023 points (higher than 330ºC).

Table 4. Chemical composition of biocrude at different temperatures. Time of reaction: 0 min. Stirring: 100 rpm.

Compound	Formula	Temperature (ºC)				
		240	270	300	320	340
cetene	$C_{16}H_{32}$			X	X	
1-Pentadecene	$C_{15}H_{30}$				X	X
1-Octadecene	$C_{18}H_{36}$			X		
1-Tridecene	$C_{13}H_{26}$				X	

1-Tricosene	$C_{23}H_{46}$			X		
3-Heptadecene, (Z)-	$C_{17}H_{34}$				X	
2-Tridecanone	$C_{13}H_{26}O$			X		
2-Pentadecanone	$C_{15}H_{30}O$					X
2-Heptadecanone	$C_{17}H_{34}O$			X		
Cyclotridecanone	$C_{13}H_{24}O$					
2(3H)-Furanone, 5-dodecyldihydro-	$C_{16}H_{30}O_2$					
Hexadecane, 2,6,10,14-tetramethyl-	$C_{20}H_{42}$			X		
Tridecanoic acid	$C_{13}H_{26}O$					
Tetradecanoic acid	$C_{14}H_{28}O_2$	X			X	
9-Hexadecenoic acid	$C_{16}H_{30}O$					
9-Octadecenoic acid, (E)-	$C_{18}H_{34}O_2$					X
Palmitoleic acid	$C_{16}H_{30}O_2$	X				
n-Hexadecanoic acid	$C_{16}H_{30}O_2$	X	X	X	X	X
Oleic Acid	$C_{18}H_{34}O$	X	X	X	X	
Octadecenoic acid	$C_{18}H_{34}O$	X				
Dodecanoic acid	$C_{12}H_{24}O_2$				X	
6-Octadecenoic acid	$C_{18}H_{34}O$		X			
Octadecane	$C_{18}H$	X				X
Hexadecane	$C_{16}H_{34}$			X		
Dodecane			X			

4-Methyldocosane	$C_{23}H_{48}$					
1-Chloroeicosane	$C_{20}H_{41}Cl$					
Cyclotetradecane	$C_{14}H_{28}$			X		X
Cyclooctacosane	$C_{28}H_{56}$			X		
Cyclododecane	$C_{12}H_{24}$				X	
Eicosane	$C_{20}H$	X				
1-Nonadecene	$C_{19}H_{38}$	X	X			
Nonadecane	$C_{19}H_{40}$			X		
1-Decene	$C_{10}H$					
Galaxolide 1	$C_{18}H_{26}O$					
Hexadecanoic acid, methyl ester	$C_{17}H_{34}O$					X
trans-13-Octadecenoic acid	$C_{18}H_{34}O_2$					X
N-Methyldodecanamide	$C_{13}H_{27}NO$				X	
Hexadecanoic acid, dodecyl ester	$C_{28}H_{56}O_2$					
9-Octadecenoic acid (Z)-, methyl ester	$C_{19}H_{36}O$	X	X			
Hexadecanamide	$C_{16}H_{33}NO$				X	X
1-Hexadecyne	$C_{16}H_{32}$			X		
9-Octadecenamide, (Z)-	$C_{18}H_{35}NO$	X	X			X
Octadecanamide	C18H37NO			X		
Dodecanamide	$C_{12}H_{25}NO$			X		

11-Dodecen-1-ol trifluoroacetate	$C_{14}H_{23}F_3O_2$					
1,13-Tetradecadiene	$C_{14}H_{26}$				X	
Dodecane, 2,6,10-trimethyl-	$C_{15}H_{32}$			X		
Methyl stearate	$C_{19}H_{38}O_2$	X				
14-Methyl-heptadecanoic acid, pyrrolidide	$C_{17}H_{34}O_2$				X	
Bis(2-ethylhexyl) phthalate	$C_{24}H_{38}O$	X				
9-Tetradecenal, (Z)-	$C_{14}H_{26}O$			X		
E-14-Hexadecenal	$C_{16}H_{30}O$					X
E-15-Heptadecenal	$C_{17}H_{32}O$				X	
Cholest-3-ene, (5.beta.)-	$C_{27}H_{46}$			X	X	X
Cholest-2-ene, (5.alpha.)-	$C_{27}H_{46}$					X
Cholest-4-ene	$C_{27}H_{46}$			X	X	X
Cholest-5-ene	$C_{27}H_{46}$			X	X	X
Cholesta-3,5-diene	$C_{27}H_{44}$				X	X
Cholest-7-ene, (5.alpha.)-	$C_{27}H_{46}$				X	

3.3.3. TGA

TG analysis in a nitrogen atmosphere was applied to evaluate the simulation process of biocrude to establish its thermal stability. the three stages of weight loss of the biocrude.

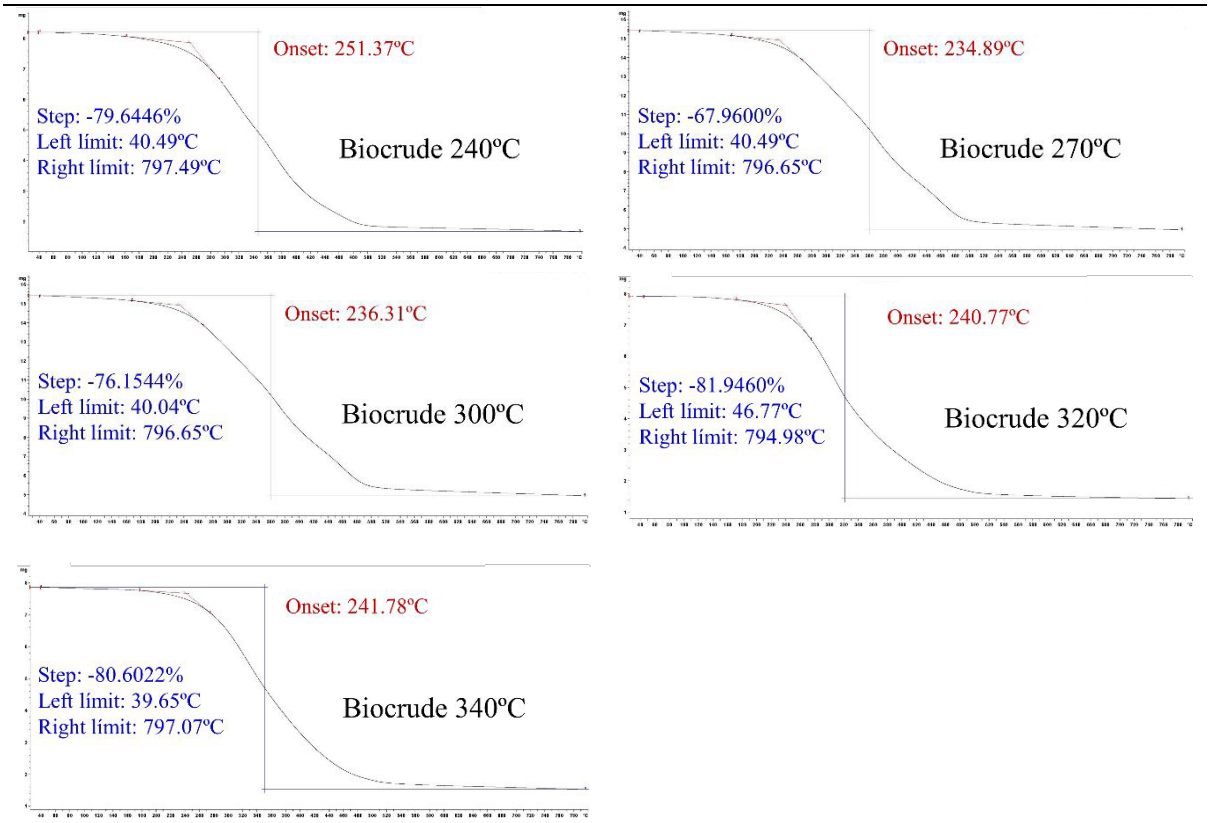

Figure 5. TGA of biocrude at different temperatures. Time of reaction: 0 min. Stirring: 100 rpm.

As it can be observed, all samples of biocrude present the TG curve of the five samples present a similar tendency. The differences between the weight loss from the five samples were small. Weight loss values were 79.64 % for biocrude at 240ºC; 67.96 % for biocrude at 270°C; 76.15 % for biocrude at 300°C; 81.95 % for biocrude at 320°C and 80.60 % for biocrude at 340°C. Normally, in typical biocrude curves, there is a first mass loss from 75 to 100ºC, which

corresponds to the loss of water and volatile oils (Watson et al., 2020). In all cases of biocrude presented in Figure 5, it can be seen that at 100ºC, the mass loss has been less than 2%, which confirms that the biocrude contains almost no water and that it does not contain large amounts of volatile oils. On the other hand, more than half of the mass has been lost around 330-350ºC. From over 100ºC and these values, the mass loss is caused by the decomposition of less volatile substances. Over 350ºC to 700ºC, more or less 50% of the sample was lost, corresponding to the volatilization of high molecular weight substances and long chain hydrocarbons produced during the repolymerisation (Amin et al., 2016).

3.3.4. ^{1}H NMR and FT-IR

FTIR spectroscopy detects functional groups present in biocrude, based on which the entire biocrude can be classified by different classes of compounds. Figure 5 shows FTIR spectra for biocrudes after hydrothermal liquefaction at 240ºC, 270ºC, 300ºC, 320ºC and 340ºC for the same reaction time (0 min).

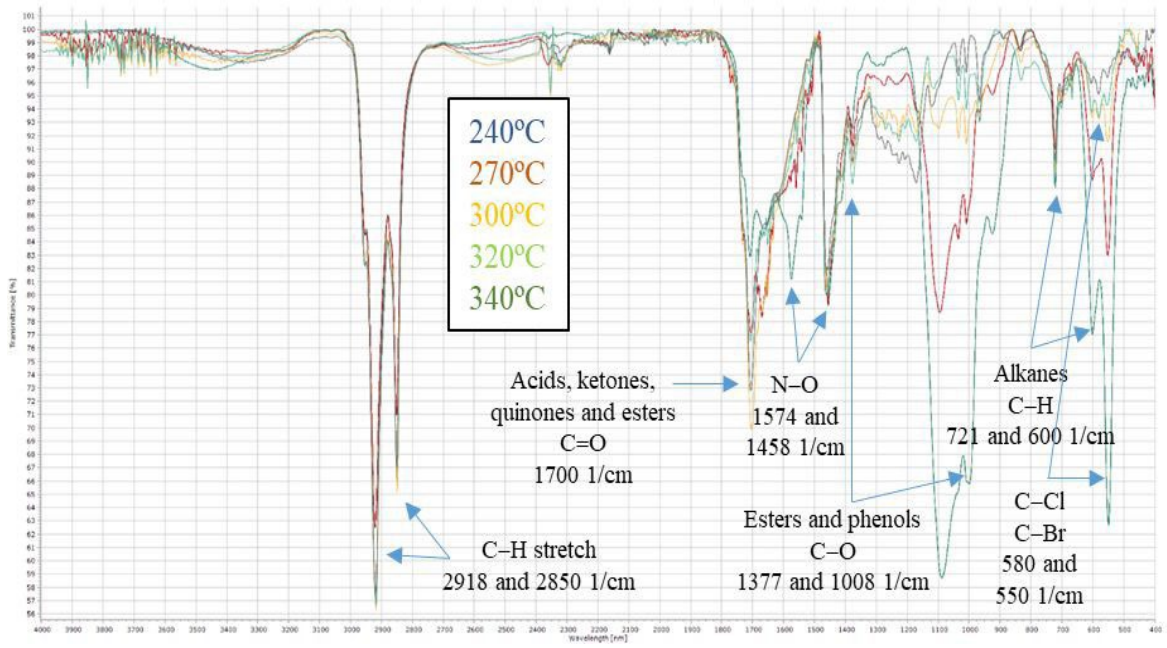

Figure 4. FT-IR of biocrude at different temperatures. Time of reaction: 0 min. Stirring: 100 rpm.

The high content of carbon and hydrogen in the elemental analyzed was observed here as well. The increase in the intensity of peaks at 2918 and 2850 cm^{-1} illustrates a high concentration of alkanes in the fraction with CH_2 and CH_3 bending and high peaks near 721 and 600 cm^{-1} belonged to unsaturated stretching. Biocrude was detected with C-O stretching peaks (1008–1377 cm^{-1}) that belong to esters and phenols. C=O stretching peaks around 1704 cm^{-1} and 1707 cm^{-1} correspond to the functional groups of carboxylic acids, ketones, quinones and esters as detected by GCMS. The moderate protein content in primary sludge was transformed into biocrude with N-O bending peaks around 1574 cm^{-1} and 1458 cm^{1}. The peaks around 580 cm^{-1} and 550 cm^{-1} showed the presence of C-Br or C-Cl bonds. All spectra were comparable. They present the same functional groups. Yet, along with the increase of temperature, less intensity of C=O and C-Br or C-Cl peaks was observed and more intensity of CH bonds was noted.

NMR spectra added more functional group information to FT-IR spectra. Figure 6 presents the ^{1}H NMR spectra of samples of biocrude at 240ºC, 270ºC, 300ºC, 320ºC and 340ºC for the same reaction time (0 min).

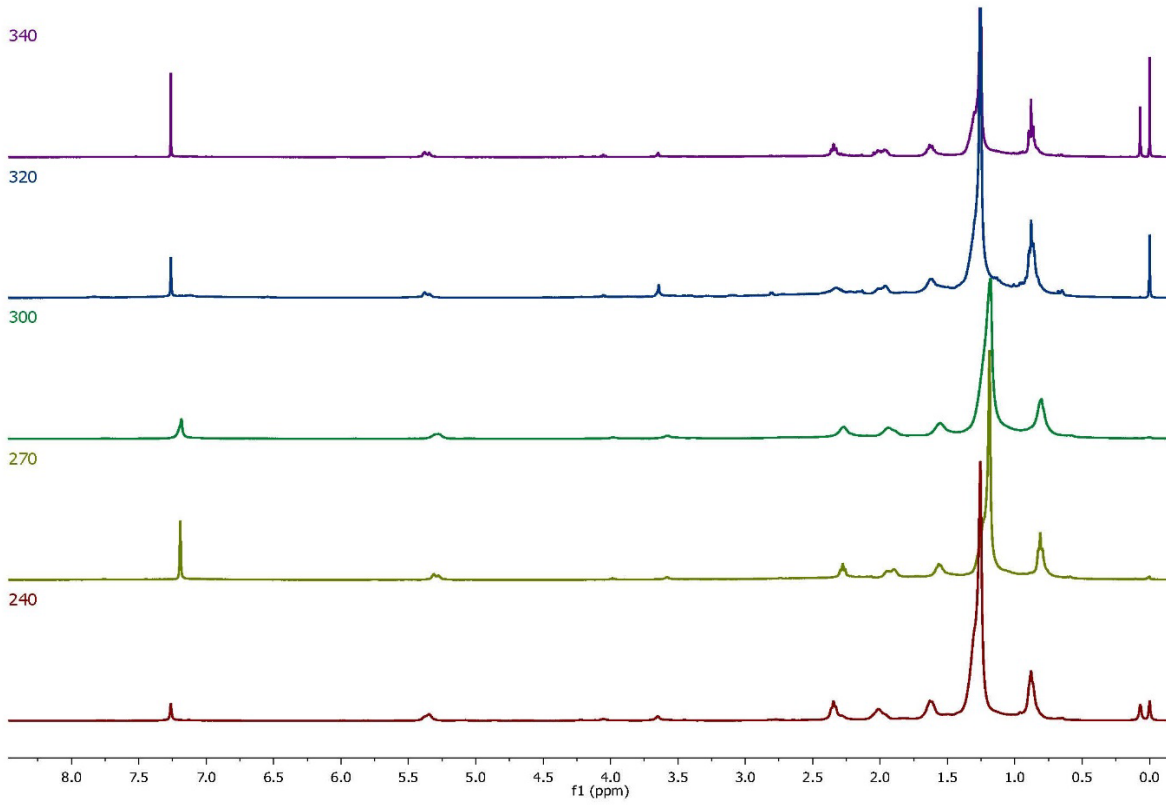

Figure 6. ^{1}H NMR plot of sample of HTL biocrude at all temperature. Reaction time: 0 min. Stirring: 100 rpm.

In all spectra, similar to FT-IR, ^{1}H NMR spectra showed a percentage of aliphatic functional groups of alkane functional groups (0.7–1.0 ppm). HTL biocrude displayed unsaturated functionality (1.9–2.5 ppm). Though, the same range can be assigned to carboxylic acids, ketones and esters. The high peak intensity here confirmed that decomposition of lipid-derived compounds in biocrude was derived from lipids in sludge (Masoumi et al., 2021). The high

peak around 7.2 ppm corresponded to the solvent used. The chemical alterations, located between 5.22 to 5.5 ppm, denoted amide protons, that can be associated to the large number of nitrogen compounds. Aromatics were also observed (2.0–2.5 ppm) in agreement with results from FTIR. Even though all conditions supplied the same functional groups, but their peak intensities were different. It can be noted clearly that by increasing the temperature, more saturated compounds and less unsaturated compounds were produced. This was also confirmed by GC/MS and FTIR.

3.3.5. SARA fractions quantification of biocrude

SARA analysis was done for the light phase obtained from the separation with Soxhlet. It was performed for all conditions and all the results are listed in table 5. Oils contained maltenes, fractioned into saturates, aromatics and resins.

Table 2. SARA analysis of maltenes at different temperatures. Time of reaction: 0 min. Stirring: 100 rpm.

Temperature (ºC)	Maltenes (% $w/w_{Biocrude}$)	Saturates (% $w/w_{Biocrude}$)	Aromatics (% $w/w_{Biocrude}$)	Resins (% $w/w_{Biocrude}$)	Asphaltenes (% $w/w_{Biocrude}$)
240	61.8	32.7	4.1	25.0	38.2
270	57.3	36.1	4.9	16.3	42.7
300	50.1	27.5	5.0	17.6	79.9
320	55.0	40.3	0.8	13.9	45.0

The heavy phase was counted as asphaltenes. The amount of asphaltenes was always lower than 50 % of the total amount of biocrude obtained. However, with the increase of temperature, asphaltene percentage reached a maximum value of 49.91 % at 300 ºC then decreased to 15.40 % at 340 ºC. The distribution of maltenes, the predominant part of biocrude, into saturates, aromatics and resins were very distinct depending on the condition. The amount of saturates was similar (≈ 33%) at all temperatures except that at 340ºC where a huge amount of saturates was detected (72.58%). Aromatics were few in biocrude, but more found at lower conditions. The amount of resins was decreasing along with the increase of temperature from 25.14% to 10.36%. The results obtained from SARA analysis complied with the peaks detected by GCMS, ^{1}H NMR and FTIR. Chromatograms of the three fractions obtained in the biocrude are presented in Figure 7.

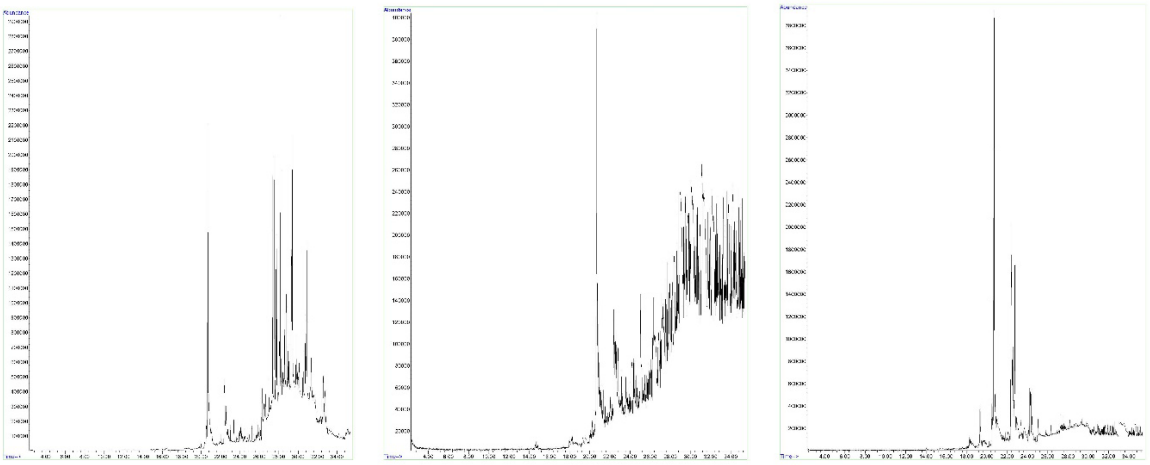

Figure 7. Chromatograms of (a) saturate, (b) aromatic and (c) polar phases of biocrude at 300ºC of temperature, 0 min of reaction time and 100 rpm of stirring rate.

3.3.6. Simulated Distillation Sim-Dis

Chromatograms from GC-FID were processed according to ASTM D 2887 methods to obtain distillation curves for each biocrude sample. Gasoline, jet fuel, diesel, vacuum gas oil and vacuum residue distillation cuts are presented in Figure 8.

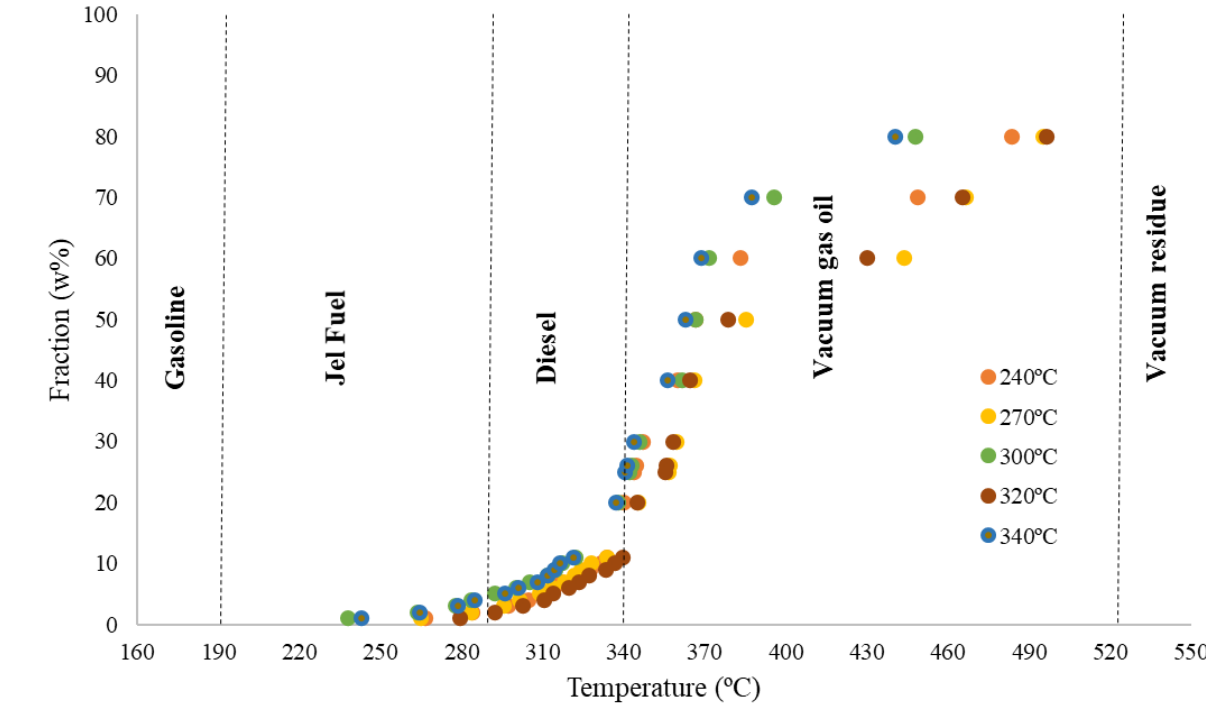

Figure 8. Sim-Dis results of biocrude produced from HTL at 0 min.

Biocrude, at all conditions, provide very similar fractions. The effect of temperature was not important. In all the scenarios, none of the biocrude contained a fraction in the gasoline cut. Only less than 5% of the biocrude has a fraction in the range of jet fuel. Likewise, less than 20% of the biocrude fraction belonged to diesel range. The biocrude, characterized by high molecular weight compounds, is associated with high vacuum gasoil cut (more than 65%). These results agree with the fact that biocrude should be subjected to additional treatment to be utilized as an alternative practicable transport fuel. Gasoline and diesel fractions should be

optimized by maximizing low boiling point and high value products other works. To achieve that, hydro-treatment followed by fractionation is processed (Ghadge et al. 2022). Values of composition of biocrudes by fractional cuts are listed in Table 6. Boiling cuts used in the table were taken from the study of Haider (Haider et al., 2018).

Table 3. Fractional distribution of biocrude at different temperatures. Time of reaction: 0 min. Stirring: 100 rpm.

Fractional cuts	BP range	Composition				
		240ºC	270ºC	300ºC	320ºC	340ºC
Gasoline	< 190ºC	0%	0%	0%	0%	0%
Jet fuel	190-290ºC	2%	3%	5%	2%	4%
Diesel	290-340ºC	17%	17%	18%	10%	20%
Vacuum gas oil	340-538ºC	73%	65%	69%	80%	69%
Vacuum residue	>538ºC	7%	16%	9%	9%	7%

3.4. Aqueous liquid phase and its characterization

After the completion of separation process, aqueous phase was collected apart and subjected to different experimental analysis allowing the quantification of organics. The liquid phase is mainly the water content of primary sludge, containing water soluble organic species. The influence of temperature on the aqueous phase composition is illustrated in Table 7. TN concentration was increasing along with the temperature from 1387 to 1476 mg/L, marking more nitrogenous compounds. COD and TOC concentrations were decreasing from 18168 to 10130 mg/L and from 6135 to 5330 mg/L along with the increase of temperature; Or, maximum percentages of TOC removal and COD removal were noted at 270ºC with 19.95% and at 340ºC with 71.21%. Obviously, the high values of TOC and COD obtained can be explained by the dissolution of the high content of organics contained in primary sludge in the aqueous phase produced from HTL. Both the COD and TOC values marked that a considerable amount of

energy remained in the HTL-AP, which suggests that further valorisation of HTL-AP would help the energy recovery of the HTL system. The number of proteins and carbohydrates dissolved in the aqueous phase was lower than that retrieved initially in primary sludge.

Table 7. Quantification of aqueous phase after HTL at different temperatures. Time of reaction: 0 min. Stirring: 100 rpm

	Temperature				
	240ºC	270ºC	300ºC	320ºC	340ºC
Weight (g)	455.34	445.52	442.33	423.20	445.39
Yield (%, VS basis)	5.73	4.44	3.83	2.11	2.01
Proteins (%, TS basis)	2.42	2.46	2.24	1.5	1.83
Carbohydrates (%, TS basis)	0.23	0.15	0.10	0.04	0.04
TN (mg/L)	1387	1335	1375	1480	1476
TOC (mg/L)	6135	5035	5270	4956	5330
TOC removal (%)	2,46	19,95	16,22	21,21	15,26
COD (mg/L)	18168	11356	14695	12434	10130
COD removal (%)	48.36	67.72	58.23	64.66	71.21
pH	5.61	6.90	6.59	7.49	7.81
TS (%, dry basis)	0.97	0.75	0.63	0.35	0.34
Ash (%, TS basis)	15.03	15.06	15.93	27.39	26.20
VS (%, TS basis)	84.97	84.94	84.10	72.61	73.80

In previous studies, it was indicated that proteins and carbohydrates favour to be dissolved in the aqueous phase. For this reason, aqueous phase is frequently rich in organic acids coming from the breakdown of either monomeric sugars or carbohydrates, and cyclic amine derivatives and N/O heterocyclic compounds derived from protein hydrolysis and deamination (Watson et al., 2020). pH values were slowly increasing with temperature, demonstrating the existence of N-rich compounds. The percentage of dissolved solids in the aqueous phase was observed in low amounts. Ash content and VS were affected oppositely by the increase of temperature. While ash content was increasing along with temperature, VS content was dropping, but

slightly. SEM images and EDX spectra of ash in aqueous phase are presented in Figure 9. Few heavy metals were detected in the ash of the dissolved solid in the aqueous phase.

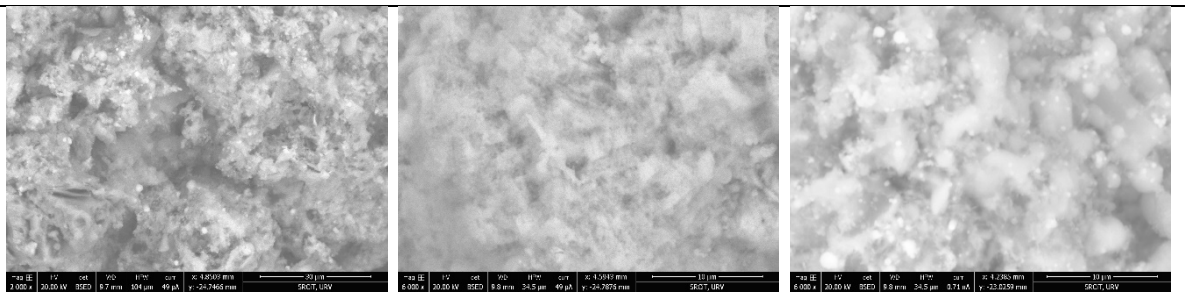

SEM image location (a) SEM image location (b) SEM image location (c)

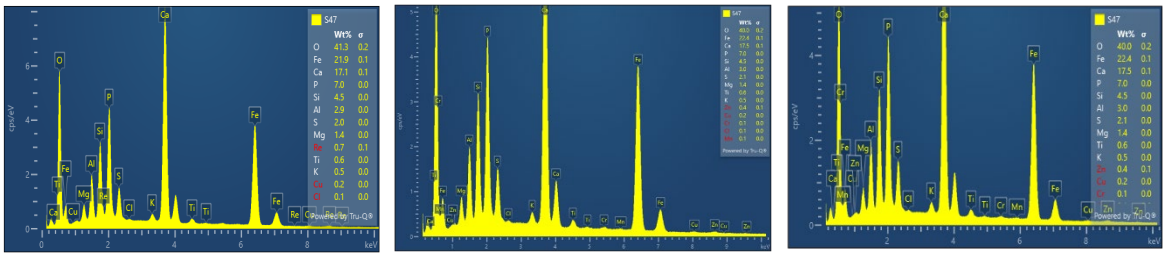

EDX spectra location (a) EDX spectra location (b) EDX spectra location (c)

Figure 9. SEM and EDX of ash in solid phase at 340ºC. Time of reaction: 0 min. Stirring: 100 rpm. (a), (b) and (c) represent three different observation locations of the sample.

3.5. Biochar

3.5.1. Quantification results

Biochar is the solid phase recuperated from HTL process. It's a black solid, distributed between volatiles and ashes. The results obtained from its analysis and quantification are mentioned in Table 8. Biochar yield was negatively affected by the increase of temperature. From 240ºC until 300ºC, the percentage of biochar decreased from 37.45 until 20.76% (w/w). At higher conditions, this percentage remained almost constant, around 20.50 % (w/w). Ash content (inorganic fraction) and volatile content (organic fraction) were analysed after each

experiment. In general, ashes were consumed in the biochar and organics were transferred to biocrude along with the increase of temperature.

Table 8. Solid phase yield and characterization after HTL at different temperatures. Time of reaction: 0 min. Stirring: 100 rpm.

Temperature (ºC)	Biochar weight (g)	Biochar % (TS basis)	Ash % (Biochar basis)	VS % (Biochar basis)
240	8.07	37.45	29.83	70.17
270	5.95	28.28	42.67	57.33
300	4.15	20.73	61.71	38.29
320	4.92	21.37	69.99	30.01
340	4.37	20.26	76.45	23.55

3.5.2. Elemental composition and HHV analysis

HHV with C, H, N and O values of biochar at all conditions are presented in Table 9. HTL process of primary sludge was able to form a product with high energy source. especially at high conditions. Solid phase reached a maximum HHV of 41.84 MJ/kg with a maximum carbon content of 80.78 % at 300ºC. Consequently, biochar could be implemented in the heat and power generation and adsorption treatments (Amin et al. 2016). Also, it can improves significantly plant growth and it is appropriate as a soil amendment (Santos et al. 2018).

Table 9. Elemental analysis and HHV of biochar at different temperatures. Time of reaction: 0 min. Stirring: 100 rpm.

Conditions		% C	% H	% N	% O	HHV% (MJ/kg) *
t=0 mins	240ºC	53.93	7.66	2.63	35.78	22.78
	270ºC	59.30	7.94	3.09	29.67	26.09
	300ºC	80.78	10.71	4.26	4.24	41.84
	320ºC	79.53	10.74	3.43	6.31	41.08
	340ºC	76.03	9.88	4.94	9.15	38.17

* Calculated with Dulong equation (Hong et al., 2021)

3.5.3. Heavy metals

SEM images and EDX spectra ash in biochar are presented in Figure 10. In general, heavy metals were detected in different quantities in the biochar. The most abundant ones retrieved were Fe, Ca, P, Si, Al, S, and Mg. In fact, inorganic salts and heavy metals are mainly converted into solid phase as they could not be liquified easily through the process (Liu et al. 2018).

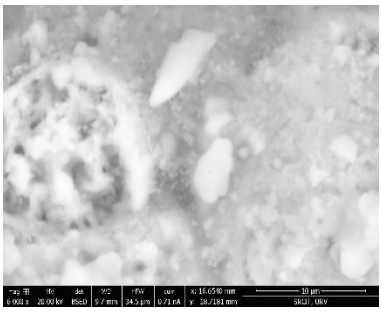

SEM image location (a)

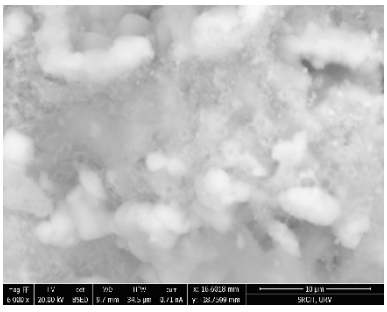

SEM image location (b)

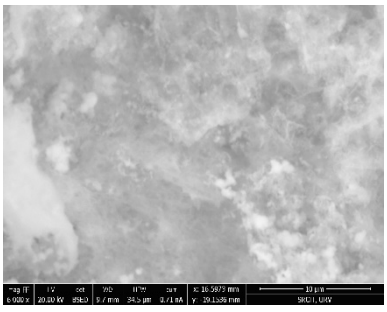

SEM image location (c)

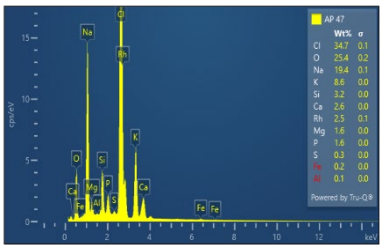

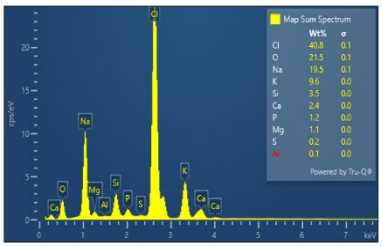

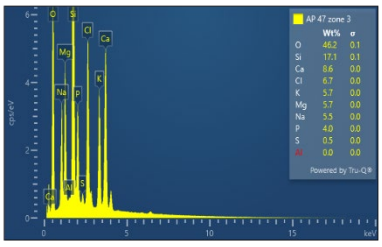

EDX spectra location (a) EDX spectra location (b) EDX spectra location (c)

Figure 10. SEM images and EDX spectra (a), (b) and (c) of ash in aqueous phase. HTL operation conditions: temperature at 340ºC. Time of reaction: 0 min. Stirring: 100 rpm. represent three different observation locations of the sample.

2165

2166 **3.6. Biogas**

2167 The composition of biogas produced from HTL of primary sludge at different temperatures for
2168 0 min are shown in table 10. Only small fractions of biogas were generated. At all conditions,
2169 0.004 mol % C_2H_4 was produced. At 240ºC, 0.042 mol % CO_2 was obtained. CH_4 was detected
2170 at higher temperatures. Gas composition at 300 ºC and 320ºC was very similar. CH_4 was
2171 observed with 0.035 mol % and 0.038 mol %. CO_2 was detected with 0.0487 mol % and 0.0495
2172 mol %. At 320 ºC alone, some CO was found with 0.115 mol %. At 340 ºC, more CH_4 was
2173 detected, 0.133 mol % respectively and 0.0465 mol % of CO_2 was noted. The increase of
2174 temperature promoted the production of more gases.

Table 10. Biogas composition at different temperatures. Reaction time: 0 min. Stirring: 100 rpm.

Conditions		Yield (%, VS basis)	Biogas composition (mol%)				
			CH_4	CO	CO_2	C_2H_4	C_3H_6
t=0 mins	240ºC	21.46	N.D.	N.D.	0.047	0.004	N.D.
	270ºC	31.93	N.D.	N.D.	N.D.	N.D.	N.D.
	300ºC	37.14	0.035	N.D.	0.0485	0.004	N.D.
	320ºC	40.33	0.038	0.115	0.0495	0.004	N.D.
	340ºC	41.96	0.133	N.D.	0.0465	0.004	N.D.

N.D.: Not detected

4. Conclusions

Primary sludge supplied by WWTP of Reus is a convenient feedstock for HTL conversion process as it contains high moisture content (95.70 %) and more importantly high organic contents (77.12 %). The parameter of temperature has significantly affected the yield and quality of products obtained. The optimum condition was 300ºC with 38.30 % (w/wVS) of biocrude. At the same temperature, the percentage of biochar was 20.75 % (w/wVS). After HTL conversion, biocrude should be subjected to further treatments in order to improve its quality. Similarly, biochar and aqueous phase, containing still organic fractions, should be studied more for valorization purposes.

Acknowledgment

Authors thank the collaboration of the public company Gestió Ambiental i Abstament S.A. (WWTP in Reus, Spain). Jacky Cheikhwafa thanks the Agència de Gestió d'Ajuts Universitaris i de Recerca (AGAUR) of Catalan Government for the pre-doctoral contract (Ajuts per a la contractació de personal investigador predoctoral en formació, 2019 FI-B 00743). This work

is part of the PECT “Cuidem el que ens uneix/Pobles Vius i Actius/Ebrebioterritori" project, within the frame of the RIS3CAT and ERDF Catalonia Operational Programme 2014-2020. It is co-financed by the Catalan Government and the Provincial Council of Tarragona. The authors from Universitat Rovira i Virgili are recognised by the Comissionat per a Universitats i Recerca del DIUE de la Generalitat de Catalunya (2017-SGR-396) and supported by the Universitat Rovira i Virgili (2017PFR-URV-B2-33).

References

Amin, F. R., Huang, Y., He, Y., Zhang, R., Liu, G., & Chen, C. W. (2016). Biochar applications and modern techniques for characterization. Clean Technologies and Environmental Policy, 18(5), 1457-1473. *https://doi.org/10.1007/s10098-016-1218-8*

APHA. (2012). Standard method 2540G (22nd ed.).

APHA. (2012). Standard method 5520E (22nd ed.).

Biller, P., Johannsen, I., dos Passos, J. S., & Ottosen, L. D. M. (2018). Primary sewage sludge filtration using biomass filter aids and subsequent hydrothermal co-liquefaction. *Water Research*, *130*, 58–68. *https://doi.org/10.1016/j.watres.2017.11.048*

Budych-Gorzna, M., Szatkowska, B., Jaroszynski, L., Paulsrud, B., Jankowska, E., Jaroszynski, T., & Oleskowicz-Popiel, P. (2021). Towards an Energy Self-Sufficient Resource Recovery Facility by Improving Energy and Economic Balance of a Municipal WWTP with Chemically Enhanced Primary Treatment. *Energies*, *14*(5), 1445. *https://doi.org/10.3390/en14051445*

Dubois et. al., (1956). Total sugar determination by phenol sulphuric method. Analytical Chemistry, 28 (1956), 350-356.

Fan, Y., Fonseca, F. G., Gong, M., Hoffmann, A., Hornung, U., & Dahmen, N. (2021). Energy valorization of integrating lipid extraction and hydrothermal liquefaction of lipid-

extracted sewage sludge. Journal of Cleaner Production, 285, 124895. https://doi.org/10.1016/j.jclepro.2020.124895

Ghadge, R., Nagwani, N., Saxena, N., Dasgupta, S., & Sapre, A. (2022). Design and scale-up challenges in hydrothermal liquefaction process for biocrude production and its upgradation. Energy Conversion and Management: X, 14, 100223. *https://doi.org/10.1016/j.ecmx.2022.100223*

Hao, B., Xu, D., Jiang, G., Sabri, T. A., Jing, Z., & Guo, Y. (2021). Chemical reactions in the hydrothermal liquefaction of biomass and in the catalytic hydrogenation upgrading of biocrude. *Green Chemistry*, *23*(4), 1562–1583. *https://doi.org/10.1039/d0gc02893b*

Hao, B., Yang, W., Wang, Y., Xu, D., Kapusta, K., & Guo, Y. (2022). Hydrothermal liquefaction of municipal sludge: Coupling effects of temperature and time on nitrogen migration. *Journal of Analytical and Applied Pyrolysis*, *165*, 105562. https://doi.org/10.1016/j.jaap.2022.105562

Incorporating hydrothermal liquefaction into wastewater treatment – Part I: Process optimization for energy recovery and evaluation of product distribution. Chemical Engineering Journal,137838. *https://doi.org/10.1016/j.cej.2022.137838*.

Li, R., Ma, Z., Yang, T., Li, B., Wei, L., & Sun, Y. (2018). Sub–supercritical liquefaction of municipal wet sewage sludge to produce bio-oil: Effect of different organic–water mixed solvents. Journal of Supercritical Fluids, 138, 115–123. *https://doi.org/10.1016/j.supflu.2018.04.011*

Liu, H., Basar, I., Eskicioglu, C. (2023). Hydrothermal liquefaction for sludge-to-energy conversion: An evaluation of biocrude production and management of waste streams. *Energy, 128268*. *https://doi.org/10.1016/j.energy.2023.128268*.

Liu, R., Tian, W., Kong, S., Meng, Y., Wang, H., & Zhang, J. (2018). Effects of inorganic and organic acid pretreatments on the hydrothermal liquefaction of municipal secondary sludge. Energy Conversion and Management, 174, 661-667. *https://doi.org/10.1016/j.enconman.2018.08.058*

Lowry et. al., (1951). Protein measurement with the folin phenol reagent. Biological Chemistry, 193(1951), 265-275.

Marrone, P. A. (2016). Genifuel Hydrothermal Processing Bench-Scale Technology Evaluation Report. *Water Intelligence Online*, *15*(0), 9781780408408-9781780408408. *https://doi.org/10.2166/9781780408408*

Mishra, S., & Mohanty, K. (2020). Co-HTL of domestic sewage sludge and wastewater treatment derived microalgal biomass – An integrated biorefinery approach for sustainable biocrude production. *Energy Conversion and Management*, *204*, 112312. *https://doi.org/10.1016/j.enconman.2019.112312*

Nazem, M. A., & Tavakoli, O. (2017). Bio-oil production from refinery oily sludge using hydrothermal liquefaction technology. *The Journal of Supercritical Fluids*, *127*, 33–40. *https://doi.org/10.1016/j.supflu.2017.03.020*

Obeid, R., Smith, N., Lewis, D. M., Hall, T., & van Eyk, P. (2022). A kinetic model for the hydrothermal liquefaction of microalgae, sewage sludge and pine wood with product characterisation of renewable crude. *Chemical Engineering Journal*, *428*, 131228. https://doi.org/10.1016/j.cej.2021.131228

Penke, C., Moser, L., & Batteiger, V. (2021). Modeling of cost optimized process integration of HTL fuel production. *Biomass and Bioenergy*, *151*, 106123. *https://doi.org/10.1016/j.biombioe.2021.106123*

Qian, L., Wang, S., & Savage, P. E. (2020). Fast and isothermal hydrothermal liquefaction of sludge at different severities: Reaction products, pathways, and kinetics. *Applied Energy*, *260*, 114312. https://doi.org/10.1016/j.apenergy.2019.114312

Qian, L., Wang, S., & Savage, P. E. (2020). Fast and isothermal hydrothermal liquefaction of sludge at different severities: Reaction products, pathways, and kinetics. Applied Energy, 260, 114312. *https://doi.org/10.1016/j.apenergy.2019.114312*

Saner, A., Carvalho, P., Catalano, J., & Anastasakis, K. (2022). Renewable adsorbents from the solid residue of sewage sludge hydrothermal liquefaction for wastewater treatment. *Science of The Total Environment*, 156418. *https://doi.org/10.1016/j.scitotenv.2022.156418*

Santos, F. M., & Pires, J. C. (2018). Nutrient recovery from wastewaters by microalgae and its potential application as bio-char. Bioresource Technology, 267, 725-731. https://doi.org/10.1016/j.biortech.2018.07.119

Shah, A. A., Toor, S., Conti, F., Nielsen, A. H., & Rosendahl, L. (2020). Hydrothermal liquefaction of high ash containing sewage sludge at sub and supercritical conditions. Biomass and Bioenergy, 135, 105504. https://doi.org/10.1016/j.biombioe.2020.105504

Snowden-Swan, Lesley J., Zhu, Yunhua, Bearden, Mark D., Seiple, Timothy E., Jones, Susanne B., Schmidt, Andrew J., Billing, Justin M., Hallen, Richard T., Hart, Todd R., Liu, Jian, Albrecht, Karl O., Fox, Samuel P., Maupin, Gary D., & Elliott, Douglas C.. *Conceptual Biorefinery Design and Research Targeted for 2022: Hydrothermal Liquefacation Processing of Wet Waste to Fuels*. United States. *https://doi.org/10.2172/1415710*

Song, H., Yang, T., Li, B., Tong, Y., & Li, R. (2022). Hydrothermal liquefaction of sewage sludge into biocrude: Effect of aqueous phase recycling on energy recovery and pollution mitigation. *Water Research*, *226*, 119278. *https://doi.org/10.1016/j.watres.2022.119278*

Thomsen, L.,Carvalho, P., Passos, J., Anastakis, K., Bester, K., & Biller, P. (2020). Hydrothermal liquefaction of sewage sludge; energy considerations and fate of micropollutants during pilot scale processing. *Water Research*, *183*, 116101. https://doi.org/10.1016/j.watres.2020.116101

Thomsen, L., Anastasakis, K., & Biller, P. (2022). Wet oxidation of aqueous phase from hydrothermal liquefaction of sewage sludge. *Water Research, 209,* 117863. https://doi.org/10.1016/j.watres.2021.117863

Wang, J., Liu, G., Shao, Y., Zhang, Q., Wei, Q., Luo, F., Sun, W., Liu, S., Liu, Y., Zhang, J., Qi, L., & Wang, H. (2021). Regulation of anaerobic fermentation for producing short-chain fatty acids from primary sludge in WWTPs by different alkalis. *Journal of Environmental Management*, *299*, 113623. https://doi.org/10.1016/j.jenvman.2021.113623

Watson, J., Wang, T., Si, B., Chen, W. T., Aierzhati, A., & Zhang, Y. (2020). Valorization of hydrothermal liquefaction aqueous phase: pathways towards commercial viability. *Progress in Energy and Combustion Science*, *77*, 100819. https://doi.org/10.1016/j.pecs.2019.100819

Xu, D., Lin, G., Liu, L., Wang, Y., Jing, Z., & Wang, S. (2018). Comprehensive evaluation on product characteristics of fast hydrothermal liquefaction of sewage sludge at different temperatures. Energy, 159, 686–695. https://doi.org/10.1016/j.energy.2018.06.191

Xu, Y. H., & Li, M. F. (2021). Hydrothermal liquefaction of lignocellulose for value-added products: Mechanism, parameter and production application. *Bioresource Technology*, *342*, 126035. https://doi.org/10.1016/j.biortech.2021.126035

Yang, J. H., Shin, H. Y., Ryu, Y. J., & Lee, C. G. (2018). Hydrothermal liquefaction of Chlorella vulgaris: Effect of reaction temperature and time on energy recovery and nutrient recovery. *Journal of Industrial and Engineering Chemistry*, *68*, 267–273. https://doi.org/10.1016/j.jiec.2018.07.053

Zhu, Y., Zhao, Y., Tian, S., Zhang, X., & Wei, X. (2022). Catalytic hydrothermal liquefaction of sewage sludge: Effect of metal support heterogeneous catalysts on products distribution. *Journal of the Energy Institute*. https://doi.org/10.1016/j.joei.2022.04.0

2314

4

Depolymerization of lipid-based primary sludge to high-quality biocrude with homogeneous and heterogeneous catalysts

ABSTRACT

Hydrothermal liquefaction process is a promising technique that converts the wet biomass, primary sludge, to biocrude and other valuable products. The introduction of catalysts in the process for the purpose of optimization gained a great attention. Homogeneous catalysts including $CuSO_4$, Na_2CO_3 and K_2CO_3 and heterogeneous catalysts including Pt/Al, Pd/Al, MoS_2, TgS_2, TiO_2 and Ni over Si/Al were employed in HTL process in different amounts and their influence on the products distribution was studied. Among all, biocrude yield was improved to 42.20, 41.52 and 40.13 % with 10 % of $CuSO_4$, 5% of TiO_2 8 g of Pt/Al. Though, the effect of catalyst on the quality of biocrude and other products was either negligeable or negative. Biocrude contained heavy and long chain compounds with a HHV not higher than 39.24 MJ/kg. Biochar, having high ash content and low carbon content, reached a HHV lower than 20 MJ/kg. Whereas, for aqueous phase, the presence of catalyst didn´t make any important change on its properties. The composition of biogas varied between CO, CO_2 and hydrocarbons, but in small fractions.

1. Introduction

Municipal waste sludge is a nutrient-rich by-product generated from the wastewater treatment process. The composition of sludge is complex and difficult to treat as it contains organic contaminants. Conventional treatments of sewage sludge include incineration, landfarming, biological composting and oxidations. However, they have changing degrees of limitations in processing cost, efficiency and effectiveness (Dang et al., 2021). Hydrothermal liquefaction (HTL), performed at high temperature and high pressure, represents a promising route to convert a wet organic feedstock (municipal sludge) into an intermediate fuel (Bio-crude) by mean of a solvent, usually water, without high-cost drying steps. It is accomplished by the hydrolysis of bio-constituents of the wet biomass and by the improvement of the depolymerization products to simple organic molecules (Prestigiacomo et al., 2021). Solid phase noted as Bio-char, gaseous phase and aqueous phase containing water-soluble products are co-products (Dimitriadis et al., 2017). Biocrude yield from HTL of municipal sewage sludge changes from 10 to 48 wt % in the previous studies (Qian et al., 2017). Lately, the researchers have considered different strategies to improve the quality and production of biocrude from municipal sewage sludge. The effect of temperature (260 – 350 °C) on the products distribution was studied by Xu et al. in the HTL of secondary municipal sludge. It was found that high temperature improved the quality of biocrude and the yield of gas and lowered the yield of solid phase and the total organic carbon in the aqueous phase (Xu et al., 2018). Hao et al. investigated the influence of time (10 – 50 mins) on the HTL process. The results showed that long reaction time increased the yield of biocrude and decreased the yield of solid phase (Hao et al., 2022). However, Biocrude obtained in HTL is generally very viscous at room temperature and has a very high heteroatom content (mainly oxygen and nitrogen) and has low heating

value to be used directly as fuel, so it needs important upgrading (Haider et al., 2020 and Galadima et al., 2018). At present, some studies have introduced the catalyst in HTL process for helping the extraction efficiency of biocrude (Dang et al., 2021). The acquisition of catalysts in HTL of wet biomass could improve biocrude yield and decreases its O, N and S concentrations (Prestigiacomo et al., 2021). Homogeneous catalysts like organic acids or alkali catalysts and *heterogeneous catalysts* such as *supported metal catalysts* or zeolite have been considered, respectively (Hosseini et al., 2022). Significant studies proved that homogeneous alkaline catalysts (like K_2CO_3, and KOH) were able to effectively improve the quality and yield of biocrude by restraining repolymerization reactions (Shah et al., 2020). The optimum conditions 300 °C with 5 % $FeSO_4$ were reported for maximum bio-crude yield (47.79 %) (Malins et al., 2015). The highest yield of biocrude (47.45 %) from municipal sewage sludge was attained with $CuSO_4$ catalyst at 270 °C for 30 min (Wang et al., 2018). Whereas, heterogeneous catalysts are seen to be a very attracting option as they assist the upgrading of biocrude during its production and, generally, they can be separated from the reaction products (Prestigiacomo et al., 2021). For example, Ru/C was selected as the best catalyst to remove heteroatoms from biocrude elsewhere (Costanzo et al., 2016). 34.2 wt% was the highest biocrude yield obtained from dewatered sewage sludge with 10 wt% Co-Mo/ATP catalysts at 320 °C for 15 min reaction time (Zhu et al., 2022). Primary sludge, containing high moisture and volatile content, was considered as a convenient feedstock for the HTL process. The effects of temperature and reaction time on the products distribution and the quality of biocrude were completed as well. Yet, biocrude produced contained a critical amount of oxygen, diminishing its use in further applications (Cheikhwafa et al.,). Therefore, a hypothesis using different type of catalysts in HTL of PS to improve biocrude yield, energy efficiency and quality was

proposed. The purpose of this work is to utilize various catalysts (homogeneous and heterogeneous) for improvement of biocrude production. The elemental and chemical composition of biocrude and other co-products were analysed.

2. Experimental part

2.1. Materials

Reagents

Dichloromethane 99,9 % (ref.: 32222) was obtained from Honeywell. n-Hexane 95 % (ref.: 363242), high performance chromatography grade, and phenol crystalline (ref: 144852.1211) were supplied by PanReacAppliChem. Sulfuric acid reagent (ref: 34632), orange reagent (ref: 131130.1612), sulfuric acid 95.0–97.0 % (ref: 30743), bovine serum albumin (BSA) (ref: A9647), sodium hydroxide 98 % (ref: 30620), sodium carbonate (ref: 222321), potassium sodium tartrate tetrahydrate (ref: 217255), copper (II) sulphate pentahydrate (ref: 209198), Folin&Ciocalteu's phenol reagent (ref: F9252), magnesium sulphate monohydrate (ref: 434183), anhydrous sodium sulphate (ref: 239313), and fuming hydrochloric acid (ref: 84418), high analytical reagent grade, were purchased from Sigma - Aldrich.

Catalysts

Homogeneous catalysts including sodium carbonate, ACS reagent, anhydrous granular 99.5 % (ref: 22231), potassium carbonate GR for analysis 100 % (ref: 1066830500) and cupric sulfate anhydrous 99 % (C-1297) and heterogeneous catalysts comprising Titanium (IV) oxide 99-100.5 % (ref:14027), platinum on alumina 0.5 wt % loading, pellets (ref: 206016), palladium on alumina 0.5 wt % loading, pellets (ref: 205745), Molybdenum (IV) sulfide 98 %

(ref:234842), Tungsten (IV) sulfide 99 % (ref:243639) and Nickel on silica/alumina (ref:208779) were all purchased from Sigma-Aldrich.

Primary sludge: Collection and management

The municipal wastewater treatment plant of Reus in Tarragona, Spain provided samples of primary sludge. 500 ml bottles of sludge were sampled after partial gravity thickening of the primary treatment. They were deposit in a freezer at -15 °C and defrosted in an oven at 60 °C for 5 hours. The bottles of sludge were utilized directly as received.

Characterization

A full characterization of primary sludge was repeated at least three times. Total solids (TS), volatile solids (VS) and ash content were analyzed according to standard methods 2540B and 2540E respectively (Rice et al., 2012). Extraction of lipids was completed in a Soxhlet apparatus using hexane as a solvent, according to standard method 5520E (Rice et al., 2012). Total carbohydrate percentage was measured by phenol-sulfuric acid Dubois method (Dubois et al., 1956). Shortly, 0.05 mL of 80 % phenol solution was added to 2 mL of diluted sludge sample in a glass tube. Then, 5 mL concentrated sulfuric acid was quickly added. The tubes were kept under room temperature for 10 min and then placed into a thermostatic bath at 30 ℃ another 15 min. The absorbance was measured at 480 nm. Protein content was detected with Lowry method (Lowry et al., 1951). The protein solubilization in the sludge samples was completed by heating the samples with 2 M sodium hydroxide at 100°C for 10 min in a digester. The absorbance was measured at 750 nm. Finally, elemental analysis was acquired by Serveis Técnics de Recerca at Universitat de Girona. Analysis was carried out using an elemental

analyzer (Perkin Elmer model EA2400). C, H and N were determined, and O was calculated by difference.

2.2. Experimental procedure: Catalytic Hydrothermal liquefaction

The experiments were accomplished in a 1 L Stainless Steel Autoclave (Autoclave Engineers model EZE Seal) surrounded by a movable heating shell, a fixed MagneDrive® stirrer (magnetically coupled, packless rotary impeller system) and an operating condition controller. The reactor is connected to a gas line through an inlet valve allowing the purging of nitrogen. The outlet valve is connected to a gas flow meter and a Tedlar bag push lock valve 0.6 L (Superlco 30289-U) for gas collection. A bottle containing approximately 500 g of primary sludge was unloaded in the reactor. Pure nitrogen gas was introduced three times to create an atmosphere free of oxygen and then pressurized up to 1 bar as an initial pressure. HTL experiments were always completed at a temperature of 300°C (~86.9 bar), a reaction time of 30 min and an agitation rate of 100 rpm. Catalysts (homogeneous and heterogeneous) were added at 5 wt%, 10 wt% and 20 wt% with respect to dry feedstock. The pressure of the reaction was not controlled and retained as auto generated with respect to its reaction temperature. The heating up time was recorded as 2 hours, based on the condition chosen. After achievement of each batch experiment, the reactor was cooled down in a room temperature water bath (~25°C) until going back to its initial condition.

2.3. Products separation

Figure 1 presents the schematic diagram of the experimental separation procedures after HTL of PS. The products obtained from the hydrothermal liquefaction of primary sludge are distributed into 4 different phases: gas, organic, aqueous and solid.

When the reactor was returned to laboratory ambient temperature and atmospheric pressure, the gas phase was vented. The output gas was passed through a flow meter, indicating the volume of the gas mixture, and collected in the gas bag. Then, the reactor was opened, and the mixture was poured into a large beaker. The solid phase was separated from the liquid phase through vacuum filtration. The filtrate, mainly containing the aqueous phase and a small part of the organic phase, was moved into a bottle. Simultaneously, the reactor was washed with dichloromethane several times until being totally clean to recover the organic remaining part, deposited on the walls, on the cover of the reactor and, in the agitation module. After that, the mixture, where a part of solids was captured by the organics, was separated via vacuum filtration. The liquid part (organic phase and dichloromethane) was transferred into another bottle. The solid retained on the filter paper, biochar and ashes, was washed with dichloromethane repeatedly. The biochar was dried in the oven for 24 hours at 105ºC. In the scenarios where heterogeneous catalysts were used in the form of pellets, they were collected with the solid phase, dried in the oven and recuperated separately. The quantification of biochar was done by taking into account the amount of catalyst used.

A small amount of dichloromethane was added to the aqueous phase. Then, the mixture was centrifuged at 8000 rpm for 5 minutes. The upper phase containing the dichloromethane and organics was added to the organic phase previously separated. The lower phase is the aqueous phase containing soluble organic molecules.

Dichloromethane was separated from the organic phase by the rotary evaporation, at 65ºC and atmospheric pressure. The viscous organic liquid obtained is the bio-crude, that it was further weighted for quantification. Finally, bio-crude was divided into oils and asphaltenes by Soxhlet extraction using 200 mL of hexane. Hexane was evaporated from oils by rotary evaporation at

65ºC and vacuum pressure of 273 bar. Asphaltenes were calculated by the difference between biocrude and oils.

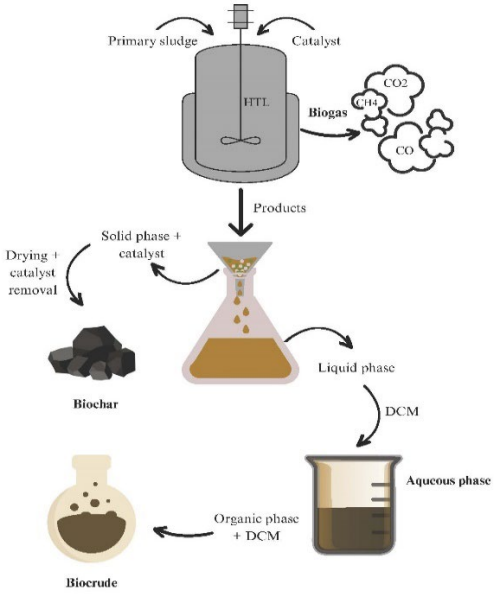

Figure 1. Process overview of catalysed HTL of primary sludge.

2.4. Analytical method

2.4.1. Biocrude

The characterization of biocrude was very wide. The weight and ash content were done. Gas chromatography/mass spectrometry (GC/MS), thermogravimetric analysis (TGA), elemental (ultimate) analysis, determination of higher heating value (HHV), Fourier transform infrared spectroscopy (FTIR), nuclear magnetic resonance (NMR) and simulated distillation (SimDis) were achieved. Finally, saturated, aromatics, resins and asphaltenes (SARA) fractions of biocrude were considered.

Gas chromatography/mass spectrometry spectroscopy of biocrude

The samples of biocrude with all catalysts were characterized by gas chromatography-mass spectroscopy (GC/MS) using a Perkin Elmer Turbo Mass Gold GC/MS, equipped with a Supelco SLB®-5ms capillary GC column (L × I.D. 30 m × 0.25 mm, d_f 0.25 μm). Solvent used was dichloromethane. The GC oven was maintained at 70ºC for 1 min, heated to 180ºC at a rate of 7ºC/min, then heated to 240ºC at a rate of 12ºC/min and finally 7 min hold at 330ºC.

Thermogravimetric analysis of biocrude

The weight loss properties of biocrudes were studied by thermogravimetric analysis (TGA). In each test, about 3 to 4 mg of sample was heated from 30°C to 800°C at a nitrogen flow of 60 mL/min and a 10 K/min heating rate (Zhu et al., 2022).

Ultimate analysis and HHV of biocrude

Ultimate analysis of biocrude samples was also realized by Serveis Técnics de Recerca at Universitat de Girona as commented in section 2.4. C, H and N were quantified, and O calculated by difference. Then, the higher heating values of (HHVs) of biocrude were calculated (Hong et al., 2021).

FTIR of biocrude

FTIR spectra were collected using a Thermo Nicolet Nexus 670 Fourier Transform Infrared Spectrophotometer equipped with a single-bounce diamond attenuated total reflectance (ATR) accessory (Specac Golden Gate) and KBr beam splitter. Spectra were collected from 4000 to 500 cm^{-1} with 0.98-cm^{-1} resolution and averaged over 50 replicate scans using Omnic software.

Background scans were conducted of the dry accessory at ambient temperature. The spectra were then collected after smearing about 30 mg of sample directly on the ATR crystal surface.

^{1}H NMR of biocrude

^{1}H NMR spectra were collected using a Varian Unity 400-MHz spectrometer outfitted with a 5-mm broadband probe. 50–75 mg of biocrude were dissolved in deuterated chloroform containing 0.03% tetramethylsilane (TMS) as an internal reference. Samples were then filtered (0.22-lm PTFE) to remove any suspended particulates before loading into 5 mm diameter NMR tubes. ^{1}H spectra were acquired with a 90^{o} pulse angle, spinner frequency of 20 Hz, sweep width of 8000 Hz across 32 transients.

Simulated distillation of biocrude

Simulated distillations were modeled after ASTM-D2887 method and performed using a HP 5890 Series II FID gas chromato-graph and a Durabond DB-HT-SimDis GC column by Agilent-J&WScientific (5 m0.53 mm id, 0.15µm film). Helium (56.4 mL/min) was used as the carrier gas. The oven temperature was initially set to 36°C, and raised to 400°C at 10°C/min and then held constant for 10 min. The injector volume was set to 0.5 µL and the injector temperature was set to 350ºC. Detector temperature was set to 375°C, hydrogen gas set to 40 ml/min, airflow set to 400 ml/min, and helium makeup set to 24 ml/min. Samples (1% w/w) and reference standards (0.5% w/w) were dissolved in DCM. Samples were filtered (0.22 µm PTFE) to remove any suspended particulates. Boiling points were determined in accordance to a D2887 calibration mix and a D2887 Reference Gas Oil standard, both purchased from sigma Aldrich. Data (retention time and areas) were collected. Each sample was distributed between fractions (%wt) and boiling points were calculated accordingly.

Quantification of SARA fractions of biocrude

SARA fractions of biocrude were analysed. The separation of light phase and heavy phase was repeated as mentioned above, but with n-heptane. Maltenes were separated into saturated hydrocarbons with 20 mL of n-heptane using activated alumina in a glass chromatographic column. Then, aromatics were extracted by mean of 20 mL of toluene. Finally, polars were removed from the adsorbent using 20 mL of a mixture of toluene and 2-propanol (1:1). Remaining resins were also removed using 20 ml of methanol. Each eluted fraction was recovered by solvent removal using a Rotary evaporator.

2.4.2. Biochar

Total solids, moisture content, volatile solids and ash content were determined in biochar according to standard methods 2540B and 2540E respectively (Rice et al., 2012). Also, ultimate analysis and heavy metals detection were done by following the same procedures described above.

2.4.3. Aqueous phase characterization

COD, TOC, TN, proteins, and carbohydrates were measured or analysed for the aqueous phase. COD analysis was performed according to standard method 5220D (Rice et al., 2012). TOC was analysed by using a TOC analyser TOC-L Series based on a specific standard calibration curve. Total organic carbon (TOC) was measured by ASI-L auto sampler Shimadzu into a Shimazdu TOC-L CSN TOC analyser provided with a NDIR detector and calibrated with standard solutions of hydrogen potassium phthalate. Total dissolved nitrogen was measured in the same TOC analyser coupled with TNM-L ROHS unit (Ponces-Robles et al., 2018). Protein

amount was measured according to Lowry method (Lowry et al., 1951) and carbohydrates were quantified following Dubois method (Dubois et al., 1956) as described in the previous section (2.3). Total solid (TS), volatile solid (VS) and ash content were measured in the aqueous phase as well. A specific volume of aqueous phase was dried in a weighted crucible for 24 hours in the oven at 100ºC then burned in the furnace at 550ºC for 1 hour, as detailed by the standard methods 2540B and 2540E respectively (Rice et al., 2012). Measurement of pH value in the HTL aqueous phase was performed by pH meter. Heavy metals were analysed in the ash of the solid dissolved in the aqueous phase by following the same procedure mentioned before.

2.4.4. Biogas

Identification and quantification of biogas were finalized by a gas chromatograph (micro-GC, Agilent, 990) equipped with a thermal conductivity detector (TCD). A MS5A SS 10MX0.25MMX30UM BF RTS, CP-PORABOND Q 5MX0.25MMX3UM column (column 1) was used to separate the light gases using Argon as a carrier gas and a PORAPLOT Q UM 10MX0.25MMX8UM BF, CP-PORABOND Q 1MX0.25MMX3UM column (column 2) was used to separate heavy gases using helium as a carrier gas. Column 1 was maintained at injector temperature 100ºC, injection time 40 ms, column temperature 100ºC and initial pressure 200 kPa. Column 2 was maintained at injector temperature 100ºC, injection time 40 ms, column temperature 60ºC and initial pressure 150 kPa. The run time was 120 s. The mole percentage of each gas was determined with respect to gas standards prepared by Carburos Metálicos, S.A.

2.5.Calculations

The bio-oil yield was calculated from equation (1):

$$Bio-crude\ yield\ (\%) = \frac{Mass\ of\ bio-crude}{Mass\ of\ volatile\ solids} \times 100 \quad (1)$$

The aqueous phase yield was calculated from equation (2):

$$Aqueous\ phase\ yield\ (\%) = \frac{Mass\ of\ solids\ dissolved\ in\ aqueous\ phase}{Mass\ of\ volatile\ solids} \times 100 \quad (2)$$

The solid yield was calculated from equation (3):

$$Biochar\ yield\ (\%) = \frac{Mass\ of\ solid\ residue}{Mass\ of\ volatile\ solids} \times 100 \quad (3)$$

In some cases, the amount of catalyst should be subtracted from the total amount of solid phase obtained after drying.

The gas yield was calculated from equation (4):

$$Gas\ yield\ (\%) = \frac{Mass\ of\ gas}{Mass\ of\ volatile\ solids} \times 100 \quad (4)$$

In all the equations, mass of volatile solids is referred to that of primary sludge.

HHV is calculated through Dulong formula and expressed in MJ/kg.

$$\mathrm{HHV}\ (\%) = 0.3383 \cdot \mathrm{C} + 1.443 \cdot \left(\mathrm{H} - \frac{\mathrm{O}}{8}\right) \quad (5)$$

C, H and O are the mass percentages of carbon, hydrogen, and oxygen from the ultimate analysis of the samples, respectively.

3. Results and discussion

3.1. Characterization of feedstock

Table 1 presents the physiochemical properties of primary sludge. The wet primary sludge contained 95.70 % of moisture. Total solids accounted to 4.30 % of wet primary sludge. 77.15 % of total solids were volatile solids, occupying 3.32 % of wet primary sludge in total solids basis. The rest, 0.98 % were ashes.

Carbohydrate, protein and lipid contents were considered as organic content in primary sludge. Carbohydrate occupied the highest fraction (29.84 %). Definitely, the values of proteins (21.15 %) and lipids (oil, greases, fats and long fatty acids) (23.41 %) were considered important. Ashes were 22.88 %. In terms of energy source, primary sludge covered low nitrogen content (3.71 %), low hydrogen content (5.34 %), but high carbon content (36.86 %) and high oxygen content (54.12 %), resulting in a higher heating value (HHV) of 10.37 MJ/kg. The total solid percentage was very low, less than 5 %. The initial concentration of the primary sludge used in the HTL conversion of wastewater solids to fuels was 4.5 wt % (Marrone et al., 2018). The density of primary sludge was 1.01 g/ml, similar to that of water. HTL process is a convenient alternative for handling high moisture content solids as water is used as medium to hydrolyse the organic matter into nearly simpler chemicals at high temperatures and pressures (Krishnan et al., 2022). Lipids in PS are produced from free fatty acids in the range of C10 to C18 which are precursors for esters production. Also, proteins are confirmed to be supporters for biocrude production through HTL. Maillard reactions represent a significant part in the distribution of biocrude and composition, originated from the reaction of amine groups present in proteins with carbonyl groups present in reducing carbohydrates (Fan et al., 2021). PS, including a high moisture content, is rich in lipids, proteins and carbohydrates. Therefore, HTL is supposed to be an ideal option for thermally hydrolysing the macromolecules into valuable chemicals and PS helps in validating an economically viable and energy-efficient sludge biorefinery approach.

Table 1. Physiochemical properties of primary sludge received from WWTP of Reus.

Moisture content*	**Ash content***	**Organic matter***		
		Protein	**Carbohydrate**	**Lipid**
95.7	22.9	21.2	29.8	23.4
Elemental composition				**HHV (MJ/kg)**
C	**H**	**N**	**O****	
47.81	6.93	4.81	40.45	18.83
TOC (mg/L)	**Density (g/mL)**	**COD (mg/L)**		
6290	1.01	35180		

*Average of at least three assays

** Calculated by difference

3.2. The effect of catalyst on products distribution and quality

Series of HTL experiments were performed using different catalysts, either homogeneous or heterogeneous, either powder or pellets, to understand the product distribution profiles obtained (biocrude, biochar, biogas and aqueous phase). In all the scenarios, the parameters were set to 300 ºC for temperature, 30 min for reaction time and 100 rpm for agitation rate. An experiment at the same conditions without any catalyst was used as a control test. Figure 2 present the yields of biocrude and Table 4 present the composition of biocrude, asphaltenes and oils.

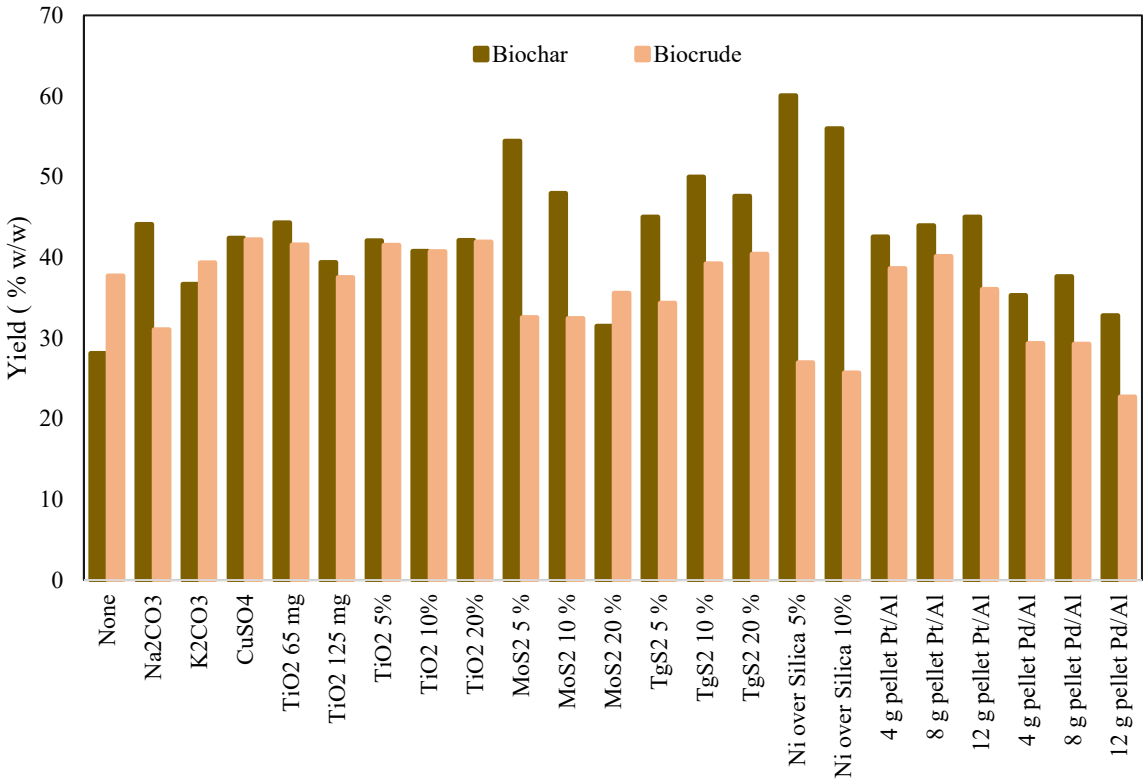

Figure 2. Biochar and biocrude yields from HTL using different types of catalyst, 300 ºC of temperature, 30 min of reaction time and 100 rpm of stirring rate.

3.2.1. Biocrude

Biocrude yield without any added catalyst was 37.70 % with 23.96 % of oils and 13.74 % of asphaltenes. Based on the results obtained, it´s clear that the addition of catalyst has an influence not only on the biocrude yield, but also on the quality of biocrude (yields of oils and asphaltenes). In some scenarios, the yield of biocrude has been improved. In some others, the introduction of catalyst has worsened the production process. A more detailed explanation is provided below.

3.2.1.1. Homogeneous catalyst

All the homogeneous catalysts were added at the same ratio, 10 % of the total solid of primary sludge. With $CuSO_4$, the highest yield of biocrude was reached, 42.20 %, with 27.93 % of oils and 14.26 % of asphaltenes. The results from the HTL of sewage sludge with $CuSO_4$ displayed as well better yield of biocrude (47.45 %) than that without any catalyst (Wang et al. 2018). $CuSO_4$ encourage the production of esters and suppress the *decarboxylation* of fatty acid, resulting a better quality of bio-crude (Fan et al. 2023). K_2CO_3 has contributed to the increase of yield by almost 2 % with 21.95 % of oils and 17.38 %. Runs of HTL of corn stover with K_2CO_3 have showed significant effects on biocrude yield (Carpio et al. 2022). However, the K_2CO_3 showed a less improvement than $CuSO_4$ on biocrude yield, but this improvement verified that K_2CO_3 could promote the liquefaction process. It was not the case with Na_2CO_3. The yield of biocrude was shifted into lower value (31.03 %). It has been reported that alkali catalysts ameliorate the degradation of biomass polymer, which induce hydrolysed intermediate products in the aqueous phase (Hwan et al. 2019). However, high quantity of alkali catalyst can promote the repolymerization (Carpio et al. 2022). In our study, the concentration of Na_2CO_3 could have been enough high to support the repolymerization, demonstrated by the results obtained.

3.2.1.2. Heterogeneous catalyst

Heterogeneous catalysts were distributed between two categories: powder and pellets. The powder ones were used in three different ratios: 5, 10 and 20 %. Whereas, the pellet ones were added in three different amounts: 4, 8 and 12 g.

When HTL was achieved with powder heterogeneous catalysts, yield of biocrude was affected obviously. The presence of MoS_2 didn´t promote the production of biocrude until it´s added in

a high fraction. With 20 %, the yield of biocrude became 35.58 % with 25.45 % of oils and 10.13 % of asphaltenes. When used in small quantities, that yield turned into a lower value (≈ 32.50 %). In the case of TgS_2, a fraction of 10 % was enough to increase the percentage of biocrude to 39.23 % with 26.81 % of oils and 12.41 % of asphaltenes. HTL experiments performed with Ni over Si/Al catalysts produced very low yield of biocrude, 25.85 % approximately. The use of TiO_2, regardless its amount, showed a positive effect on HTL process. Biocrude yield was increased to a percentage higher than 40 % with around 24.8 % of oils and 16.59 % of asphaltenes.

The addition of catalyst in pellet form also has altered the biocrude yield. With Pt/Al, when added in small (4 g) and moderate (8 g) amounts, the biocrude yield has increased to 38.64 % and 40.13 %. However, when the dosage was exceeded (12 g), that percentage has been dropped slightly to 36.06 %. With Pd/Al, the biocrude yield was always in decrement to less than 30 %, despite the quantity added.

Regarding all the results obtained, it´s clear that the introduction of catalyst did influence the biocrude yield and its quality. Among all the catalysts used, the optimum yield of biocrude was achieved when TiO_2 was applied with 20 % dosage. TiO_2 has clearly promoted the hydrolysis of macromolecules in primary sludge. This is confirmed also by the high percentage of oils present (27.78 %). Titanium Oxide (TiO_2) is a proper catalyst for HTL process optimization. It is an extensively accepted promoter for technical research and industrial production as it is characterized by high thermal stability and activity in oxidation-reduction catalysis (Wang et al. 2018). Even though 10 % of $CuSO_4$ resulted high biocrude yield, it´s a homogeneous catalyst. The use of heterogeneous catalyst is more favourable as it´s easy to handle, separate, recover and can be recycled (Rani et al. 2023).

Gas chromatography/mass spectrometry spectroscopy (GC/MS)

GC/MS reports the molecular information of biocrude obtained from HTL of primary sludge using different catalysts. Generally, many substances could be detected by GC/MS in the biocrude. However, here, the identification was limited due to the column temperature. The substances found were derived from the conversion reactions of primary sludge. The detailed compound information of all the biocrude samples can be found in Tables SM1 and SM2 (supplementary materials). The main composition of biocrude included hydrocarbons, esters, acids, ketones, alcohols, phenols and nitrogen-rich compounds. During the high-pressure conversion, the reformation and depolymerization reactions of biomass components, mainly carbohydrates, promoted the production of phenols (Biswas et al., 2020). The hydrolysis of carbohydrates produces phenols. N-compounds and O-compounds could be synthesized in Maillard reaction between the hydrolysis product of carbohydrates and proteins (Yang et al., 2021). The presence of catalysts, either homogeneous or heterogeneous, promoted the production of more acids and esters. n-hexadecanoic acid, dodecanoic acid, octadecanoic acid and tetradecanoic acid were observed in all the biocrudes, which was attributed to the hydrolysis of lipids (Galadima et al., 2018). The N-containing compounds, amides and N-containing heterocycle compounds like hexadecamide, octadecanamide, dodecanamide came from the proteins present in primary sludge. Amide compounds were products of the reaction between fatty acids and amines formed from the cracking of amin acids (Lu et al., 2020). Esters including hexadecenoic acid, methyl ester, hexadecenoic acid, dodecyl ester and hexadecenoic acid, tetradecyl ester were predominant. Ketones were mainly observed in the form of 2-heptadecanone and 2-pentadecanone. Cyclic hydrocarbons like cholest-3-ene, cholest-4-ene, cholest-5-ene were products of the recombination reactions between the hydrophilic molecules in sludge (Xiao et al., 2019).

Thermogravimetry analysis (TGA)

TGA analysis was performed to study the weight loss stages of the biocrude. The TGA curves of the samples of biocrude from HTL of primary sludge are shown in Figure 3.a, 3.b and 3.c. For comparisons, thermograms of the same category of catalyst are plotted in the same figure. In Figure 4.a, biocrudes produced from HTL using homogeneous catalysts presented similar decomposition process. A relatively significant weight loss took place at 210 °C in HTL-Na_2CO_3 with 66.91% of weight loss, 200 °C in HTL-K_2CO_3 with 73.18 % of weight loss and 243.80 °C in HTL-$CuSO_4$ with 90.19 % of weight loss. Considering the samples of biocrude produced from HTL using powder heterogeneous catalysts, an important weight loss took place near 230 ºC in HTL-TiO_2 with around 75 % of weight loss, near 230 ºC in TgS_2 with around 80 % of weight loss, near 235 ºC in HTL-MoS_2 with around 80 % of weight loss and near 170 ºC in HTL-Ni over Si/Al with around 71 % of weight loss. While in the case of heterogeneous pellet catalyst, biocrude samples faced an important weight loss near 220 ºC in HTL-Pd/Al with around 75 % of weight loss and near 240 ºC in HTL-Pt/Al with around 75 % of weight loss.

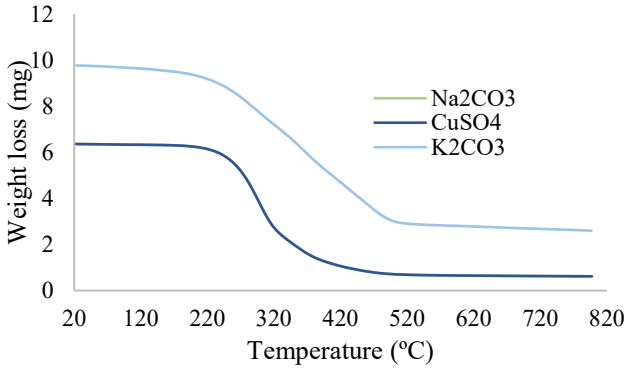

Figure 3.a. TGA curves of samples of biocrude: (a) Na_2CO_3; (b) $CuSO_4$; (c) K_2CO_3. 300 ºC of temperature, 30 min of reaction time and 100 rpm stirring rate.

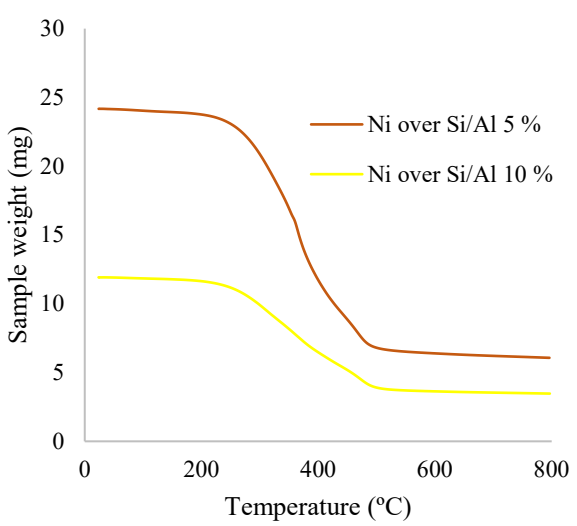

(a)

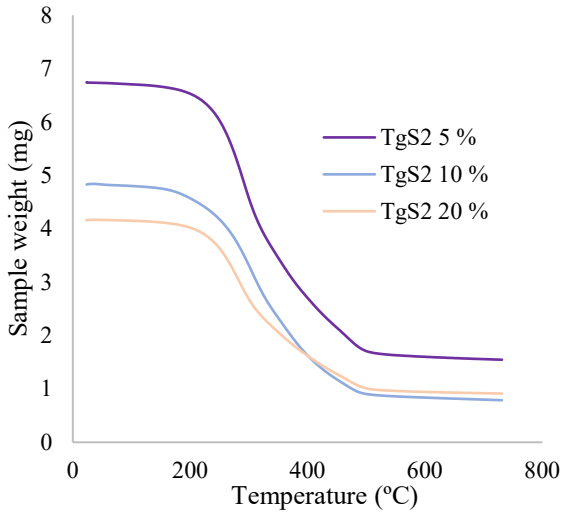

(b)

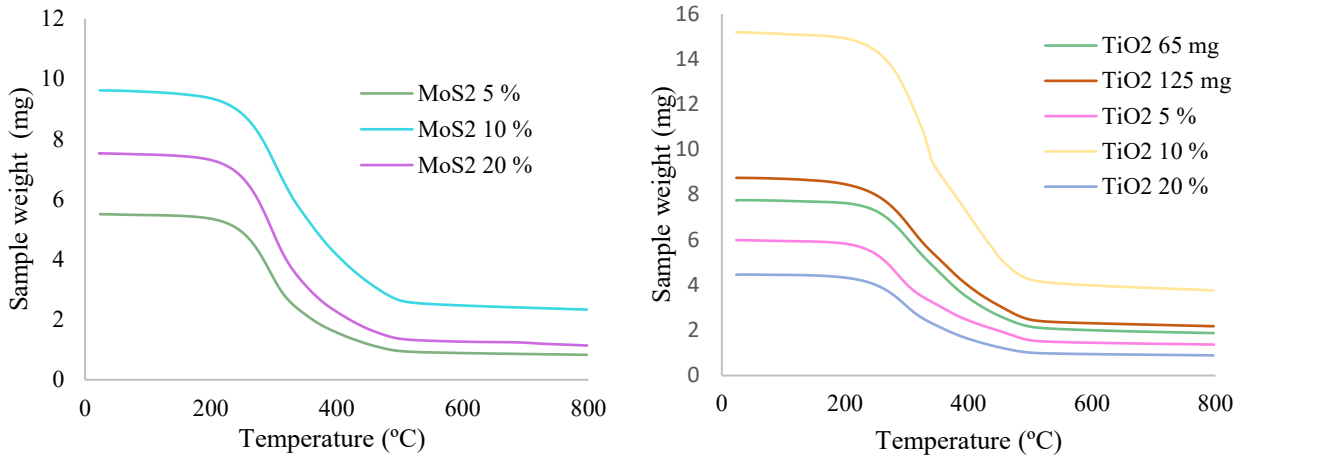

(c) (d)

Figure 3.b. TGA curves of samples of biocrude: (a) Ni over Si/Al, (b) TgS_2, (c) MoS_2 and (d) TiO_2, 300 ºC of temperature, 30 min of reaction time and 100 rpm of stirring rate.

2715

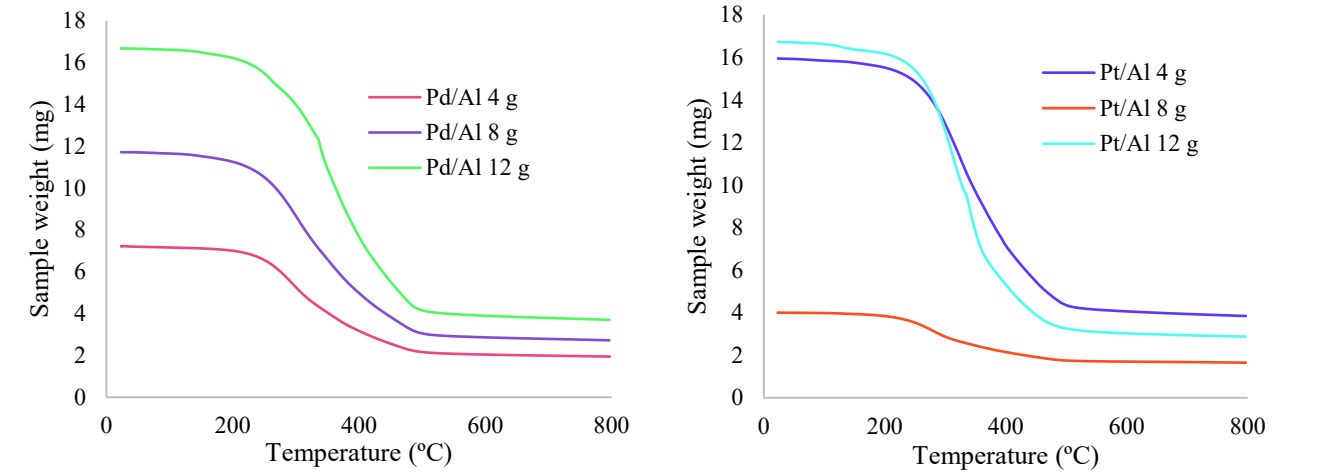

(a) (b)

Figure 3.c. TGA curves of samples of biocrude: (a) Pd/Al and (b) Pt/Al, 300 ºC of temperature, 30 min of reaction time and 100 rpm of stirring rate.

2716

Ultimate analysis and HHV

The ultimate composition C, H, N and O, higher heating values HHV and the energy recovery ER of biocrude are presented in Table 2. Generally, through the HTL process, primary sludge was converted into a product with higher energetic value. However, the optimization of the process by adding a catalyst was not that convenient. Based on the results obtained, it´s clear that none of the catalysts was able to boost the energetic property of biocrude. While the HHV of biocrude produced from HTL without using any catalyst reached 39.99 MJ/kg, the HHV of biocrude produced from HTL using catalyst, either homogeneous or heterogeneous, didn´t pass that value. Very close attaints were observed in the HTL-$CuSO_4$ where HHV of biocrude was 39.24 MJ/kg with 75.01 % of carbon, 10.97 % of hydrogen, 3.08 % of nitrogen and 10.94 % of oxygen. Also, the quality of biocrude produced from HTL without using any catalyst was very close to that of petroleum, 42.75 MJ/kg (Shah et al., 2020). Regarding the results of energy recovery, the increase noticed in the HT-$CuSO_4$ from 80.06 % to 87.93 % is due to the improvement of biocrude yield (see Figure 2).

Table 2. Ultimate analysis. HHV and energy recovery of biocrude produced from HTL using different catalysts at 300 ºC of temperature. 30 min of reaction time and 100 rpm of stirring rate.

Catalyst	Elemental composition (wt%)				HHV (MJ/kg)	ER %
	C	H	N	O*		
None	75.06	11.31	4.07	9.56	39.99	80.06
Na_2CO_3 10 %	59.66	8.30	2.88	29.16	26.90	44.08
K_2CO_3 10 %	63.88	8.77	3.69	23.66	30.00	62.66
$CuSO_4$ 10 %	75.01	10.97	3.08	10.94	39.24	87.93
TiO_2 65 mg	68.07	9.43	3.60	18.90	33.23	73.35
TiO_2 125 mg	66.83	9.06	3.27	20.84	31.93	63.62
TiO_2 5%	64.20	9.22	3.00	23.58	30.77	67.85
TiO_2 10 %	70.63	9.81	3.42	16.14	35.14	76.00
TiO_2 20 %	69.64	9.67	3.34	17.35	34.39	77.69
TgS_2 5 %	68.95	9.57	2.95	18.53	33.80	61.60
TgS_2 10 %	71.23	10.15	3.15	15.47	35.96	74.91
TgS_2 20 %	69.39	9.69	3.30	17.62	34.28	73.55
MoS_2 5 %	73.27	10.59	3.05	13.09	37.71	65.18
MoS_2 10 %	71.17	9.72	3.76	15.35	35.34	60.87
MoS_2 20 %	72.52	10.44	3.13	13.91	37.09	78.27
4 g pellet Pd/Al	67.93	9.38	3.65	19.04	33.08	51.54
8 g pellet Pd/Al	67.55	9.51	3.70	19.24	33.11	51.42
12 g pellet Pd/Al	69.11	9.82	3.57	17.50	34.40	41.49
4 g pellet Pt/Al	67.93	9.48	3.59	19.00	33.24	68.20
8 g pellet Pt/Al	63.69	9.16	3.80	23.35	30.55	65.12
12 g pellet Pt/Al	70.32	10.39	3.31	15.98	35.90	68.76
Ni over Si/Al 5%	65.51	8.97	2.87	22.65	31.02	42.99
Ni over Si/Al 10%	64.22	8.74	3.10	23.94	30.02	40.93

The percentage of catalysts added is represented by (w/wTS).

*O is calculated by difference, considering that biocrude is ash-free.

FT-IR

FTIR spectroscopy gives more information about the functional groups present in the biocrude. FTIR spectra of biocrudes produced from HTL using homogeneous catalysts, heterogeneous powder catalysts and heterogeneous pellet catalysts are separated in Figure 4.a, 4.b and 4.c. All the spectra were similar in shape, but different in intensity. So, all biocrudes are composed from the same functional groups. The presence of C and H detected by ultimate analysis is explained here by the important C-H stretching with CH_2 and CH_3 bending around 2961 cm^{-1} and 2852 cm^{-1}, double bond C stretching around 1655 cm^{-1}, triple bond C stretching around 2260 cm^{-1} and aromatics around 722 cm^{-1}. Esters and phenols are represented by C-O stretching peaks near 1030–1450 cm^{-1}. C=O stretching peaks ranging between 1707 cm^{-1} and 1590 cm^{-1} belong to the functional groups of carboxylic acids, ketones and esters as detected by GC/MS analysis. Wide peaks around 3200 cm^{-1} and 3500 cm^{-1} correspond to N-compounds or OH compounds. The peaks around 500 cm^{-1} could be identified as compounds containing C-Cl or C-F bonds. Among all the homogeneous catalysts used, it can be observed that in HTL with acidic catalyst, the intensity of hydrocarbon peaks is higher; whereas, in HTL with basic catalyst, the intensity of acids and esters peaks is higher. Regarding the spectra of HTL using heterogeneous catalysts, in the powder case, it can be observed that with TiO_2, TgS_2 and MoS_2, the intensity of peaks is very comparable. However, with Ni over Si/Al, it´s clear that the intensity of C=O groups is much higher. In the case of heterogeneous pellet catalyst, the intensity of peaks when using Pt/Al was more visible than that of Pd/Al.

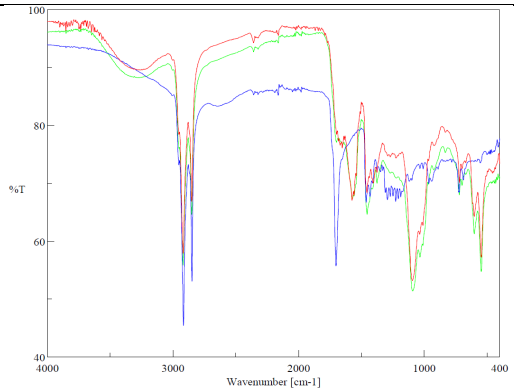

Figure 4.a. FT-IR results of biocrude from HTL using Na_2CO_3 (red), K_2CO_3 (green) and $CuSO_4$ (blue) as homogeneous catalyst, 300 ºC of temperature, 30 min of reaction time and 100 rpm of stirring rate.

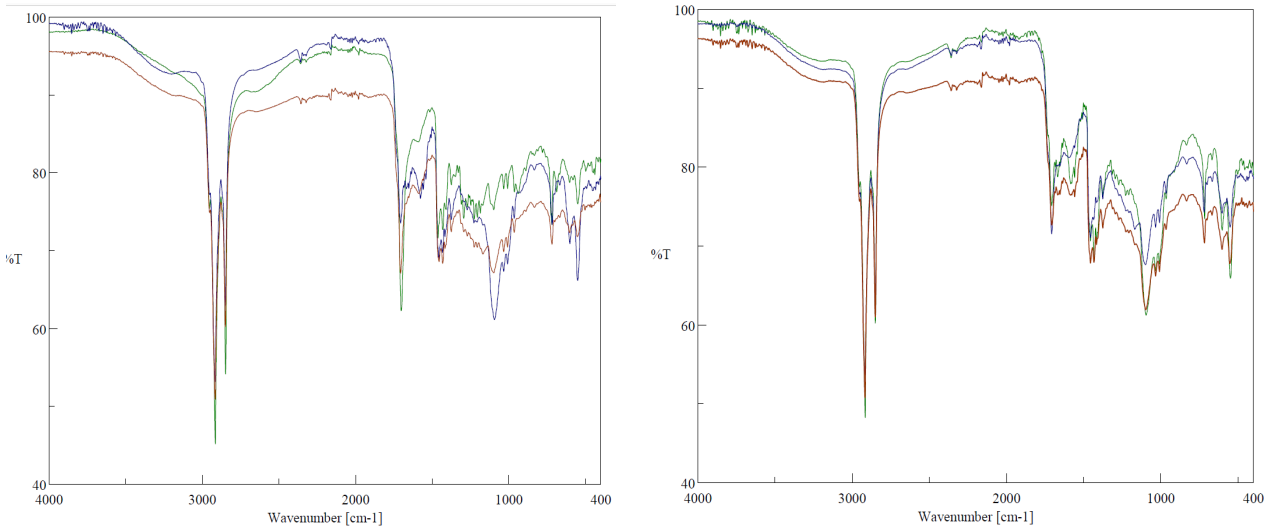

(a) (b)

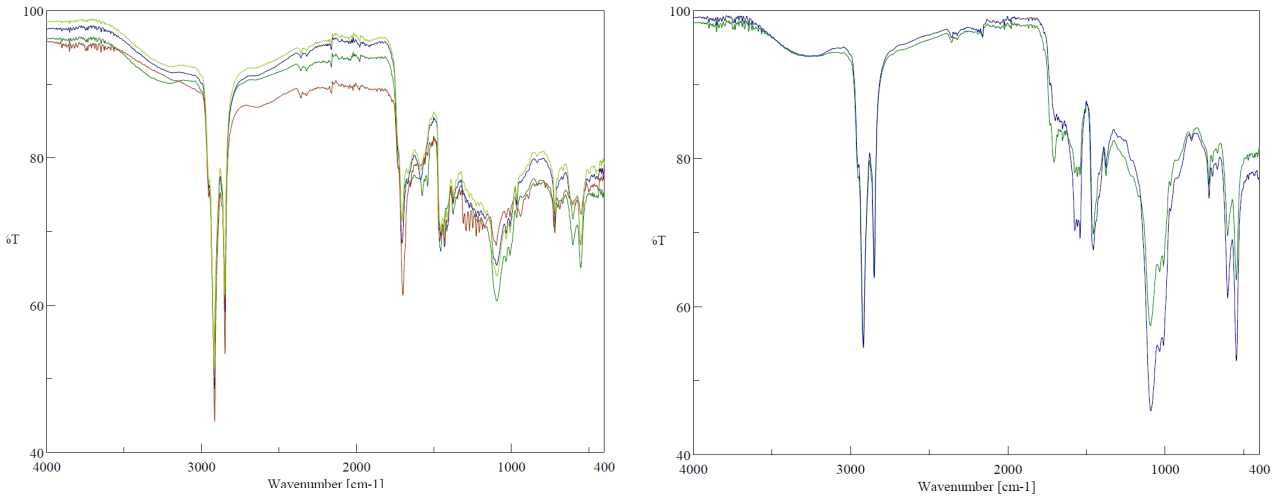

(c) (d)

Figure 4.b. FT-IR results of biocrude from HTL using MoS2 (a), TgS2 (b), TiO2 (c) and Ni over Si/Al (d) as heterogeneous powder catalyst, 300 ºC of temperature, 30 min of reaction time and 100 rpm of stirring rate.

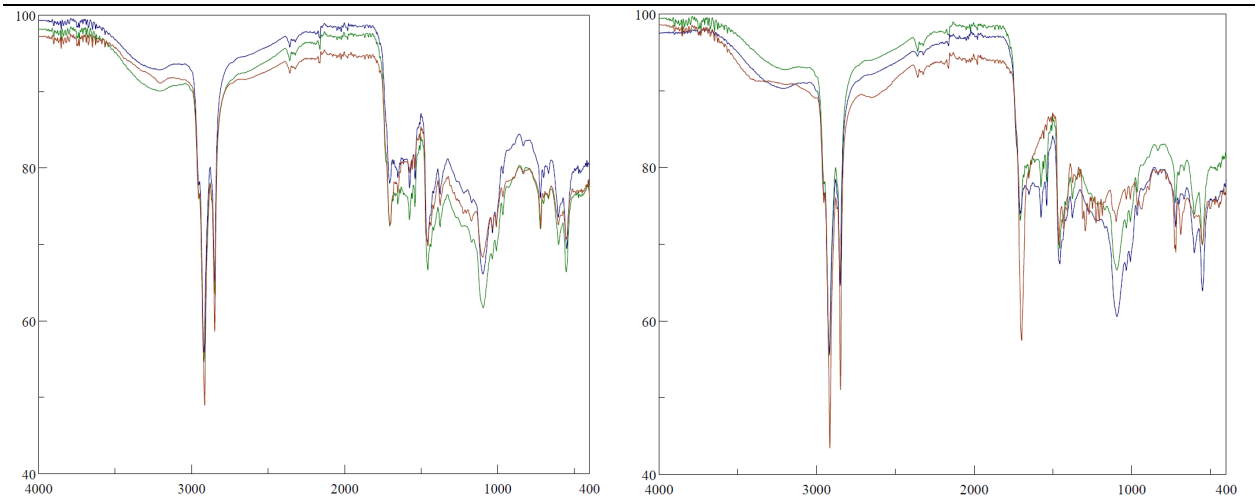

(a) (b)

Figure 4.c. FT-IR results of biocrude from HTL using Pd/Al (a) and Pt/Al (b) as heterogeneous pellet catalyst, 300 ºC of temperature, 30 min of reaction time and 100 rpm of stirring rate.

^{1}H NMR

Similar to FTIR, NMR provides additional functional group information. Figure 5.a, 5.b and 5.c present the ^{1}H NMR spectra of samples of biocrude produced from HTL using different catalysts (homogeneous and heterogeneous). H corresponding to the functional group of alkanes appears near 0.9 ppm and 1.8 ppm. Unsaturated hydrocarbons (alkenes) are observed around 2.1 ppm. However, the same spectra could belong to esters, carboxylic acids, amine, amide and ketones. The chemical shifts, located between 5 and 5.5 ppm are assigned to alcohol and phenols. Also, the same chemical shifts could belong to amide. The peak around 7.2 ppm correspond to the solvent used. Generally, all the biocrude contain the same functional groups, but with different intensity. The distribution of the groups and their intensity was dependent on the catalyst used. Regarding the results obtained from biocrudes HTL-homogeneous catalyst, it can be noted that Na_2CO_3 promoted the formation of hydrocarbons compounds whereas $CuSO_4$ promoted the formation of C=O compounds, (see Figure 6.a). Considering the results obtained from biocrudes HTL-heterogeneous catalyst, by increasing the amounts of MoS_2 and Pt/Al, less hydrocarbons were produced. With 5 % of Ni over Si/Al, more hydrocarbons were observed, while with 10 % of Ni over Si/Al, more C=O compounds were noted. With TiO_2, Pd/Al and TgS_2, no significant changes were found, (see Figure 6.b and 6.c). ^{1}H NMR spectra comply with FTIR and GC/MS analysis. As mentioned before, carboxylic acids and esters were derived from the lipids, phenols and alcohol could be originated from carbohydrates and nitrogenous compounds were produced from proteins; all together constitute the main ingredients of primary sludge.

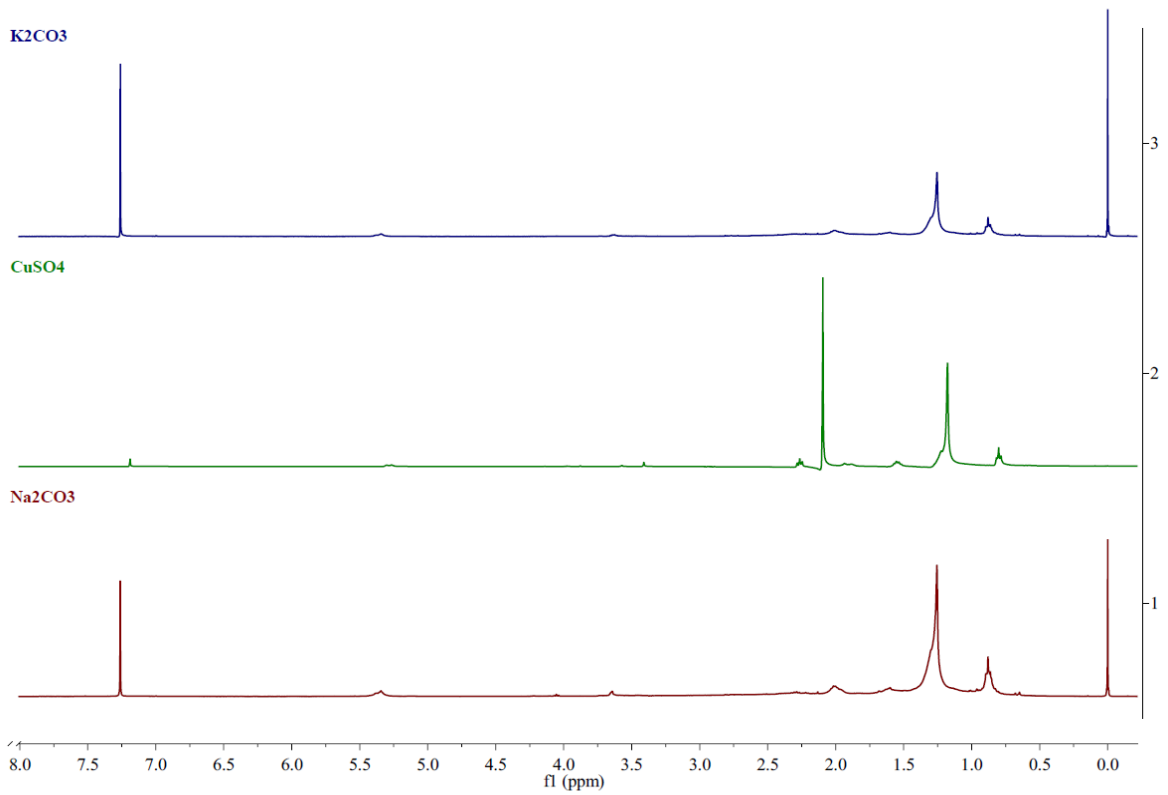

Figure 5.a. ^{1}H NMR results of biocrude from HTL using Na_2CO_3, K_2CO_3 and $CuSO_4$ as homogeneous catalyst, 300 ºC of temperature, 30 min of reaction time and 100 rpm of stirring rate.

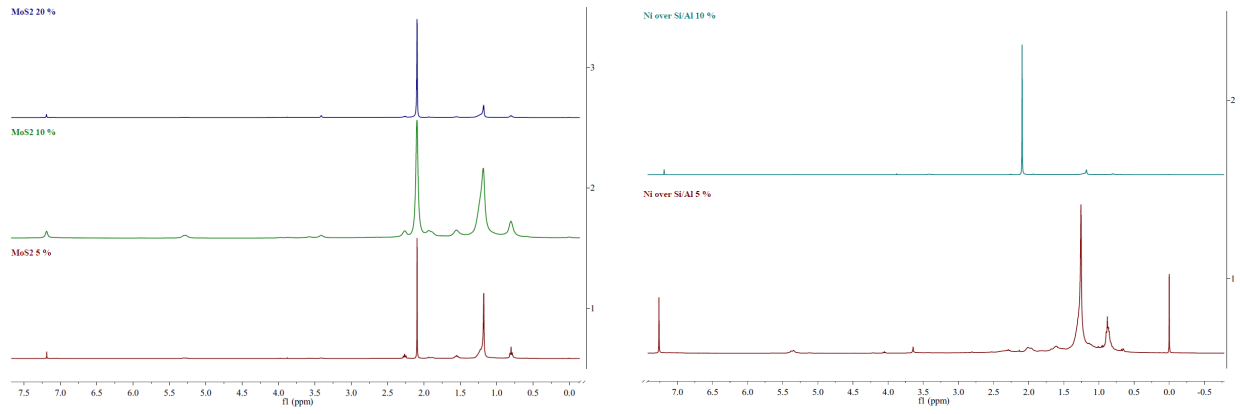

(a) (b)

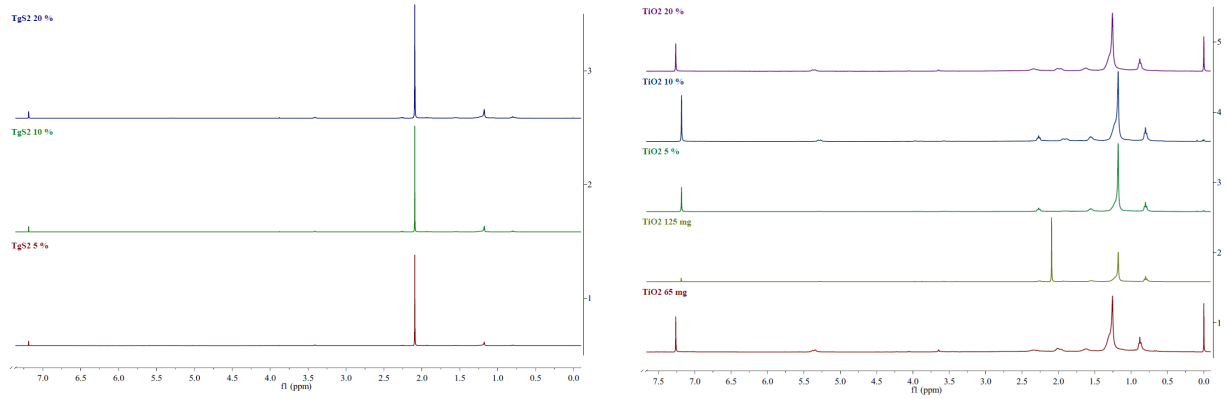

(c) (d)

Figure 5.b. ^{1}H NMR results of biocrude from HTL using MoS_2 (a), Ni over Si/Al (b), TgS_2 (c) and TiO_2 (d) as heterogeneous powder catalyst, 300 ºC of temperature, 30 min of reaction time and 100 rpm of stirring rate.

2777

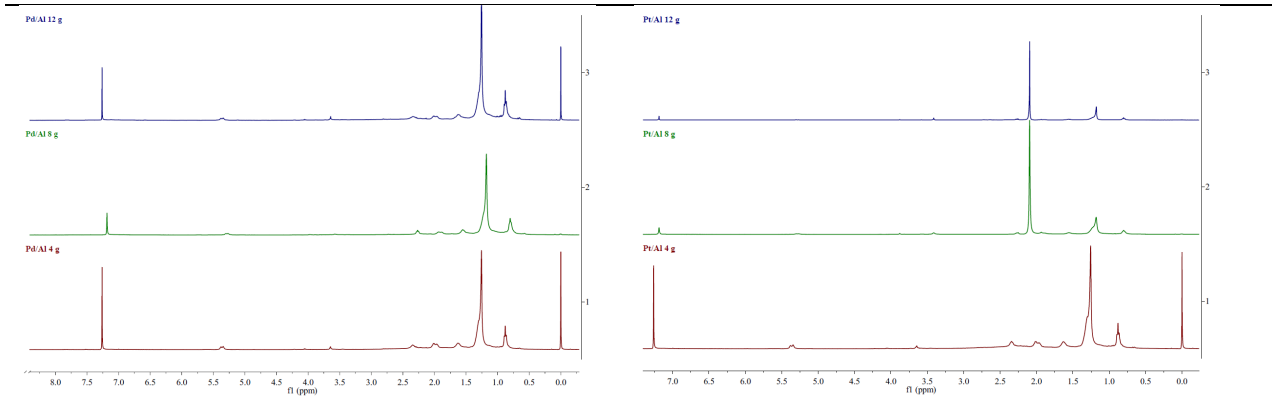

(a) (b)

Figure 5.c. ^{1}H NMR results of biocrude from HTL using Pd/Al (a) and Pt/Al (b) as heterogeneous pellet catalyst, 300 ºC of temperature, 30 min of reaction time and 100 rpm of stirring rate.

2778

Simulated Distillation (Sim-Dis)

The fractional cuts of biocrude, produced from HTL using different catalysts (homogeneous or heterogeneous), are represented in Figure 6.a, 6.b and 6.c. It´s clear that all the biocrudes present similar behaviour. The composition of biocrude is divided into fractions, from gasoline to vaccum residue. In other words, the fractions were detected in the form of boiling points in an ascending way from light to heavy with the mass fractions. As it can be observed, none of the biocrude contain a fraction in the range of gasoline. Only less than 5 % of the biocrude fraction is in the Jet Fuel range, except with 5 % of TiO_2 where no fractions in that range was detected. Proteins and lignin are probably the promoters for the production of substances in that fractional cut (Al-juboori et al., 2023). Likewise, less than 15 % of the biocrude fraction is in the Diesel range. Most of the substances in this fractional cut are mainly produced from proteins, and in small quantity from carbohydrates and lipids (Al-juboori et al., 2023). In fact, the most significant fractions of the biocrude belong to the vacuum gasoil range. Between 70 and 90 % were detected, demonstrating the presence of heavy and long chain molecules in the biocrude generated from lipids (Al-juboori et al., 2023). This confirms that biocrude should be subjected to further treatment in order to improve its quality. As the major substances produced from lipids are fatty acids, one solution could be the hydrodeoxygenation of fatty acids to produce alkanes. This linear – chain paraffin can be blended perfectly to biodiesel, helping in low temperature fluidity and better antioxidation stability (Mondal et al., 2017). Table SM3 (supplementary material) lists the values of composition of biocrudes by fractional cuts. The reference boiling cuts were obtained from Haider (Haider et al., 2018).

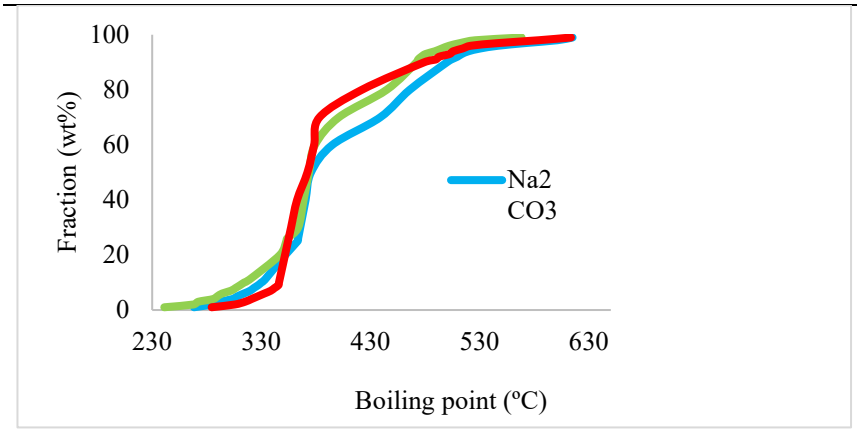

Figure 6.a. Simulated distillation of biocrude from HTL using homogeneous catalysts, 300 ºC of temperature, 30 min of reaction time and 100 rpm of stirring rate.

2800

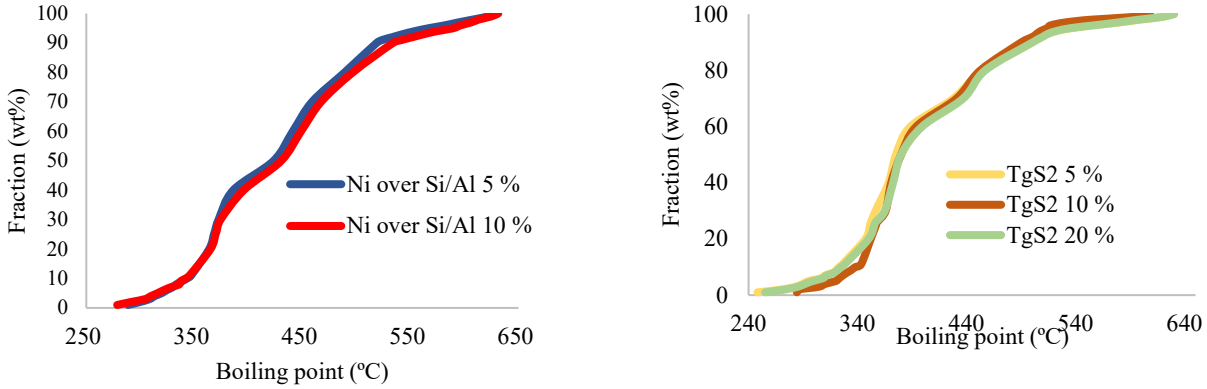

(a) (b)

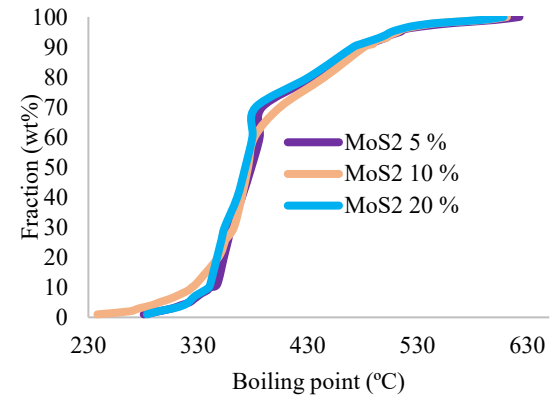

(c)

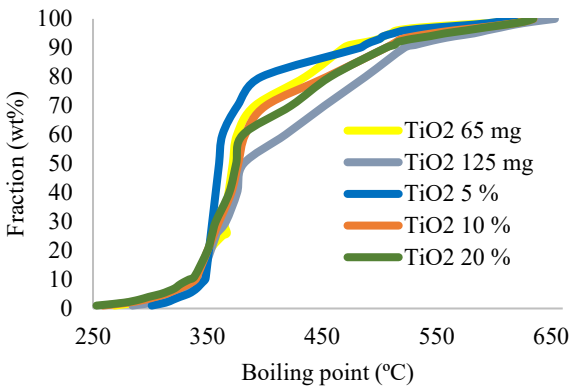

(d)

Figure 6.b. Simulated distillation of biocrude from HTL using Ni over Si/Al (a), TgS_2 (b), MoS_2 (c) and TiO_2 (d) as heterogeneous powder catalyst heterogeneous powder catalysts, 300 ºC of temperature, 30 min of reaction time and 100 rpm of stirring rate.

2801

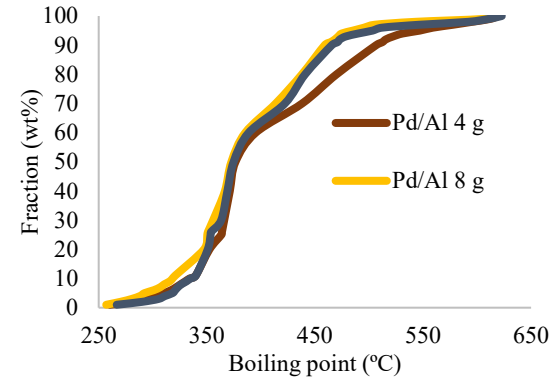

(a)

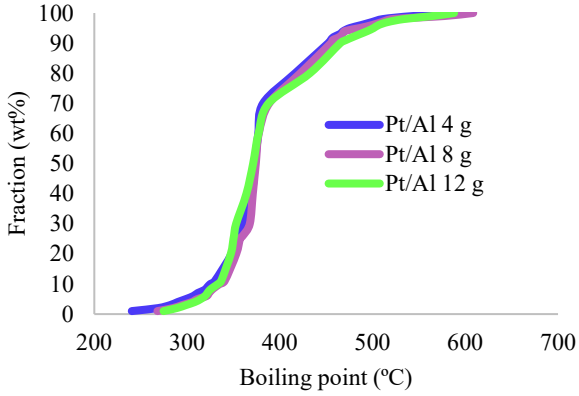

(b)

Figure 6.c. Simulated distillation of biocrude from HTL using Pd/Al (a) and Pt/Al (b) as heterogeneous pellet catalysts, 300 ºC of temperature, 30 min of reaction time and 100 rpm of stirring rate.

2802

Saturates, aromatics, resins and asphaltenes (SARA)

SARA fractions quantification was performed to all conditions and the results are presented in Table 3. Biocrude was distributed between asphaltene and maltenes containing saturates, aromatics and resins. The composition of biocrude (asphaltenes and maltenes) as well as the composition of light phase (saturates, aromatics, resins) was dependent on the type and amount of catalyst. Biocrude produced from HTL without using any catalyst contained 68.35 % of saturates, 11.17 % of aromatics and 20.48 % or polars. Generally, maltene was predominant in biocrude, except with TiO_2 (65 and 125 mg), Pt/Al and Pd/Al (12 g). By focusing on the quality of biocrude, using a heterogeneous catalyst was more favourable than using a homogeneous one. Specifically, 20 %TgS_2 and 8 g of Pt/Al could have promoted the production of more saturates compounds to 72.94 % and 75 %. It seems that most of the remaining catalysts have helped in the production of heavy and long chain compounds, either aromatics or polars.

Table 3. SARA of biocrude samples after HTL using different catalysts at 300 ºC of temperature. 30 min of reaction time and 100 rpm of stirring rate.

Catalyst	Asphaltene %	Oils			
		Yield %	Saturates %	Aromatics %	Resins %
No catalyst	13.74	23.96	68.35	11.17	20.48
Na_2CO_3 10 %	17.59	13.45	54.19	35.67	10.14
K_2CO_3 10 %	17.38	21.95	45.02	31.33	23.65
$CuSO_4$ 10 %	14.26	27.93	48.68	7.87	43.45
TiO_2 65 mg	28.67	12.89	42.65	49.95	7.40
TiO_2 125 mg	20.92	16.60	53.26	19.24	27.50
TiO_2 5 %	18.95	22.57	39.16	12.15	48.69
TiO_2 10%	16.67	24.05	61.43	2.47	36.10
TiO_2 20 %	14.14	27.78	52.01	21.00	26.99
Pt/Al 4 g	18.62	20.02	60.39	4.76	34.85
Pt/Al 8 g	14.41	25.72	75.00	3.94	21.06
Pt/Al 12 g	21.69	14.38	25.40	14.11	60.50
Pd/Al 4 g	7.60	21.73	39.78	55.28	4.94
Pd/Al 8 g	9.51	19.74	32.73	42.04	25.23
Pd/Al 12 g	12.21	10.50	33.89	1.55	64.56
MoS_2 5 %	11.54	21.00	42.31	7.88	49.81
MoS_2 10 %	6.99	25.45	63.45	23.44	13.11
MoS_2 20 %	10.13	25.45	67.75	13.59	18.66
TgS_2 5 %	11.56	22.76	5.26	0.03	51.15
TgS_2 10 %	12.41	26.81	9.29	80.47	10.24
TgS_2 20 %	16.36	24.04	72.94	19.61	7.45
Ni over Si/Al 5 %	7.05	19.04	26.24	36.85	36.91
Ni over Si/Al 10 %	6.93	18.74	63.94	7.98	28.09

The percentage of catalysts added is represented by (w/wTS).

3.2.2. Biochar

Biochar yield after HTL at 300 ºC, for 30 min and without addition of any catalyst was 28.10 % with 60.60 % of ashes and 39.40 % of volatiles. Regarding the results obtained in Figure 2, the presence of catalyst has affected the biochar yield. In some cases, it has increased the percentage, while in others it has decreased the percentage. A further interpretation is provided.

3.2.2.1. Homogeneous catalyst

. It´s demonstrated that biochar, ash and volatile yields were not significantly affected by the presence of catalyst. With Na_2CO_3 and $CuSO_4$, biochar yield was increased to 30.62 % and 30.05 % with 56.38 % and 55.71 % of ash and 43.62 % and 44.29 % of volatile. Whereas with K_2CO_3, 28.18 % of biochar were produced with 57.84 % of ash and 42.16 % of volatile.

Elsewhere, slight or no changes were shown in the solid percentage when K_2CO_3 was added (Carpio et al. 2022). In other studies, the acidic catalyst $CuSO_4$ improved both biocrude and biochar yields as well, implying that $CuSO_4$ encourage the water-soluble intermediates secret into biocrude and additional polymerized into biochar (Fan et al. 2023). It´s said in other studies that $NaCO_3$ promote the hydrolysis of carbohydrate and diminish the conversion of protein and lipids (Shakya et al. 2015). Even though primary sludge contained a significant amount of carbohydrate, neither biocrude yield was improved nor biochar yield was decreased.

3.2.2.2. Heterogeneous catalyst

Biochar yield was changing with the type of catalyst utilized respectively. According to the results obtained from the HTL with heterogeneous catalyst in the form of powder, the amount of solid residue was altered. When MoS_2 and TgS_2 were used with 5 % and 10 % loading, biochar percentage increased moderately. When used in high portion 20 %, MoS_2 showed a negative effect on biochar yield while TgS_2 showed a noticeable increment on that yield. TiO_2 diminished the biochar yield, regardless the amount used. Ni over Si/Al always demonstrated a positive effect on the biochar yield, but more when used with 5 %.

On the other hand, HTL performed with the use of heterogeneous catalyst in the form pellets generated solid residue with higher yield when Pt/Al was employed and lower yield when Pd/Al was applied. However, there was no significant variation in the percentage when looking at the fractions respectively.

Ash content and HHV

The ash content, the ultimate analysis and HHV of the solid phase, biochar, is presented in Table 4. Solid phase from HTL without using a catalyst reached a HHV of 33.48 MJ/kg. With

the employment of catalysts, either homogeneous or heterogeneous, the energetic density of biochar has decreased. The highest HHV of biochar produced from HTL with catalysts couldn´t reach higher than 20 MJ/kg. The ash content in the solid phase produced after HTL with catalysts was quite high, leading to a low organic content. Also, this is confirmed by the low amount of carbon obtained. While the percentage of carbon in the solid phase produced from HTL without catalysts was 71.47 %, it decreased to not higher than 35 % when a catalyst was added. By comparing the quality of biochar produced from HTL without catalyst to the one produced from HTL with catalyst, it can be concluded that the presence of catalyst has inhibited the energetic value of biochar, preventing its usage in different applications.

Table 4. Ultimate composition. HHV and ash content of biochar after HTL using different catalysts at 300 ºC of temperature. 30 min of reaction time and 100 rpm of stirring rate.

Catalyst	Ash (wt%) #	Elemental composition (wt%)				HHV (MJ/kg)
		C	H	N	O*	
None	60.60	71.47	9.75	2.97	15.81	33.48
Na_2CO_3 10 %	47.14	31.00	4.66	1.17	16.03	14.32
K_2CO_3 10 %	42.01	32.21	4.36	1.27	20.15	13.55
$CuSO_4$ 10 %	37.74	34.77	5.11	1.40	20.98	15.35
4 g pellet Pd/Al	60.89	25.69	3.74	1.34	8.34	12.58
8 g pellet Pd/Al	63.84	24.72	2.96	1.35	7.13	11.35
12 g pellet Pd/Al	62.35	29.48	3.85	1.42	2.90	15.00
4 g pellet Pt/Al	51.51	30.36	3.91	1.47	4.72	15.06
8 g pellet Pt/Al	52.99	36.88	5.46	1.43	3.24	19.77
12 g pellet Pt/Al	52.87	37.38	5.30	1.58	2.87	19.78
TiO_2 65 mg	61.54	24.21	3.08	1.28	9.89	10.85
TiO_2 125 mg	59.37	15.69	1.48	1.26	22.20	3.44
TiO_2 5%	58.55	10.81	1.10	0.71	28.83	0.04
TiO_2 10%	69.09	11.67	1.12	0.76	17.36	2.43
TiO_2 20%	65.78	19.99	2.22	1.27	10.74	8.03
TgS_2 5 %	59.73	32.48	4.63	1.20	1.96	17.31
TgS_2 10 %	58.85	31.44	4.49	1.20	4.02	16.39
TgS_2 20 %	54.17	27.53	3.84	0.95	13.51	12.42
MoS_2 5 %	56.86	30.90	4.15	1.22	6.87	15.20

MoS_2 10 %	36.90	26.91	3.81	1.01	31.37	8.94
MoS_2 20 %	9.70	25.46	3.49	0.89	60.46	2.74
Ni over Si/Al 5%	52.88	35.85	5.35	1.18	4.74	18.99
Ni over Si/Al 10%	48.55	29.76	4.32	1.03	16.34	13.35

The percentage of catalysts added is represented by (w/wTS).

*O is calculated by difference considering the percentage of ash.

Ash content in biochar is catalyst-free

Heavy metals

SEM images and EDX spectra of ash in biochar are also presented in Figure 7. According to the results obtained, ash was rich in oxides and salts containing Fe, Ti, Ca, Si, Al, W, P, Cl, Mg and S. The variety and amount of elements present mean that heavy metals are richly concentrated in the solid phase, biochar (Zhou et al., 2023).

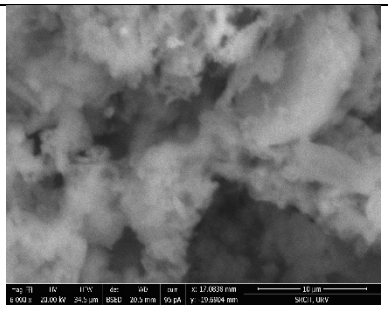

SEM image (a)

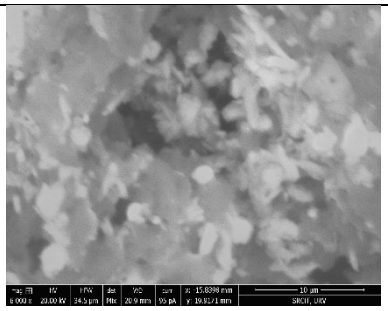

SEM image (b)

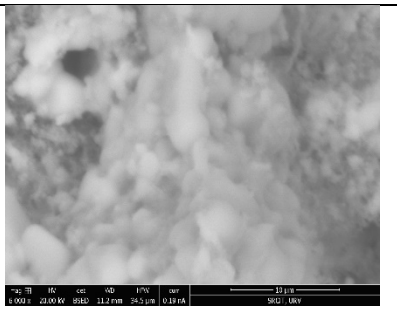

SEM image (c)

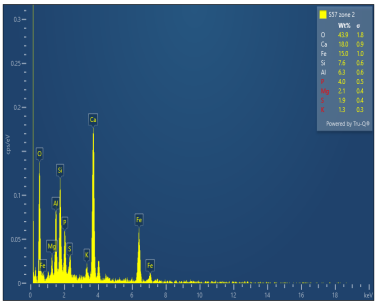

EDX spectra (a)

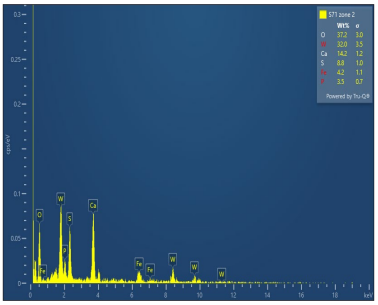

EDX spectra (b)

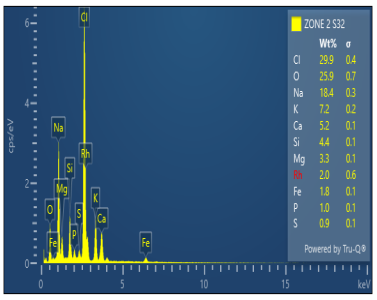

EDX spectra (c)

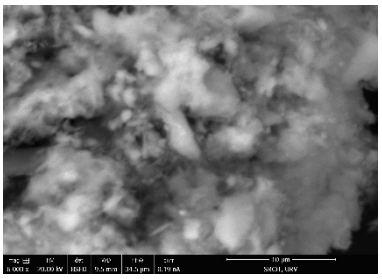

SEM image (d)

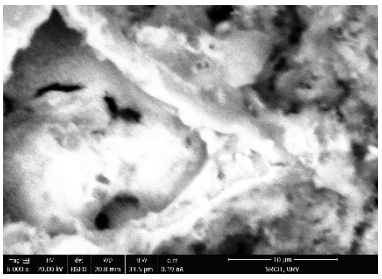

SEM image (e)

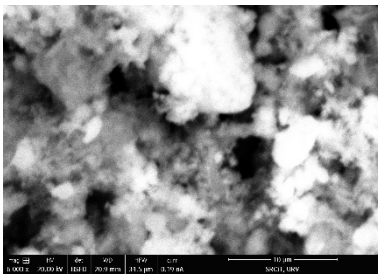

SEM image (f)

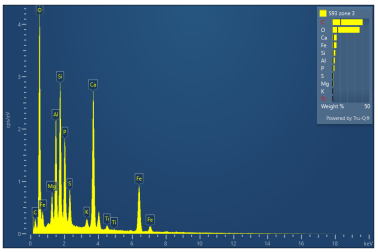

EDX spectra (d)

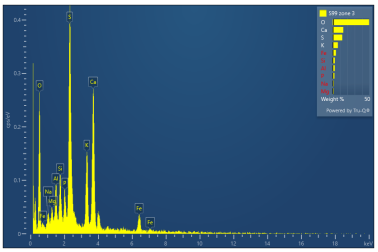

EDX spectra (e)

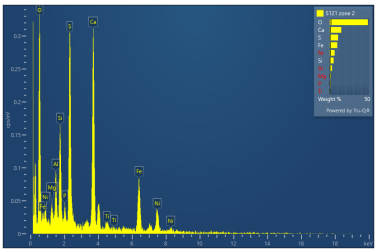

EDX spectra (f)

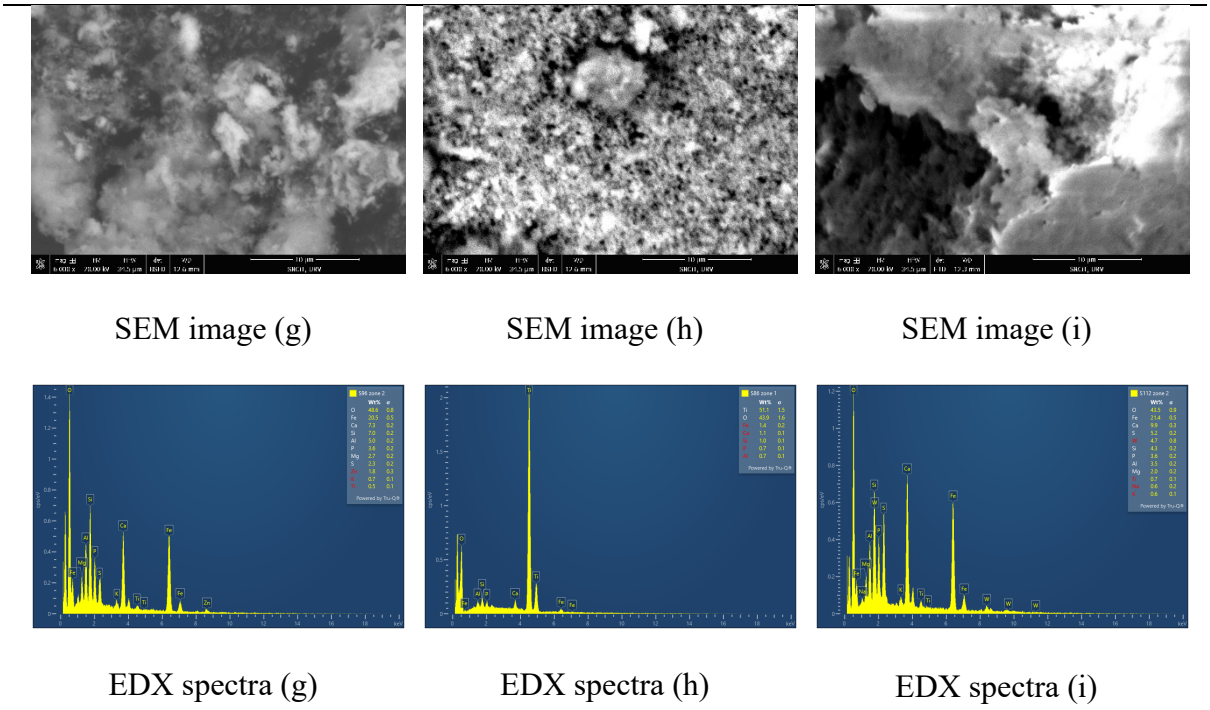

Figure 7. SEM images and EDX spectra of ash in biochar from HTL using: (a) Na_2CO_3, (b) K_2CO_3, (c) $CuSO_4$, Pt/Al (d), MoS_2 (e), Ni over Si/Al (f), Pd/Al (g), TiO2 (h) and TgS_2 (i). 300 ºC of temperature, 30 min of reaction time and 100 rpm of stirring rate

3.2.3. Aqueous phase

Aqueous phase contained a small percentage of proteins, carbohydrates and ashes without any catalyst regarding the initial properties of primary sludge. Also, the value of COD decreased and the value of TOC was comparable. In this study, the characteristics of aqueous phase change depending on the catalyst used whether it´s homogeneous or heterogeneous, in the form of powder or pellets. After each experiment, TOC, COD, proteins, carbohydrates and ash of soluble solids were determined in the aqueous phase obtained, presented in Table 5.

Table 5. Aqueous phase characterization after HTL using different catalysts at 300ºC of temperature. 30 min of reaction time and 100 rpm of stirring rate.

Catalyst	TOC	COD	Protein % (TS basis)	Carbohydrate % (TS basis)	Ash (g) (TS of AP basis)
None	5696	11649	1.01	0.03	0.39
Na_2CO_3 10 %	6737	18062	2.15	0.12	1.22
K_2CO_3 10 %	7245	14999	2.19	0.03	0.97
$CuSO_4$ 10 %	6570	13729	1.84	0.05	0.16
TiO_2 65 mg	6215	17540	1.59	0.07	0.45
TiO_2 125 mg	6920	1285	1.61	0.04	0.23
TiO_2 5%	9370	14175	1.26	0.06	0.64
TiO_2 10%	6910	12850	1.66	0.04	1.47
TiO_2 20%	7495	21368	1.59	0.04	1.09
MoS_2 5%	6752	15300	2.18	0.07	0.51
MoS_2 10%	5873	14820	1.78	0.07	0.44
MoS_2 20%	6160	13490	1.93	0.07	0.46
TgS_2 5%	4432	11360	2.02	0.07	0.80
TgS_2 10%	4889	18934	2.19	0.09	0.63
TgS_2 20%	4272	18977	2.01	0.08	0.43
Ni over Si/Al 5%	3193	12750	2.29	0.11	0.52
Ni over Si/Al 10%	4660	16646	2.02	0.09	0.48
4 g pellet Pt/Al	5805	19620	1.86	0.04	0.68
8 g pellet Pt/Al	6240	16500	2.01	0.04	0.62
12 g pellet Pt/Al	6895	18900	1.58	0.04	0.77
4 g pellet Pd/Al	2677	21620	1.83	0.04	0.72
8 g pellet Pd/Al	2910	12800	1.49	0.05	0.49
12 g pellet Pd/Al	2815	17880	1.30	0.04	0.58

The percentage of catalysts added is represented by (w/wTS).

Also, a microorganism analysis through ESEM was performed for the ashes of the dissolved solids in the aqueous phase, presented in Figure 8.

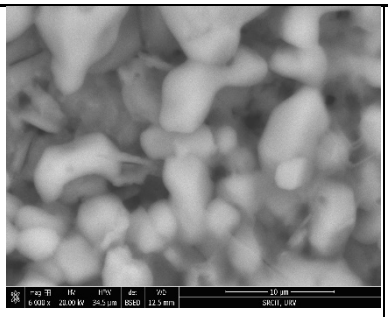	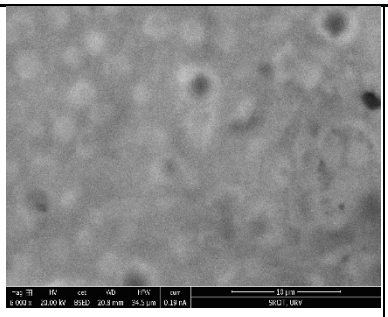	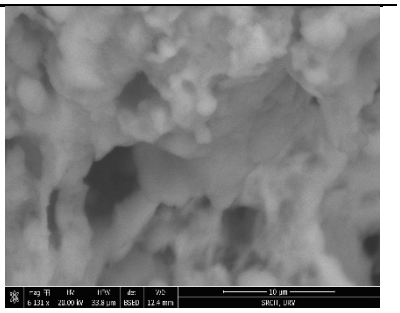
SEM image (a)	SEM image (b)	SEM image (c)
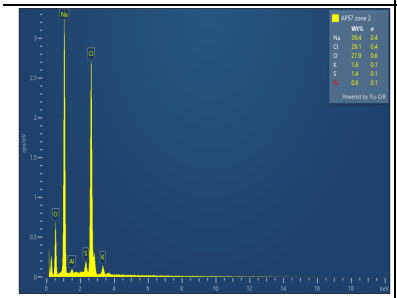	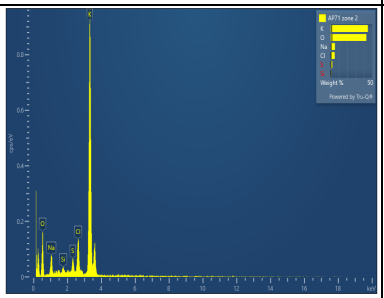	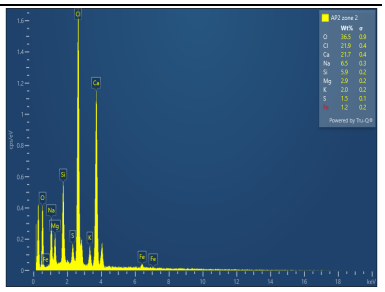
EDX spectra (a)	EDX spectra (b)	EDX spectra (c)
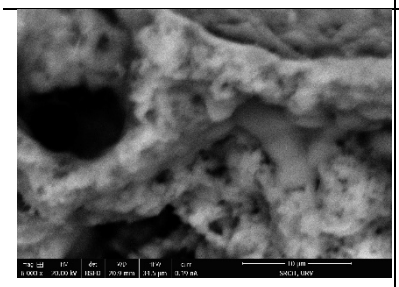	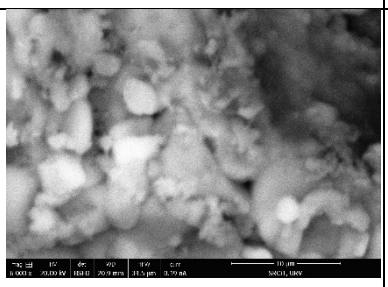	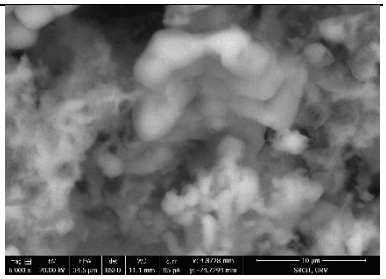
SEM image (d)	SEM image (e)	SEM image (f)
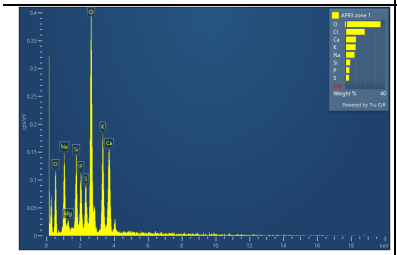	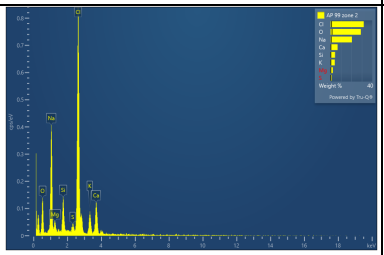	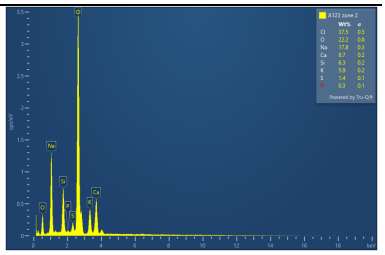
EDX spectra (d)	EDX spectra (e)	EDX spectra (f)

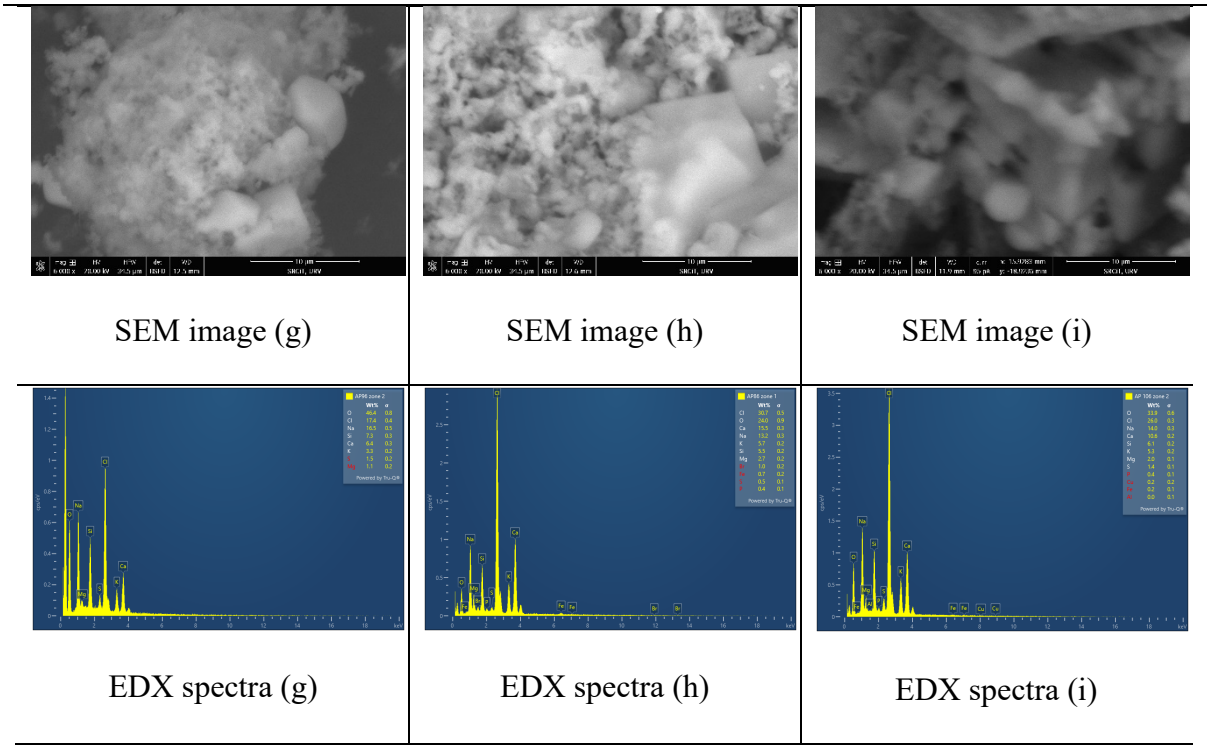

Figure 9. SEM images and EDX spectra of ash of the dissolved solid in the aqueous phase from HTL using: (a) Na_2CO_3, (b) K_2CO_3, (c) $CuSO_4$, Pt/Al (d), MoS_2 (e), Ni over Si/Al (f), Pd/Al (g), TiO_2 (h) and TgS_2 (i). 300 ºC of temperature, 30 min of reaction time and 100 rpm of stirring rate.

3.2.3.1. Homogeneous catalyst

The percentages of protein and carbohydrates in the aqueous phase produced from HTL using homogeneous catalyst were low, concerning primary sludge composition. However, without any use of catalyst, these percentages became even lower. These organic matters have been transformed into biocrude. Also, COD values decreased sharply to lower than 18100 mg/L. While TOC concentrations marked a slight increment. Values were ranging between 6500 mg/L and 7300 mg/L. TOC and COD results assume that some organic species in the initial

biomass were dissolved in the aqueous phase produced after HTL. Ash occupied less than 1 %, which can be negligeable.

3.2.3.2. Heterogeneous catalyst

HTL aqueous phase presented low amounts of carbohydrate and protein when heterogeneous catalysts were applied, demonstrating the conversion of organics into biocrude. Ash percentage was always less than 1 %. COD showed the same trend as carbohydrate and protein. However, here, the type of catalyst altered the quality of aqueous phase. Results of COD were different, but all way lower than that of primary sludge. TOC values were changing with the type of catalyst respectively. When Ni over Si/Al, TgS2 and Pd/Al were used, TOC values decreased. While, with the rest, TOC values increased. Results obtained, specifically COD and TOC, propose that a part of organic components were dissolved in the aqueous phase.

3.2.4. Biogas

The identification and relevant composition of biogas obtained from the catalytic HTL are listed in Table 6. Mainly, the percentage of gas produced was small. The abundant compounds were CO and CO_2, the saturated hydrocarbons CH_4, C_2H_6 and C_3H_8 and the unsaturated ones C_2H_4 and C_3H_6. As shown in table 5, it´s clear that more amount and diversity of gases were observed when heterogeneous catalysts were used. When employing homogeneous catalyst in the runs, few gases were released with percentages lower than 0.08 %. While adding heterogeneous catalyst liberated more gases. It can be noted that unsaturated gases were predominant. Also, significant amounts of CO and CO_2 were detected. Finally, the introduction of catalysts, specifically heterogeneous, promoted the production of biogas.

Table 6. Biogas composition after HTL at 300ºC. 30 mins and 100 rpm using different catalysts.

Catalyst		Biogas composition (mmol %)						
		CH_4	CO	CO_2	C_2H_4	C_2H_6	C_3H_6	C_3H_8
Homogeneous	Na_2CO_3 10% (w/wTS)	ND	ND	0.054	0.004	ND	0.001	ND
	$CuSO_4$ 10% (w/wTS)	0.081	ND	0.047	0.004	ND	0.001	ND
Heterogeneous	Pt/Al 4 g pellet	0.127	0.713	0.148	0.032	0.035	0.331	0.034
	Pt/Al 8 g pellet	0.132	0.767	0.148	0.042	0.052	0.469	0.051
	Pt/Al 12 g pellet	0.017	ND	0.051	0.004	ND	ND	ND
	Pd/Al 4 g pellet	0.095	ND	0.052	0.004	ND	ND	ND
	Pd/Al 8 g pellet	0.417	0.8	0.143	0.059	0.057	0.489	0.056
	Pd/Al 12 g pellet	0.166	0.493	0.16	0.028	0.032	0.286	0.034
	TiO_2 5 % (w/wTS)	0.13	0.141	0.074	0.004	0.006	0.067	0.007
	TiO_2 10 % (w/wTS)	ND	ND	0.05	0.004	ND	0.001	ND
	TiO_2 20 % (w/wTS)	0.016	ND	0.05	0.043	0.004	ND	ND
	MoS_2 5 % (w/wTS)	ND	ND	0.052	0.004	ND	ND	ND
	MoS_2 10 % (w/wTS)	0.446	2.363	1.812	0.186	0.13	0.801	0.12
	MoS_2 20 % (w/wTS)	0.051	0.059	ND	0.05	0.004	0.001	ND
	TgS_2 5 % (w/wTS)	0.131	0.14	0.404	0.011	0.01	0.122	0.011
	TgS_2 10 % (w/wTS)	0.156	0.736	0.97	0.039	0.039	0.328	0.037
	TgS_2 20 % (w/wTS)	0.14	0.418	0.327	0.044	0.037	0.322	0.037

ND: not defined

4. Conclusion

The introduction of catalyst into HTL process did improve the biocrude yield. According to the study achieved, 42.20 % (w/w_{VS}) of biocrude was achieved with 10 % $CuSO_4$ (homogeneous catalyst) and 41.90 % (w/w_{VS}) of biocrude was obtained with 20 % of TiO_2. Though, the use of heterogeneous catalyst was always a better option as it can be recovered easily and reused. On the other hand, the effect of catalyst was negligeable on the quality improvement of biocrude and other products. Heavy compounds were still observed in the biocrude. The energetic density of biochar and biocrude decreased. The percentage of ash

in biochar increased. Aqueous phase was not greatly affected by the employment of catalyst. Definitely, the optimization of HTL process of primary sludge by the use of catalyst is a convenient pathway, but with either a further post-refining step or with a change in the conditions.

Reference

Al-juboori, J.M., Lewis, D.M., Hall, T., van Eyk, P.J. 2023. Characterisation of chemical properties of the produced organic fractions via hydrothermal liquefaction of biosolids from a wastewater treatment plant. Biomass and Bioenerg, 170, 106703. *https://doi.org/10.1016/j.biombioe.2023.106703*

Biswas, B., Kumar, A., Fernandes, A. C., Saini, K., Negi, S., Muraleedharan, U. D., & Bhaskar, T. (2020). Solid base catalytic hydrothermal liquefaction of macroalgae: Effects of process parameter on product yield and characterization. *Bioresource Technology*, *307*, 123232. *https://doi.org/10.1016/j.biortech.2020.123232*

Carpio, R. B., Avendaño, C. I. L., Basbas, C. A., Habulan, A. a. A., Guerrero, G. E. G., Detras, M. C. M., & Bambase, M. E. (2022). Assessing the effect of K2CO3 and aqueous phase recycling on hydrothermal liquefaction of corn stover. *Bioresource Technology Reports*, *18*, 101093. https://doi.org/10.1016/j.biteb.2022.101093.

Costanzo, W., Hilten, R., Jena, U., Das, K., & Kastner, J. R. (2016). Effect of low temperature hydrothermal liquefaction on catalytic hydrodenitrogenation of algae biocrude and model macromolecules. *Algal Research*, *13*, 53–68. *https://doi.org/10.1016/j.algal.2015.11.009*

Dang, Z., Zhu, X., Wang, L., & Ji, G. (2021). Titanium dioxide catalytic hydrothermal liquefaction to treat oily sludge: As hydrogen production catalyst. *Chemical Engineering Journal Advances*, *8*, 100139. *https://doi.org/10.1016/j.ceja.2021.100139*

Dimitriadis, A., & Bezergianni, S. (2017). Hydrothermal liquefaction of various biomass and waste feedstocks for biocrude production: A state of the art review. *Renewable and Sustainable Energy Reviews*, *68*, 113–125. https://doi.org/10.1016/j.rser.2016.09.120

DuBois, M., Gilles, K.A., Hamilton, J.K., Rebers, P.A., Smith, F. 1956. Total sugar determination by phenol sulphuric method. Anal Chem, 28, 350-356.

Fan, Y., Fonseca, F., Gong, M., Hoffmann, A., Hornung, U., & Dahmen, N. (2021). Energy valorization of integrating lipid extraction and hydrothermal liquefaction of lipid-extracted sewage sludge. *Journal of Cleaner Production*, *285*, 124895. *https://doi.org/10.1016/j.jclepro.2020.124895*

Fan, Y., Meyer, L., Gong, M., Krause, B., Hornung, U., & Dahmen, N. (2023). Understanding the fate of nitrogen during catalytic hydrothermal liquefaction of sewage sludge. *Fuel*, *339*, 126948. *https://doi.org/10.1016/j.fuel.2022.126948*

Galadima, A., & Muraza, O. (2018). Hydrothermal liquefaction of algae and bio-oil upgrading into liquid fuels: Role of heterogeneous catalysts. *Renewable and Sustainable Energy Reviews*, *81*, 1037–1048. https://doi.org/10.1016/j.rser.2017.07.034

Haider, M.S., Castello, A., Michalski, K.M., Pedersen, T.H., Rosendahl, L.A. 2018. Catalytic hydrotreatment of microalgae biocrude from continuous hydrothermal liquefaction: heteroatom removal and their distribution in distillation cuts. Energies, 11, 3360. *https://doi.org/10.3390/en11123360*

Haider, M. S., Castello, D., & Rosendahl, L. A. (2020). Two-stage catalytic hydrotreatment of highly nitrogenous biocrude from continuous hydrothermal liquefaction: A rational design of the stabilization stage. *Biomass and Bioenergy*, *139*, 105658. *https://doi.org/10.1016/j.biombioe.2020.105658*

Hao, B., Yang, W., Wang, Y., Xu, D., Kapusta, K., & Guo, Y. (2022). Hydrothermal liquefaction of municipal sludge: Coupling effects of temperature and time on nitrogen migration. *Journal of Analytical and Applied Pyrolysis*, *165*, 105562. https://doi.org/10.1016/j.jaap.2022.105562

Hosseini, M., Hatefirad, P., Salimi, S., & Tavasoli, A. (2022). Hydrothermal liquefaction of granular bacteria to high-quality bio-oil using Ni–Ce catalysts supported on functionalized activated carbon. *Energy*, *241*, 122875. https://doi.org/10.1016/j.energy.2021.122875

Hwang, H., Lee, J. S., Choi, I., & Choi, J. Y. (2019). Comprehensive characterization of hydrothermal liquefaction products obtained from woody biomass under various alkali catalyst concentrations. *Environmental Technology*, *40*(13), 1657–1667. https://doi.org/10.1080/09593330.2018.1427799

Krishnan, R. Y., Manikandan, S., Subbaiya, R., Kim, W., Karmegam, N., & Govarthanan, M. (2022). Advanced thermochemical conversion of algal biomass to liquid and gaseous biofuels: A comprehensive review of recent advances. Sustainable Energy Technologies and Assessments, 52, 102211. https://doi.org/10.1016/j.seta.2022.102211

Lowry, O.H., Rosebrough, N.J., Farr, A.L., Randall, R.J. 1951. Proteins measurement with the folin phenol reagent. Biol Chem, 193, 265-275.

Lu, J., Wu, J., Zhang, L., Liu, Z., Wu, Y., & Yang, M. (2020). Catalytic hydrothermal liquefaction of microalgae over mesoporous silica-based materials with site-separated acids and bases. *Fuel*, *279*, 118529. https://doi.org/10.1016/j.fuel.2020.118529

Malins, K., Kampars, V., Brinks, J., Neibolte, I., Murnieks, R., & Kampare, R. (2015). Bio-oil from thermo-chemical hydro-liquefaction of wet sewage sludge. *Bioresource Technology*, *187*, 23–29. https://doi.org/10.1016/j.biortech.2015.03.093

Mondal, S., Singuru, R., Shit, S. C., Hayashi, T., Irle, S., Hijikata, Y., Mondal, J., & Bhaumik, A. (2017). Ruthenium Nanoparticle-Decorated porous organic network for direct hydrodeoxygenation

of Long-Chain fatty acids to alkanes. *ACS Sustainable Chemistry & Engineering*, *6*(2), 1610–1619. https://doi.org/10.1021/acssuschemeng.7b02772

Prestigiacomo, C., Proietto, F., Laudicina, V. A., Siragusa, A., Scialdone, O., & Galia, A. (2021). Catalytic hydrothermal liquefaction of municipal sludge assisted by formic acid for the production of next-generation fuels. *Energy*, *232*, 121086. https://doi.org/10.1016/j.energy.2021.121086

Qian, L., Wang, S., & Savage, P. E. (2017). Hydrothermal liquefaction of sewage sludge under isothermal and fast conditions. *Bioresource Technology*, *232*, 27–34. https://doi.org/10.1016/j.biortech.2017.02.017

Rani, M. a. a. B. A., Karim, N. A., Shamsul, N. S., & Kamarudin, S. K. (2023). Titanium oxide/nickel foam (TiO2/NF) catalyzed the conversion of glucose to 5-hydroxymethylfurfural in subcritical solvothermal liquefaction. *Fuel*, *345*, 128271. https://doi.org/10.1016/j.fuel.2023.128271

Rice, E.W., Baird, R.B., Eaton, A.D., Clesceri, L.S. 2012. Standard Methods for the Examination of Water and Wastewater, 22nd edn. APHA AWWA WEF, Washington.

Shah, A. A., Toor, S. S., Conti, F., Nielsen, A. H., & Rosendahl, L. A. (2020). Hydrothermal liquefaction of high ash containing sewage sludge at sub and supercritical conditions. *Biomass and Bioenergy*, *135*, 105504. https://doi.org/10.1016/j.biombioe.2020.105504

Wang, W., Yu, Q., Meng, H., Han, W., Li, J., & Zhang, J. (2018). Catalytic liquefaction of municipal sewage sludge over transition metal catalysts in ethanol-water co-solvent. *Bioresource Technology*, *249*, 361–367. https://doi.org/10.1016/j.biortech.2017.09.205

Wang, W., Xu, Y., Wang, X., Zhang, B., Tian, W., & Zhang, J. (2018). Hydrothermal liquefaction of microalgae over transition metal supported TiO2 catalyst. *Bioresource Technology*, *250*, 474–480. https://doi.org/10.1016/j.biortech.2017.11.051

Xiao, H., Zhai, Y., Xie, J., Wang, T., Wang, B., Li, S., Li, C. 2019. Speciation and transformation of nitrogen for spirulina hydrothermal carbonization. Bioresource Technol, 286, 121385. *https://doi.org/10.1016/j.biortech.2019.121385*

Xu, D., Lin, G., Liu, L., Wang, Y., Jing, Z., & Wang, S. (2018). Comprehensive evaluation on product characteristics of fast hydrothermal liquefaction of sewage sludge at different temperatures. *Energy*, *159*, 686–695. *https://doi.org/10.1016/j.energy.2018.06.191*

Yang, J., Hong, C., Xing, Y., Zheng, Z., Li, Z., Zhao, X., & Qi, C. (2021). Research progress and hot spots of hydrothermal liquefaction for bio-oil production based on bibliometric analysis. *Environmental Science and Pollution Research*, *28*(7), 7621–7635. *https://doi.org/10.1007/s11356-020-11942-2*

Zhou, A., Yu, Sh., Deng, Sh., Mikulčić, H., Tan, H., Wang, X. (2023). Enrichment characteristics and environmental risk assessment of heavy metals in municipal sludge pyrolysis biochar. Journal of the Energy Institute, 111, 101417. *https://doi.org/10.1016/j.joei.2023.101417*

Zhu, Y., Zhao, Y., Tian, S., Zhang, X., & Wei, X. (2022). Catalytic hydrothermal liquefaction of sewage sludge: Effect of metal support heterogeneous catalysts on products distribution. *Journal of the Energy Institute*, *103*, 154–159. https://doi.org/10.1016/j.joei.2022.04.008

5

Doping WWTP primary sludge HTL products by solvent

ABSTRACT

Hydrothermal liquefaction (HTL) can directly convert primary sludge (PS) to biocrude without pre-treatment. This research study considered the effect of sludge percentage (2 and 8 % (w/w_{TS})) and the effect of solvents and co-solvents (methanol (100%; 50% and 65%), ethanol (100% and 50%), ethyl acetate (100%) and acetone (100%)) on biocrude, biochar, aqueous phase and biogas production. All the products were characterized and yields were calculated. High moisture biomass can effectively increase the yield and quality of biocrude, which implies the efficiency of the process. At 300 °C, the highest biocrude yield 32.10 % (w/w_{VS}) with 16.71 % (w/w_{VS}) of oils and high heating value (HHV) of 41.82 MJ/kg were obtained. Compared to the hydrothermal liquefaction in water at 200 °C, the highest biocrude yield 51.37 % (w/w_{VS}) with 48.82 % (w/w_{VS}) of oils and high heating value (HHV) of 45.95 MJ/kg were obtained when using pure methanol. In addition, the use of alcohol boost the formation of ester compounds.

3031

1. Introduction

Wastewater treatment plants have been established to treat wastewater to required standards before release to the receiving environment. During the process, an excess amount of residue called sludge is produced. Sewage sludge has the potential to be utilized as a resource for landfilling, agricultural application, incineration and sea dumping. However, the application of these conventional methods has been restricted because of environmental problems such as contamination with pathogens, heavy metals, emission of toxic substances into the atmosphere and micropollutants (Jahromi et al. 2022). Therefore, it´s necessary to develop a process that resolve the issue of waste generation in an efficient way. On the other hand, to minimize fossil fuel demands and greenhouse gas emissions, waste-to-energy conversion has received a great attention worldwide (Li et al., 2021). Sludge, characterized by its availability and high nutrient and carbon contents, has driven the society to look at it as a very promising feedstock, able to generate energy or interesting molecules (Fan et al. 2021).

Hydrothermal liquefaction (HTL) is a thermochemical process that operates at high temperatures (280-350 °C) and high vapour pressures (100-221 bar at these temperatures). Particularly, it can convert biomass into a biocrude and other high-added valued products without any pre-drying (Barreiro et al. 2022; Dimitriadis et al., 2017). Subsequently, HTL can highly minimize waste volume, destroy organic pollutants, and remove pathogens during a short period of time (less than 1 hour). Some lab scale research suggested that HTL primary sludge at 325- 350 ºC for less than 20 min could attain a high energy recovery (up to 69 %) (Thomsen et al., 2020). Recently, researchers have been trying to improve the yield of biocrude by optimizing the process reaction conditions. One of the possibilities is to replace partially or totally the water by organic solvents, characterized by their lower critical point when compared to water, allowing to perform HTL at lower temperature and pressure (Li et al. 2018; Masoumi

et al. 2021). The employment of organic solvent in HTL process is potential to enhance the yield and quality of biocrude (Caporgno et al., 2016), specifically, to improve carbon content and higher heating value (HHV) and decrease viscosity (Yerrayya et al., 2022). Co-solvents can affect significantly the extraction and thermal depolymerization reactions when there are strong interactions with solutes like hydrogen bonds (Baloch et al., 2021). These solvents can be recycled through evaporation after HTL (Patil et al., 2014). For example, the critical conditions of ethanol (243.1 ºC, 6.3 MPa) are lower than that of water. Using ethanol in HTL can improve the dissolution of carbohydrates and lignin as it has lower dielectric constant and weaker H-bond than water (Kim et al., 2022). Also, ethanol acts by itself as a reactant in the conversion reactions of aldehydes to esters (Balcho et al., 2021). The HTL of kitchen wastes with ethanol (ratio 5:3) at 260 ºC, allowed a yield of biocrude close to 48 %, when the HTL realized with water alone, only produced less than 10 % of yield (Yan et al. 2023). Methanol, another organic solvent, produced from various sources, is characterized by its Lewis acidity when compared to other alcohols and expected to be part of the redox reactions resulting in the cleavage of bonds during HTL process (Yerrayya et al., 2022). Specific thermodynamic properties (enthalpy, entropy, etc.) of alcohol-water binary solvents provide faster reaction rate of decarboxylation, hydrolysis and condensation than is possible in water (Isa et al., 2018). For example, the HTL of Nannochlopsis gladina with a mixture of methanol: water at a ratio of 3:1 (Masoumi et al. 2021), improved the biocrude yield from 15 to 47 %. While in the HTL of sewage sludge at 260 ºC, a maximum yield of biocrude of more than 42 % was obtained with a mixture methanol: water with a ratio of 1:1 (Tong et al. 2021). Acetone belongs to the aprotic polar solvent category. Previous investigations of acetone (as solvent and co-solvent) observed changes in the reaction mechanism. Its presence supported the production of phenolic and ketonic compounds (Arturi et al., 2019). Another parameter that affects the HTL conversion is

the concentration of the feedstock. When the amount of water is higher, the hydrolysis of sludge is faster, resulting in an increase in the yields of biocrude and aqueous phase due to the production of more organic compounds (Māliņš et al., 2015). An elevated level of moisture content could potentially delay the dehydration reactions of water-soluble compounds, preventing them from becoming less polar and can be effectively integrated into the biocrude phase (Xu et al., 2008). In one study, the results obtained suggested that a sewage sludge with higher moisture content can be readily converted to water-soluble and gas product at a short time. While at longer time, the compounds of the aqueous phase might be converted to lighter compounds, causing more production of volatiles leading to higher bio-crude yield (Qian et al., 2017).

The literature undoubtedly demonstrated the presence of synergistic effects from co-solvents during biomass liquefaction, leading to improved bio-oil yield and quality. For this reason, the effect of the solvent or of a mixture of solvents was evaluated in HTL of a balanced primary sludge from the WWTP Reus in Spain ([carbohydrates] ≈ [lipids] ≈ [proteins] ≈ [ashes]. In a first part of the work, water was used as a solvent in different concentrations with respect to dried total solids. Operating conditions were maintained at 300°C of temperature and 30 min of time. In a second part of the study, several solvents including methanol, ethanol, ethyl acetate and acetone were used alone or in a mixture with water as methanol-water or ethanol-water. Different ratios of the mixture were tested in the HTL process. In these experiments, temperature and time of reaction were set at 200°C and 30 min. All the products were fully recuperated. Quantification and characterization of products was completed following corresponding protocols and analysis.

2. Materials and methods

2.1. Reagents

Dichloromethane (ref.: 32222), with a purity of 99.9%, Toluene (ref.: 32249) with a purity of 99.7%, and 2-Propanol (ref.: 59300) with a purity of 99.9% were purchased from Honeywell. Methanol (ref.: 412722), HPLC-GOLD-Ultragradient grade, was obtained from Carlo Erba reagents. n-Hexane (ref.: 363242), with a purity of 95%, high-performance chromatography grade, and phenol crystalline (ref: 144852.1211), ethanol with a concentration of 96% (ref: 212800.1212), as well as n-heptane (ref.: 162062.1611), were provided by PanReacAppliChem. Sulfuric acid reagent (ref: 34632), orange reagent (ref: 131130.1612), sulfuric acid (ref: 30743) with a concentration of 95.0-97.0%, ethyl acetate with a concentration of 99.5% (ref: 319902), bovine serum albumin (BSA) (ref: A9647), sodium hydroxide with a purity of 98% (ref: 30620), sodium carbonate (ref: 222321), potassium sodium tartrate tetrahydrate (ref: 217255), copper (II) sulphate pentahydrate (ref: 209198), Folin&Ciocalteu's phenol reagent (ref: F9252), magnesium sulphate monohydrate (ref: 434183), anhydrous sodium sulphate (ref: 239313), and fuming hydrochloric acid (ref: 84418), all of high analytical reagent grade, were supplied by Sigma - Aldrich. Acetone was bought from Icopresa Acetona.

2.2. Primary sludge collection and managing

Primary sludge was supplied by the municipal wastewater treatment plant of Reus in Tarragona, Spain. Bottles were filled with 500 ml of primary sludge after partial gravity thickening of the primary treatment. They were stored in a freezer at -15°C and defrosted in an oven at 60°C for 5 hours. Water part was removed by evaporation through rotary evaporator at 95°C and very low vacuum pressure, and recuperated separately. Remaining solids were dried completely in the oven at 105°C for 24 hours.

2.3. Characterization of primary sludge

The characterisation of primary sludge was done before the drying process and was realized three times. Total solids (TS), volatile solids (VS) and ash content were analysed according to standard methods 2540B and 2540E respectively (Rice et al., 2012). Lipid extraction was completed in a Soxhlet apparatus using hexane as a solvent, according to standard method 5520E (Rice et al., 2012). Total carbohydrates content was detected by phenol-sulfuric acid Dubois method (Dubois et al., 1956). Briefly, 0.05 mL of 80% phenol solution was added to 2 mL of diluted sludge sample in a glass tube. Then, 5 mL concentrated sulfuric acid was quickly added. The tubes were kept under room temperature for 10 min and then placed into a thermostatic bath at 30°C another 15 min. The absorbance was measured at 480 nm. Proteins percentage was determined with Lowry method (Lowry et al., 1951). The proteins solubilization in the sludge samples was achieved by heating the samples with 2 M sodium hydroxide at 100°C for 10 min. The absorbance was measured at 750 nm. Finally, ultimate analysis was provided by Serveis Técnics de Recerca at Universitat de Girona. Analysis was done using an ultimate analyser (Perkin Elmer model EA2400). C, H and N were determined, and O was calculated by difference. A field emission of variable pressure environmental scanning electron microscopy (ESEM) with X-ray microanalysis (Quanta 600, FEI Company), characterised by a high resolution (3 nm) was utilized to detect heavy metals of primary sludge.

2.4. Hydrothermal liquefaction of primary sludge

The experiments were conducted using a 1 L Stainless Steel Autoclave (Autoclave Engineers model EZE Seal), which was equipped with a movable heating shell, a fixed MagneDrive® stirrer (a packless rotary impeller system that operates magnetically), and an operating

condition controller. To facilitate gas flow, the reactor was connected to a gas line through an inlet valve, allowing the introduction of nitrogen. The outlet valve was connected to a gas flow meter and a Tedlar bag push lock valve 0.6 L (Superlco 30289-U) for collecting gas. The reactor was initially filled with approximately 500 g of the mixture primary sludge-solvent. In the first experimental part, water was used as a solvent with different percentages of primary sludge: 2 % (w/w) and 8 % (w/w). HTL experiments were performed at 300°C (~86.9 bar) of temperature, 30 min of reaction time and 100 rpm of stirring rate. The heating time was 2 hours. In the second experimental part, the percentage of sludge was maintained at 4 % (w/w). Water (100%), methanol (100%; 50% and 65%), ethanol (100% and 50%), ethyl acetate (100%) and acetone (100%) were used as solvents and co-solvents. HTL experiments were conducted at subcritical condition, 200°C (~33.7 bar). The reaction time after reaching the desired temperature was always 30 minutes, with continuous agitation at 100 rpm. The heating time was 1 hour. To create an oxygen-free environment, pure nitrogen gas was purged three times, and then the pressure was increased to 1 bar. The pressure of the reaction was not manually controlled but instead automatically generated based on the reaction temperature. After each batch experiment, the reactor was cooled down in a water bath at room temperature (~25°C) until it returned to its initial condition.

2.5. Cleaning of the reactor and separation of products

Figure 1 depicts the schematic diagram illustrating the separation procedures conducted after hydrothermal liquefaction of primary sludge.

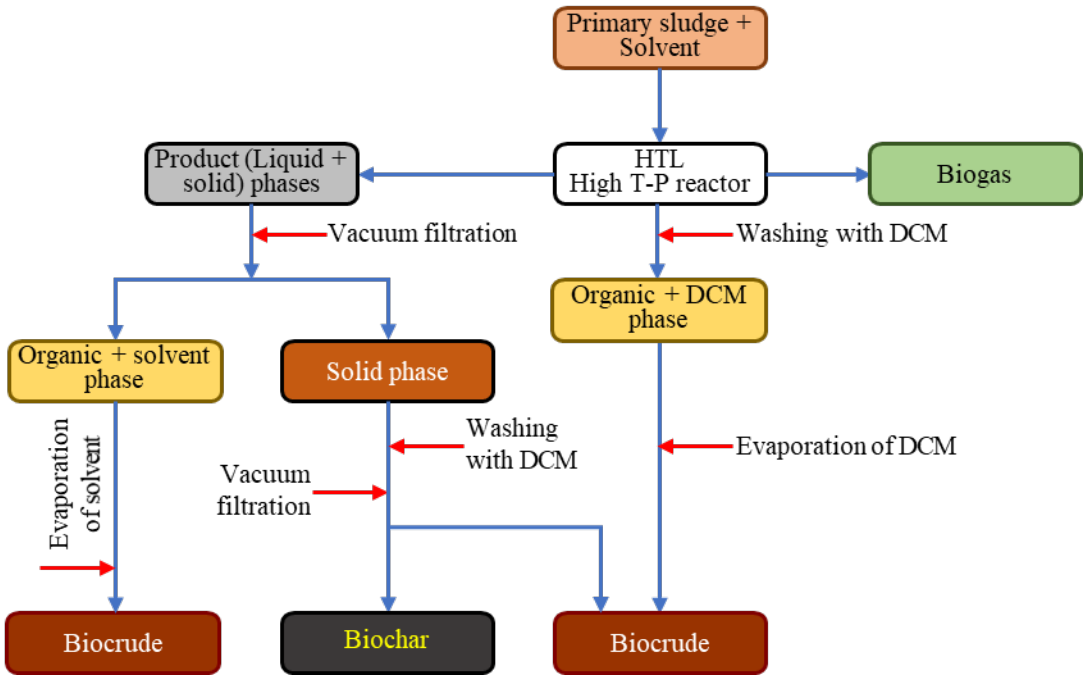

Figure 1. Process overview of HTL of primary sludge.

The resulting products were divided into four distinct phases: gas, organic, aqueous, and solid. Once the reactor returned to atmospheric pressure and the laboratory ambient temperature, the gas phase was released. The gas mixture passed through a flow meter to measure its volume and was collected in a gas bag. Subsequently, the reactor was opened, and the mixture was poured into a large beaker. Vacuum filtration was employed to separate the solid component from the liquid component. The liquid portion, consisting mainly of the solvent used-organic phase, was transferred into a bottle. Meanwhile, the reactor underwent repeated washing with dichloromethane to fully recover any remaining organic components adhering to the reactor walls and cover, as well as the agitation module. The resulting mixture, containing some solids entrapped within the organic phase, was separated again using vacuum filtration. The liquid portion, comprising the remaining organic phase and dichloromethane, was transferred into another bottle. The solid residue retained on the filter paper, consisting of biochar and ashes, was subjected to several washes with dichloromethane. The biochar was then dried in an oven

at 105ºC for 24 hours and weighed for quantification. Organic phases collected from both solvents underwent rotary evaporation to remove the dichloromethane and the solvent used. The resulting viscous organic liquid, known as biocrude, was weighed for further quantification. Finally, the biocrude was subjected to Soxhlet extraction using 200 mL of hexane to separate it into oils and asphaltenes. The oils were subsequently separated from the hexane by rotary evaporation at 65ºC and atmospheric pressure. Asphaltenes were quantified by the difference between biocrude and oils. The biocrude yield was calculated from equation (1):

$$\text{Biocrude yield (\%)} = \frac{\text{Mass of biocrude from DCM+Mass of biocrude from solvent used}}{\text{Mass of volatile solids}} \times 100 \quad (1)$$

The aqueous phase yield was calculated from equation (2):

$$\text{Aqueous phase yield (\%)} = \frac{\text{Mass of solids dissolved in aqueous phase}}{\text{Mass of volatile solids}} \times 100 \quad (2)$$

The solid yield was calculated from equation (3):

$$\text{Solid yield (\%)} = \frac{\text{Mass of solid residue}}{\text{Mass of volatile solids}} \times 100 \quad (3)$$

The gas yield was calculated from equation (4):

$$\text{Gas yield (\%)} = \frac{\text{Mass of gas}}{\text{Mass of volatile solids}} \times 100 \quad (4)$$

In all the equations, mass of volatile solids corresponds to the mass of primary sludge.

2.6. Biocrude characterization and quantification

A comprehensive characterization was conducted on the biocrude, encompassing various analyses. These analyses included weight determination, ash content determination, gas chromatography/mass spectrometry (GC/MS), thermogravimetric analysis (TGA), elemental (ultimate) analysis, determination of higher heating value (HHV), Fourier transform infrared spectroscopy (FTIR), nuclear magnetic resonance (NMR), and simulated distillation (SimDis).

Additionally, the saturated, aromatics, resins, and asphaltenes (SARA) fractions of the biocrude were characterized.

2.6.1. Gas chromatography/mass spectrometry spectroscopy of biocrude

The biocrude samples at all temperatures underwent characterization using gas chromatography-mass spectrometry (GC/MS). The analysis was performed using a Perkin Elmer Turbo Mass Gold GC/MS instrument, equipped with a Supelco SLB®-5ms capillary GC column (length × inner diameter: 30 m × 0.25 mm, with a film thickness of 0.25 μm). Dichloromethane was employed as the solvent for the analysis. The GC oven was programmed to start at 70ºC for 1 minute, followed by a temperature ramp to 180ºC at a rate of 7ºC per minute. Subsequently, the temperature was further increased to 240ºC at a rate of 12ºC per minute, and the final temperature was held at 330ºC for 7 minutes.

2.6.2. Thermogravimetric analysis of biocrude

The thermogravimetric analysis (TGA) was employed to investigate the weight loss characteristics of the biocrudes. For each test, approximately 3 to 4 mg of the sample was subjected to heating from 30°C to 800°C. The analysis was conducted under a nitrogen flow rate of 60 mL/min, with a heating rate of 10 K/min.

2.6.3. Elemental analysis and HHV of biocrude

Serveis Técnics de Recerca at Universitat de Girona conducted the ultimate analysis of the biocrude samples, as mentioned in section 2.2. The analysis involved the quantification of carbon (C), hydrogen (H), and nitrogen (N) content, while oxygen (O) content was determined by difference. Subsequently, the higher heating values (HHVs) of the biocrude were calculated

using the Dulong formula (equation 5), as described in Hong's study. The HHVs were expressed in MJ/kg (Hong et al., 2021).

$$\mathrm{HHV}\ (\%) = 0.3383 \cdot \mathrm{C} + 1.443 \cdot \left(\mathrm{H} - \frac{\mathrm{O}}{8}\right) \quad (5)$$

C, H and O are the mass percentages of carbon, hydrogen, and oxygen from the ultimate analysis of the samples, respectively.

The energy recovery of biocrude is calculated using the equation below:

$$\mathrm{ER}\ (\%) = \cdot\ \text{Biocrude yield}\ (\%) \cdot \frac{HHV\ Biocrude}{HHV\ Primary\ sludge} \quad (6)$$

2.6.4. FTIR of biocrude

FTIR spectra were obtained using a Thermo Nicolet Nexus 670 Fourier Transform Infrared Spectrophotometer. The instrument was equipped with a single-bounce diamond attenuated total reflectance (ATR) accessory known as Specac Golden Gate, as well as a KBr beam splitter. Spectra were collected in the range of 4000 to 500 cm-1 with a resolution of 0.98 cm-1. To ensure accuracy, 50 replicate scans were averaged using Omnic software. Prior to sample analysis, background scans were performed on the dry accessory at ambient temperature. The spectra were then obtained by directly applying approximately 30 mg of the sample onto the surface of the ATR crystal.

2.6.5. ^{1}H NMR of biocrude

The ^{1}H NMR spectra were obtained using a Varian Unity 400-MHz spectrometer equipped with a 5-mm broadband probe. For analysis, 50-75 mg of biocrude was dissolved in deuterated chloroform, which contained 0.03% tetramethylsilane (TMS) as an internal reference. To remove any suspended particulates, the samples were filtered using a 0.22-µm PTFE filter before being loaded into 5 mm diameter NMR tubes. The ^{1}H spectra were acquired with a 90°

pulse angle, a spinner frequency of 20 Hz, a sweep width of 8000 Hz, and a total of 32 transients.

2.6.6. Simulated distillation of biocrude

Simulated distillations were conducted following the ASTM-D2887 method. A HP 5890 Series II FID gas chromatograph and a Durabond DB-HT-SimDis GC column by Agilent-J&W Scientific (5 m length, 0.53 mm inner diameter, 0.15 μm film thickness) were employed for the analysis. Helium was used as the carrier gas with a flow rate of 56.4 mL/min. The oven temperature was initially set to 36°C and then increased to 400°C at a rate of 10°C/min, followed by a 10-minute hold at that temperature. The injector volume was set to 0.5 μL, and the injector temperature was maintained at 350ºC. The detector temperature was set to 375°C, with a hydrogen gas flow rate of 40 mL/min, an airflow of 400 mL/min, and a helium makeup flow rate of 24 mL/min.

For the analysis, samples containing 1% w/w and reference standards containing 0.5% w/w were dissolved in dichloromethane (DCM). Prior to analysis, the samples were filtered using a 0.22 μm PTFE filter to eliminate any suspended particulates. The boiling points were determined using a D2887 calibration mix and a D2887 Reference Gas Oil standard, both obtained from Sigma Aldrich. Data, including retention time and peak areas, were collected. Each sample was divided into fractions (%wt), and the corresponding boiling points were calculated accordingly.

2.6.7. Gas chromatography/mass spectroscopy of oils separated from biocrude

The oils were subjected to characterization using gas chromatography-mass spectrometry (GC/MS). The same procedure employed for the biocrude analysis (as described in section 2.6.1) was followed, but with the utilization of hexane as the solvent.

2.6.8. Quantification of SARA fractions of biocrude

The SARA fractions of the biocrude were analysed. The process of separating the light phase and heavy phase was repeated, following the procedure mentioned above, but this time utilizing n-heptane. The separated maltenes were then fractionated into saturated hydrocarbons by passing 20 mL of n-heptane through an activated alumina-packed glass chromatographic column. Subsequently, aromatic compounds were extracted by employing 20 mL of toluene. Additionally, resins were separated from the adsorbent using 20 mL of methanol. Each eluted fraction was recovered by removing the solvent using a rotary evaporator.

2.7. Biochar characterization and quantification

The determination of total solids, moisture content, volatile solids, and ash content in the biochar was carried out using standard methods 2540B and 2540E, as outlined in Rice et al. (2012). Additionally, the ultimate analysis and detection of heavy metals in the biochar were performed following the same procedures described earlier.

2.8. Aqueous phase characterization

Several parameters were measured or analysed in the aqueous phase, including COD (Chemical Oxygen Demand), TOC (Total Organic Carbon), TN (Total Nitrogen), proteins, and carbohydrates. The COD analysis was performed according to standard method 5220D as

described in Rice et al. (2012). TOC analysis was carried out using a TOC analyser from the TOC-L Series, utilizing a specific standard calibration curve. The measurement of TOC was conducted by ASI-L auto sampler Shimadzu, which was connected to a Shimadzu TOC-L CSN TOC analyser equipped with an NDIR (Non-Dispersive Infrared) detector and calibrated with standard solutions of hydrogen potassium phthalate. Total dissolved nitrogen was determined using the same TOC analyser coupled with the TNM-L ROHS unit, following the methodology outlined in Ponces-Robles et al. (2018). Protein content was measured using the Lowry method described by Lowry et al. (1951), while carbohydrates were quantified using the Dubois method outlined in Dubois et al. (1956), as previously discussed in section 2.3.

The aqueous phase was also subjected to measurements of total solids (TS), volatile solids (VS), and ash content. A specific volume of the aqueous phase was dried in a weighed crucible for 24 hours in an oven set at 100ºC. Subsequently, it was burned in a furnace at 550ºC for 1 hour, following the procedures described in standard methods 2540B and 2540E as detailed in Rice et al. (2012). The pH value of the HTL aqueous phase was measured using a pH meter. Additionally, heavy metals were analysed in the ash of the solid dissolved in the aqueous phase, following the same procedure mentioned earlier.

2.9. Gas phase characterization

Figure 1 also depicts the characterization performed on the gas phase. The identification and quantification of biogas components were conducted using a gas chromatograph (micro-GC, Agilent, 990) equipped with a thermal conductivity detector (TCD). Two different columns were employed for separating the light and heavy gases. Column 1, MS5A SS 10MX0.25MMX30UM BF RTS, CP-PORABOND Q 5MX0.25MMX3UM, was utilized to separate the light gases with Argon employed as the carrier gas. Column 2, PORAPLOT Q UM

10MX0.25MMX8UM BF, CP-PORABOND Q 1MX0.25MMX3UM, was used to separate the heavy gases with helium as the carrier gas.

For column 1, the injector temperature was maintained at 100ºC, with an injection time of 40 ms. The column temperature was set to 100ºC, and the initial pressure was 200 kPa.

For column 2, the injector temperature was also set at 100ºC with an injection time of 40 ms. The column temperature was maintained at 60ºC, and the initial pressure was 150 kPa.

The run time for the analysis was 120 seconds. The mole percentage of each gas component was determined using gas standards prepared by Carburos Metálicos, S.A., serving as reference for calibration purposes.

3. Results and discussion

3.1. Characterization of primary sludge and suitability of its use in HTL

Table 1 provides an overview of the characterization conducted on the primary sludge. The as-received primary sludge was found to contain approximately 4.3 ± 0.1% total solids (w/w wet sludge basis). By difference, the moisture content accounted for 95.7 ± 0.1% (w/w wet sludge basis). These values align closely with those reported in previous studies on primary sludge from the Reus WWTP (Tarragona, Spain), such as 4.2 ± 1.2% (Olkiewicz et al., 2015) or 3.9 ± 0.1% (Glinska et al., 2020). The ash content, expressed as a percentage of the total solids, was determined to be 22.9 ± 0.3%. Consequently, the volatile solids were calculated as the difference from the ash content, resulting in 77.1 ± 0.3% (w/w total solids basis). Notably, the density of the primary sludge was found to be 1.012 g/mL, comparable to that of water.

Regarding the analysis of volatile solids, the primary sludge was examined for its carbohydrate, protein, and lipid contents. Carbohydrates were identified as the predominant fraction, accounting for 29.84%.

Table 1. Characterization of primary sludge from WWTP of Reus.

Proximate analysis	TS as received (% $w/w_{primary\ sludge}$) *	95.7 ± 0.1
	Moisture (% $w/w_{primary\ sludge}$) *,#	4.3 ± 0.1
	Ashes (% w/w_{TS}) *	23.9 ± 0.3
	VS (% w/w_{TS}) *,#	77.1 ± 0.3
	Proteins (% w/w_{TS}) *	21.2 ± 1.7
	Carbohydrates (% w/w_{TS}) *	29.8 ± 1.2
	Lipids (% w/w_{TS}) *	23.4 ± 0.8
	TOC (mg/L)	6290
	COD (mg/L)	35180
Ultimate analysis (ash free)	C (%)	47.81
	H (%)	6.93
	N (%)	4.81
	O (%)	40.45
Calorific value	HHV (MJ/kg)	18.83

* Average of at least three assays

By difference

The values obtained for lipids (23.41%) and proteins (21.15%) were considered significant. These findings are consistent with those from previous studies on primary sludge from the same source, reporting lipids (19.6 ± 0.6%), carbohydrates (31.3 ± 0.1%), proteins (27.7 ± 0.1%), and ashes (16.0 ± 0.1%) in a cellulose recovery study (Glinska et al., 2020), as well as lipids (27.2 ± 0.4%), carbohydrates (26.2 ± 2.6%), proteins (24.2 ± 1.4%), and ashes (20.1 ± 0.4%) in a study on biodiesel production from primary sludge. It is worth noting that the

primary sludge from the Reus WWTP consistently exhibits a similar composition of ingredients, all falling within the 20-30% range on a w/w total solids basis.

The ultimate analysis of the primary sludge revealed low nitrogen content (3.71%), low hydrogen content (5.34%), high carbon content (36.86%), and a remarkably high oxygen content (31.19%), determined by difference. These values allowed for the calculation of the higher heating value (HHV) of the dried primary sludge. In this calculation, the mass of the ashes was excluded to obtain a more realistic value. Under these conditions, the HHV was determined to be 14.55 MJ/kg. This value aligns with those obtained in other works, such as 10.55 MJ/kg (Kulikova et al., 2022) or 17.31 MJ/kg (Adedeji et al., 2022).

SEM images and EDX spectra of the ash in the primary sludge are presented in Figure 2. The SEM images illustrate the irregular structure of the ashes, consisting of particles of different sizes and shapes.

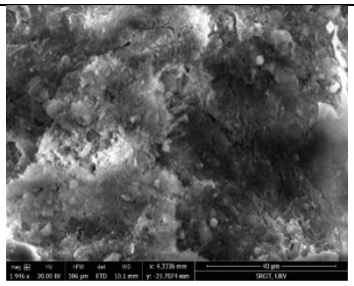

SEM image location (a)

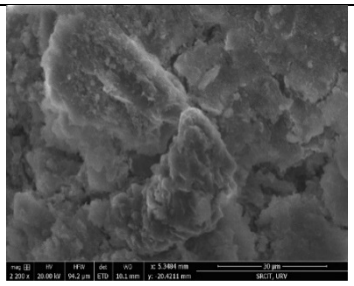

SEM image location (b)

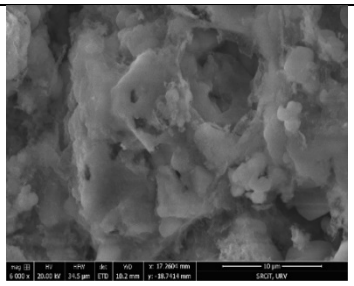

SEM image location (c)

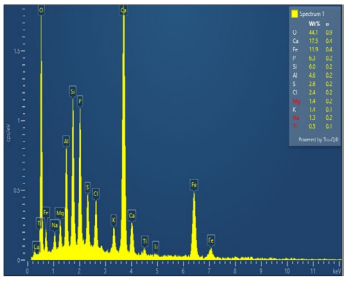

EDX spectra location (a)

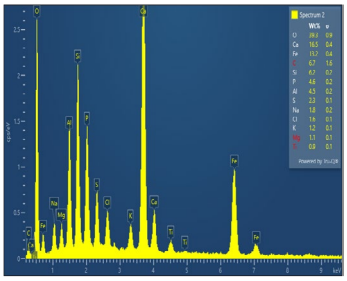

EDX spectra location (b)

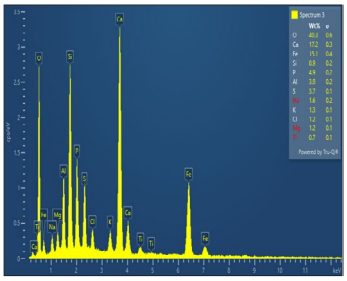

EDX spectra location (c)

Figure 2. SEM images and EDX spectra of ash in primary sludge. (a), (b) and (c) represent three different zones of the sample.

Larger particles appear to be formed by the aggregation of smaller ones. When magnified 6000 times, asymmetric cavities and a granule-covered surface can be observed. The EDX spectra of the ash indicated the presence of various elements, with average identified percentages of O (41.2%), Ca (17.1%), Fe (13.4%), Si (7.0%), P (5.3%), Al (4.3%), S (2.9%), Cl (1.7%), Na (1.6%), K (1.3%), Mg (1.2%), and Ti (0.7%). The origin of these oxides can be attributed to factors such as the high calcium content in the drinking water, dust carried by rainwater, and erosion within the sewage system.

Regarding the suitability of primary sludge for the HTL process, it exhibits a low total solids content of 4.3% (w/w wet sludge basis). This value is consistent with those reported in other studies, typically ranging from 1% to 5%, such as 5.0% (Biller et al., 2018) or 4.5% (Marrone et al., 2018). Consequently, the primary sludge contains a high-water content, making it an ideal candidate for the HTL process, which is specifically designed for the treatment of wet biomass, utilizing water as the medium for organic matter degradation.

The presence of lipids in the primary sludge, derived from free fatty acids within the C10 to C18 range, serves as precursors for ester production. Additionally, proteins are known to play a role in promoting biocrude production through HTL, with Maillard reactions playing a crucial part in the distribution and composition of biocrude. The primary sludge from WWTP is rich in lipids, proteins, and carbohydrates. Thus, HTL represents a suitable option for thermally hydrolysing these macromolecules into valuable chemicals. Consequently, primary sludge supports the demonstration of an economically viable and energy-efficient approach to sludge biorefinery.

3.2. Hydrothermal liquefaction of primary sludge

Sample containing around 500 g of wet primary sludge was used for the experiments. In the first part, the concentrations of TS in water chosen were 2 % (w/w) and 8 % (w/w). Runs were always performed at 300ºC of temperature, 30 min of reaction time and 100 rpm of stirring rate. In the second part, the temperature was decreased to 200ºC and reaction time and stirring rate were maintained at 30 min and 100 rpm. Different scenarios were completed: methanol (100%), ethanol (100%), ethyl acetate (100%), acetone (100%), aqueous phase (100%), methanol-water (1:1), methanol water (2:1) and ethanol-water (1:1). After the achievement of the experiment, the reactor was cooled to room temperature after the reaction time had passed. The designated experimental procedure shown in Figure 1 Subsequently, the four products (gaseous phase, biocrude, organics-containing aqueous phase, and biochar) were separated. The following sections will outline the quantification and characterization of the products obtained during the hydrothermal liquefaction (HTL) of the sludge.

3.3. Effect of ratio TS:water on characteristics of biocrudes

3.3.1. Results

The biocrude yields from HTL of primary sludge with different TS: Water ratios realised at 300ºC are presented in Table 2. In the scenarios where the volume of water was modified, obviously, the yield of biocrude has increased from 21.06% (w/w_{VS}). to 32.10 % (w/w_{VS}). along with the increase of concentration of sludge from 2 w_{TS}% to 8 w_{TS}%. The percentage of bio-oil increased slightly from 13.57 (w/w_{VS}) to 16.71 (w/w_{VS}). Typically, a great amount of moisture leads to higher bio-crude yields, mainly because it enhances the speed of hydrolysis reaction by improving the solubility of the organic fragments. In the study of Qian and his

colleagues, when the water content has increased from 9.6 to 49.7%., biocrude yield has been improved from 22.4 to 27.3% (w/w) (Qian et al. 2017). However, herein, the volume of water remained high in both cases (higher than 92%) and enough to still boost the depolymerization and decomposition reactions of primary sludge.

Table 2. Effect of TS:Water ratio on biocrude, oils and asphaltenes yields (T = 300ºC; Time = 30 min; Stirring = 100 rpm).

TS: Water	Biocrude		Bio-oil *		Asphaltene *	
Ratio	Weight (g)	(%)	Weight (g)	(%)	Weight (g)	(%)
2 %	1.67	21.06	1.08	13.57	0.59	7.49
8 %	10.12	32.10	5.27	16.71	4.85	15.39

* Bio-oil was extracted from biocrude with hexane and asphaltene was calculated by difference

3.3.2. Ultimate analysis and high caloric value of biocrudes, effect of TS:water ratio

The percentages of elements C, H, N and O, the higher heating value HHV and the energy recovery for HTL using different concentrations of TS and for HTL using different solvents and co-solvents are listed in Table 3.

Table 3. Elemental analysis and HHV of biocrude using different TS:water ratios, (T = 300ºC; Time = 30 min; Stirring = 100 rpm).

		Elemental analysis (%)					
Samples		C	H	N	O	HHV (MJ/kg) *	ER (%) **
Ratio TS:Water	2 %	69.84	9.10	4.37	16.69	45.81	40.96
	8 %	71.75	8.27	6.64	13.34	41.82	71.30

* Calculated using equation (5)

** Calculated using equation (6)

Regarding Table, it's clear that the increase in the concentration of TS didn't really affect the ultimate composition of biocrude. In both cases, HHV was higher than 40 MJ/kg. The percentages of C, H, N and O in biocrudes from HTL using 2% and 8% of TS were very comparable. They were 69.84 % and 71.75 %, 9.10 % and 8.27 %, 4.37 % and 6.64 % and 16.69 % and 13.34 %. A higher energy recovery was observed with a ratio of 8% (71.30%).

3.3.3. GC/MS of biocrudes, effect of TS:water ratio

Chemical compounds found in biocrude produced from the different HTL runs were identified by GC/MS analysis. Only compounds with boiling point lower than 330 ºC could have been detected. Through the analysis process, compounds with an identification probability more than 70% were considered. The detailed compound information of the biocrude from HTL with different ratios TS:Water is presented in Table 4.

Table 4. GCMS analysis of biocrude from HTL using different TS:water ratios, (T = 300ºC; Time = 30 min; Stirring = 100 rpm).

Time (min)	Substance	Formula	Time (min)	Ratio TS:Water 2%	Ratio TS:Water 8%
	cis-2-Methyl-7-octadecene	$C_{19}H$	14.87		X
	1-Heptadecene	$C_{17}H$	17.19		X
	E-14-Hexadecenal	$C_{16}H_{30}O$	17.20	X	
	2-Pentadecanone	$C_{15}H_{30}O$	17.31	X	X
	1-Nonadecene	$C_{19}H_{38}$	19.03		X
	2-Heptadecanone	$C_{17}H_{34}O$	19.97	X	X

Time (min)	Substance	Formula	Time (min)	Ratio TS:Water 2%	8%
	Methyl stearate	$C_{19}H_{38}O_2$	22.20	X	
	Hexadecanoic acid, methyl ester	$C_{17}H_{34}O_2$	20.23	X	X
	9-Octadecenoic acid, (E)-	$C_{18}H_{34}O$	20.42	X	X
	2,6,10,14-Tetramethyl-7-(3-methylpent-4-enylidene) pentadecane	$C_{25}H_{48}$	20.56	X	
	n-Hexadecanoic acid	$C_{16}H_{32}O_2$	20.67	X	X
	Oleic Acid	$C_{18}H_{34}O_2$	22.41	X	X
	Hexadecanamide	$C_{16}H_{33}NO$	22.74	X	X
	1-Octadecanamine	$C_{18}H_{39}N$	23.02		X
	Z-11-Pentadecenol	$C_{15}H_{30}O$	23.17	X	
	11-Tricosene	$C_{23}H$	23.44	X	
	2(3H)-Furanone, dihydro-5-tetradecyl-	$C_{18}H_{34}O$	23.87	X	X
	9-Octadecenamide, (Z)-	$C_{18}H_{35}NO$	24.23	X	X
	Octadecanamide	$C_{18}H_{37}NO$	24.41	X	X
	9-Tricosene, (Z)-	$C_{23}H_{46}$	25.58		X
	Pyrrolidine, 1-(1-oxooctadecyl)-	$C_{22}H_{43}NO$	25.81		X
	14-Methyl-heptadecanoic acid, pyrrolidide	$C_{17}H_{34}O$	25.83	X	
	Cholest-3-ene, (5.beta.)-	$C_{27}H_{46}$	27.38	X	X
	Cholest-5-ene	$C_{27}H_{46}$	27.55	X	X
	Cholest-7-ene, (5.alpha.)-	$C_{27}H_{46}$	27.56		X
	Cholest-4-ene	$C_{27}H_{46}$	27.68		X
	Cholesta-3,5-diene	$C_{27}H_{44}$	27.68		X
	Cholestan-3-one, (5.alpha.)-	$C_{27}H_{46}O$	29.50		X
	Hexadecanoic acid, hexadecyl ester	$C_{32}H_{64}O_2$	30.87		X

3459

3460 During the hydrothermal liquefaction process, the initial step involves the hydrolysis of
3461 biomolecules such as lipids, proteins, and carbohydrates. This hydrolysis leads to the formation

of fatty acids (which are the predominant form of lipids) as well as nitrogenous compounds like amino acids and sugars (Masoumi et al. 2021). As it can be seen in the table, even though both biocrudes presented many similarities, but more compounds were detected when the concentration of sludge was higher. Both biocrudes contained a variety of hydrocarbons like cholest-4-ene, cholest-5-ene, 1-heptadecene, 1-nonadecene , acids like methyl stearate, n-hexadecanoic acid, oleic acid, 9-octadecenoic acid, (E)-, ketones like 2-heptadecanone, 2-pentadecanone and cholestan-3-one, (5.alpha.)- , esters like hexadecanoic acid, methyl ester and hexadecanoic acid, hexadecyl ester, and nitrogenous compounds like hexadecanamide, octadecanamide and 1-octadecanamine, originated from the main ingredients of primary sludge. The decarboxylation of fatty acids has promoted the formation of hydrocarbons (Ateş et al., 2016). While phenolic compounds found in the bio-oil predominantly originated from the cleavage of carbon-oxygen (C-O) bonds under subcritical water conditions (Li et al., 2020). The presence of nitrogen compounds can be attributed to the promotion of in inorganic nitrogen present in the raw sludge, transitioning from the solid phase to the liquid phase at the given temperature (Xu et al., 2018).

3.3.4. TGA of biocrudes, effect of TS:water ratio

TGA analysis was applied to study the stages of weight loss of HTL biocrude. The TGA curves of the samples of biocrude from HTL using different percentages of primary sludge are shown in Figure 3. In general, all HTL biocrudes presented the same TGA curve progression, with a comparable decomposition process. Regarding the change of percentages of TS, an important weigh loss took place at 335°C with 78.21% of weight loss in HTL 2% of TS and 338°C with 80.56% of weight loss in HTL 8% of TS. TGA analysis showed three decomposition stages: the first one includes the evaporation of water (Biswas et al., 2021). The second one, which is

the strongest, is observed mainly because of the decomposition of ingredients of primary sludge (proteins, carbohydrates and lipids) (Peng et al., 2001). In the third zone, gasification occurs and CO and CO2 are produced (Agrawal et al., 2013).

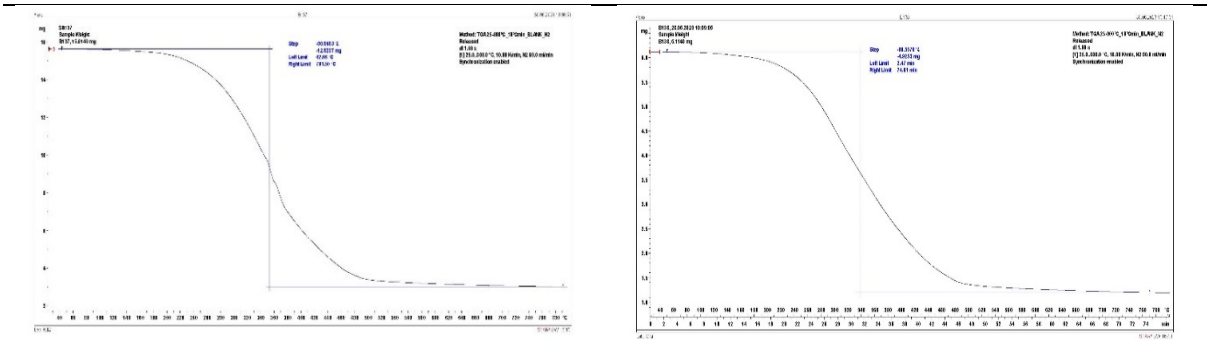

Primary sludge, 2% TS Primary sludge, 8% TS

Figure 3. Thermal gravimetric analysis of samples of biocrude, using different TS:water ratios, (T = 300ºC; Time = 30 min; Stirring = 100 rpm).

3.3.5. FTIR of biocrudes, effect of TS:water ratio

FTIR spectroscopy provides detailed information about the functional groups present in biocrude and allows for a more clarification of these groups when compared with GCMS analysis. Figure 4 presents FTIR spectra for biocrude produced from HTL using different ratios TS:water.

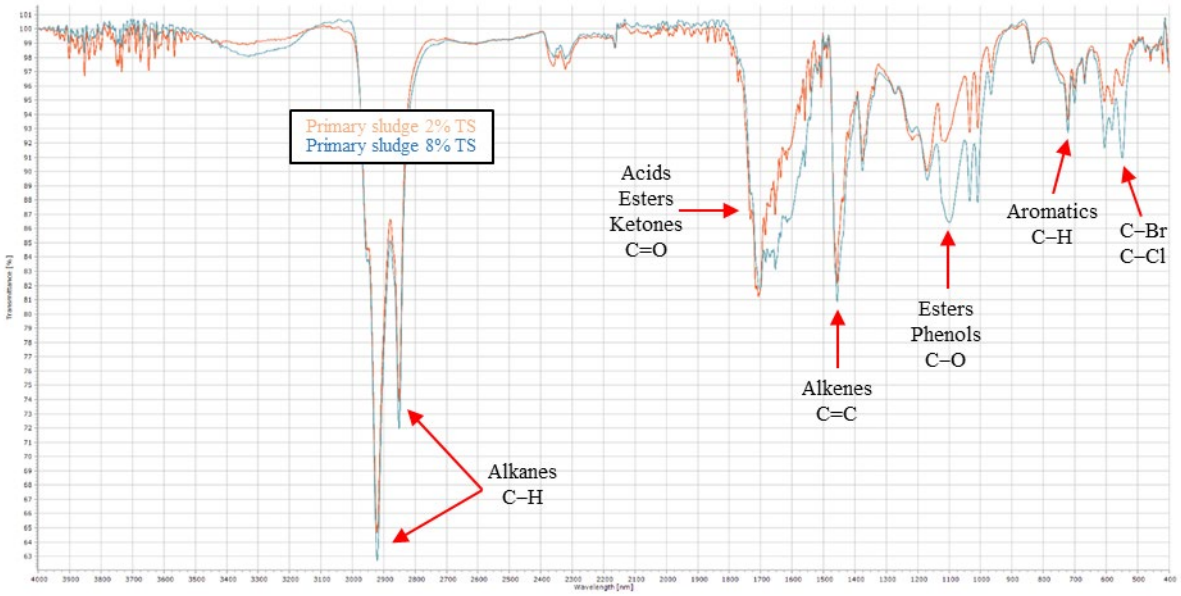

Figure 4. FT-IR of samples of biocrude, using different TS:water ratios, (T = 300ºC; Time = 30 min; Stirring = 100 rpm).

According to the figure, the high content of hydrocarbon compounds produced important saturated C-H stretching with CH_2 and CH_3 bending 2910 cm^{-1} and 2870 cm^{-1}, unsaturated stretching between 1400 and 1500 cm^{-1} and aromatics around 725 cm^{-1}. C-O stretching peaks around 1100 cm^{-1} correspond to esters and phenols. C=O stretching peaks were observed near 1700 cm^{-1}, demonstrating the presence of carboxylic acid, ketone, ester and quinone compounds as shown previously by GCMS analysis. Stretching peak between 3200 and 3400 cm^{-1} designates the presence of nitrogenous compounds. The peaks between 500 cm^{1} and 600 cm^{-1} indicated the presence of C-Br or C-Cl bonds. Both spectra were very comparable, including the same compounds. The amount of water didn't affect the biocrude composition in terms of functional groups. However, the intensity of peaks of biocrude from HTL 8% of TS was higher in most of the areas, indicating the presence of wider variety spectra of the HTL of biocrude at 340ºC detected more peaks that correspond to C=O functional groups, indicating

the presence of an extensive variety of acids, ketone, esters, hydrocarbons, ether, amide and amine.

3.3.6. ^{1}H NMR of biocrudes, effect of TS:water ratio

NMR spectra offer additional functional group information to FTIR spectra. Figure 5 show the ^{1}H NMR spectra of samples of biocrude produced from HTL using different ratios TS:water.

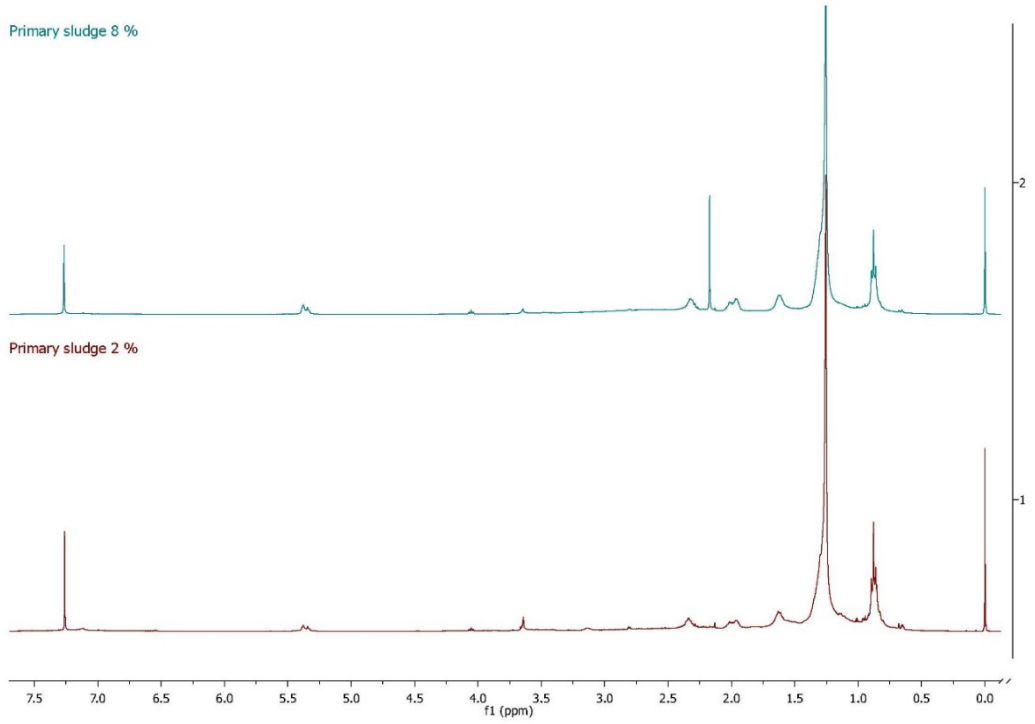

Figure 5. ^{1}H NMR plots of samples of biocrude , using different TS:water ratios, (T = 300ºC; Time = 30 min; Stirring = 100 rpm).

As it can be seen in the figure, the behaviour is similar to FTIR, ^{1}H NMR spectra presented a huge peak of aliphatic functional groups of alkanes (0.8-1.0 ppm; 1.0-1.5 ppm). HTL biocrude showed unsaturated bonds, alkenes (1.8-2.2 ppm) and alkynes (2.2-2.4 ppm). Aromatics were

as well perceived (2.1-2.2 ppm). The peaks in the range 3.5-3.7 ppm belong to carboxylic acids, ketones and esters. N-O group peaks were observed in the range of 4.0-4.2 ppm and N-H groups were detected by the chemical shifts in the range of (5.2-5.5 ppm). The last peak around 7.2 ppm is attributed to the solvent used. Summarising, the spectra of both biocrudes are very close. However, the intensity of peaks was different. In the case of HTL 2%, the peaks corresponding to C=O groups and unsaturated hydrocarbons were more intense. While in the case of HTL 8%, the peak that belong to saturated hydrocarbons was higher. This interpretation was also observed through FT-IR analysis.

3.3.7. SARA separation of biocrudes, effect of TS:water ratio

The results of the SARA separation for biocrudes are presented in Table 5. The light phase, maltenes, was distributed into saturates, aromatics and polars fractions. In most of the cases, maltenes was the abundant part in biocrude. Considering the influence of the ratio TS:water, by increasing the percentage from 2 to 8% (w/w), the amount of saturates decreased from 59.92 to 38.24%. While aromatics and resins have increased from 3.17 to 7% and from 36.90 to 54.76% respectively.

Table 5. SARA fractions of biocrude from HTL using different TS:water ratios (T = 300ºC; Time = 30 min; Stirring = 100 rpm).

Ratio TS:water	Oils fraction (% w/$w_{maltenes}$)		
	Saturates	Aromatics	Polars
2%	59.92	3.17	36.90
8%	38.24	7.00	54.76

The results are in accordance when compared to the peaks identified by GC/MS, FTIR and NMR. Chromatograms of GC/MS of the three phases with identified peaks were listed in Figure 6 and Table 6. In another study, polars and aromatics were detected in n-pentane extract with 22.1% and 72.6%. Also, the same was observed with toluene extract with 13.3% and 55.6% (Badoga et al., 2023). Similarly, as detected by GC-MS, polar compounds were found not only in the methanol extract, but also in n-hexane and toluene extracts, explaining the presence of acids in all the phases. Also, as interpreted by NMR, in the case of HTL 2%, more saturates were observed than that of HTL 8%.

Table 6. Principal substances identified by GC-MS in SARA fractions of biocrude, with different TS:water ratios (T = 300ºC; Time = 30 min; Stirring = 100 rpm).

Fraction	Substances
Saturates	Hexadecanoic acid, methyl ester; n-Hexadecanoic acid; Methyl stearate; 9-Octadecenoic acid, (E)-; 1-Eicosene; 9-Octadecenamide, (Z)-
Aromatics	6-Octadecenoic acid, (Z)-; 3-Cyclopentylpropionamide, N,N-dimethyl-; Octanamide, N,N-dimethyl-; 9-Octadecenamide, (Z)-; 2-Ethylacridine
Resins	Oleic Acid; Hexadecanamide; Methyl-6-nonenamide; Octadecanamide; E-2-Octadecadecen-1-ol

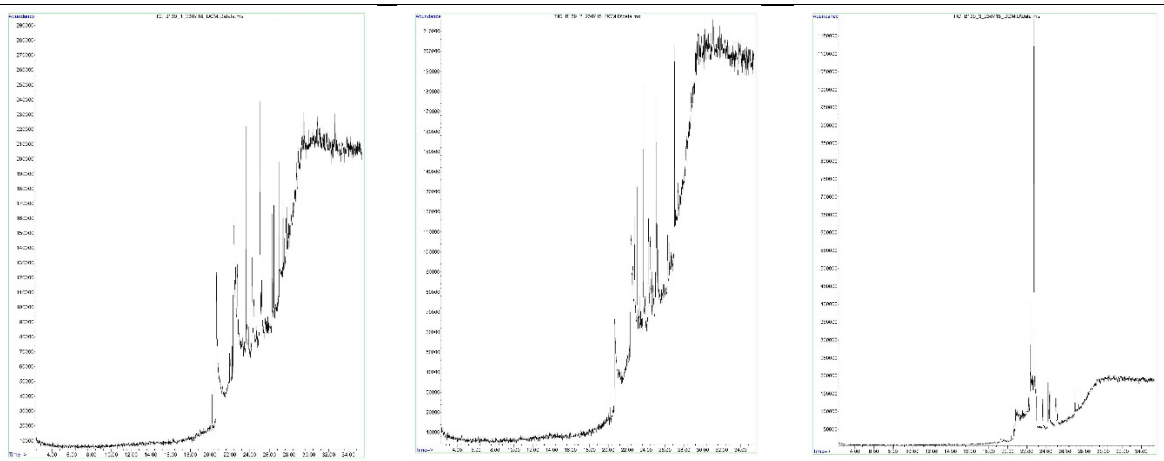

Saturates (a) Aromatics (b) Resins (c)

Figure 6. Chromatograms of saturated oils, aromatic oils and resins oils of biocrude.

3.3.8. Simulated distillation of biocrudes, effect of TS:water ratio

Figure 7 show the fractional cuts by boiling point of the biocrude samples obtained by simulated distillation. As shown in the figure, biocrudes present very similar classification of fractions. The difference between the results is considered negligeable. The curves of biocrudes produced with different TS:water ratios are quasi-identical. The fractions are almost the same. None of them contains a fraction in the gasoline cuts. Only 4% belongs to the range of jet fuel. Around 12% is in the Diesel range. The fraction of vacuum gas is the predominant. It represents near 74% of the biocrude. Only 4% belongs to the range of jet fuel. Biocrude produce from HTL 2% contained 13% in the Diesel range while biocrude produced from HTL 8% contained 11%. Around 12% is in the Diesel range. The difference in the vacuum gas fractions for both biocrude samples was only 1% (75% for HTL 2% and 74% for HTL 8%). Consequently, 8% of vacuum residue remained in the biocrude of HTL 2% while 11% remained in that of biocrude of HTL 8%. As mentioned before, by increasing the amount of water, the hydrolysis becomes faster, resulting in lighter molecules with lower boiling points. That´s why biocrude produced

from HTL 2% contained more compounds in lower boiling point ranges than that produced from HTL 8%.

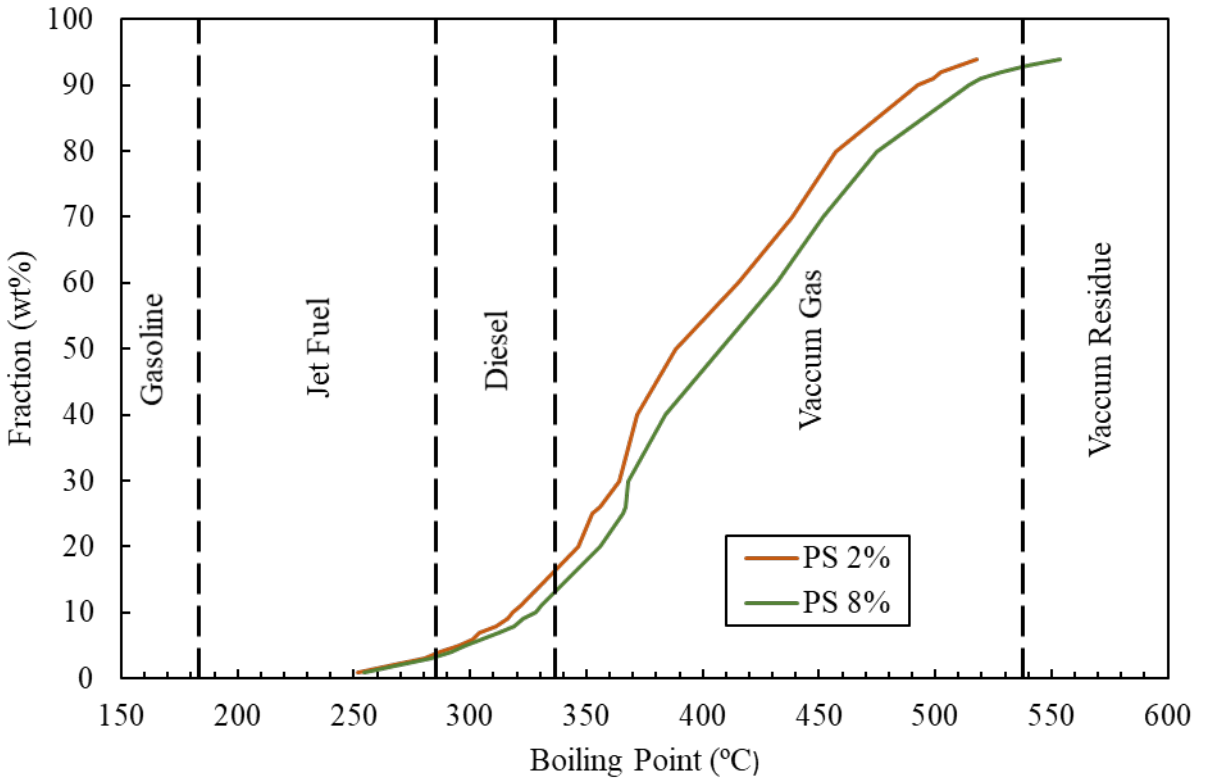

Figure 7. Simulated distillation of biocrude from HTL with different TS:water ratios (T = 300ºC; Time = 30 min; Stirring = 100 rpm).

3.4. Effect of solvents on characteristics of biocrudes

3.4.1. Yields of biocrude, effect of solvents

The biocrude yields from HTL of primary sludge using different solvents are presented in Table 7. Biocrude yield produced from HTL of PS using pure water was 30.354 (w/w_{VS}) at 200 ºC of temperature and 30 min of reaction time. However, when organic solvents and co-solvents were added, the yield of biocrude became higher. The maximum value, 51.373(w/w_{VS}), was achieved with 100% of methanol.

Table 7. Biocrude, oils and asphaltenes yields after HTL experiment using different solvents (T = 200ºC; Time = 30 min; Stirring = 100 rpm).

Solvent	Biocrude		Bio-oil *		Asphaltene *	
	Weight (g)	(%)	Weight (g)	(%)	Weight (g)	(%)
Water 100%	3.99	30.35	3.69	28.11	0.30	2.25
MeOH 100%	6.69	51.37	6.36	48.82	0.33	2.56
MeOH: H_2O 1:1	4.15	33.32	0.79	6.10	3.36	27.22
MeOH: H_2O 2:1	5.51	42.28	1.59	12.18	3.92	34.08
Acetone 100%	6.03	46.26	5.67	43.50	0.36	2.76
Ethyl Acetate 100%	5.08	38.97	2.54	19.47	2.54	19.50
Ethanol 100 %	6.62	50.81	1.77	13.60	4.85	37.21
Ethanol:H_2O 1:1	5.51	43.90	3.34	25.63	2.17	18.27

* Bio-oil was obtained from biocrude by separation with hexane and asphaltene was calculated by difference

Moreover, when looking at the results obtained from HTL using different MeOH: H_2O ratios, biocrude yield was always in increment from 33.32% to 51.37% along with the increase of the amount of methanol from MeOH:H_2O 1:1 to MeOH 100%. In another study, biocrude yield obtained from dewatered sludge with 100% of methanol at 240ºC for 20 min was 54.20% (Huang et al., 2014). This increase in the yield can be attributed to methanol´s lower dielectric constant and less polar nature, which facilitate the diffusion of the solvent in the biomass. In addition, methanol´s slightly higher acidity compared to water acted as a hydrogen donor, catalysing HTL process, enhancing biocrude yields and decreasing solid residue (Masoumi et al. 2021; Yerrayya et al. 2022). Also, 42.2% of biocrude was produced from HTL of sewage sludge and MeOH: H_2O 50:50 at 260 ºC for 40 min (Tong et al. 2021). In fact, the effect of

ethanol and methanol on primary sludge is the same. Either with EtOH 100% or with MeOH 100%, the difference between the results obtained is negligeable. While when alcohols were mixed with water, their synergistic effect was different. Eventhough in other studies it was demonstrated that co-solvent of alcohol:water gives better results than alcohol alone (Madikizela et al., 2022), in our case it was the opposite. As primary sludge is rich in lipids, it can be possible that the esterification reactions are more efficient in the presence of pure alcohol. The effect of other solvents and co-solvents on the biocrude yield cannot be ignored. With Acetone 100% and Ethyl Acetate 100%, the yields of biocrude were improved to 46.26, 38.97 (w/wVS), respectively. The improvement of biocrude yields in the presence of solvents comes in this order: MeOH 100% > EtOH 100% > Acetone 100% > EtOH: H_2O 1:1 > MeOH: H_2O 2:1 > Ethyl Acetate 100% > MeOH: H_2O 1:1. In a study elsewhere, they have investigated the effect of methanol, ethanol and acetone on biocrude HTL of sewage sludge. The results showed similar effect (same order), Methanol (54.62%) > Ethanol (53.71%) > Acetone (51.35%) (Huang et al., 2014).

3.4.2. Ultimate analysis and high caloric value of biocrudes, effect of solvents

The percentages of elements C, H, N and O, the higher heating value HHV and the energy recovery for HTL using different solvents and co-solvents are listed in Table 8.

Table 8. Elemental analysis and HHV of biocrude after HTL experiment using different solvents (T = 200ºC; Time = 30 min; Stirring = 100 rpm).

	Samples	% C	% H	% N	% O	HHV (MJ/kg) *	ER (%) **
Solve	Water 100 %	64.27	7.17	1.89	26.67	58.53	90.90

Methanol 100%	69.97	10.93	2.12	16.98	45.95	125.35
MeOH: H_2O 1:1	73.22	11.82	2.1	12.86	41.00	72.55
MeOH: H_2O 2:1	62.25	8.92	5.25	23.58	53.12	119.26
Acetone 100 %	72.45	11.61	2.45	13.49	41.68	97.17
Ethyl Acetate 100 %	68.27	10.77	2.89	18.07	46.96	102.39
Ethanol 100 %	67.55	10.45	2.96	19.04	48.16	129.95
EtOH: H_2O 1:1	58.54	9.14	5.14	27.18	56.97	132.82

* Calculated with Dulong equation (5)

** Calculated using equation (6)

Regarding the ultimate analysis of biocrude produced from HTL using different solvents and co-solvents, the energy value and contents of C, H, N and O were dependent on the condition chosen. However, the HHV was always improved when compared to that of primary sludge. The highest HHV attained was when pure water was used with 58.53 MJ/kg and containing 64.27 % of carbon, 7.17 % of hydrogen, 1.89 % of nitrogen and 26.67 % of oxygen. The calorific value of the biocrude obtained was higher than that of heavy crude oil or bitumen (36.5 MJ/kg) (Baloch et al., 2021). Energy recovery was quite high in all scenarios. However, in some runs, ER value has exceeded 100%. This could be explained by the participation of the solvent in the reaction solvent system and supplied a certain energy source (Tong et al., 2021).

3.4.3. GC/MS of biocrudes, effect of solvents

The detailed compound information of the biocrude from HTL with different ratios TS:Water is presented in Table 9.

Table 9. GCMS analysis of biocrude using different solvents (T = 200ºC; Time = 30 min; Stirring = 100 rpm).

Substance	Formula	Solvent							
		Water 100%	Methanol 100%	Methanol 50%	Methanol 67%	Ethanol 100%	Ethanol 50%	Acetone	Ethyl acetate
Methyl tetradecanoate	$C_{15}H_{30}O_2$		X	X	X				
Pentadecanoicacid, methyl ester	$C_{16}H_{32}O$		X	X	X				
Hexadecanoicacid, methyl ester	$C_{17}H_{34}O_2$		X						
n-Hexadecanoic acid	$C_{16}H_{32}O_2$	X	X	X	X	X	X	X	X
9-Octadecenoic acid(Z)-, methyl ester	$C_{19}H_{36}O_2$		X						
9-Octadecenoic acid, methyl ester,(E)-	$C_{19}H_{36}O$		X	X					
Methylstearate	$C_{19}H_{38}O_2$		X	X	X	X		X	X
Oleic acid	$C_{18}H_{34}O_2$		X	X	X	X	X	X	
Octadecanoic acid	$C_{18}H_{36}O_2$	X	X		X	X	X		
Eicosanoic acid, methyl ester	$C_{21}H_{42}O$		X						
Docosanoic acid, methyl ester	$C_{23}H_{46}O$		X		X				
Tetracosanoic acid, methyl ester	$C_{25}H_{50}O_2$		X						
Cholest-3-ene, (5.beta.)-	$C_{27}H_{46}O_2$		X						
Dodecanoic acid, methyl ester	$C_{13}H_{26}O$		X	X				X	
Tridecanoic acid, 12-methyl-, methyl ester	$C_{15}H_{30}O$	X	X	X	X		X	X	X
Methyl13-methyltetradecanoate	$C_{16}H_{32}O_2$		X	X	X				
11-Hexadecenoic acid, methyl ester	$C_{17}H_{32}O_2$		X						
Hexadecanoic acid, methyl ester	$C_{17}H_{34}O_2$		X	X	X	X		X	
Hexadecanoic acid,14-methyl-, methyl ester	$C_{18}H_{36}O_2$		X	X	X				
Octadecanoic acid,10-oxo-, methyl ester	$C_{19}H_{36}O_3$		X						
Methyl18-methylnonadecanoate	$C_{21}H_{42}O_2$		X						

Substance	Formula	Solvent							
		Water 100%	Methanol 100%	Methanol 50%	Methanol 67%	Ethanol 100%	Ethanol 50%	Acetone	Ethyl acetate
Tridecanoic acid, methyl ester	$C_{14}H_{28}O$			X	X				
Z-5-Nonadecene	$C_{19}H_{38}$								
Tetradecanoic acid	$C_{14}H_{28}O_2$	X		X	X		X	X	X
Pentadecanoic acid, 14-methyl-, methyl ester	$C_{17}H_{34}O$			X					
Methyl hexadec-9-enoate	$C_{17}H_{32}O_2$			X					
Hexadecanoic acid, 15-methyl-, methyl ester	$C_{18}H_{36}O_2$			X					
Heptadecanoic acid, methyl ester	$C_{18}H_{36}O$			X		X	X		X
9-Octadecenoic acid, methyl ester	$C_{19}H_{36}O$			X	X				
9-Octadecenoic acid, methyl ester,(E)-	$C_{19}H_{36}O$			X	X			X	
Octadecanoic acid	$C_{18}H_{36}O_2$			X				X	X
Docosanoic acid, methyl ester	$C_{23}H_{46}O$			X					
Tetracosanoic acid, methyl ester	$C_{25}H_{50}O_2$			X					
Cholestan-3-ol, (3.beta., 5.beta.)-	$C_{27}H_{48}O$			X					
Hexadecanoic acid, ethyl ester	$C_{18}H_{36}O_2$			X		X	X		
6-Octadecenoic acid, methyl ester,(Z)-	$C_{19}H_{36}O_2$			X					
9-Octadecenoic acid, (E)-	$C_{18}H_{34}O_2$			X		X			X
Octadecanoic acid, ethyl ester	$C_{20}H_{40}O_2$			X	X	X	X		
Dodecanoic acid, methyl ester	$C_{13}H_{26}O$				X				
Dodecanoic acid	$C_{12}H_{24}O_2$				X			X	
Pentadecanoic acid	$C_{15}H_{30}O_2$				X				
Hexadecanoic acid, 15-methyl-, methyl ester	$C_{18}H_{36}O_2$				X				
Docosanoic acid, methyl ester	$C_{23}H_{46}O$				X				
1,4-Benzenedicarboxylic acid, dimethyl ester	$C_{10}H_{10}O$								

Substance	Formula	Solvent							
		Water 100%	Methanol 100%	Methanol 50%	Methanol 67%	Ethanol 100%	Ethanol 50%	Acetone	Ethyl acetate
1-Nonadecene	$C_{19}H_{38}$				X	X			
8-Octadecenoic acid, methyl ester	$C_{19}H_{36}O_2$								
10-Octadecenoic acid, methyl ester	$C_{19}H_{36}O$				X				
Tetradecanoic acid, ethyl ester	$C_{16}H_{32}O_2$					X	X		
2-Heptadecanone	$C_{17}H_{34}O$	X				X	X	X	X
Ethyl14-methyl-hexadecanoate	$C_{18}H_{36}O_2$					X			
6-Octadecenoicacid, (Z)-	$C_{18}H_{34}O_2$					X			
Ethyl Oleate	$C_{20}H_{38}O_2$					X			
Methyl19-methyl-eicosanoate	$C_{22}H_{44}O_2$.					X			
Dodecanoic acid, ethyl ester	$C_{14}H_{28}O_2$					X	X		
1,4-Benzenedicarboxylicacid, diethyl ester	$C_{12}H_{14}O$					X			
Ethyltridecanoate	$C_{15}H_{30}O_2$					X			
Tetradecanoicacid,2-methyl-, methyl ester	$C_{16}H_{32}O$					X			
Octadecanoicacid,17-methyl-, methyl ester	$C_{20}H_{40}O_2$					X			
Ethyl13-methyl-tetradecanoate	$C_{17}H_{34}O_2$					X	X		
Pentadecanoicacid, ethyl ester	$C_{17}H_{34}O_2$					X	X		
Palmitoleicacid	$C_{16}H_{30}O_2$					X			
Ethyl15-methyl-hexadecanoate	$C_{19}H_{38}O$					X			
11-Octadecenoicacid, methyl ester	$C_{19}H_{36}O_2$					X		X	
8-Octadecenoicacid, methyl ester, (E)-	$C_{19}H_{36}O_2$					X			
Methyltetradecanoate	$C_{15}H_{30}O_2$							X	
6-Octadecenoicacid	$C_{18}H_{34}O_2$	X						X	X
Octadec-9-enoicacid	$C_{18}H_{34}O_2$							X	

Substance	Formula	Solvent							
		Water 100%	Methanol 100%	Methanol 50%	Methanol 67%	Ethanol 100%	Ethanol 50%	Acetone	Ethyl acetate
Dodecanamide,N,N-diethyl-	$C_{16}H_{33}NO$							X	
Terephthalicacid,di(4-octyl)ester	$C_{23}H_{36}O_4$							X	
Cholestan-3-one, (5.alpha.)-	$C_{27}H_{46}O$							X	
9-Octadecenoicacid(Z)-, tetradecyl ester	$C_{32}H_{62}O$							X	
cis-13-Octadecenoicacid, methyl ester	$C_{19}H_{36}O$								X
14-Pentadecenoicacid	$C_{15}H_{28}O_2$								X
9-Octadecenamide, (Z)-	$C_{18}H_{35}NO$								X
Cholestan-3-one	$C_{27}H_{46}O$								X
Cholest-8(14)-ene, (5.alpha.)-	$C_{27}H_{46}O$	X							
Cholestane,3,4-epoxy-, (3.alpha.,4.alpha.,5.alpha.)-	$C_{27}H_{46}O$	X							

The composition of biocrudes at all conditions was very comparable. With pure water, few compounds were observed. Probably, the operating temperature, 200 ºC, was not enough to complete the polymerization process. Consequently, high molecular weight compounds with high boiling points were still present and their detection by GC/MS got failed. In the presence of solvents and co-solvents, a wide range of acids, esters, ketones, hydrocarbons were detected. The presence of methanol and ethanol in the system can potentially increase the likelihood of esterification reactions with fatty acids, consequently reducing the quantity of phenolic and nitrogenous compounds and increasing the quantity of esters (Masoumi et al. 2021; Wang et al. 2018). Also, oxygenated compounds in biocrude products, including acids, ketones, and alcohols, could be formed through the hydrolysis and dehydration reactions of cellulose and

hemicellulose (Zhao et al. 2022). Chromatograms of biocrude samples produced from HTL experiments using different solvents are shown in Figure 8.

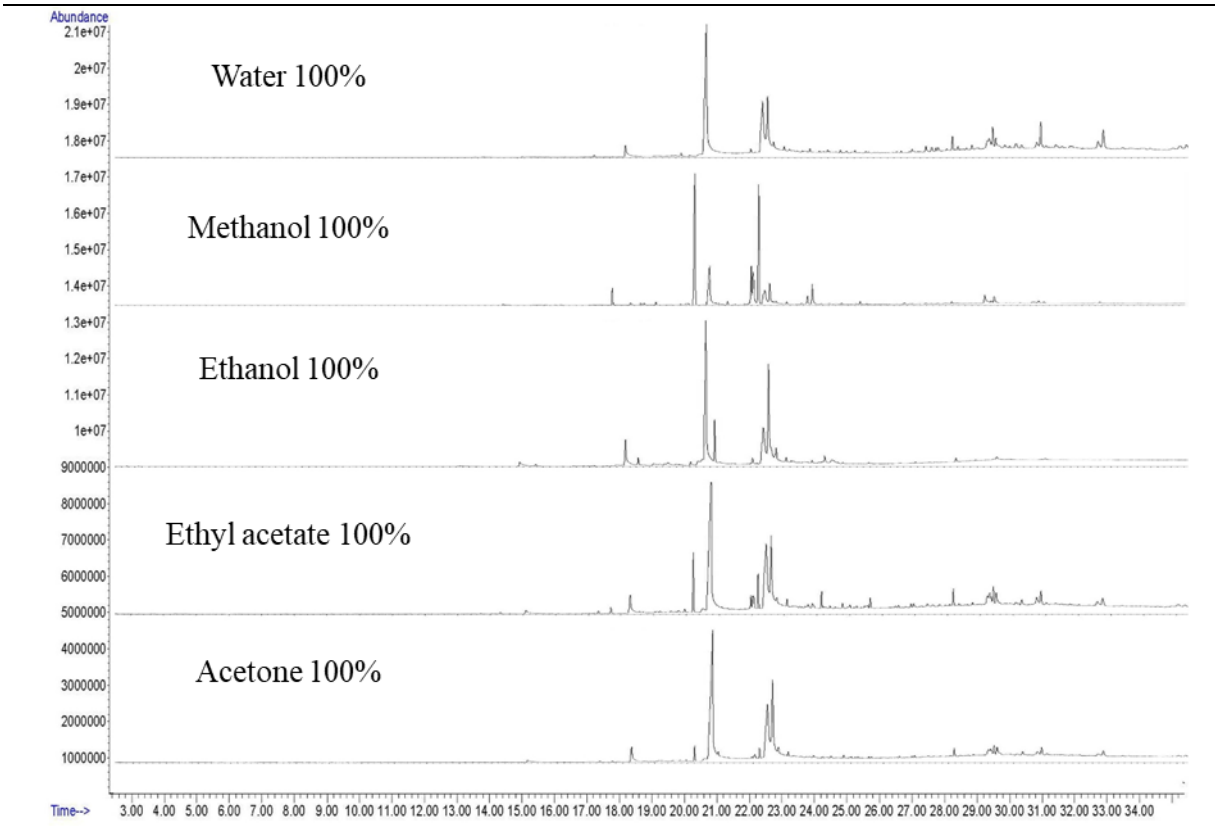

Figure 8. Chromatograms of biocrudes using different solvents (T = 200ºC; Time = 30 min; Stirring = 100 rpm).

3.4.4. TGA of biocrudes, effect of solvents

The TGA curves of the samples of biocrude from HTL using solvents and co-solvents are shown in Figure 9. As it can be seen in the figure, a significant weight loss took place at 315°C with 81.06% of weight loss when using pure water, at 360°C with 94.75% of weight loss when using pure methanol, at 245°C with 59.61% of weight loss and at 359°C with 35.33% of weight loss when using methanol-water (1:1), at 150°C with 8.66% of weight loss and at 317°C with 75.00% of weight loss when using methanol-water (2:1), at 85°C with 2.31% of weight loss

and at 319°C with 83.83% of weight loss when using pure ethanol, at 340°C with 95.38% of weight loss when using ethanol-water (1:1), at 130°C with 3.62% of weight loss and at 345°C with 88.64% of weight loss when using pure acetone, and at 325°C with 91.02% of weight loss when using pure ethyl acetate.

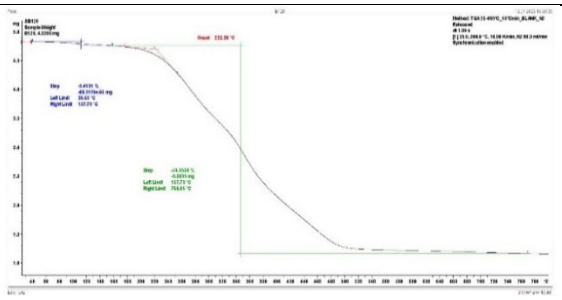

Water 100%

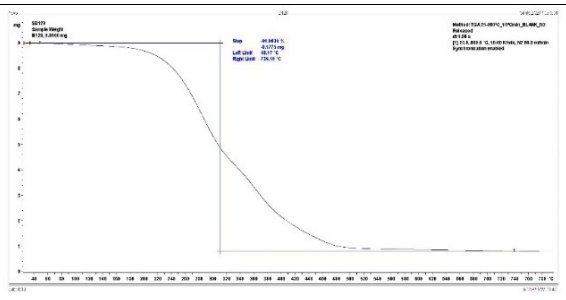

Methanol 100%

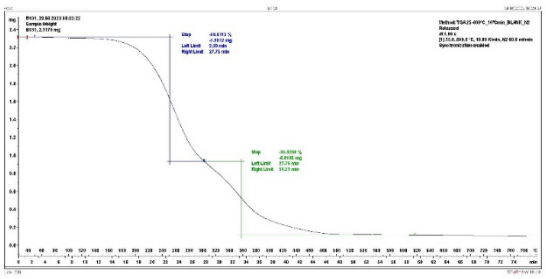

MeOH:H_2O 1:1

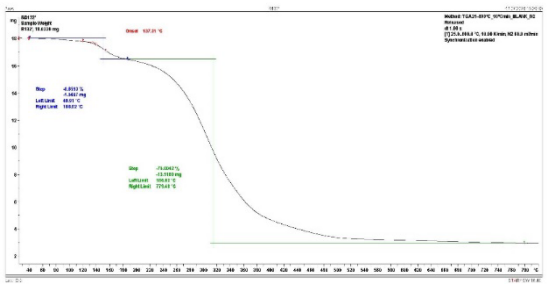

MeOH:H_2O 2:1

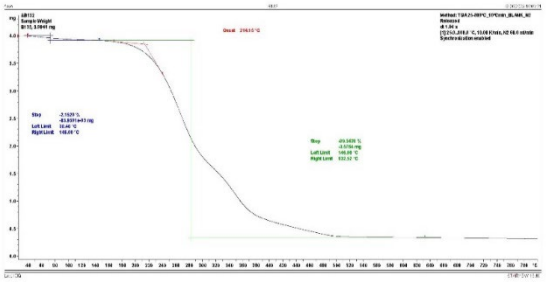

Ethanol 100%

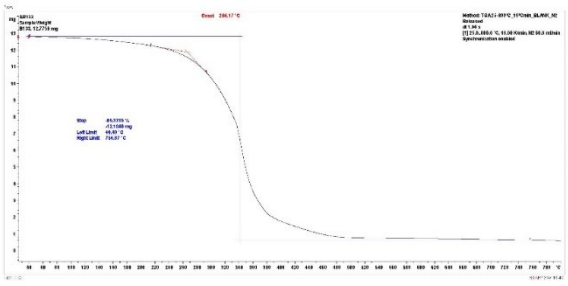

EtOH:H_2O 1:1

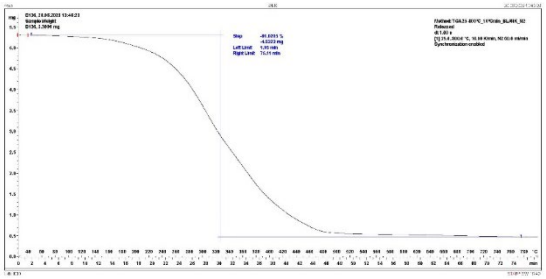

Acetone 100%

Ethyl Acetate 100%

Figure 9. Thermal gravimetric analysis of samples of biocrude using different solvents (T = 200ºC; Time = 30 min; Stirring = 100 rpm).

3.4.5. FTIR of biocrudes produced with different solvents

Figure 10 presents FTIR spectra for biocrude produced from HTL using different solvents and co-solvents. Figure 10 presented a very similar distribution of peaks as in the case of Figure 4 with some modifications. Biocrude from HTL with different solvents and co-solvents did not present any peak in the range of 3200 and 3400 cm^{-1}. The intensity of peaks in the range of acids, ketone, ester and hydrocarbons was more significant, demonstrating the effect of solvents (other than water) and co-solvents on the quality of biocrude.

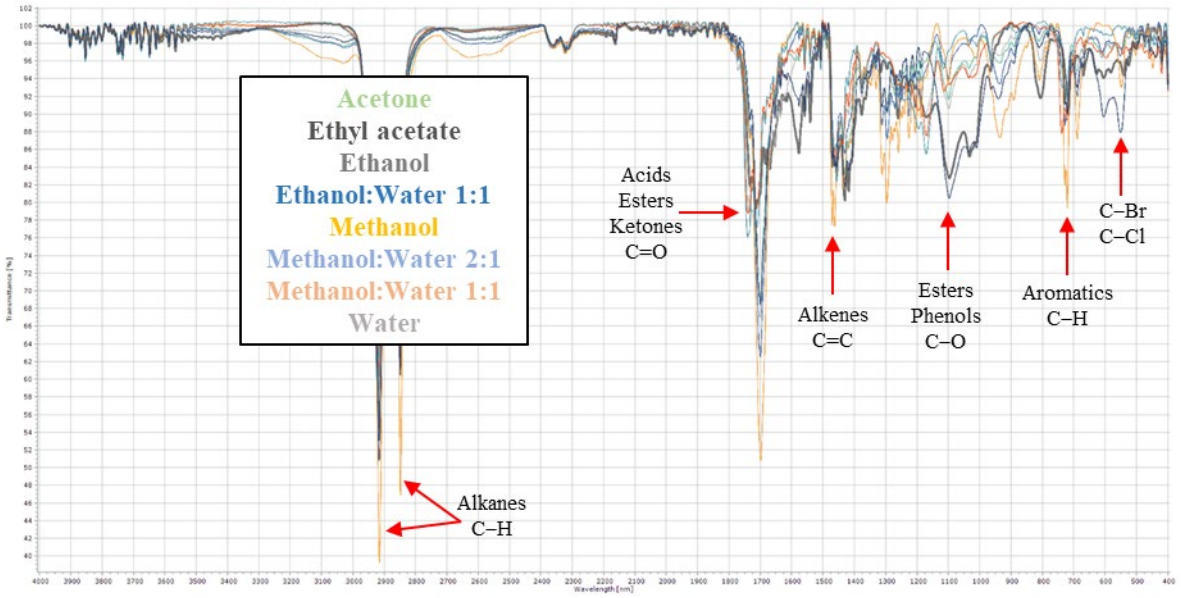

Figure 10. FT-IR of samples of biocrude, using different solvents (T = 200ºC; Time = 30 min; Stirring = 100 rpm).

3.4.6. ^{1}H NMR of biocrudes, effect of solvents

Figure 11 show the ^{1}H NMR spectra of samples of biocrude produced from HTL using different solvents and co-solvents. In Figure 11, the distribution of peaks in biocrudes from HTL using different solvents and co-solvents was very similar to that obtained from HTL using different concentration of sludge. The intensity of peaks was dependent on the solvent chosen. For example, the peak of hydrocarbons was the highest when water was used as a solvent. Whereas the peak of carboxylic acids was the optimal when methanol and water were added together in a ratio of 2:1. Overall, the results of ^{1}H NMR are confirmed by the ones obtained from GCMS and FTIR analysis.

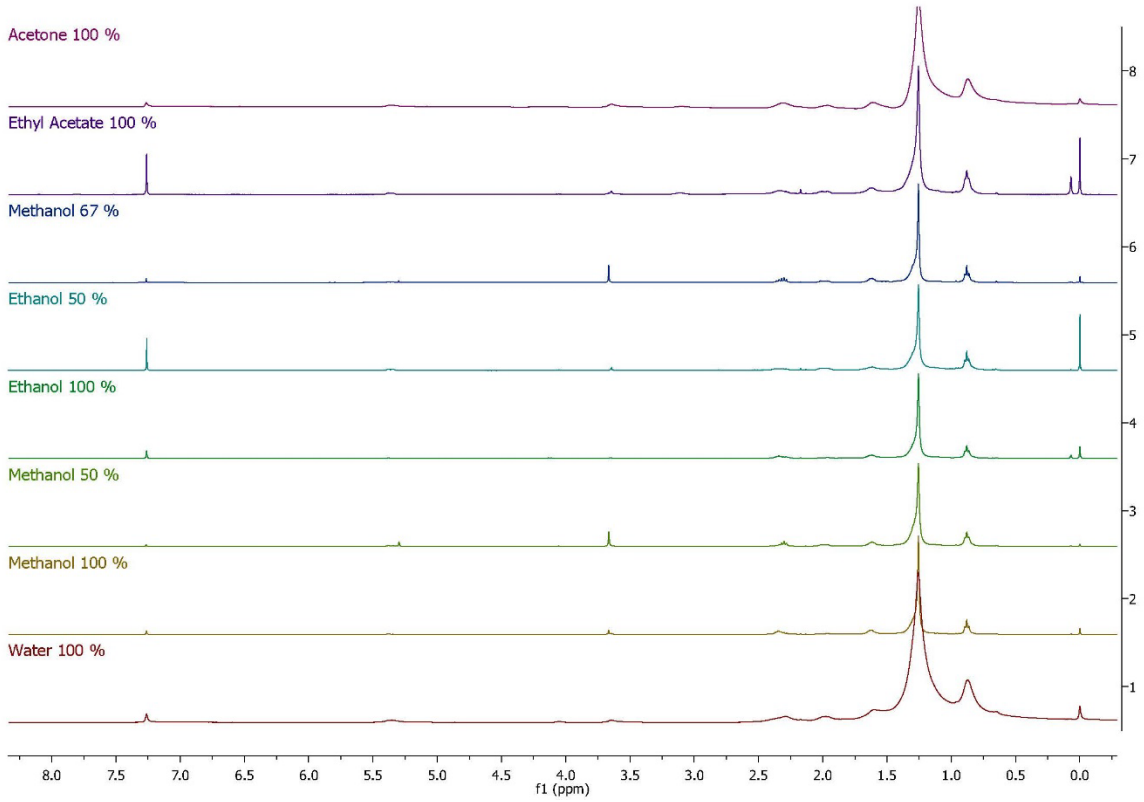

Figure 11. ^{1}H NMR plots of samples of biocrude, using different solvents (T = 200ºC; Time = 30 min; Stirring = 100 rpm).

3.4.7. SARA separation of biocrudes, effect of solvents

SARA fractions determination was achieved for the HTL biocrude at all conditions and the results are presented in Table 10. The light phase, bio-oil, was distributed into saturates, aromatics and polars. In most of the cases, maltenes was the abundant part in biocrude. Considering the change of the percentages of TS in HTL, by increasing the percentage from 2 to 8 % (w/w), the amount of saturates has decreased from 59.92 to 38.24 %. While aromatics and resins have increased from 3.17 to 7 % and from 36.90 to 54.76 %.

Regarding the effect of the solvent on the biocrude, the distribution of phases was dependent on the solvent chosen. For example, with pure water, saturates, aromatics and resins were

detected with 51.35 %, 20.50 % and 28.15 %. While with Ethanol- Water (1:1), saturates were 59.00 %, aromatics were 36.64 % and resins were 4.36 %. The results obtained were reasonable when compared to the peaks identified by GC/MS, FTIR and NMR. Chromatograms of GC/MS of the three phases with identified peaks were listed in Figure X and Table X.

Table 10. SARA fractions of biocrude from HTL using different solvents and ratios (T = 200ºC; Time = 30 min; Stirring = 100 rpm).

	Oils fraction (% w/$w_{maltenes}$)		
Solvent (cosolvent ratio)	Saturates	Aromatics	Polars
Water (pure)	51.35	20.50	28.15
Methanol (pure)	74.83	8.92	16.26
Methanol:water (1:1)	56.97	38.86	4.17
Methanol:water (2:1)	33.72	49.18	17.10
Ethanol (pure)	25.78	48.06	26.16
Ethanol:water (1:1)	59.00	36.64	4.36
Acetone (pure)	59.00	27.58	13.42
Ethyl Acetate (pure)	81.48	16.99	1.52

3.4.8. Simulated distillation of biocrude, effect of solvents

Figure 12 shows the fractional cuts of biocrude samples obtained with different solvents. As shown in the figure, the behaviour is very close for all biocrudes. The difference between the results is nearby to be negligeable. None of the biocrudes contains a fraction in the gasoline cut. Biocrude obtained with acetone does not contain as well a fraction in the range of jet fuel. The rest, contain a fraction lower than 7%, possibly because of the mild hydrotreating temperature. The fraction of diesel in the case of ethyl acetate and acetone is only around 7%. Jet fuel and diesel cuts are related to the presence of lipid-derived molecules in sludge (Passos

et al., 2022). Whereas the others have around 20% of Diesel cuts in the biocrude. vacuum gas is noted as the most significant part in biocrude. It occupies more than 65% in the biocrude. More interestingly, HTL with acetone produced biocrude containing around 92% of vacuum gas cuts. This can be explained by the high presence of oxygen containing compounds (Sharma et al., 2021). The category of high boiling point compounds detected here was not visible on GC-MS. The use of biocrude as fuels imposes further post refining to upgrade characteristics after the hydrothermal liquefaction.

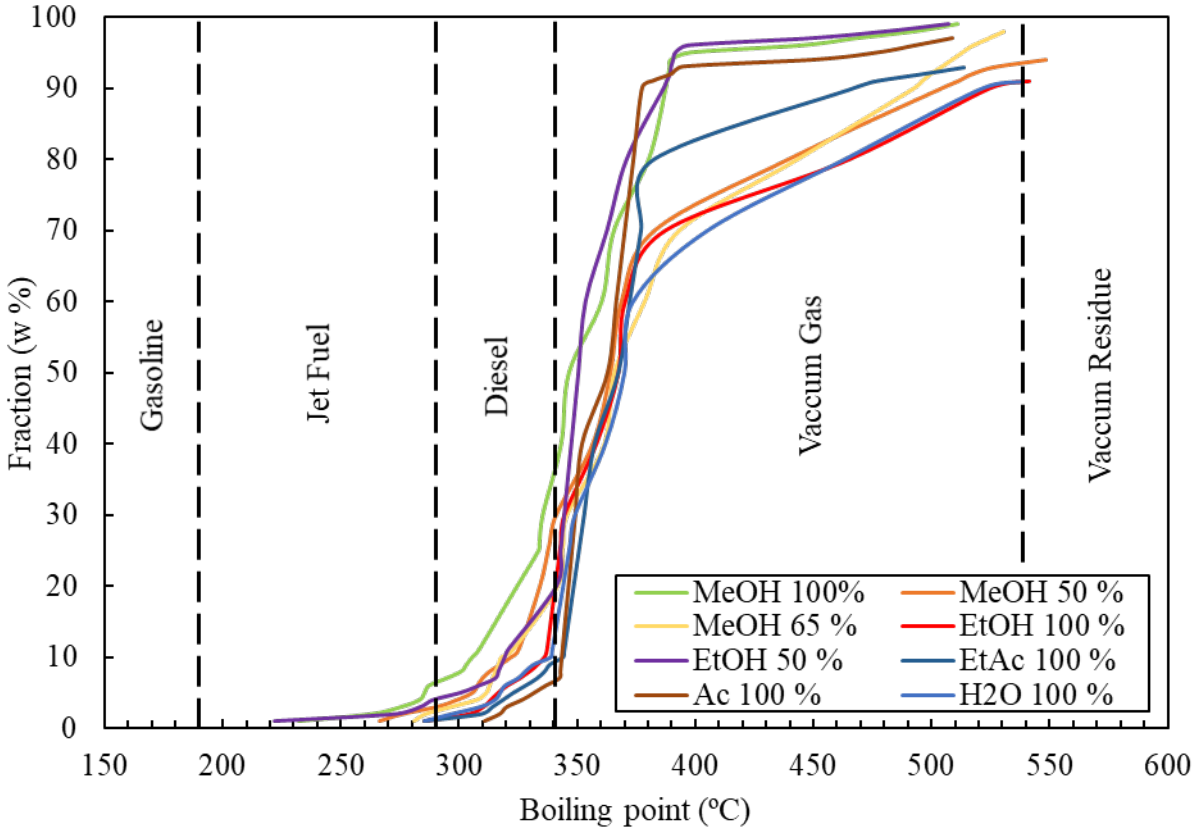

Figure 12. Simulated distillation of samples of biocrude, using different solvents (T = 200ºC; Time = 30 min; Stirring = 100 rpm).

The increase of temperature could promotes the hydrolysis of heavier compounds (vacuum gas and vacuum residue fractions), resulting in the formation of lower boiling point compounds that belong to jet fuel cuts (Da Costa Magalhães., et al. 2023).

3.5. Effect of TS:water ratio and solvents on the aqueous liquid phase

The aqueous phase is the liquid phase obtained from HTL using co-solvents after separation. The full characterization of aqueous phase resulted from HTL using Water 100%, MeOH: H_2O 1:1, MeOH: H_2O 2:1 and EtOH: H_2O 1:1 and using 2 % and 8 % of TS is listed in Table 11. The liquid phase is defined as the water content of primary sludge with water soluble organic species.

Table 11. Aqueous phase characterization after HTL.

Parameters	Solvents: 200ºC; 30 min; 100 rpm				TS: 300ºC; 30 min; 100 rpm	
	Water 100 %	MeOH:H_2O 1:1	MeOH:H_2O 2:1	EtOH:H_2O 1:1	2 % (w_{TS})	8 % (w_{TS})
Weight (g)	469.50	204.69	152.58	149.40	451.27	402.24
Proteins (%, TS basis)	7.22	18.99	16.29	18.17	0.35	0.18
Carbohydrates (%, TS basis)	1.70	6.91	3.95	3.69	0.59	0.22
TOC (mg/L)	4224	2300	2850	575	244.5	1185
COD (mg/L)	10102	186000	316300	151700	7550	9230
pH	6.78	5.88	4.47	3.86	7.89	7.49
TS (%, dry basis)	0.66	1.25	1.25	1.90	0.28	0.92
Ash (%, TS basis)	15.93	14.65	19.25	28.73	22.94	18.58
VS (%, TS basis)	84.07	85.35	80.75	71.27	77.06	81.42

In all the scenarios, when changing the solvent at 200ºC or changing the concentration of sludge at 300ºC, TOC values were lower from that of the initial feedstock. However, the behaviour of COD was different. In the case when the concentration of TS was 2% and 8% at 300 C, COD concentration decreased after HTL experiment to 7.55 and 9.23 g/L. The same change was noticed when pure water was added at 200 ºC. While, when methanol and ethanol were mixed with water, COD values increased clearly to higher values: 18.6 g/L with MeOH: H_2O 1:1, 31.6 g/L with MeOH: H_2O 2:1 and 15.200 g/L with EtOH: H_2O 1:1. The variation of pH was dependent on the condition used. When water was used as solvent, regardless the temperature and the concentration of sludge, pH was near 7, indicating the presence of N-compounds originated from proteins. However, when methanol and ethanol were introduced to the system, pH became acidic, demonstrating the presence of acidic compounds. Carbohydrates and proteins percentages were noticed in small quantities in the aqueous phase after HTL, but more were dissolved in the scenarios of methanol and ethanol. The analysis of the aqueous phase obtained from HTL is important for identifying the optimal approach for studying its potential reusability. Herein, the quality obtained could propose a solution for valorising the aqueous phase. The re-use of dissolved organics through circulation could boost the biocrude yield and reduce the presence of aqueous phase products (Hong et al., 2021). The percentage of dissolved solids in the aqueous phase was respectively negligeable. VS was always higher than 70 %; consequently, ash content remained low. SEM images and EDX spectra of ash in aqueous phase are presented in Figure 13. Very little heavy metals remained in the ash of the dissolved solid in the aqueous phase.

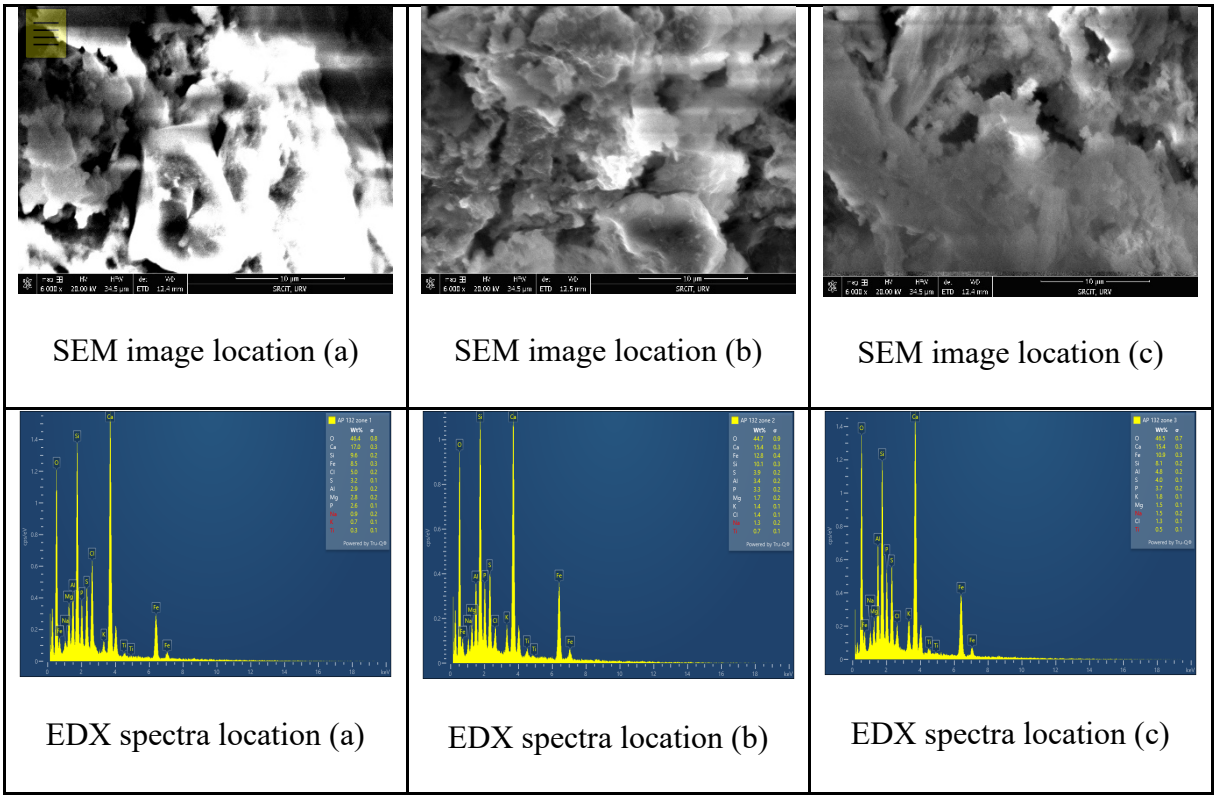

Figure 13. SEM images and EDX spectra of ash in the aqueous phase. (a), (b) and (c) represent three different zones of the sample.

3.6. Effect of TS:water ratio and solvents on the biochar

3.6.1. Experimental results

Biochar is the solid phase product recuperated after process. It's a black solid divided into volatiles and ashes. The yields obtained from HTL with different concentrations of TS and using different solvents and co-solvents are presented in Table 12. Firstly, it´s clear that the change of concentration of TS didn´t affect neither the biochar yield nor its composition. Biochar yield obtained from 2 and 8 % of TS was 36.99 and 36.28 % (w/w). VS and ash percentages were 46.12 and 49.49.30 % (w/w) and 53.88 and 50.70 % (w/w). Whereas in the scenarios where the parameter of solvent was changed, the biochar yield and its properties were dependent on the solvent or co-solvents chosen. However, the results obtained were still very similar. The percentage of biochar was always higher than 40 % (w/w). Organic contents were

3791 always predominant. They have covered more than 50 % of the biochar. The significant amount
3792 of biochar and more importantly the quality of biochar, the high content of volatiles, open a
3793 new pathway for its valorisation and its usage in further applications.

3794

3795 Table 12. Biochar characterization.

	Composition				Ultimate analysis				
Concentration: 300ºC; 30 min; 100 rpm	Weight (g)	Yield (%, d)	VS (%, d)	Ash (%, d)	% C	% H	% N	% O	HHV (MJ/kg) *
2 %	3.72	36.99	46.12	53.88	64.27	7.17	1.89	26.67	58.53
8 %	14.52	36.28	49.30	50.70	69.97	10.93	2.12	16.98	45.95
Solvent: 200ºC; 30 min; 100 rpm	Weight (g)	Yield (%, d)	VS (%, d)	Ash (%, d)	% C	% H	% N	% O	HHV (MJ/kg) *
Water 100 %	8.24	48.28	70.55	29.45	78.81	7.73	2.81	10.66	40.48
Methanol 100%	8.89	52.49	62.86	37.14	41.03	5.97	5.15	47.85	81.14
MeOH: H_2O 1:1	8.29	48.98	58.03	41.97	47.92	6.94	3.58	41.55	74.29
MeOH: H_2O 2:1	7.87	46.47	54.53	45.47	46.98	6.57	4.11	42.34	75.18
Acetone 100 %	9.38	55.39	66.90	33.10	46.53	6.36	5.62	41.48	73.83
Ethyl Acetate 100 %	7.39	43.67	51.03	48.97	46.02	6.10	5.98	41.90	74.30
Ethanol 100 %	10.78	63.63	67.09	32.91	45.26	6.22	6.01	42.51	74.89

EtOH: H_2O 1:1	9.37	55.32	66.90	33.10	56.89	7.62	4.08	31.41	62.73

3.6.2. Ultimate analysis

The distribution of elements and the value of HHV of the solid phase, biochar, from HTL using different concentrations of sludge and using different solvents and co-solvents are also presented in Table 12. Generally, solid phase from HTL of primary sludge could be employed in different applications because it presents a high energy value and high carbon percentage. In the HTL where the concentration of sludge was modified, solid phase reached a HHV higher than 45 MJ/kg with a carbon content higher than 64 %. While in the case when the solvent added was changed, solid phase attained a HHV higher than 73 MJ/kg with carbon content higher than 46 %. Consequently, biochar can be considered an important bioenergy feedstock. It has a wide range of applications, serving as an adsorbent, catalyst, and solid fuel, among others. Its versatility is presented in its ability to effectively remove various substances like dyes and heavy metals from water-based solutions. Though, the use of biochar extends beyond that, as it addresses the issue of secondary pollution caused by the mentioned pollutants. Specifically, it has proven effective in removing organic pollutants such as ammonia, phosphorus, and nitrate from municipal wastewater, providing a sustainable solution to water purification challenges (Mahima et al., 2021). SEM images of biochar and ash in biochar are presented in Figure 14.

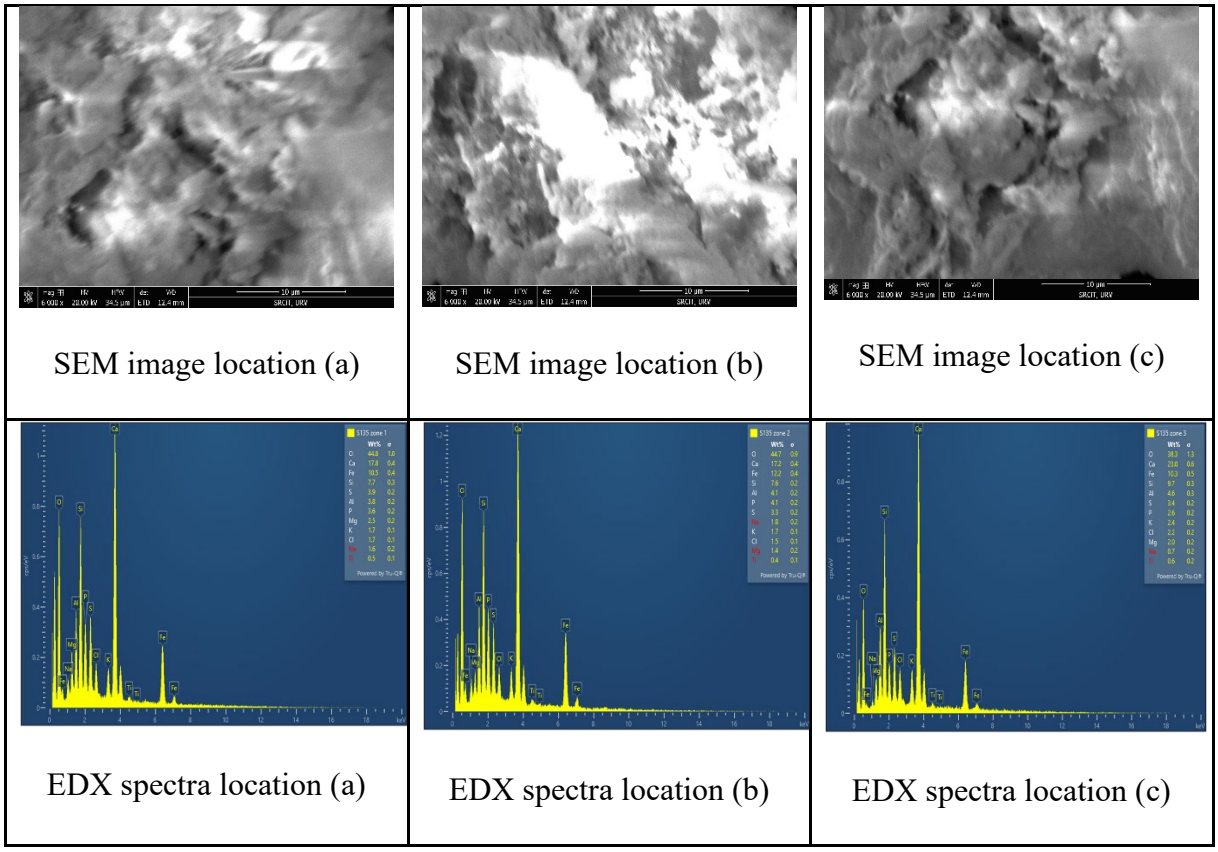

Figure 14. SEM images and EDX spectra of ash in the solid phase. (a), (b) and (c) represent three different zones of the sample.

3.6.3. Heavy metals

EDX spectra of ash in biochar are also presented in Figure 14. As carbon was the predominant element in biochar, heavy metals were considered almost negligeable. Ash was rich in salts or oxides including Ca, Fe, Si, S, Al, P, Mg, K and Cl. The high ash content confirmed the mineral species were retained during HTL process of sewage sludge (Tong et al., 2021).

3.7. Biogas

The composition of biogas produced from HTL of primary sludge is presented in Table 13.

Table 13. Biogas composition.

	Biogas volume (ml)	Biogas composition (mmol %)								
		H_2	CH_4	CO	CO_2	C_2H_4	C_2H_6	C_3H_6	C_3H_8	SO_2
[TS]: 300ºC; 30 min; 100 rpm										
TS: 2%	496.0	1.19	0.20	ND	37.34	0.14	0.04	0.43	0.05	ND
TS: 8%	1401.0	0.71	0.31	0.01	57.50	0.26	0.07	0.62	0.10	ND
Solvent: 200ºC; 30 min; 100 rpm										
Water 100%	176.7		0.06	ND	12.45	0.01	0.01	0.09	0.05	ND
MeOH 100%	161.2		0.01	ND	1.67	0.01	ND	ND	ND	0.01
MeOH: H_2O 1:1	201.5		ND	ND	2.66	0.01	ND	ND	ND	0.01
MeOH: H_2O 2:1	ND		ND	ND	ND	ND	ND	ND	ND	ND
Acetone 100%	190.4		0.03	1.44	ND	0.01	ND	ND	ND	ND
Ethyl Acetate 100%	124.0		0.05	1.77	ND	0.01	ND	ND	ND	ND
Ethanol 100 %	241.8		ND	ND	ND	ND	ND	ND	ND	ND
Ethanol 1:1	145.7		ND	ND	ND	ND	ND	ND	ND	ND

Based on the results obtained in the table, both biocrudes obtained with different water ratios presented a very similar gas composition. However, it's clear that by increasing the concentration of sludge from 2 to 8%, higher volume of gases was detected. Additionally, the percentage of each gas increased, except for hydrogen that decreased from 1.19 to 0.71 mmol %. CO was absent in the case where the concentration of sludge was 2%. While it was detected at 8% with a low amount (0.01 mmol %). CH_4, CO_2, C_2H_6, C_3H_6 and C_3H_8 were clearly improved along with the increase of concentration of primary sludge. Regarding the results obtained with different solvents, the volume of gas produced was quite lower in all cases. Because of the low volume attained, only few gases were detected. In the case where pure water was added, CO_2 was predominant with 12.45 mmol %. CH_4, C_2H_4, C_2H_6, C_3H_6 and C_3H_8

were detected with 0.059, 0.004, 0.001, 0.092 and 0.048 mmol %. In the case where methanol was used, CH_4 was noted with 0.004 mmol % when it was added purely. When mixed with water, CO_2 increased from 1.67 to 2.65 mmol %. The amounts of C_2H_4 and SO_2 remained the same. The composition of gases when pure acetone and pure ethyl acetate were used is the same. CH_4 was 0.02 and 0.05 mmol %, CO was 1.43 and 1.77 mmol % and C_2H_4 was 0.002 and 0.006 mmol %.

4. Conclusions

- The effect of TS:water ratio and of the utilisation of several solvents hydrothermal liquefaction of primary sludge was evaluated
- At 300ºC, more biocrude was obtained with a TS:water ratio of 8% (32.10% w/w_{VS}) than for a 8% ratio (21.06% w/w_{VS})
- At 200°C, the yield of biocrude obtained with pure water was 30.35% (w/w_{VS}). The utilisation of pure methanol has significantly boosted the yield of biocrude to 51.37 % (w/w_{VS}).
- The effect of pure ethanol was very similar to that of pure methanol 50.81% (w/w_{VS}).
- Other organic pure solvents like acetone or ethyl acetate also improved the yield of biocrude but they didn´t give the optimum results
- The utilisation of pure alcohol gave better results than that of alcohol:water
- Bio-oil yield from HTL in different solvent was in the order of pure ethanol > pure acetone > ethanol-water (1:1)> pure ethyl acetate> methanol: water (2:1)> methanol: water (1:1)
- The calorific value of biocrude has improved to a value higher than 40 MJ/kg
- The addition of solvents produced less N-compounds and more esters

- Aqueous phase still contains after HTL process high organic matters and few number of heavy metals
- Biochar is an important feedstock as an energy source due to its high content of carbon and high HHV.

Acknowledgements

The authors would like to express their gratitude to the collaboration of Gestió Ambiental i Abastament S.A., the public company operating the WWTP in Reus, Spain. Jacky Cheikhwafa acknowledges the support of the Agència de Gestió d'Ajuts Universitaris i de Recerca (AGAUR) of the Catalan Government for the pre-doctoral contract (Ajuts per a la contractació de personal investigador predoctoral en formació, 2019 FI-B 00743).

This work is conducted as part of the PECT "Cuidem el que ens uneix/Pobles Vius i Actius/Ebrebioterritori" project, which falls within the framework of the RIS3CAT and ERDF Catalonia Operational Programme 2014-2020. The project is co-financed by the Catalan Government and the Provincial Council of Tarragona.

The authors affiliated with the Universitat Rovira i Virgili are recognized by the Comissionat per a Universitats i Recerca del DIUE de la Generalitat de Catalunya (2017-SGR-396) and are supported by the Universitat Rovira i Virgili (2017PFR-URV-B2-33).

References

Adedeji, A.M., Russack, J.S., Molnar, L.A., Bauer, S.K. 2022. Co-hydrothermal liquefaction of sewage sludge and beverage waste for high-quality bio-energy production. Fuel, 324, 124757. *https://doi.org/10.1016/j.fuel.2022.124757*.

Arturi, K. R., Kucheryavskiy, S., Nielsen, R. P., Maschietti, M., Vogel, F., Bjelić, S., & Søgaard, E. G. (2019). Molecular footprint of co-solvents in hydrothermal liquefaction (HTL) of Fallopia Japonica. *Journal of Supercritical Fluids*, *143*, 211–222. https://doi.org/10.1016/j.supflu.2018.08.010

Ateş, F., & Erginel, N. (2016). Optimization of bio-oil production using response surface methodology and formation of polycyclic aromatic hydrocarbons (PAHs) at elevated pressures. Fuel Processing Technology, 142, 279–286. https://doi.org/10.1016/j.fuproc.2015.10.026.

Baloch, H. A., Siddiqui, M. M., Nizamuddin, S., Riaz, S., Haris, M., Mubarak, N. M., Griffin, G., & Srinivasan, M. (2021). Effect of solvent on hydro-solvothermal co liquefaction of sugarcane bagasse and polyethylene for bio-oil production in ethanol–water system. Chemical Engineering Research & Design, 148, 1060–1069. https://doi.org/10.1016/j.psep.2021.02.015.

Barreiro, D. L., Martin-Martinez, F. J., Zhou, S., Sagastagoia, I., Del Molino Pérez, F., Morales, F. J. A., & Buehler, M. J. (2022). Biobased additives for asphalt applications produced from the hydrothermal liquefaction of sewage sludge. Journal of Environmental Chemical Engineering, 10(6), 108974. https://doi.org/10.1016/j.jece.2022.108974.

Biller, P., Johannsen, I., dos Passos, J.S., Ottosen, L.D.M. 2018. Primary sewage sludge filtration using biomass filter aids and subsequent hydrothermal co-liquefaction. Water Res, 130, 58–68. https://doi.org/10.1016/j.watres.2017.11.048.

Cabrera, D.V., Barria, D.A., Camu, E., Celis, C., Tester, J.W. Labatut, R.A. 2023. Enhancing energy recovery of wastewater treatment plants through hydrothermal liquefaction. Environ Sci-Wat Res, 9, 474-488. *https://doi.org/10.1039/d2ew00752e*.

Caporgno, M. P., Pruvost, J., Legrand, J., Lépine, O., Tazerout, M., & Bengoa, C. (2016). Hydrothermal liquefaction of Nannochloropsis oceanica in different solvents. *Bioresource Technology*, *214*, 404–410. https://doi.org/10.1016/j.biortech.2016.04.123

Da Costa Magalhães, B., Checa, R., Lorentz, C., Afanasiev, P., Laurenti, D., & Geantet, C. (2023). Catalytic hydroconversion of HTL micro-algal bio-oil into biofuel over NIWS/AL2O3. Algal Research-Biomass Biofuels and Bioproducts, 71, 103012. *https://doi.org/10.1016/j.algal.2023.103012*.

Dimitriadis, A., & Bezergianni, S. (2017). Hydrothermal liquefaction of various biomass and waste feedstocks for biocrude production: A state of the art review. *Renewable & Sustainable Energy Reviews*, *68*, 113–125. https://doi.org/10.1016/j.rser.2016.09.120

DuBois, M., Gilles, K.A., Hamilton, J.K., Rebers, P.A., Smith, F. 1956. Total sugar determination by phenol sulphuric method. Anal Chem, 28, 350-356.

Fan, Y., Fonseca, F. C., Gong, M., Hoffmann, A., Hornung, U., & Dahmen, N. (2021). Energy valorization of integrating lipid extraction and hydrothermal liquefaction of lipid-extracted sewage sludge. Journal of Cleaner Production, 285, 124895. https://doi.org/10.1016/j.jclepro.2020.124895.

Glińska, K., Stüber, F., Fabregat, A., Giralt, J., Font, J., Mateo-Sanz, J.M., Torrens, E., Bengoa, C. 2020. Moving municipal WWTP towards circular economy: Cellulose recovery from primary sludge with ionic liquid. Resour Conserv Recycl Adv, 154, 104626. https://doi.org/10.1016/j.resconrec.2019.104626.

Hong, C., Wang, Z., Si, Y., Li, Z., Xing, Y., Jiashuo, H., & Li, Y. (2021). Effects of aqueous phase circulation and catalysts on hydrothermal liquefaction (HTL) of penicillin residue (PR): Characteristics of the aqueous phase, solid residue and bio oil. Science of the Total Environment, 776, 145596. *https://doi.org/10.1016/j.scitotenv.2021.145596*.

Isa, K. M., Abdullah, T. a. T., & Ali, U. F. M. (2018). Hydrogen donor solvents in liquefaction of biomass: A review. *Renewable & Sustainable Energy Reviews*, *81*, 1259–1268. https://doi.org/10.1016/j.rser.2017.04.006

Jahromi, H. K., Rahman, T., Roy, P., & Adhikari, S. (2022). Hydrotreatment of solvent-extracted biocrude from hydrothermal liquefaction of municipal sewage sludge. Energy Conversion and Management, 263, 115719. *https://doi.org/10.1016/j.enconman.2022.115719*.

Kim, S., Kim, G., & Um, B. (2022). Use of an alkaline catalyst with ethanol-water as a co-solvent in the hydrothermal liquefaction of the Korean native kenaf: An analysis of the light oil and heavy oil characteristics. *Energy*, *249*, 123509. https://doi.org/10.1016/j.energy.2022.123509

Kulikova, Y., Babich, O., Tsybina, A., Sukhikh, S., Mokrushin, I., Noskova, S., Orlov, N. 2022. Feasibility of Thermal Utilization of Primary and Secondary Sludge from a Biological Wastewater Treatment Plant in Kaliningrad City, Energies, 15, 5639. https://doi.org/10.3390/en15155639.

Li, B., Yang, T., Li, R., & Kai, X. (2020). Co-generation of liquid biofuels from lignocellulose by integrated biochemical and hydrothermal liquefaction process. Energy, 200, 117524. *https://doi.org/10.1016/j.energy.2020.117524*.

Li, S., Jiang, Y., Snowden-Swan, L., Askander, J. A., Schmidt, A. J., & Billing, J. M. (2021). Techno-economic uncertainty analysis of wet waste-to-biocrude via hydrothermal liquefaction. *Applied Energy*, *283*, 116340. *https://doi.org/10.1016/j.apenergy.2020.116340*

Lowry, O.H., Rosebrough, N.J., Farr, A.L., Randall, R.J. 1951. Proteins measurement with the folin phenol reagent. Biol Chem, 193, 265-275.

Mahima, J., Sundaresh, R. K., Gopinath, K. P., Rajan, P. S. S., Arun, J., Kim, S. H., & Pugazhendhi, A. (2021). Effect of algae (Scenedesmus obliquus) biomass pre-treatment on bio-oil production in hydrothermal liquefaction (HTL): Biochar and aqueous phase utilization studies. Science of the Total Environment, 778, 146262. *https://doi.org/10.1016/j.scitotenv.2021.146262*.

Māliņš, K., Kampars, V., Brinks, J., Neibolte, I., Mūrnieks, R., & Kampare, R. B. (2015). Bio-oil from thermo-chemical hydro-liquefaction of wet sewage sludge. *Bioresource Technology*, *187*, 23–29. https://doi.org/10.1016/j.biortech.2015.03.093

Marrone, P., Elliott, D. S., Billing, J. M., Hallen, R., Hart, T., Kadota, P., Moeller, J. C., Randel, M. A., & Schmidt, A. (2018). Bench-Scale Evaluation of Hydrothermal Processing Technology for Conversion of Wastewater Solids to Fuels. *Water Environment Research*, *90*(4), 329–342. https://doi.org/10.2175/106143017x15131012152861.

Masoumi, S., Boahene, P. E., & Dalai, A. K. (2021). Biocrude oil and hydrochar production and characterization obtained from hydrothermal liquefaction of microalgae in methanol-water system. Energy, 217, 119344. https://doi.org/10.1016/j.energy.2020.119344.

Olkiewicz, M., Fortuny, A., Stüber, F., Fabregat, A., Font, J., Bengoa, C. 2015. Effects of pre-treatments on the lipid extraction and biodiesel production from municipal WWTP sludge. Fuel, 141, 250-257. https://doi.org/10.1016/j.fuel.2014.10.066.

Passos, J. S. D., Matayeva, A., & Biller, P. (2022). Synergies during hydrothermal liquefaction of cow manure and wheat straw. Journal of environmental chemical engineering, 10(5), 108181. *https://doi.org/10.1016/j.jece.2022.108181*.

Patil, P. T., Armbruster, U., & Martin, A. (2014). Hydrothermal liquefaction of wheat straw in hot compressed water and subcritical water–alcohol mixtures. *Journal of Supercritical Fluids*, *93*, 121–129. https://doi.org/10.1016/j.supflu.2014.01.006

Qian, L., Wang, S., & Savage, P. E. (2017). Hydrothermal liquefaction of sewage sludge under isothermal and fast conditions. Bioresource Technology, 232, 27–34. https://doi.org/10.1016/j.biortech.2017.02.017.

Rice, E.W., Baird, R.B., Eaton, A.D., Clesceri, L.S. 2012. Standard Methods for the Examination of Water and Wastewater, 22nd edn. APHA AWWA WEF, Washington.

Sharma, K., Castello, D., Haider, M. S., Pedersen, T. G., & Rosendahl, L. (2021). Continuous co-processing of HTL bio-oil with renewable feed for drop-in biofuels production for sustainable refinery processes. Fuel, 306, 121579. *https://doi.org/10.1016/j.fuel.2021.121579*.

Thomsen, L. B. S., Carvalho, P. N., Passos, J. S. D., Anastasakis, K., Bester, K., & Biller, P. (2020). Hydrothermal liquefaction of sewage sludge; energy considerations and fate of micropollutants during pilot scale processing. *Water Research*, *183*, 116101. https://doi.org/10.1016/j.watres.2020.116101

Tong, Y., Yang, T., Li, B., Kai, X., & Li, R. (2021). Two-stage liquefaction of sewage sludge in methanol-water mixed solvents with low-medium temperature. *The Journal of Supercritical Fluids*, *168*, 105094. https://doi.org/10.1016/j.supflu.2020.105094.

Wang, W., Yu, Q., Meng, H., Han, W., Li, J., & Zhang, J. (2018). Catalytic liquefaction of municipal sewage sludge over transition metal catalysts in ethanol-water co-solvent. Bioresource Technology, 249, 361–367. *https://doi.org/10.1016/j.biortech.2017.09.205*.

Xu, C., & Lancaster, J. (2008). Conversion of secondary pulp/paper sludge powder to liquid oil products for energy recovery by direct liquefaction in hot-compressed water. *Water Research*, *42*(6–7), 1571–1582. https://doi.org/10.1016/j.watres.2007.11.007

Xu, D., Lin, G., Liu, L., Wang, Y., Jing, Z., & Wang, S. (2018b). Comprehensive evaluation on product characteristics of fast hydrothermal liquefaction of sewage sludge at different temperatures. Energy, 159, 686–695. https://doi.org/10.1016/j.energy.2018.06.191.

Yan, M., Liu, Y., Wen, X., Yang, Y., Cui, J., Chen, F., & Yan, M. (2023). Effect of operating conditions on hydrothermal liquefaction of kitchen waste with ethanol-water as a co-solvent for bio-oil production. Renewable Energy, 118949. https://doi.org/10.1016/j.renene.2023.118949.

Yerrayya, A., Nikunj, A., Prashanth, P. F., Chakravarthy, S. R., Natarajan, U., & Vinu, R. (2022). Optimization of bio-crude yield and its calorific value from hydrothermal liquefaction of bagasse using methanol as co-solvent. Energy, 244, 123192. https://doi.org/10.1016/j.energy.2022.123192.

Zhao, B., Wang, H., Xu, S., Qian, L., Li, H., Gao, J., Zhao, G., Ray, M. B., & Xu, C. (2022). Influence of extraction solvents on the recovery yields and properties of bio-oils from woody biomass liquefaction in sub-critical water, ethanol or water–ethanol mixed solvent. Fuel, 307, 121930. https://doi.org/10.1016/j.fuel.2021.121930.

4018

6

Waste to Energy: Employment of HTL and co-HTL processes to reach sustainability

ABSTRACT

The deficiency in conventional energy resources imposed the researcher to look for another alternative. Because agricultural and municipal wastes and microalgae are carbon rich sources, they were considered to good biomasses for bioenergy production. One feasible technique is the hydrothermal liquefaction process that treats wet biomass at high temperature and pressure. In this study, HTL and co-HTL were performed on different biomasses to demonstrate the difference between the biomasses and their effects on the yield and quality of biocrude and other products. From the results obtained, the highest yield was reached from the HTL of primary sludge with 37.66 %. While the most noticeable improvement was noticed through the co-HTL of rice straw with primary sludge from 16.11 % to 29.03 %. Biochar yield was always less than 30 %. Aqueous phase contained high amount of organics even after the conversion processes. Biogas was composed from hydrocarbons, CO, CO_2 and H_2.

4020

1. Introduction

There is no doubt that energy is of the most important parameters for global success. The rapid population expansion and the advancement in industrialization and modernization, respectively, have given rise to the demand of energy in recent years (Paramati et al., 2022). Consequently, the depletion of conventional resources like natural gas, oil and coal has started. Nevertheless, a severe environmental pollution, specifically the pollution of water and air resources became a significant issue, along with the depletion of ozone layer and the increase of global temperature (Xu et al., 2022). Nowadays, most of the energy resource is the non-reproducible fossil fuels that cause negative impact on ecosystem due to high carbon dioxide emissions (Zhang et al., 2022). Therefore, many researchers from the sustainable energy field considered finding environmentally gentle processes to produce bioenergy an important topic (A. Parvathy Eswari et al., 2023). Biomass-originated energy is nowadays being developed on a worldwide scale (Iqbal et al., 2023). It absorbs a noticeable amount of CO2 emitted into the air, providing a carbon-neutral path for biofuels. Agricultural wastes. Municipal waste and microalgae are all considered as an organic matter waste or biomass (Duc Bui et al., 2023). They can be converted to liquid and gaseous transportation fuel, electricity, heat, etc (Tolessa 2023). Hydrothermal liquefaction (HTL) offers a direct and efficient process for treating wet biomass without the need for energy-intensive and costly drying processes (Hao et al., 2022). HTL processes are typically operated at mild temperatures (200–400 °C) and elevated pressures (5–25 MPa) in the presence of water to hydrolyse the macromolecules of the biomass into biocrude containing light molecules (Wang et al., 2023). For example, the highest biocrude yield (36.4 wt%) was obtained from rice straw at 350 °C of temperature and 30 min of reaction time (Harinsakar et al., 2022). Also, the highest yield of biocrude (24.2 wt%) was reached from

microalgae at 325 °C of temperature and 60 min of reaction time (Zhang et al., 2022). Recently, hydrothermal co-liquefaction has fascinated much research concern. Using mixed feedstocks instead of one type is more practical and economically feasible. Also, due to the synergistic effects between biomass components, the biocrude yield could improve (Yan et al., 2022). The hydrothermal co-liquefaction of microalgal biomass with faecal sludge produced 38 % of biocrude at 1 hour of reaction time and 300 °C of temperature, 28.4 % and 23.3 % higher than the HTL of microalgae and faecal sludge individually (Islam et al., 2022). In another study, the hydrothermal co-liquefaction of municipal sewage sludge and rice straw has produced 32.45 % of biocrude at 20 minute of reaction time and 300 °C of temperature, 23.67% and 22.74% higher than the HTL of rice straw and municipal sewage sludge individually (Leng et al., 2018a).

The first part of this study focused on the hydrothermal liquefaction of different biomasses separately: primary sludge, rice straw, spirulina plantesis, swine manure, buffalo's powder (BP) Alphitobius diaperinus and frass. All the experiments were conducted at 300 °C of temperature, 30 minute of reaction time, 4 % of solid loadings and 100 rpm of stirring rate. In the second part, hydrothermal co-liquefaction of primary sludge blended with each biomass alone was completed at a ratio of 1:1 by respecting the 4 % of solid loadings, temperature of 300 °C, reaction time of 30 minute and stirring rate of 100 rpm. A full characterization was completed for all the feedstocks and all the products obtained from HTL and co-HTL at all conditions.

2. Materials and methods

2.1. Reagents

Dichloromethane (ref.: 32222), Toluene (ref.: 32249), and 2-Propanol (ref.: 59300) were purchased from Honeywell. Methanol (ref.: 412722), HPLC-GOLD-Ultragradient grade, was obtained from Carlo Erba reagents. n-Hexane 95% (ref.: 363242), high-performance chromatography grade, and phenol crystalline (ref: 144852.1211) along with n-heptane (ref.: 162062.1611) were provided by PanReacAppliChem. Sulfuric acid reagent (ref: 34632), orange reagent (ref: 131130.1612), sulfuric acid 95.0–97.0% (ref: 30743), bovine serum albumin (BSA) (ref: A9647), sodium hydroxide 98% (ref: 30620), sodium carbonate (ref: 222321), potassium sodium tartrate tetrahydrate (ref: 217255), copper (II) sulfate pentahydrate (ref: 209198), Folin&Ciocalteu's phenol reagent (ref: F9252), magnesium sulfate monohydrate (ref: 434183), anhydrous sodium sulfate (ref: 239313), and fuming hydrochloric acid (ref: 84418), high analytical reagent grade, were supplied by Sigma - Aldrich.

2.2. Waste collection and managing

Samples of primary sludge were provided by the municipal wastewater treatment plant of Reus in Tarragona, Spain. 500 mL bottles of primary sludge were sampled after partial gravity thickening of the primary treatment. Frass was supplied by Iberinsect S.L. Reus. Buffalo's powder (BP) Alphitobius diaperinus was bought from Kreca Ento-Food. Before any use, it was grinded. Spirulina Plantesis was contributed by Plateforme R&D AlgoSolis, Saint-Nazaire, France. Rice straw was brought from Caubra Drossera de la Dreta, Amposta, Spain. Swine Manure was supplied by Romero-Polo Company, Lleida, Spain. All the wastes were stored in a freezer at -15 °C. Defrosting in an oven at 60°C for 5 hours was required for high moisture wastes before any use.

2.3. Characterization of biomass

The characterization of all biomasses was conducted in triplicate. The percentages of Total Solids (TS), Volatile Solids (VS), and Ash content were determined according to standard methods 2540B and 2540E, respectively (Rice et al., 2012). Lipid extraction was performed using a Soxhlet apparatus with hexane as a solvent for sludge, frass, buffalo, spirulina plantesis and ethanol- toluene (1:2) as a solvent for rice straw and swine manure, following standard method 5520E (Rice et al., 2012). Total carbohydrate percentage was determined using the phenol-sulfuric acid Dubois method (Dubois et al., 1956). Briefly, 0.05 mL of 80% phenol solution was added to 2 mL of sample in a glass tube. Subsequently, 5 mL of concentrated sulfuric acid was rapidly added. The tubes were left at room temperature for 10 minutes, followed by 15 minutes in a thermostatic bath at 30°C. The absorbance was then measured at 480 nm. For protein content determination, the Lowry method was employed (Lowry et al., 1951). Proteins in the samples were solubilized by heating them with 2 M sodium hydroxide at 100°C for 10 minutes. The absorbance was measured at 750 nm. Ultimate analysis was carried out by Serveis Técnics de Recerca at Universitat de Girona using an ultimate analyzer (Perkin Elmer model EA2400). This analysis determined C, H, and N, with O being calculated by difference. Additionally, a field emission of variable pressure environmental scanning electron microscopy (ESEM) with X-ray microanalysis (Quanta 600, FEI Company) was utilized for heavy metal detection, offering high resolution (3 nm).

2.4. HTL and co-HTL of biomass

The experiments were conducted in a 1 L Stainless Steel Autoclave (Autoclave Engineers model EZE Seal) equipped with a movable heating shell, a fixed MagneDrive® stirrer (a magnetically coupled, packless rotary impeller system), and an operating condition controller. The reactor was connected to a gas line through an inlet valve to introduce nitrogen, while the

outlet valve was connected to a gas flow meter and a Tedlar bag push lock valve 0.6 L (Superlco 30289-U) for gas collection. In the first part, HTL was performed for each biomass separately at the same conditions. To start each experiment, approximately 4 % (w_{TS}) was added to the reactor, and pure nitrogen gas was purged three times to create an oxygen-free atmosphere. The reactor was then pressurized up to an initial pressure of 1 bar. Hydrothermal Liquefaction (HTL) experiments were performed at 300 °C (~86.9 bar). The reaction time after reaching the desired temperature was consistently set at 30 minutes, while continuous agitation at 100 rpm was maintained throughout the experiments. The pressure inside the reactor was not externally controlled but rather allowed to auto-generate based on the reaction temperature.

The heating-up time was around 2 hours. After each batch experiment, the reactor was cooled down in a room-temperature water bath (approximately 25 °C) until it returned to its initial condition. In the second part, in the co-HTL, two types of biomasses were combined, respecting a total percentage of total solids (4 % (w_{TS})). Four different conditions were achieved: primary sludge with swine manure, primary sludge with rice straw, primary sludge with spirulina plantesis, primary sludge with buffalo and primary sludge with Frass. The temperature, the reaction time and the stirring rate were maintained at 300 °C, 30 mins and 100 rpm. The experimental procedure was done by following the same steps of part 1.

2.5. Cleaning of the reactor and separation of products

Figure 1 illustrates the schematic diagram of the experimental separation procedures conducted after hydrothermal liquefaction of biomass. The products obtained from the liquefaction process are distributed into four distinct phases: gas, organic, aqueous, and solid. Once the reactor returned to atmospheric pressure and temperature, the gas phase was released. The gas mixture was passed through a flow meter, measuring its volume, and collected in a gas bag for

further analysis. Next, the reactor was opened, and the mixture was transferred to a large beaker. The solid part was separated from the liquid part through vacuum filtration. The liquid part primarily contained the aqueous phase along with a small portion of the organic phase. This liquid portion was transferred into a separate bottle. Meanwhile, the reactor was repeatedly washed with dichloromethane to recover any remaining organic components, which might be deposited on the reactor's walls, cover, or agitation module. The mixture collected during this washing process, including solids entrapped in the organics, was separated by vacuum filtration. The liquid part, containing the organic phase and dichloromethane, was transferred into another bottle. The solid retained on the filter paper, consisting of biochar and ashes, was washed several times with dichloromethane. The biochar was then dried in an oven at 105 °C for 24 hours and weighed for quantification purposes. A small volume of dichloromethane was added to the aqueous phase, and the mixture was centrifuged at 8000 rpm for 5 minutes. The upper phase consisted of dichloromethane containing a small portion of the organic phase, which was combined with the previously separated organic phase. The lower phase contained soluble organic molecules and represented the aqueous phase. All the organic parts were collected together and were subjected to rotary evaporation at 65 °C and atmospheric pressure to remove the dichloromethane, resulting in a viscous organic liquid known as biocrude. The biocrude was further weighed for quantification. Finally, the biocrude was separated into oils and asphaltenes using Soxhlet extraction with 200 mL of hexane. Oils were separated from hexane by rotary evaporation at 65 °C and atmospheric pressure. The quantity of asphaltenes was determined by calculating the difference between the total biocrude and the separated oils. Products yield were calculated using equations (1), (2), (3) and (4).

Biocrude (BC) yield was calculated from equation (1):

$$\text{Biocrude yield (\%)} = \frac{\text{Mass of biocrude}}{\text{Mass of volatile solids}} \times 100 \quad (1)$$

Aqueous phase (AP) yield was calculated from equation (2):

$$\text{Aqueous phase yield (\%)} = \frac{\text{Mass of solids dissolved in aqueous phase}}{\text{Mass of volatile solids}} \times 100 \quad (2)$$

Biochar yield (BCH) was calculated from equation (3):

$$\text{Solid yield (\%)} = \frac{\text{Mass of solid residue}}{\text{Mass of volatile solids}} \times 100 \quad (3)$$

Biogas yield (BG) was calculated from equation (4):

$$\text{Gas yield (\%)} = 100 - \text{BC yield} - \text{AP yield} - \text{BCH yield} \quad (4)$$

In all the equations, mass of volatile solids is referred to that of initial biomass(es) used.

2.6. Biocrude characterization and quantification

Extensive characterization of the biocrude was carried out, including various analytical techniques. Gas Chromatography/Mass Spectrometry (GC/MS), thermogravimetric Analysis (TGA), ultimate Analysis and higher heating value (HHV), Fourier Transform Infrared Spectroscopy (FTIR), nuclear Magnetic Resonance (NMR), simulated Distillation (SimDis), saturates, aromatics, resins and asphaltenes (SARA) were characterized, providing detailed understanding of its properties and potential energy.

2.6.1. Gas chromatography/mass spectrometry spectroscopy of biocrude

The biocrude samples at all conditions were subjected to gas chromatography-mass spectrometry (GC/MS) analysis using a Perkin Elmer Turbo Mass Gold GC/MS instrument, equipped with a Supelco SLB®-5ms capillary GC column (dimensions: 30 m × 0.25 mm, df 0.25 μm). For the analysis, dichloromethane (DCM) was used as solvent. The GC oven temperature was programmed as follows: it was initially maintained at 70 ºC for 1 minute, then gradually increased to 180 ºC at a rate of 7 ºC/min. Subsequently, the temperature was further raised to 240 ºC at a rate of 12 ºC/min and finally held at 330 ºC for 7 minutes. GC/MS analysis

provided the identification and quantification of the biocrude components at different conditions.

2.6.2. Thermogravimetric analysis of biocrude

The thermogravimetric analysis (TGA) was employed to investigate the weight loss properties of the biocrudes. Each analysis involved heating approximately 3 to 4 mg of the biocrude sample from 30 °C to 800 °C. TGA was carried out under a nitrogen flow of 60 mL/min, and the heating rate was set at 10 K/min.

2.6.3. Elemental analysis and HHV of biocrude

Ultimate analysis of biocrude samples was also realized by Serveis Técnics de Recerca at Universitat de Girona as commented in section 2.2. C, H and N were quantified, and O calculated by difference. Then, the higher heating values of (HHVs) of biocrude were calculated using Dulong formula (5), taken from Hong's study, where HHV is expressed in MJ/kg (Hong et al., 2021):

The ultimate analysis of biocrude samples was conducted by Serveis Técnics de Recerca at Universitat de Girona, as previously mentioned in section 2.2. It involved quantifying the percentages of carbon (C), hydrogen (H), and nitrogen (N) present in the biocrude. The oxygen content (O) was then calculated by the difference. Subsequently, the higher heating values (HHVs) of the biocrude were calculated using the Dulong equation (5), expressed in MJ/kg according to Hong's study (Hong et al., 2021).

$$\mathrm{HHV}\ (\%) = 0.3383 \cdot \mathrm{C} + 1.443 \cdot \left(\mathrm{H} - \frac{\mathrm{O}}{8}\right) \quad (5)$$

C, H and O are the mass percentages of carbon, hydrogen, and oxygen from the ultimate analysis of the samples, respectively.

2.6.4. FTIR of biocrude

FTIR spectra were recorded using a Thermo Nicolet Nexus 670 Fourier Transform Infrared Spectrophotometer, equipped with a single-bounce diamond attenuated total reflectance (ATR) accessory known as the Specac Golden Gate and KBr beam splitter. The spectra wavenumbers ranged from 4000 to 400 cm^{-1}, with a resolution of 0.98 cm^{-1}. To enhance accuracy and reliability, each spectrum was averaged over 50 replicate scans utilizing Omnic software. Background scans were performed with the dry accessory at ambient temperature to provide a reference for subsequent sample measurements. For sample analysis, approximately 30 mg of the biocrude sample was directly smeared onto the ATR crystal surface.

2.6.5. ^{1}H NMR of biocrude

^{1}H NMR spectra were recorded using a Varian Unity 400-MHz spectrometer equipped with a 5-mm broadband probe. For each analysis, 50–75 mg of biocrude was dissolved in deuterated chloroform, including 0.03% tetramethylsilane (TMS) as an internal reference. Samples were filtered through 0.22-µm PTFE filters to remove any suspended particulates. Subsequently, the filtered samples were loaded into 5 mm diameter NMR tubes for analysis. ^{1}H spectra were obtained using a 90^{o} pulse angle and a spinner frequency of 20 Hz, sweep width was set at 8000 Hz across 32 transients.

2.6.6. Simulated distillation of biocrude

Simulated distillations were conducted following the ASTM-D2887 method using a HP 5890 Series II FID gas chromatograph equipped with a Durabond DB-HT-SimDis GC column by Agilent-J&W Scientific (5 m × 0.53 mm id, 0.15 µm film). Helium was used as the carrier gas

at a flow rate of 56.4 mL/min. The oven temperature was initially set to 36 °C and then ramped up to 400 °C at a rate of 10°C/min, held constant for 10 minutes. The injector volume was set to 0.5 µL, and the injector temperature was maintained at 350 ºC. The detector temperature was set to 375 °C, with hydrogen gas flowing at 40 ml/min, airflow at 400 ml/min, and helium makeup at 24 ml/min. For analysis, samples (1% w/w) and reference standards (0.5% w/w) were dissolved in DCM. Prior to analysis, the samples were filtered through 0.22 µm PTFE filters to remove any suspended particulates. Boiling points were determined using a D2887 calibration mix and a D2887 Reference Gas Oil standard, both purchased from Sigma Aldrich. Data, including retention times and peak areas, were collected. Each sample was then distributed into different fractions (% wt), and boiling points were calculated accordingly.

2.6.7. Quantification of SARA fractions of biocrude

SARA fractions of biocrude were analysed through a series of separation steps. The extraction of light phase from heavy phase was done using n-heptane and following the method mentioned previously. Maltenes (light phase) were further fractionated through a glass chromatographic column containing activated alumina. Saturates were extracted using 20 mL of n-heptane. Next, aromatic compounds were removed using 20 mL of toluene. Subsequently, resins were isolated using 20 mL of methanol. Each eluted fraction was recovered by removing the solvents using a Rotary evaporator.

2.7. Biochar characterization and quantification

Beside the yield of biochar, total solids, moisture content, volatile solids and ash content were determined according to standard methods 2540B and 2540E respectively (Rice et al., 2012).

Ultimate analysis and heavy metals detection were done as well by following the same procedures described above.

2.8. Aqueous phase characterization

The amount of aqueous phase obtained was measured. COD, TOC, TN, proteins, and carbohydrates were measured or analysed. COD analysis was done according to standard method 5220D (Rice et al., 2012). TOC and TN were analysed in ASI-L auto sampler Shimadzu into a Shimazdu TOC-L CSN TOC analyser coupled with TNM-L ROHS unit provided with a NDIR detector and calibrated with standard solutions of hydrogen potassium phthalate (Ponces-Robles et al., 2018). Protein amount was determined according to Lowry method (Lowry et al., 1951) and carbohydrates were measured following Dubois method (Dubois et al., 1956) as described in the previous section (2.3). Total solid (TS), volatile solid (VS) and ash content of the dissolved solid in the aqueous phase were measured. A specific volume of aqueous phase was dried in a weighted crucible for 24 hours in the oven at 100 ºC then burned in the furnace at 550 ºC for 1 hour, as detailed by the standard methods 2540B and 2540E respectively (Rice et al., 2012). Measurement of pH value in the HTL aqueous phase was achieved by pH meter. Heavy metals were analysed in the ash of the solid dissolved in the aqueous phase by following the same procedure mentioned before.

2.9. Gas phase characterization

Identification and quantification of biogas were completed by a gas chromatograph (micro-GC, Agilent, 990) equipped with a thermal conductivity detector (TCD). A MS5A SS 10MX0.25MMX30UM BF RTS, CP-PORABOND Q 5MX0.25MMX3UM column (column 1) was used to separate the light gases using Argon as a carrier gas and a PORAPLOT

Q UM 10MX0.25MMX8UM BF, CP-PORABOND Q 1MX0.25MMX3UM column (column 2) was used to separate heavy gases using helium as a carrier gas. Column 1 was maintained at injector temperature 100 ºC, injection time 40 ms, column temperature 100 ºC and initial pressure 200 kPa. Column 2 was maintained at injector temperature 100 ºC, injection time 40 ms, column temperature 60 ºC and initial pressure 150 kPa. The run time was 120 s. The mole percentage of each gas was determined with respect to gas standards prepared by Carburos Metálicos, S.A.

3. Results and discussion

3.1. Feedstock characterization

The characterisation of all the feedstocks is outlined in Table 1. As it can be observed, the primary sludge, as received, contained 4.3 % of total solids (w/w wet basis), very close to 3.9 % (Glinska et al., 2020). The moisture accounted to 95.7 % (w/w wet basis). Ashes were 22.9 % (w/w total solids basis) of the total solids. Primary sludge was characterized by its significant carbohydrate, lipid and protein contents with 29.84 %, 23.41 % and 21.15 %, respectively. Spirulina Platensis contained 26.76 % of total solids (w/w wet basis). The moisture accounted to 73.24 % (w/w wet basis). Ashes were 7.57 % (w/w total solids basis) of the total solids. Buffalo contained 98.6 % of total solids (w/w wet basis). The moisture accounted to 1.40 % (w/w wet basis). Ashes were 5.50 % (w/w total solids basis) of the total solids. Spirulina platensis and buffalo were characterized by their high protein contents with 63.35 % and 60.62 %, respectively. Frass contained 88.18 % of total solids (w/w wet basis). The moisture accounted to 11.82 % (w/w wet basis). Ashes were 17.81 % (w/w total solids basis) of the total solids. Swine manure contained 32.10 % of total solids (w/w wet basis). The moisture accounted to 67.10 % (w/w wet basis). Ashes were 14.40 % (w/w total solids basis) of the total

solids. Rice straw contained 93.73 % of total solids (w/w wet basis). The moisture accounted to 6.27 % (w/w wet basis). Ashes were 9.49 % (w/w total solids basis) of the total solids, close to 11.56 (w/w total solids basis) (Leng et al., 2018c). Frass, swine manure and rice straw were characterized by their high carbohydrate contents with 52.81 %, 64.90 % and 71.44 %, respectively. The percentage of carbohydrates in swine manure attained 80.08 % elsewhere (Shah et al., 2021).

Among all the biomasses employed, only primary sludge could have been used as received as it contained very high-water content. Adjustment of total solid loading to 4 % into the HTL reactor was required for the other biomasses by adding specific amount of water as it is used as the medium for hydrolysing the organic matter.

Lipids are formed from free fatty acids in the range of C10 to C18 which are building blocks for esters production. Also, proteins are approved to be promoters for biocrude production through HTL. Maillard reactions represent a significant part in the distribution of biocrude and composition, originated from the reaction of amine groups present in proteins with carbonyl groups present in reducing carbohydrates (Fan et al., 2021). All the feedstocks are rich in lipids, proteins and/or carbohydrates. Therefore, HTL is assumed to be a suitable option for thermally hydrolysing the macromolecules into valuable chemicals. More importantly, co-HTL is considered to be a feasible path for taking advantage from the composition of the combined feedstocks used and converting them together into valuable products.

Table 1. Characterization of different feedstocks.

Feedstock	TS	Moisture	Ash	Volatile			TOC	COD
				Carbohydrate	Lipid	Protein		
Primary sludge	4,304	95,696	21,23	29,8	23,4	21,2	35180	6290
Spirulina Platensis	26,76	73,24	7,57	25,63	4,25	63,35	13595	
Buffalo	98,6	1,4	5,5	10,3	23,38	60,62	ND	ND
Frass	88,18	11,82	17,81	52,81	ND	28,1	ND	ND
Swine manure	32,1	67,9	14,4	64,9	2,35	20,22	ND	ND
Rice straw	93,73	6,27	9,487	71,44	2,45	ND	ND	ND

3.2. HTL and co-HTL of feedstocks

HTL and co-HTL experiments were always performed at a reaction time of 30 minutes and a stirring rate of 100 rpm and an operating temperature of 300 ºC. After the completion of the reaction time, the reactor was cooled down to ambient conditions and the four products (gaseous phase, biocrude, containing organics aqueous phase and biochar) were separated following experimental procedure depicted in Figure 1. The quantification and characterization of the products obtained during HTL and co-HTL runs will be presented in the different sections presented below.

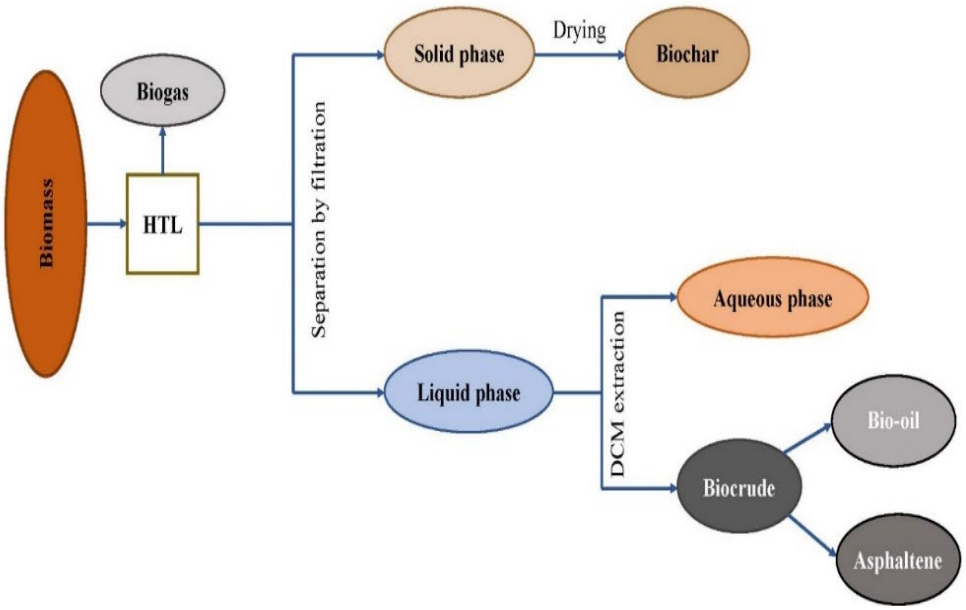

Figure 5. Process and separation overview of HTL.

3.3. Main product: Biocrude

3.3.1. Yield

The biocrude yields from HTL using different biomasses separately and co-HTL of primary sludge with other biomasses are illustrated in Table 2. The maximum value of biocrude was produced from HTL of primary sludge, 37.66 % (w/wVS) including 23.96 % (w/wVS) of oils. This value is comparable to the one obtained from the HTL of mixed sludge (primary and secondary) in another study with 37.3 % of biocrude at 350 ºC for 15 minutes (Liu et al. 2023). The addition of primary sludge to other biomasses showed an important improvement in the biocrude yield. Concerning the results obtained from co-HTL runs, the yields of biocrude obtained from co-HTL of primary sludge with frass, primary sludge with buffalo, primary sludge with rice straw, primary sludge with spirulina platensis have increased from 23.44 to 25.43 % (w/wVS), 7.76 to 26.81 % (w/wVS), 16.11 to 29.03 % (w/wVS) and 18.74 to 25.08

% (w/wVS). While in the co-HTL of primary sludge with swine manure, the percentage of biocrude has decreased slightly from 19.20 to 17.66 % (w/wVS). In another study, the combination of municipal sewage sludge with rice straw has improved the yield of biocrude by 5-10 % and the property of biocrude by decreasing the percentage of asphaltenes (Leng et al., 2018b). Also, the co-processing of sewage sludge of microalgae has reached a maximum biocrude yield of 28.68 % (dry basis) (Xu et al., 2019). The interaction between swine manure and sewage sludge produced biocrude with a yield of 42 % (Shah et al., 2021). Co-liquefaction boosts interactions of free radicals or intermediates from different biomass, resulting in higher biocrude production (Leng et al., 2018c). In other words, when a biomass is co-liquified with sludge, the minerals in the sludge could catalytically help the hydrolysis and depolymerization of that biomass, resulting in better yield and quality of biocrude (Chan et al., 2023).

Table 2. Biocrude, Bio-oil and asphaltene yields from HTL and co-HTL at 300ºC of temperature, 30 min of reaction time and 100 rpm of stirring rate.

Feedstock	Biocrude %		Bio-oil %		Asphaltene %	
Experiment	HTL	Co-HTL	HTL	Co-HTL	HTL	Co-HTL
Buffalo	7.76	26.81	0.86	16.07	6.90	10.74
Frass	23.44	25.43	15.26	8.36	8.18	17.07
Rice straw	16.11	29.03	7.82	1.92	8.30	27.11
Spirulina Platensis	18.74	25.08	2.61	10.67	16.13	14.41
Primary sludge	37.66		23.96		13.7	
Swine manure	19.20	17.66	ND	6.90	ND	10.76

3.3.2. Ultimate analysis and HHV

The results from the ultimate analysis, C, H, N and O, and higher heating values HHV of biocrude from HTL and co-HTL are presented in Table 3. The ultimate composition of biocrude was not really affected by the biomass selected as the results were very similar. It can be noted that in the HTL experiments, the produced biocrude contained around 72 % of carbon, 8 % of hydrogen, 5 % of nitrogen and 18 % of oxygen. With these values, HHV didn´t reach higher than 40 MJ/kg. Also, the employment of primary sludge with other biomass through the co-HTL process didn´t really improve the energetic value of biocrude. A slight decreased was noted in the percentage of carbon, resulting in an increase in the percentage of oxygen. Considering the HHV, according to the results obtained, no important change was noticed. However, in any case, the energetic quality of biocrude should be improved as it is still lower than that of petroleum, 42.75 MJ/kg (Shah et al., 2020).

Table 3. Ultimate analysis and HHV of biocrude of HTL and co-HTL, 300 ºC of temperature, 30 min of reaction time and 100 rpm stirring rate.

Feedstock	C %		H %		N %		O %*		HHV MJ/kg)	
	HTL	co-HTL	HTL	co-HTL	HTL	co-HTL	HTL	co-HTL	HTL	co-HTL
Primary sludge	75.06		11.31		4.07		9.56		39.99	
Swine manure	ND	65.75	ND	8.83	ND	3.22	ND	22,2	ND	30.98
Spirulina	66.94	68.56	9.44	9.59	5.84	2.46	17.78	19.39	33.06	33.53
Rice straw	72.01	66.44	7.16	8.93	2.08	3.81	18.75	20.82	31.31	31.61
Frass	71.50	67.34	8.27	8.74	6.64	3.66	13.34	20.26	33.80	31.74
Buffalo	72.32	69.7	9.86	9.70	5.56	3.98	12.26	16.62	36.48	34.58

O % was calculated from the equation (100 – H % – N % – C %)

3.3.3. GC/MS analysis

Chemical compounds of the biocrude obtained from HTL of different feedstocks and from co-HTL of primary sludge with other biomass were identified through GC/MS analysis. Usually, there are more of 300 substances detected in the biocrude. However, only the ones with boiling points lower than 330 ºC were identified. The detailed compounds information is listed in Table 4.a and Table 4.b. These compounds were additionally classified into alcohols, phenols, esters, hydrocarbons, and N and O containing compounds. The hydrolysis of the lipids in the feedstock produces long chain fatty acids and esters (Mishra et al., 2020). Whereas, the decomposition and dehydration of proteins and amides produces N rich compounds (Chen et al., 2019). On

the other hand, more types of N-containing long-chain structure molecules were found in biocrude, implying the improved combination of alkane with amine generated from the deamination of the organics in the feedstock (Leng et al., 2020). The co-HTL process has increased the amount of ester and hydrocarbon compounds and decreased the amount of N-containing compounds. These results are compatible with a study mentioned elsewhere (Koley et al., 2018).

Table 4.a. Substances identified in the chromatograms of biocrude from HTL, 300ºC of temperature, 30 min of reaction time and 100 rpm stirring rate.

Compounds	Formula	Biomass			
		Buffalo	Rice Straw	Frass	Primary sludge
Pentadecanoic acid, 14-methyl-, methyl ester	C17H34O	X	X		
9-Octadecenamide, (Z)-	C18H35NO	X		X	
9-Octadecenamide, N,N-dimethyl-	C18H35NO	X			
9-Octadecenamide, n-butyl-	C22H43NO	X			
Eicosane	C20H	X	X		
Pyrrolidine, 1-(1-oxo-9-octadecenyl)-	C22H41NO	X			
Pyrrolidine, 1-(12-methyl-1-oxotetradecyl)-	C22H43NO	X			
n-Hexadecanoic acid	C16H32O2	X	X	X	X
Octadecanoic acid	C18H36O	X			
cis-Vaccenic acid	C24H39NO	X			
Hexadecanamide	C16H33NO	X			X
Tridecanoic acid	C13H26O		X		X
Cholest-4-ene	C27H		X		
Tricosane	C23H		X		
Heptacosane	C27H		X		
Cyclotriacontane	C30H60		X		
Oleic Acid	C18H34O		X		
Z-5-Nonadecene	C19H38		X		
Hexacosane	C26H		X		
2-Naphthalenol, 3-methoxy-	C10H8O		X		
Octacosane	C28H		X		
Hexadecanoic acid, methyl ester	C17H34O2			X	X
1-Eicosene	C20H			X	
Methyl stearate	C19H38O			X	
9-Octadecenoic acid, (E)-	C18H34O			X	
6-Octadecenoic acid, (Z)-	C18H34O			X	
3-Cyclopentylpropionamide, N,N-dimethyl-	C5H14N2			X	
Octanamide, N,N-dimethyl-	C10H21NO			X	

2-Ethylacridine	C15H13N			X	
Cetene	C16H32				X
Ethyl N-isopropyl-3-phenylpropanimidate	C14H21NO				X
1-Heptadecene	C17H34				X
2-Dodecanone	C12H24O				X
Octadecane	C18H38				X
1,2-Benzisothiazole, 3-(hexahydro-1H-azepin-1-yl)-, 1,1-dioxide	C8H7NO3S				X
7-Acetyl-6-ethyl-1,1,4,4-tetramethyltetralin	C18H26O				X
Decane	C10H22				X
1-Nonadecene	C19H38				X
cis-9-Hexadecenoic acid	C16H30O2				X
6-Octadecenoic acid	C18H34O2				X
N, N-Dimethyldecanamide	C12H25NO				X
(Z) 9-Octadecenamide	C18H35NO				X
10-Methyl-undecanoic acid, pyrrolidide	C13H26O				X
Hexadecanoic acid, dodecyl ester	C28H56O2				X
Tetradecanoic acid	C14H28O2				X

Table 4.b. Substances identified in the chromatograms of biocrude from co-HTL, 300ºC of temperature, 30 min of reaction time and 100 rpm stirring rate.

Compound	Formula	Biomasses				
		Frass + PS	Rice straw + PS	Spirulina Platensis + PS	Swine manure + PS	Buffalo + PS
1-Pentadecene	C15H30	X			X	
6-Tridecene, 7-methyl-	C15H30	X				
3-Heptadecene, (Z)-	C17H34	X				X
2-Pentadecanone	C15H30O	X	X	X		
Tetradecanoic acid	C14H28O2	X	X	X		X
2-Heptadecanone	C17H34O	X	X			X
Pentadecanoic acid, 14-methyl-, methyl ester	C17H34O2	X				
n-Hexadecanoic acid	C16H32O2	X				
2(3H)-Furanone, 5-dodecyldihydro-	C17H32O2	X				X
Methyl stearate	C19H38O2	X	X	X		
6-Octadecenoic acid	C18H34O2	X	X	X	X	X
Octadecanoic acid	C18H36O2	X	X	X		X
Hexadecanamide	C16H33NO	X	X		X	X
2(3H)-Furanone, dihydro-5-tetradecyl-	C16H30O2	X	X	X		
9-Octadecenamide, (Z)-	C18H35NO	X	X		X	X
Octadecanamide	C18H37NO	X	X		X	
Pyridine-3-carboxamide, oxime, N-(2-trifluoromethylphenyl)-	C12H9F3N2O	X				
Cholest-3-ene, (5.alpha.)-	C27H44	X	X		X	X
Cholest-5-ene	C27H46	X				X
Cholest-4-ene	C27H46	X	X	X	X	X
Docosane	C22H46	X	X	X	X	
Cholesta-3,5-diene	C27H42	X				
Cholestan-3-one	C27H44O	X	X	X	X	

Cyclododecane	C12H24	X				
1-Octadecene	C18H36		X			
Cyclohexadecane	C16H32		X			
Ethyl 5-chloro-2-nitrobenzoate	C10H9ClNO4		X			
Cyclododecane	C12H24		X			
3-Heptadecene, (Z)-	C17H34		X			
1-Nonadecene	C19H38		X	X		
Hexadecanoic acid, methyl ester	C17H34O2		X			
n-Hexadecanoic acid	C16H32O2		X		X	X
Benz[c]acridine, 5,10-dimethyl-	C19H16		X	X		X
Vitamin E	C29H50O2		X			
Cholesterol	C27H46O		X			
Dodecanoic acid	C12H24O2		X			
Pentadecanoic acid	C15H30O2			X		
Pentadecanoic acid, 14-methyl-, methyl ester	C17H34O2			X		
Octadecanamide	C18H37NO			X		
Cholest-2-ene, (5.alpha.)-	C27H44			X		
Cholest-8(14)-ene, (5.alpha.)-	C27H44			X		
Cholestan-3-one, (5.alpha.)-	C27H44O			X		
Cyclotetradecane	C14H28			X		
Hexadecane	C16H34				X	
1,7-Trimethylene-2,3-dimethylindole	C14H19N				X	
E-14-Hexadecenal	C16H30O				X	
Heptadecane	C17H36				X	
Cyclohexadecane, 1,2-diethyl-	C18H36				X	
9-Octadecenoic acid, (E)-	C18H34O2				X	
Pyrrolidine, 1-(1-oxooctadecyl)-	C21H41NO				X	
8-Heptadecene	C17H34				X	
Heptadecanoic acid, 14-methyl-, methyl ester	C19H38O2					X
Oleic Acid	C18H34O2					X

Cholest-2-ene	C27H44					X

3.3.4. TGA analysis

TGA analysis was performed to study the weight loss stage variation in the biocrude. The TGA curves of all the samples of biocrude from HTL of different biomasses and co-HTL of primary sludge with different biomasses are shown in Figure 2.a and Figure 2.b. All HTL biocrudes showed similar TGA curve progression. Concerning the HTL experiments, a relatively significant weight loss took place at 335 °C in HTL frass with 78.21 % of weight loss, 90 °C with 1.52 % of weight loss and 314 °C with 90.09 % in HTL buffalo, 339 °C in HTL rice straw with 68.53 % of weight loss, 116 °C with 9.69 % of weight loss and 340 °C with 63.89 % in HTL spirulina platensis, 322 °C in HTL swine manure with 69.05 % of weight loss and 186.90°C in HTL primary sludge with 74.69 % of weight loss. Concerning the co-HTL experiments, a relatively significant weight loss took place at 325 °C in co-HTL frass with PS with 72.84 % of weight loss, 115 °C with 2.25 % of weight loss and 340 °C with 71.95 % in co-HTL rice straw with PS, 287 °C in co-HTL spirulina platensis with PS with 76.57 % of weight loss, 330 °C with 79.70 % of weight loss in co-HTL swine manure with PS and 130 °C with 4.13 % of weight loss and 368 °C with 65.20 % of weight loss in co-HTL buffalo with PS.

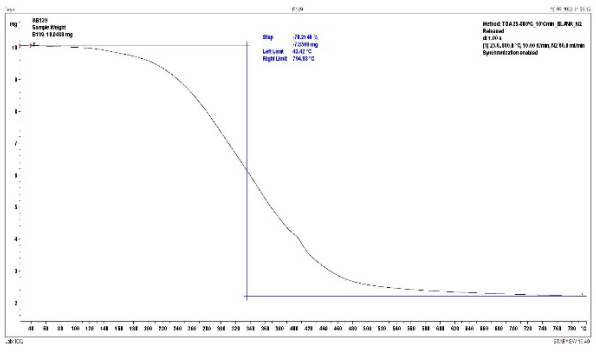

(a)

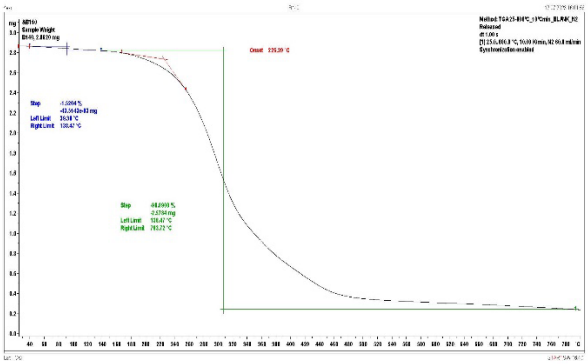

(b)

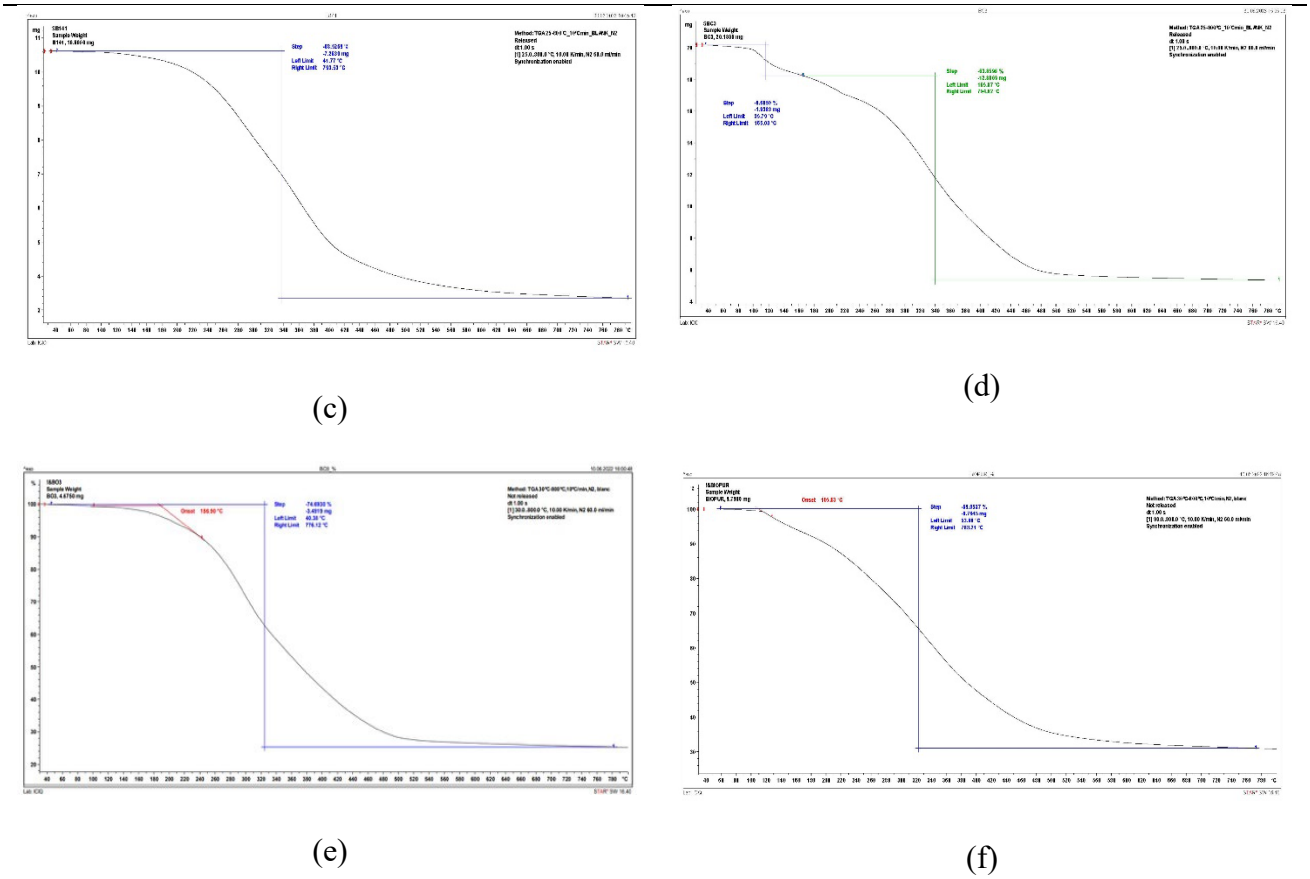

(c) (d)

(e) (f)

Figure 2.a. Thermal gravimetric analysis of samples of biocrude: (a) Frass; (b) Buffalo; (c) Rice straw; (d) Spirulina platensis; (e) Primary sludge, (f) Swine manure. 300ºC of temperature, 30 min of reaction time and 100 rpm stirring rate.

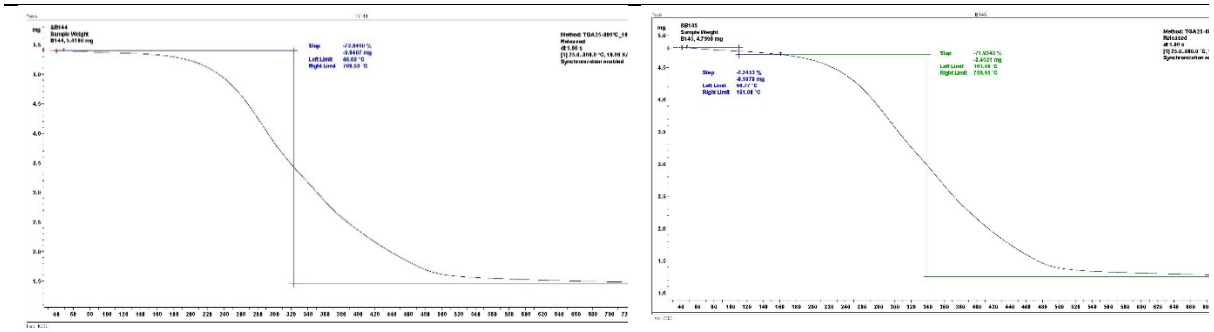

(a) (b)

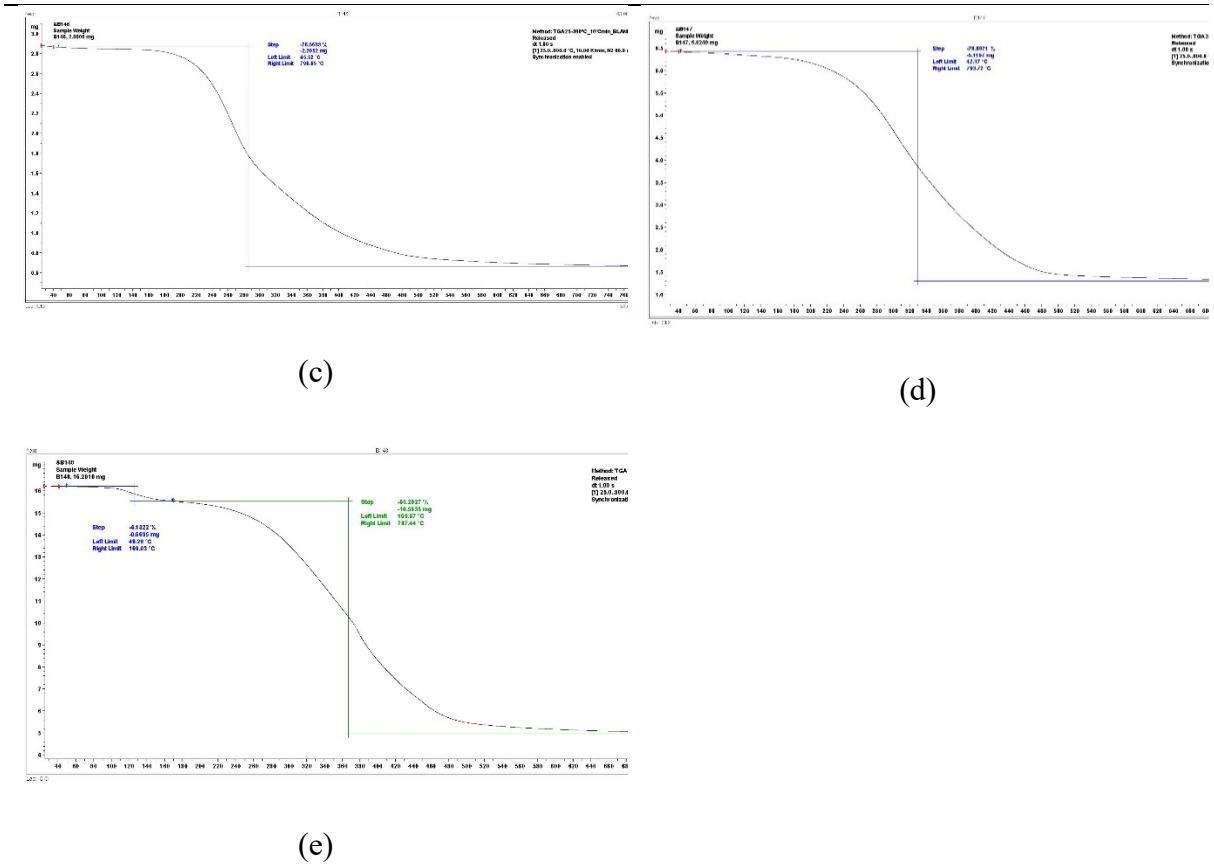

(c) (d)

(e)

Figure 2.b. Thermal gravimetric analysis of samples of biocrude: (a) Frass with PS; (b) Rice straw with PS; (c) Spirulina platensis with PS; (d) Swine manure with PS; (e) Buffalo with PS. 300ºC of temperature, 30 min of reaction time and 100 rpm stirring rate.

4407

4408 **3.3.5. FTIR**

4409 Different functional groups present in the HTL and co-HTL derived biocrudes were detected
4410 though FTIR analysis and demonstrated in Figure 3.a and Figure 3.b. The results displayed that
4411 the functional groups were almost the same in all the biocrudes which confirmed the presence
4412 of similar chemical structures within the samples of biocrude. The absorption peak near 3250
4413 cm^{-1} was from N–H/O–H stretching vibrations of amino and hydroxyl compounds. The strong
4414 and broad absorption peaks in the range of 2800 cm^{-1}–3000 cm^{-1} belonged to the C–H

stretching of $–CH_2$ and $–CH_3$ groups, showing the presence of long-chain aliphatic hydrocarbons. The peaks near 1850 cm^{-1}–1500 cm^{-1} were assigned to C=O functional groups, indicating the presence of carboxylic acids, ketones, esters and aldehydes in the biocrude. Peaks in the range of 1300 cm^{-1}–1200 cm^{-1} marked the presence of phenolic and alcoholic compounds because of C–O stretching vibrations. Despite similarity in functional groups, a significant increase in the C–H peaks was detected in the biocrudes derived from co-HTL process, suggesting the increase of hydrocarbons compounds and the decrease of N-compounds.

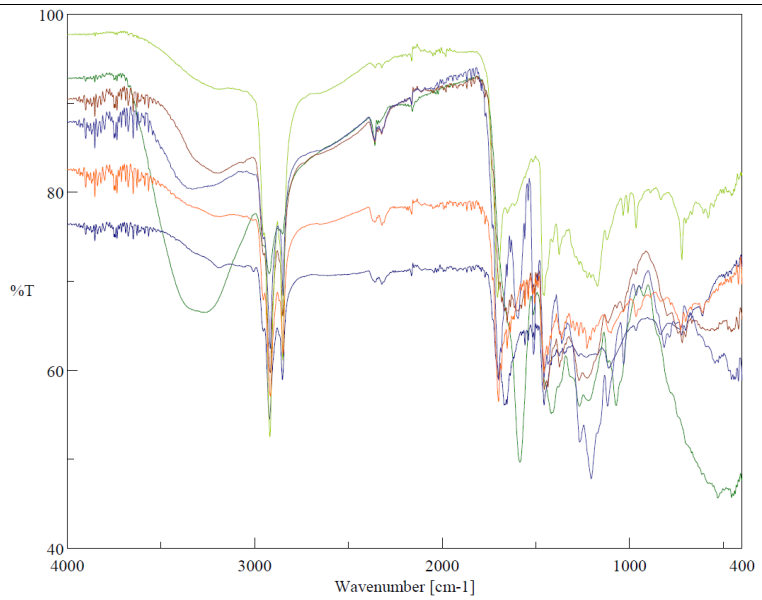

Figure 3.a. FT-IR plot of samples of biocrude: swine manure (green), buffalo (blue), frass (purple), primary sludge (yellow), rice straw (dark purple) and spirulina platensis (orange). 300ºC of temperature, 30 min of reaction time and 100 rpm stirring rate.

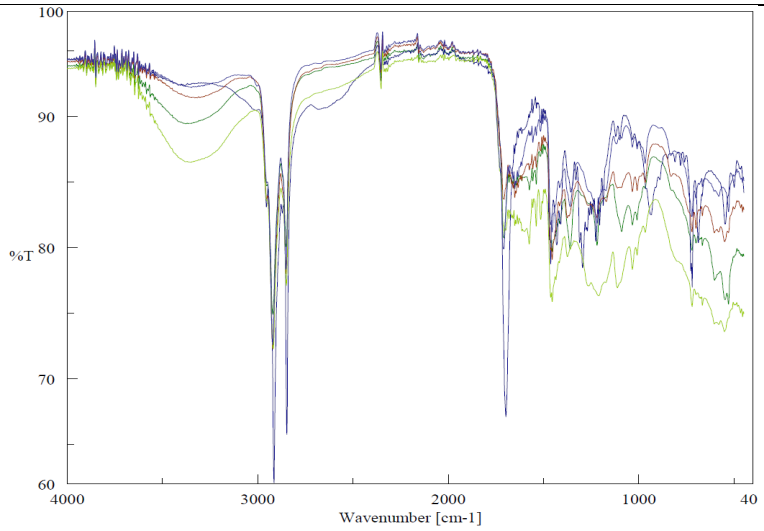

Figure 6.b. FT-IR plot of samples of biocrude: Frass + PS (green), rice straw + PS (blue), spirulina platensis + PS (red), swine manure + PS (yellow) and buffalo + PS (purple). 300ºC of temperature, 30 min of reaction time and 100 rpm stirring rate.

3.3.6. ^{1}H NMR

^{1}H NMR analysis was done for all the samples of biocrude for revealing the distribution of different functional groups in the biocrude. The spectrums looked similar regardless of which biomass was used. The spectra of all the biocrudes are listed in Figure 4.a and Figure 4.b. The most significant peaks appeared in the region of 0.5 ppm and 3.0 ppm. The peaks at 0.5-1.5 ppm determine the hydrogen atoms in alkanes. The peaks near the ranges 1.5-1.6 ppm, 1.7-2.8 ppm and 5.2-5.5 ppm demonstrate the protons in the heteroatomic functionalities, resulted from N and O compounds. Aromatics were also detected within the range 2.2–2.4 ppm. The big peak around 7.2 ppm corresponded to the solvent used, d-chloroform. In the biocrudes produced from the co-HTL process, it can be clearly noticed a high intensity in the peaks located in the range 2-2.2 ppm, resulting from the presence of high amount of esters as it was confirmed by GC/MS and FTIR analysis.

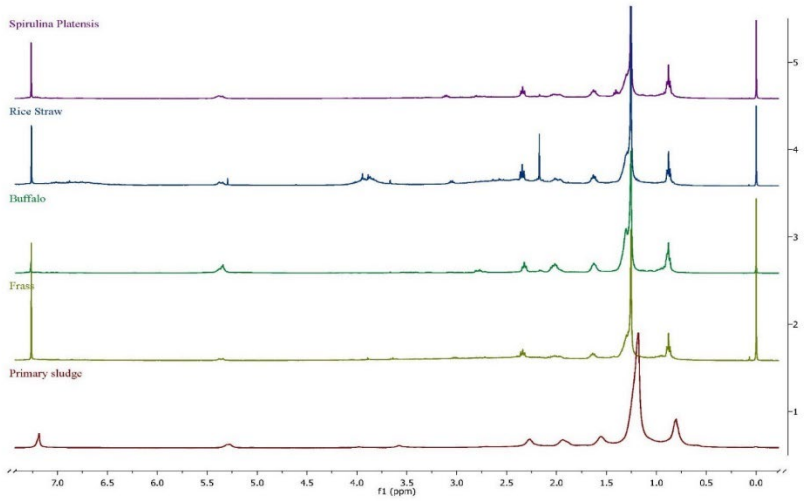

Figure 7.a. ^{1}H NMR plots of samples of HTL biocrude. 300ºC of temperature, 30 min of reaction time and 100 rpm stirring rate.

4437

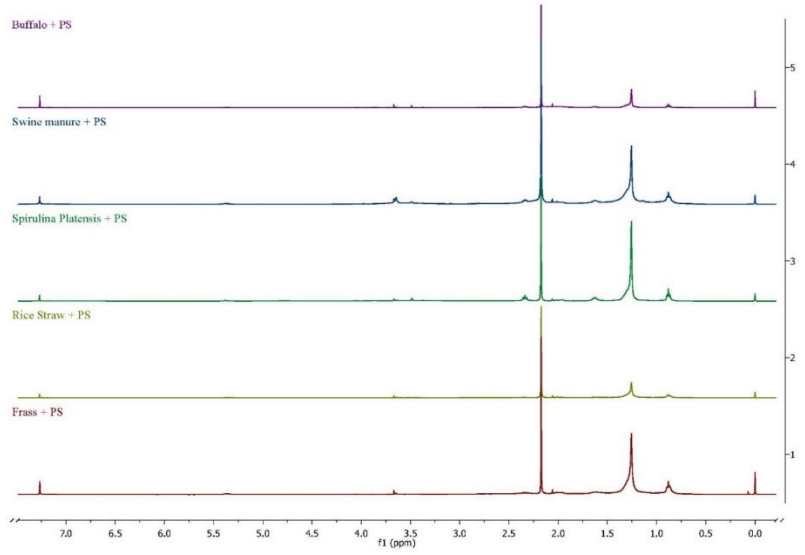

Figure 4.b. ^{1}H NMR plots of samples of co-HTL biocrude. 300ºC of temperature, 30 min of reaction time and 100 rpm stirring rate.

4438

3.3.7. Quantification of SARA fractions

SARA fractions quantification was achieved to all conditions and the results are presented in Table 5. The composition of biocrude produced was distributed between maltenes including saturates, aromatics and resins, and asphaltenes. In general, asphaltenes were predominant in the biocrude obtained, except for HTL of frass and co-HTL of buffalo and primary sludge. However, the highest percentage of asphaltene was noticed in the biocrude produced from co-HTL of rice straw and primary sludge, 93.39 %. The three fractions were observed in all the biocrudes obtained. The amount of saturates, aromatics and resins were dependent on the feedstock chosen. In the HTL of buffalo, the percentages of saturates, aromatics and polars were 1.55 %, 0.18 % and 9.35 %. While in the co-HTL of frass with primary sludge, the amounts were changed to 9.09 %, 10.53 % and 13.24 %. The results obtained from SARA analysis complied with the peaks detected by GC/MS.

Table 5. SARA fractions characterization of biocrude, 30 min of reaction time and 100 rpm stirring rate.

Feedstock	% Saturates	% Aromatics	% Resins	% Asphaltenes
Primary sludge	29,00	4,74	8,69	57,57
Frass	24,89	4,36	35,65	34,90
Frass + PS	9,09	10,53	13,24	67,13
Rice straw	25,74	5,15	17,59	51,52
Rice straw + PS	4,27	1,63	0,70	93,39
Swine manure	3,00	1,60	29,50	65,90
Swine manure + PS	5,55	27,77	5,75	60,93
Buffalo	1,55	0,18	9,35	88,92
Buffalo + PS	27,59	3,64	28,71	40,06
Spirulina Platensis	0,31	5,36	8,26	86,07
Spirulina platensis + PS	22,90	12,46	7,18	57,46

3.3.8. Simulated distillation

The simulated distillation profile of biocrudes were successfully studied through Sim-Dis analysis and the results of the distribution of boiling points with respect to the mass fractions are depicted in Figure 5. As it can be seen in the figure, all biocrudes presented relatively similar distillation profiles with respect to boiling point distributions. In other words, they all offered very similar behavior. Frass, Spirulina platensis, swine manure and buffalo contain a fraction in the range of gasoline with 4 %, 1 %, 20 % and 1 %. Less than 10 % of the biocrude fraction is in the Jet fuel range. Protein and lignin produced substances with boiling points in

the range of jet fuel (Al-juboori et al., 2023). Diesel fraction accounts to less than 30 % of the biocrude. Substances included in this fraction are mainly derived from protein, and in small quantity from carbohydrates, lipids and lignin (Al-juboori et al., 2023). The most important part in the biocrude belongs to the vacuum gasoil fraction. It accounts to around 70 %, suggesting that substances included in this fraction are mainly generated from lipids (Al-juboori et al., 2023). This study confirms that biocrude requires additional treatment in order to be considered as a feasible fuel by improving its quality. A post-refinery of the biocrude by using commercial hydrotreating hydrogen and catalysts can improve the quality of hydrocarbons and remove the heteroatoms in the biocrude (Haider et al., 2018).

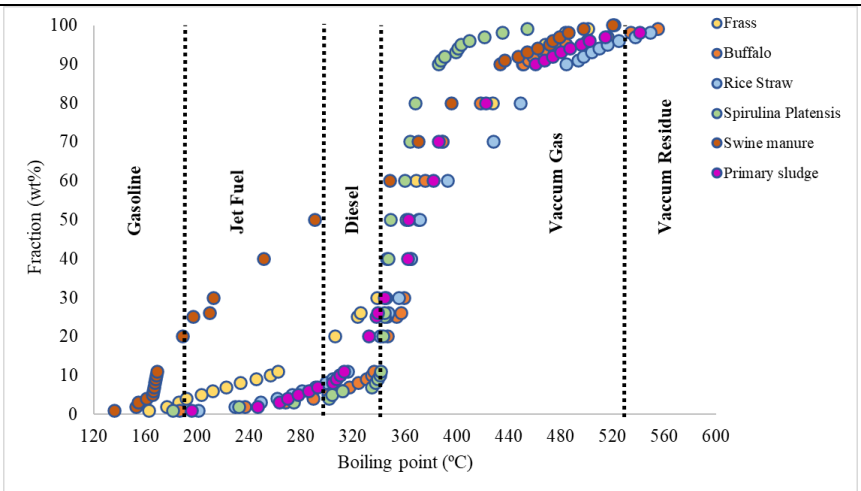

Figure 5. Simulated distillation of HTL biocrude. 300ºC of temperature, 30 min of reaction time and 100 rpm stirring rate.

3.4. Other products: Aqueous phase

3.4.1. Results

The liquid phase recuperated from the separation of organic phase and aqueous phase was fully characterized. The composition of aqueous phase was dependent on the feedstock used. Results

obtained from the analysis of liquid phase produced from HTL and co-HTL experiments are all listed in Table 6. When swine manure and rice straw were employed, pH was acidic, lower than 7, indicating the presence of acidic compounds. Whereas, when frass, buffalo, spirulina platensis and primary sludge were employed, pH was higher than or near 7, basic or neutral, indicating the presence of N-rich compounds. The percentages of carbohydrates and proteins were considered low, when compared to that of the initial feedstocks. However, it´s noted that in the scenarios of co-HTL, more proteins were detected in the liquid phase obtained. For example, in the case of buffalo, the percentages of protein and carbohydrates decreased to 0.05 % and 0.18 %. However, when it was mixed with primary sludge, the protein content increased greatly to 14.72 %. HTL involves the hydrolysis of constituents of wet biomass. Additionally, it improves the conversion of depolymerization byproducts into simpler organic compounds (Zhu et al., 2022). The concentrations of TOC and COD were lower than that of the initial feedstocks, but still high, demonstrating that large amounts of organic species in initial biomass(es) were transferred into the aqueous phase during HTL and co-HTL. For example, in the case of primary sludge, COD and TOC values decreased to 5700 mg/L and 15700 mg/L. The percentage of dissolved solids in the aqueous phase was respectively low. Ash content and VS were changing oppositely with feedstock. For example, in the scenario of spirulina platensis, the percentage of dissolved solid was just 1.59 % including 18.41 % ashes and 81.59 % volatiles. SEM images and EDX spectra of ashes in aqueous phase are depicted in Figure 6. Very little heavy metals were found in the ash of the dissolved solid in the aqueous phase.

Table 6. Aqueous phase characterization after HTL and co-HTL, 300ºC of temperature, 30 min of reaction an

100 rpm of stirring rate.

	Weight (g)	Proteins (%, db)	Carbohydrates (%, db)	TOC (mg/L)	COD (mg/L)	pH	TS (%, db)	Ash (%, db)	VS (%, db)
Primary sludge	451.14	1.40	0.10	5700	15700	6.81	0.42	22.50	77.50
Frass	442.31	0.00	0.25	1265	17125	7.89	1.05	38.89	61.11
Frass + PS	453.12	11.80	0.00		8600	6.79	0.83	29.58	70.42
Buffalo	474.91	0.05	0.18	1695	25175	9.12	1.19	13.07	86.93
Buffalo + PS	408.99	14.72	0.21			7.73	1.01	7.03	92.97
Rice straw	500.12	0.06	1.23	325	7550	3.29	0.77	48.54	51.46
Rice straw + PS	461.14	15.89	0.12		11600	4.98	0.7	22.14	77.86
Spirulina Platensis	495.6	0.53	4.07	1030	33200	7.49	1.59	18.41	81.59
Spirulina Platensis + PS	495.69	10.15	0.00		14500	8.17	0.85	23.44	76.56
Swine manure	455.32	ND	0.60	ND	16489	4.6	ND	ND	ND
Swine manure + PS	371.82	13.16	0.31		13600	5.62	0.82	22.74	77.26

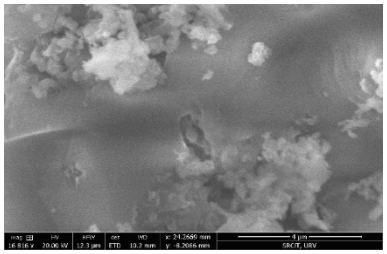

SEM image location (a)

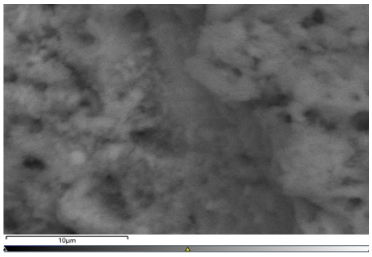

SEM image location (b)

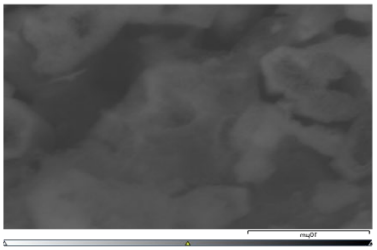

SEM image location (c)

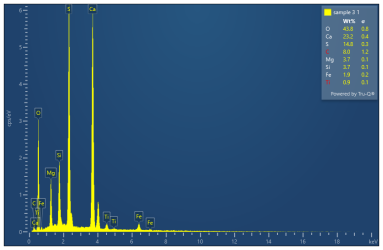

EDX spectra location (a)

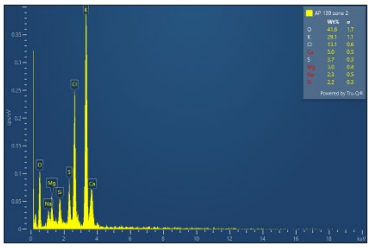

EDX spectra location (b)

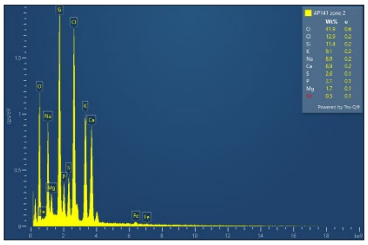

EDX spectra location (c)

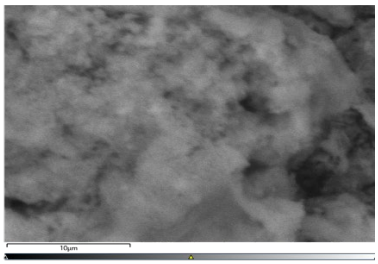

SEM image location (d)

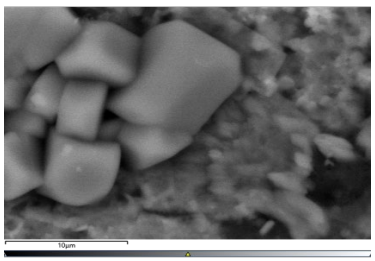

SEM image location (e)

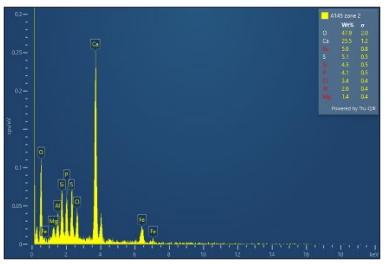

EDX spectra location (d)

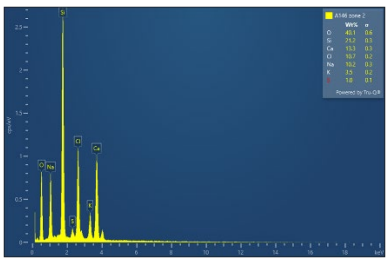

EDX spectra location (e)

Figure 6. SEM images and EDX spectra (a) primary sludge, (b) frass and (c) rice straw, (d) Frass with PS, (e) rice straw with PS of ashes in aqueous phases. HTL operation conditions: 300ºC of temperature, 30 min of reaction time and 100 rpm stirring rate.

3.5. Other products: Biochar

3.5.1. Results

Biochar is the solid phase recovered from HTL and co-HTL processes. It's a black solid that contains carbonized organics and ashes. The results obtained from its analysis are presented in Table 7. In general, the biochar yield produced was always lower than 30 % (w/w). However,

it can be demonstrated in most of the cases that the co-processing of primary sludge with other biomass improved the yield of biochar. For example, in the case of spirulina platensis, through the HTL process, only 1.35 % (w/w) of biochar was produced. However, in the co-HTL process with primary sludge, 19.44 % (w/w) were obtained. Ash and VS contents were dependent on the condition. In some cases, more volatiles were noticed, and, in some others, more ashes were noticed. However, the employment of co-HTL process decreased the volatile content in the biochar and transferred it into the biocrude.

Table 7. Biochar characterization after HTL and co-HTL, 300ºC of temperature, 30 min of reaction time and 100 rpm of stirring rate.

Feedstock	Biochar %		VS %		Ash %	
Experiment	HTL	Co-HTL	HTL	Co-HTL	HTL	Co-HTL
Buffalo	13.24	21.82	70.41	55.27	29.59	44.73
Frass	6.72	22.28	39.89	45.36	60.11	54.64
Rice straw	26.37	23.49	74.25	55.61	25.75	44.39
Microalgae	1.35	19.44	54.66	47.83	45.34	52.17
Primary sludge	28.10		39.40		60.60	
Swine manure	19.20	28.61	70.80	55.26	29.20	44.74

3.5.2. Ultimate analysis

The ultimate analysis of the solid phase, biochar, is presented in Table 8. Solid phase from HTL and co-HTL is not that useful due to its low energy density. Generally, the values of C, H, N and O didn´t bring any importance to the biochar in terms of energy resource. In the case of spirulina and frass, the presence of primary sludge has improved the carbon content of the

biochar, resulting in better HHV. On the other hand, in the case of rice straw and buffalo, the presence of primary sludge decreased the energetic value of the biochar produced.

Table 8. Ultimate analysis and HHV of biochar, 30 min of reaction time and 100 rpm stirring rate.

Feedstock	C %		H %		N %		O %*		HHV (MJ/kg)	
	HTL	co-HTL	HTL	co-HTL	HTL	co-HTL	HTL	co-HTL	HTL	co-HTL
Primary sludge	71.47		9.75		2.97		15.81		33.48	
Swine manure	ND	43.73	ND	4.40	ND	2.80	ND	49.07	ND	12.30
Spirulina	18.77	35.67	2.25	5.05	1.78	1.60	77.19	57.68	-4,32	8.95
Rice straw	57.68	36.26	4.35	4.79	2.30	1.91	35.68	57.04	19.35	8.89
Frass	28.74	40.80	2.41	5.76	2.56	1.99	66.29	51.45	1.24	12.83
Buffalo	57.59	43.69	7.47	6.45	6.61	2.18	28.33	47.67	25.15	15.49

O % was calculated from the equation (100 – ash – H % – N % – C %)

ND not defined

3.5.3. Heavy metals

EDX spectra of biochar and ash in biochar are presented in Figure 7. As carbon was the predominant part in biochar, heavy metals were detected in small quantities. It can be seen that the distribution of inorganics was not much affected by the feedstock chosen. Generally, all ashes were rich in salts or oxides containing Cl, Na, K, Ca, Fe, Si, Mg and S. It was mentioned

in a study that the majority of the inorganic elements are concentrated in the solid phase from HTL (Shah et al., 2021).

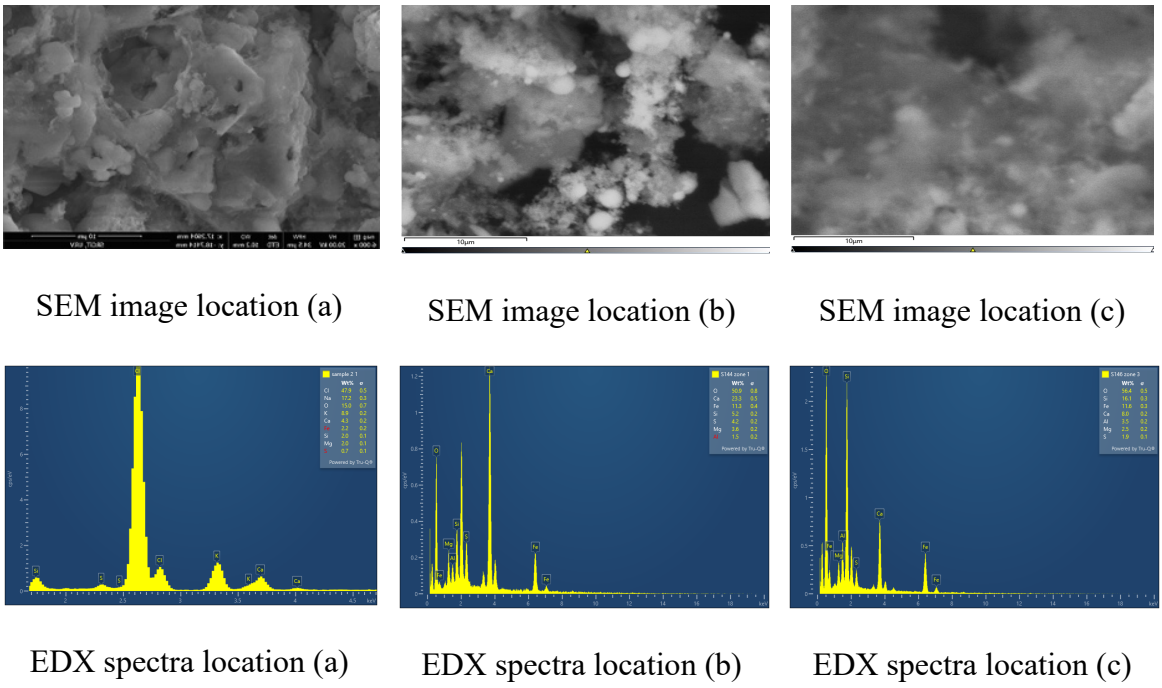

Figure 7. SEM images and EDX spectra (a) primary sludge, (b) Frass with PS, (c) rice straw with PS of ashes in biochar. HTL operation conditions: 300ºC of temperature, 30 min of reaction time and 100 rpm stirring rate.

3.6. Other products: Biogas

The composition of biogas produced from HTL of different biomasses and from co-HTL of primary sludge with other biomasses is presented in Table 9. In general, the fraction of biogas produced was dependent on the feedstock employed. From the HTL of primary sludge, only 0.038 mol % CH_4, 0.052 mol % CO_2 and 0.115 mol % CO were produced. From the HTL of frass, 0.152 mol % CH_4, 71.959 mol % CO_2, 0.093 mol % C_2H_4, 0.062 mol % C_2H_6, 2.576 mol % H_2 and 0.183 mol % C_3H_8 were produced. However, the HTL of frass with primary sludge

produced 0.233 mol % CH_4, 47.430 mol % CO_2, 0.159 mol % C_2H_4, 0.056 mol % C_2H_6, 0.463 mol % C_3H_6, 0.726 mol % H_2 and 0.045 mol % C_3H_8. From the HTL of buffalo, 1.473 mol % CH_4, 82.562 mol % CO_2, 0.152 mol % C_2H_4, 0.035 mol % C_2H_6, 0.079 mol % C_3H_6, 0.742 mol % H_2 and 0.079 mol % C_3H_8 were produced. While the HTL of buffalo with primary sludge produced 0.585 mol % CO_2, 0.001 mol % of C_2H_4 and C_2H_6, 0.028 mol % C_3H_6 and 0.663 mol % CO. In the HTL of rice straw, 2.758 mol % CH_4, 52.479 mol % CO_2, 0.140 mol % C_2H_4, 0.055 mol % C_2H_6, 0.746 mol % C_3H_6, 1.682 mol % H_2 and 0.023 mol % C_3H_8 were produced. However, the HTL of rice straw with primary sludge produced 0.291 mol % CH_4, 37.862 mol % CO_2, 0.107 mol % C_2H_4, 0.067 mol % C_2H_6 and C_3H_6, 0.374 mol % H_2 and 0.053 mol % C_3H_8 and 0.174 mol % CO. From the HTL of spirulina platensis, 0.015 mol % CH_4, 13.155 mol % CO_2, 0.02 mol % C_2H_4, 0.012 mol % C_2H_6, 0.114 mol % C_3H_6, 2.08 mol % H_2 and 0.044 mol % CO were detected. While the HTL of spirulina platensis with primary sludge produced 5.874 mol % CH_4, 35.101 mol % CO_2, 0.142 mol % C_2H_4, 0.053 mol % C_2H_6, 0.295 mol % C_3H_6, 0.434 mol % H_2 and 0.071 mol % C_3H_8. From the HTL of swine manure with primary sludge, only 0.585 mol % CO_2, 0.001 mol % C_2H_4 and C_2H_6, 0.028 mol % C_3H_6 and 0.663 mol % CO were noted.

Table 9. Biogas composition, 300ºC of temperature, 30 min of reaction time and 100 rpm stirring rate.

Biomass	Gas composition (mmol %)							
	CH_4	CO_2	C_2H_4	C_2H_6	C_3H_6	H_2	C_3H_8	CO
Primary sludge	0.038	0.052	0.004	ND	ND	ND	ND	0.115
Frass	0.152	71.959	0.093	0.062	ND	2.576	0.183	ND
Frass + PS	0.233	47.43	0.159	0.056	0.463	0.726	0.045	ND
Buffalo	1.473	82.562	0.152	0.035	0.079	0.742	0.079	ND
Buffalo + PS	ND	0.585	0.001	0.001	0.028	ND	ND	0.663
Rice straw	2.758	52.497	0.14	0.055	0.746	1.682	0.023	ND
Rice Straw + PS	0.291	37.862	0.107	0.067	0.067	0.374	0.053	0.174
Spirulina Platensis	0.015	13.155	0.02	0.012	0.114	2.08	ND	0.044
Spirulina Platensis + PS	5.874	35.101	0.142	0.053	0.295	0.434	0.071	ND
Swine manure + PS	ND	0.585	0.001	0.001	0.028	ND	ND	0.663

4. Conclusions

The highest yield of biocrude was achieved from the HTL of primary sludge with 37.66 % (w/wVS). The co-processing of primary sludge with other biomass did improve the biocrude percentage through co-HTL. The most important enhancement was noted through co-HTL of rice straw with primary sludge, where the yield of biocrude has increased from 16.11 to 29.03

% (w/wVS). The co-HTL process has decreased N- containing compounds and increased hydrocarbons and esters in biocrude. However, it still needs further treatment to improve its quality. By-products, biochar and aqueous phase, after HTL and co-HTL, contain high amount of organics, which make them interesting feedstocks for energy bioresource.

Acknowledgements

Authors express their gratitude for the collaboration with the 283àter283 company Gestió Ambiental i Abastament S.A. (WWTP in Reus, Spain). Jacky Cheikhwafa acknowledges the Agència de Gestió d'Ajuts Universitaris i de Recerca (AGAUR) of the Catalan Government for providing the pre-doctoral study (Ajuts per a la contractació de personal investigador predoctoral en formació, 2019 FI-B 00743). This work is included in the PECT "Cuidem el que ens uneix/Pobles Vius I Actius/Ebrebioterritori" project, within the frame of the RIS3CAT and ERDF Catalonia Operational Programme 2014-2020. Fundings are provided by the Catalan Government and the Provincial Council of Tarragona. The 283àter283 from Universitat Rovira i Virgili are admitted by the Comissionat per a Universitats i Recerca of the DIUE of the Generalitat de Catalunya (2017-SGR-396) and supported by the Universitat Rovira i Virgili (2017PFR-URV-B2-33).

References

A. Parvathy Eswari, Yukesh Kannah R, S. Kavitha, & J. Rajesh Banu. (2023). Recent insight into anaerobic digestion of lignocellulosic biomass for cost effective bioenergy generation. 3, 100119–100119. *https://doi.org/10.1016/j.prime.2023.100119*

Al-juboori, J.M., Lewis, D.M., Hall, T., van Eyk, P.J. 2023. Characterisation of chemical properties of the produced organic fractions via hydrothermal liquefaction of biosolids from a wastewater treatment plant. *Biomass and Bioenerg*, 170, 106703.

Anyaoha, K. E., & Zhang, Dr. L. (2022). Transition from fossil-fuel to renewable-energy-based smallholder bioeconomy: Techno-economic analyses of two oil palm production systems. *Chemical Engineering Journal Advances, 10*, 100270. *https://doi.org/10.1016/j.ceja.2022.100270*

Chan, Y. H., Lock, S. S. M., Chin, B. L. F., Wong, M. K., Loy, A. C. M., Foong, S. Y., Yiin, C. L., & Lam, S. S. (2023). Progress in thermochemical co-processing of biomass and sludge for sustainable energy, value-added products and circular economy. *Bioresource Technology*, *380*, 129061. *https://doi.org/10.1016/j.biortech.2023.129061*

Chen, W., Lin, Y. Y., Liu, H. C., Chen, T. C., Hung, C. H., Chen, C. H., & Ong, H. C. (2019). A comprehensive analysis of food waste derived liquefaction bio-oil properties for industrial application. *Applied Energy*, *237*, 283–291. *https://doi.org/10.1016/j.apenergy.2018.12.084*

Duc Bui, V., Phuong Vu, H., Phuong Nguyen, H., Quang Duong, X., Tuyen Nguyen, D., Tuan Pham, M., & Quy Phong Nguyen, P. (2023). Techno-economic assessment and logistics management of biomass in the conversion progress to bioenergy. *Sustainable Energy Technologies and Assessments*, *55*, 102991. *https://doi.org/10.1016/j.seta.2022.102991*

DuBois, M., Gilles, K.A., Hamilton, J.K., Rebers, P.A., Smith, F. 1956. Total sugar determination by phenol sulphuric method. Anal Chem, 28, 350-356.

Glińska, K., Stüber, F., Fabregat, A., Giralt, J., Font, J., Mateo-Sanz, J.M., Torrens, E., Bengoa, C. 2020. Moving municipal WWTP towards circular economy: Cellulose recovery from

primary sludge with ionic liquid. Resour Conserv Recycl Adv, 154, 104626. *https://doi.org/10.1016/j.resconrec.2019.104626*.

Haider, M.S., Castello, A., Michalski, K.M., Pedersen, T.H., Rosendahl, L.A. 2018. Catalytic hydrotreatment of microalgae biocrude from continuous hydrothermal liquefaction: heteroatom removal and their distribution in distillation cuts. *Energies*, 11, 3360. *https://doi.org/10.3390/en11123360*.

Hao, B., Yang, W., Wang, Y., Xu, D., Kapusta, K., & Guo, Y. (2022). *Hydrothermal liquefaction of municipal sludge: Coupling effects of temperature and time on nitrogen migration*. *165*, 105562–105562. *https ://doi.org/10.1016/j.jaap.2022.105562*

Harisankar, S., Vishnu Mohan, R., Vaishali Choudhary, Vinu, R. (2022). Effect of 285àter quality on the yield and quality of the products from hydrothermal liquefaction and carbonization of rice Straw. *Bioresource Technology, 351*, 127031. *https://doi.org/10.1016/j.biortech.2022.127031*

https://doi.org/10.1016/j.biombioe.2023.106703.

Iqbal, A., Noreen, N., Imran, M., Francisco Alves, J. L., da Silva, J. C. G., & Badshah, S. L. (2023). Valorization of the biomass of Rhizoclonium hookeri through slow pyrolysis and its thermokinetic investigation for bioenergy potential. *Biomass and Bioenergy, 168*, 106690. *https://doi.org/10.1016/j.biombioe.2022.106690*

Islam, Md. B., Khalekuzzaman, M., Kabir, S. B., Hossain, Md. R., & Alam, Md. A. (2022). Substituting microalgal biomass with faecal sludge for high-quality biocrude production through co-liquefaction: A sustainable biorefinery approach. *Fuel Processing Technology*, *225*, 107063. *https://doi.org/10.1016/j.fuproc.2021.107063*

Koley, S., Khadase, M. S., Mathimani, T., Raheman, H., & Mallick, N. (2018). Catalytic and non-catalytic hydrothermal processing of Scenedesmus obliquus biomass for bio-crude

4622 production – A sustainable energy perspective. *Energy Conversion and Management*,
4623 *163*, 111–121. *https://doi.org/10.1016/j.enconman.2018.02.052*
4624 Leng, L., Leng, S., Chen, J., Yuan, X., Li, J., Li, K., Wang, Y., & Zhou, W. (2018c). The
4625 migration and transformation behavior of heavy metals during co-liquefaction of
4626 municipal sewage sludge and lignocellulosic biomass. *Bioresource Technology*, *259*,
4627 156–163. *https://doi.org/10.1016/j.biortech.2018.03.019*
4628 Leng, L., Li, J., Wen, Z., & Zhou, W. (2018a). Use of microalgae to recycle nutrients in
4629 aqueous phase derived from hydrothermal liquefaction process. *Bioresource Technology*,
4630 *256*, 529–542. *https://doi.org/10.1016/j.biortech.2018.01.121*
4631 Leng, L., Li, J., Yuan, X., Li, J., Han, P., Hong, Y., Wei, F., & Zhou, W. (2018b). Beneficial
4632 synergistic effect on bio-oil production from co-liquefaction of sewage sludge and
4633 lignocellulosic biomass. *Bioresource Technology*, *251*, 49–56.
4634 *https://doi.org/10.1016/j.biortech.2017.12.018*
4635 Liu, H., Basar, I. A., & Eskicioglu, C. (2023). Hydrothermal liquefaction for sludge-to-energy
4636 conversion: An evaluation of biocrude production and management of waste streams.
4637 *Energy*, 128268. *https://doi.org/10.1016/j.energy.2023.128268*
4638 Lowry, O.H., Rosebrough, N.J., Farr, A.L., Randall, R.J. 1951. Proteins measurement with the
4639 folin phenol reagent. Biol Chem, 193, 265-275.
4640 Mishra, S., & Mohanty, K. (2020). Co-HTL of domestic sewage sludge and wastewater
4641 treatment derived microalgal biomass – An integrated biorefinery approach for
4642 sustainable biocrude production. *Energy Conversion and Management*, *204*, 112312.
4643 *https://doi.org/10.1016/j.enconman.2019.112312*

Paramati, S. R., Shahzad, U., & Doğan, B. (2022). The role of environmental technology for energy demand and energy efficiency: Evidence from OECD countries. *Renewable and Sustainable Energy Reviews*, *153*, 111735. *https://doi.org/10.1016/j.rser.2021.111735*

Rice, E.W., Baird, R.B., Eaton, A.D., Clesceri, L.S. 2012. Standard Methods for the Examination of Water and Wastewater, 22nd edn. APHA AWWA WEF, Washington.

Shah, A.A., Toor, S.S., Conti, F., Nielsen, A.H., Rosendahl, L.A. 2020. Hydrothermal liquefaction of high ash containing sewage sludge at sub and supercritical conditions. Biomass and Bioenerg, 135, 105504. *https://doi.org/10.1016/j.biombioe.2020.105504*.

Shah, A. A., Toor, S., Seehar, T. H., Sadetmahaleh, K. K., Pedersen, T. H., Nielsen, A. H., & Rosendahl, L. (2021). Bio-crude production through co-hydrothermal processing of swine manure with sewage sludge to enhance pumpability. *Fuel*, *288*, 119407. *https://doi.org/10.1016/j.fuel.2020.119407*

Tolessa, A. (2023). Bioenergy potential from crop residue biomass resources in Ethiopia. *Heliyon, 9 (2)*, e13572. *https://doi.org/10.1016/j.heliyon.2023.e13572*

Wang, H., Han, X., Zeng, Y., & Xu, C.C. (2023). Development of a global kinetic model based on chemical compositions of lignocellulosic biomass for predicting product yields from hydrothermal liquefaction. *Renewable Energy, 215,* 118956. *https://doi.org/10.1016/j.renene.2023.118956*

Xu, D., Wang, Y., Lin, G., Guo, S., Wang, S., & Wu, Z. (2019). Co-hydrothermal liquefaction of microalgae and sewage sludge in subcritical water: Ash effects on bio-oil production. *Renewable Energy*, *138*, 1143–1151. *https://doi.org/10.1016/j.renene.2019.02.020*

Xu, F., Xie, Y., & Zhou, D. (2022). Air pollution's impact on the settlement intention of domestic migrants: evidence from China. *Environmental Impact Assessment Review,95,*106761. *https://doi.org/10.1016/j.eiar.2022.106761*

Yan, S., Xia, D., Zhang, X., & Liu, X. (2022). *Synergistic mechanism of enhanced biocrude production during hydrothermal co-liquefaction of biomass model components: A molecular dynamics simulation*. *255*, 124561–124561. https://doi.org/10.1016/j.energy.2022.124561

Zhang, P., Feng, L., Su, B., & Li, X. (2022). Microalgae cultivated in wastewater catalytic hydrothermal liquefaction: Effects of process parameter on products and energy balance. *Journal of Cleaner Production*, *341*, 130895. https://doi.org/10.1016/j.jclepro.2022.130895

Zhu, Y., Zhao, Y., Tian, S., Zhang, X., Wei, X. (2022). Catalytic hydrothermal liquefaction of sewage sludge: Effect of metal support heterogeneous catalysts on products distribution. *J Energy Inst*. https://doi.org/10.1016/j.joei.2022.04.008.

4679

4680

7

Conclusion and future perspectives

- Fossil fuel is not able to cover the energy demand. In addition, it contributes to CO_2 emissions resulting in global warming.
- Biomass, a carbon source, could be implemented in the production of bioenergy.
- Primary sludge, characterized by its high organic content (lipid, protein, carbohydrate), could be used as feedstock for the conversion process into biofuels.
- Hydrothermal liquefaction is one thermochemical technique which is feasible for primary sludge as no pre-drying is required.
- Through HTL process, four products were always produced: biocrude, biochar, aqueous phase and biogas.
- Parameters including temperature, reaction time, water ratio, biomass type affect greatly the products yields and quality.
- Among all the achieved temperatures, the highest yield of biocrude was reached at 270ºC.
- The best quality of biocrude was obtained at 300 ºC regarding its composition and its energy value.
- A longer reaction time was able to improve the yield of biocrude at all temperatures.
- For process optimization, two elements could be important, the introduction of catalysts (homogeneous or heterogeneous) or the change of the solvent (using organic solvent or co-solvent with water).
- With catalyst, the highest yield of biocrude was obtained with $CuSO_4$, 42.20%.
- With solvent, the highest yield of biocrude was obtained with 100 % of Methanol, 51.37%.

- Among all the biomasses used, primary sludge reached the highest yield of biocrude.
- Co-HTL of primary sludge with other biomasses didn't improve the yield of biocrude when compared to the HTL of primary sludge alone. However, it has improved the yield of biocrude when compared to the HTL of other biomasses alone.
- After all the trials done, biocrude quality still need further treatment in order to be replaceable for fossil fuels.
- Biocrude, even though after HTL at high temperature, at longer reaction time, in the presence of catalyst, or the presence of an organic solvent contains heavy molecules.
- One way to hydrolyse these long chain molecules is the hydrotreating and hydrocracking of biocrude in the presence of catalyst in order to reduce the oxygen content and obtain more hydrocarbon chains.

Achievement

Publications:

Cheikhwafa, J., and Glinska, K., Torrens, E., Bengoa, C. Effect of Temperature on Hydrothermal Liquefaction of High Lipids and Carbohydrates Content Municipal Primary Sludge. Available at SSRN: *http://dx.doi.org/10.2139/ssrn.4584552* **Under review**

Congresses:

EUBCE 2022, online. Mini-oral presentation « Hydrothermal liquefaction of WWTP primary sludge, effect of process temperature".

XIV Congreso META 2022, Sevilla, Spain. Oral presentation "Valorization of primary sludge by hydrothermal liquefaction"

SIDISA 2020 – XI International symposium on environmental engineering, Turin, Italy. Poster "Thermochemical conversion of primary sludge into bio-energy and other value-added molecule".

MECCE2020 – 14th Mediterranean congress of chemical engineering, online. Oral presentation "Conversion of Cellulose from Rice Straw to Levulinic Acid"

Projects:

Production of biocrude from swine manure through hydrothermal liquefaction process. Romero Polo

Extraction of lipids from Buffalo and Fly Soldier by ionic liquid and production of biodiesel. FOODIE

Research mobility

Karlsruhe Institute of Technology (KIT) 2022, Karlsruhe, Germany. Hydrothermal liquefaction of lignin extracted from miscanthus.

"The Future Is Green Energy, Sustainability, Renewable Energy".

Arnold Schwarzenegger

4745

UNIVERSITAT ROVIRA i VIRGILI

4746